Experimental and Numerical Studies of Thermoregulating Textiles Incorporated with Phase Change Materials

Kashif Iqbal

Submitted for the degree of Doctor of Philosophy

Heriot-Watt University

School of Textiles and Design

April 2016

Abstract

Phase change materials (PCMs) provide thermal management solution to textiles for the protection of wearer from extreme weather conditions. PCMs are the substances which can store or release a large amount of energy in the form of latent heat at certain melting temperature. This research reports practical and theoretical studies of textiles containing PCMs.

Mono and multifilament filaments incorporated with microencapsulated phase change material (MPCM) have been developed through melt spinning process. Scanning electron microscopy (SEM) and differential scanning calorimetry (DSC) have been performed for the characterisation of MPCM polypropylene filaments. The parameters for optimum fibre processing and their effect on mechanical properties of filaments with respect to the amount of MPCM have also been studied.

A plain woven fabric has been constructed using the developed MPCM multifilament yarn. The heat transfer property of the multifilament yarn and fabric has been investigated using finite element method. The time dependent thermoregulating effect of yarn and fabric incorporated with MPCM has also been predicted according to the validated models.

The synthesis of Nanocapsules containing mixture of paraffins and Glauber's salt as PCM and its characterisation using DSC and SEM has also been carried out. Polypropylene monofilament incorporated with the nanoencapsulated paraffins was developed and its properties have been compared to its MPCM counterpart. Furthermore the developed nanocapsules were applied on a cotton fabric via a pad-dry-cure process and the resultant fabric was evaluated using DSC and SEM in comparison with MPCM treated fabric.

The research work described in this thesis has established a better understanding of use of phase change materials in textiles, the evaluation and application. It is anticipated that this research will broaden the understanding and potential use of encapsulated phase change materials in textiles especially in the field of active smart textiles.

Dedication

In love of my father and son who died during my PhD and to my beloved mother who always remembers me in her prayer

Acknowledgement

First and foremost, praises and thanks to Almighty Allah who has given me the strength to accomplish my PhD.

I wish to express my deep appreciation to **Dr. Danmei Sun**, my project supervisor, for her guidance, quick feedback and support throughout my PhD study. Whenever I had a problem, her help was right there as an advisor. My special thanks to CDI Theme, Heriot Watt University for funding this project. I would like to thank **Professor George K**. **Stylios** for his valuable feedback on my research work. My special thanks to all the technicians, librarians and staff in the School of Textile and Design for their help and support specially **Dr. Roger Spark, Mr. James McVee** and Mrs. **Ann Hardie** for their technical help.

Lastly and most importantly my deepest thanks to my wife ***Faiza Safdar*** for her unconditional love, encouragement, constant patience and unlimited support. I also want to acknowledge my lovely daughter ***Husna Kashif*** for bringing love and fun in my life. I would like to extend my gratitude to my friends and family in Pakistan and UK for their help and support.

Table of Contents

List of Tables

List of Figures

List of publications

Peer review:

1) K. Iqbal, D. Sun, G. K. Stylios, T. Lim, and D. W. Corne, "FE analysis of thermal properties of woven fabric constructed by yarn incorporated with microencapsulated phase change materials," Fibers and Polymers, vol. 16, pp. 2497-2503, 2015.

2) K. Iqbal and D. Sun, "Development of Thermal Stable Multifilament Yarn Containing Micro-encapsulated Phase Change Materials," *Fibers and Polymers*, vol. 16, pp. 1-7, 2015.

3) K. Iqbal and D. Sun, "Development of thermo-regulating polypropylene fibre containing microencapsulated phase change materials," *Renewable Energy*, vol. 71, pp. 473-479, 11// 2014.

4) K. Iqbal and D. Sun, "Finite Element Analysis of Functional Yarn with Thermal Management Characteristics" *Thermochimica Acta, (Accepted)*

Conference:

K. Iqbal and D. Sun, "Investigating thermal properties of filament yarn containing PCMs," presented at the 15th AUTEX World Textile Conference Bucharest Romania

Poster:

Finite Element Study of Thermal Properties of Filament Yarn Containing Phase Change Material. Sun, Danmei; Iqbal, Kashif. 2015. Poster session presented at SIMULIA UK Regional User Meeting, Cheshire, UK.

Chapter 1 Introduction

1.1 Background

The heat and moisture transfer behaviour of clothing has long been recognised to be critically important for human survival. Phase Change Materials (PCMs) are organic or inorganic compounds having large amount of heat energy stored in the form of latent heat, which is able to be absorbed or released when the material changes phase from solid to liquid or liquid to solid. Microencapsulated PCM (MPCM) can be either incorporated into man-made filaments or applied on to fabrics through different techniques. The temperature of the PCM keeps almost constant when the phase change is taking place. Textiles made by such smart materials are able to provide passive insulation and protect the user from extreme environment.

PCMs are used for thermal management solution in textiles because of the automatic acclimatising properties of fibres and fabrics. When the temperature of environment or body increases, phase change materials absorb extra heat from environment or body as latent heat and keep this energy stored. When the temperature falls down outside the PCM environment, it releases the stored energy to body keeping the wearer in comfortable zone.

As PCMs change their phase from solid to liquid or vice versa, so they have to be kept in protective shells to prevent from leakage. For this purpose PCMs are encapsulated within shells called microcapsules or nanocapsules which contain PCM in the core. These capsules containing PCMs are used in textiles either by direct application on fabric called coating or by incorporating into the man-made filament during different spinning processes. These filaments, yarns and coated fabrics are used to make thermoregulating garments. The potential application in the field of textiles such as space suits, sportswear, bedding, protective gloves, shoes and accessories are considered using PCMs which not only can thermally regulate the wearer but also reduce the weight and thickness of the garment.

The heat transfer studies of textiles using finite element method exploit the development of simulated model and the prediction of thermal characteristics of textiles which are sometimes impossible or difficult to achieve experimentally. The results from the analysis of simulated models can be used to get ideas of the behaviour of materials with

a specific geometry. Similarly heat transfer analysis of simulated fabric model predicts the thermoregulating effect of fabric containing MPCM which saves the time and cost of experimentation.

1.2 **Research gaps and problems**

Most of the thermoregulating textiles have been developed by applying MPCM via coating and pad-dry-cure technique using binders which are quite established techniques. The coated fabric contains thick layer of functional material which impairs the drape of the fabric adding stiffness and uncomforting characteristics to the textiles. The incorporation of MPCM within the filament during spinning process is very attractive which can enhance the life time of the thermoregulating effect of the woven or knitted fabrics made of such filament. Only few types of yarns containing MPCM have been developed using wet or dry spinning technique which are patented. Researchers are trying to develop melt spun yarn incorporated with MPCM as melt spinning does not involve the use of solvent for the preparation of fibre forming solution and most of the thermoplastic filaments are made by melt spinning technique.

Melt spinning process can be used to develop different thermoplastic fibres such as polyester, nylon, polyethylene and polypropylene. Polypropylene fibre has its unique characteristics and is applicable in active clothing. It provides best moisture transportation and insulation properties in active smart textiles because of its excellent hydrophobicity and low thermal conductivity when used in combination with hydrophilic fibres in clothing. The overall comfort of body depends on moisture and thermal management solutions. The moisture management investigation has already been established by researchers in literature using polypropylene fibre due to its excellent wicking performance. The thermoregulating solution is provided in this research by the developed polypropylene fibre containing MPCM which covers the gap in this area.

Modelling is a useful technique for property predictions, and there is published research on thermal behaviour of textiles. The published research in this field mostly lies in the heat transfer analysis on composite layered textiles including phase change materials or textiles coated by MPCM together with binders and other chemicals. The finite element based heat transfer analysis of textiles incorporated with MPCM has not been investigated for the prediction of thermoregulating effect so far.

While talking about thermoregulation of textiles, wearer comfort temperature should be considered for the development of such products. The human skin comfort temperature is found to be around 33 °C and it should be considered accordingly when developing thermoregulating textile systems. For this purpose the synthesis of encapsulated PCM is necessary which would enable phase change temperature near the skin comfort temperature. Furthermore the capsule size is critical and should be in nano range when they are being incorporated within the filament during melt spinning process to overcome the extrusion problem.

The synthesis of encapsulated hydrated salts has become a challenge as they are water soluble and difficult to get encapsulated. The suitable hydrated salt for textile is sodium sulphate decahydrate ($Na_2SO_4.10H_2O$) and it has phase change temperature of 32.4 °C which is near to the human skin comfort temperature. Sodium sulphate decahydrate is cheaper and has relatively more latent heat value than paraffin.

1.2.1 ***Problem 1***

There is no information in literature regarding the processing parameters for the synthesis of melt spun filament incorporated with MPCM. The processing parameters need to be defined for the continuous spinning of monofilament polypropylene fibre incorporated with MPCM before moving to multifilament production stage. This can provide basis to define parameters for the development of multifilament with additives.

1.2.2 ***Problem 2***

Multifilament yarns are mostly used for clothing. It was unable to produce multifilament yarn containing MPCM through regular spinneret because of the problem with uniform extrusion of all filaments. The development of a new featured spinneret needs to be addressed for manufacturing continuous multifilament polypropylene yarn.

1.2.3 ***Problem 3***

There is no published research investigating thermal properties of fabric incorporated with MPCM using finite element method (FEM). The thermoregulating effect of PCM incorporated textiles such as temperature delay of PCM with time is difficult to be tested through experiments, and it may be feasible to be predicted accurately through post processing using FEM.

1.2.4 *Problem 4*

Currently the commercially available encapsulated PCMs are paraffin based and they are in micro-scale with capsule size up to 40 microns with phase change temperature of 28 °C. The particle size would cause problem in extrusion process and blockage of the holes of spinneret. Nanoencapsulated PCM (NPCM) is needed to overcome the extrusion related problems. Furthermore the desired phase change temperature of the NPCM should be closer to human body comfort temperature.

Sodium sulphate decahydrate (Glauber's salt) has phase change temperature near to the comfort temperature of human body. It has larger amount of latent heat than paraffin and much cheaper. There is no published research work most probably due to the highly soluble nature of it hence difficulties in encapsulation, and it needs to be investigated.

1.3 **Aim and objectives of the research**

The overall aim of the research was to conduct experimental and theoretical studies of thermoregulating textiles, by developing melt spun filaments incorporated with phase change materials and predicting the thermal regulating effect of PCM incorporated textiles using finite element method.

The objectives of this research are described as follows.

1. To develop and characterise thermoregulating mono and multi filament polypropylene filaments incorporated with MPCM by optimizing the processing parameters of melt spinning and the continuous extrusion of filaments.
2. To develop finite element models and simulate the developed multifilament yarn and plain woven fabric manufactured by the developed multifilament yarn and analyse the heat transfer behaviour of textiles incorporated with MPCM using a commercial software ABAQUS.
3. To synthesise NPCM with phase change temperature near to the skin comfort temperature and particle size in nano range suitable for extrusion by encapsulating paraffin in the core.
4. To synthesis nanoencapsulated Glauber's salt by selecting suitable reaction ingredients and optimise process parameters of encapsulation.

1.4 **Overview of thesis**

This thesis comprises of seven chapters. The present chapter introduces the background of the thesis including research gaps and main problems concerned in the research field. The aim and objectives have also been described.

The second chapter contains the literature survey of the research areas of thermoregulating textiles containing phase change materials, the synthesis and general principle of microencapsulation of PCM, melt spinning technique for fibre manufacturing, and the heat transfer analysis using finite element method.

The third chapter discusses the materials and research methodologies used to conduct the research.

Fourth chapter of thesis contains two main sections describing the development of mono and multifilament polypropylene fibre incorporated with commercial MPCM. The results are discussed in detail on the basis of parameter studies. For the development of multifilament, a new spinneret designed for uniform extrusion of multifilament will also be discussed.

The fifth chapter contains information of heat transfer analysis of yarn and fabric incorporated with MPCM using finite element method. The development of geometric model using TexGen, the model validation and the results from post processing in ABAQUS will be discussed in the chapter. The thermoregulating effects of MPCM yarn and fabric will be predicted using the simulated model.

The sixth chapter describes the synthesis of NPCM containing mixture of paraffin. The detailed procedures will be explained and the results based on SEM images and DSC graphs will be discussed in detail, together with the effect of parameters on particle size. The synthesised NPCM will be compared with previously developed fibre containing commercial MPCM. This chapter will also discuss the synthesis and characterisation of NPCM Glauber's salt using PMMA (polymethylene methacrylate) shell. The application of NPCM paraffin and NPCM Glauber's salt on cotton fabric will also be discussed in this chapter.

The last chapter of the thesis discusses the conclusions and main findings based on the results discussed in previous chapters. The future works will also be recommended for further studies in this field.

Chapter 2 Literature review

This chapter presents the literature review which provides the foundation of this research. The chapter describes the background of phase change materials and its thermoregulating effect, the microencapsulation of PCM and its application in textiles, melt spinning technique for the development of polypropylene filaments, geometric modelling of textiles and heat transfer analysis using FEM.

2.1 Thermoregulating effect using phase change materials

Thermoregulation according to the textile glossary is defined as the ability of textile to maintain the constant temperature conditions without being affected by the dynamic environment conditions outside. Comfort may be divided into four categories containing thermo-physiological comfort, sensorial comfort, garment fit and psychological comfort, and the most important of these is thermo-physiological comfort [1]. Normal human body temperature is 37 °C which increases up to 38 °C, 39 °C or occasionally 40 °C during exercise [2]. The most comfortable skin temperature is 33.4 °C and when it changes more than 4.5 °C below or above the comfort temperature, human body feels uncomfortable [3]. One of the primary functions of clothes is to prevent the temperature of skin to fall or rise too far from the stated comfort temperatures [4].

As far as clothing and comfort are concerned, physical, physiological and some psychological factors influence the comfort which is a state of mind. Complete comfort is obtained with the control of thermal buffering and moisture buffering because the body feels sensation of heat or cold and skin wetness. So thermal buffering is obtained by using phase change materials which in certain cases can increase evaporative resistance impairing moisture buffering [5].

Smart textile is an emerging area in textile field which is becoming more significant by the demand of society through consumer needs. Despite the increasing impact of science and technology, smart textile demands the advancement through interdisciplinary support like fashion, design, engineering, technology, human and life sciences. In textile sector, smart textiles have application in interior textiles, technical textiles and clothing in which the last one contains higher percentage in terms of usage of smart textiles [6]. Phase change materials are kind of smart materials which were used in clothing by US National Aeronautics and Space Administration (NASA) in 1980 to make thermo-regulated garment for space and to protect apparatus in space with

drastic temperature changes [7-9]. This technology was then adopted by Outlast technologies, based in Boulder, Colorado who used PCM in textile fibres and fabric coating [10].

PCMs are attractive for storing energy in all the available heat energy storage techniques due to high density, compact storage system and high latent heat [11, 12]. The pioneer study of phase change material was applied for space crafts on small scale and then on large scale was applied in buildings and solar energy systems to build thermal energy storage system [13-15]. A large number of inorganic and organic PCMs are available in the temperature range of -5 °C to 190 °C [16-20]. The organic phase change materials ranging from 18-65 °C are used in textiles and buildings to enhance thermal comfort effect. Among all the PCMs, n-octadecane is usually used for the textile application having melting point of 28 °C [21].

Developers claim that incorporation of phase change materials in textiles will perform buffering effect keeping the skin temperature constant against extreme weather hence prolonging thermal comfort for the wearer. They also claim that using phase change materials can decrease the fabric thickness required to protect the human body from cold environment [9, 22]. Currently, phase change materials are being used in different textiles including bedding, apparel, footwear and non-woven under the trade names Outlast™, TemperTex™ and ComforTemp®. Outlast Technologies has succeeded in marketing viscose and polyacrylonitrile (PAN) fibres incorporated with MPCM [23].

2.1.1 *How PCM works*

Phase Change Materials store energy as latent heat which is the most suitable way of storing high amount of energy with a smaller difference of temperature. The stored energy is released to surroundings in a reverse cooling process. Paraffins are organic phase change materials which absorb approximately 200 J/g of latent heat during phase change. This high amount of heat is released to surroundings during reverse cooling process called crystallization. By incorporating phase change materials to textiles, their thermal management capacity can be substantially enhanced [12].

During melting and crystallization, the temperature of phase change material does not change significantly. The increase in temperature of surroundings causes phase change material to melt by absorbing heat and when temperature of surrounding environment falls down, PCM gets solidified releasing the same amount of heat energy to

environment. This interesting phenomenon makes it very important in practical applications [12]. The phase change phenomenon is explained in Figure 2.1 where shaded area indicates the amount of latent heat in J/g or KJ/Kg.

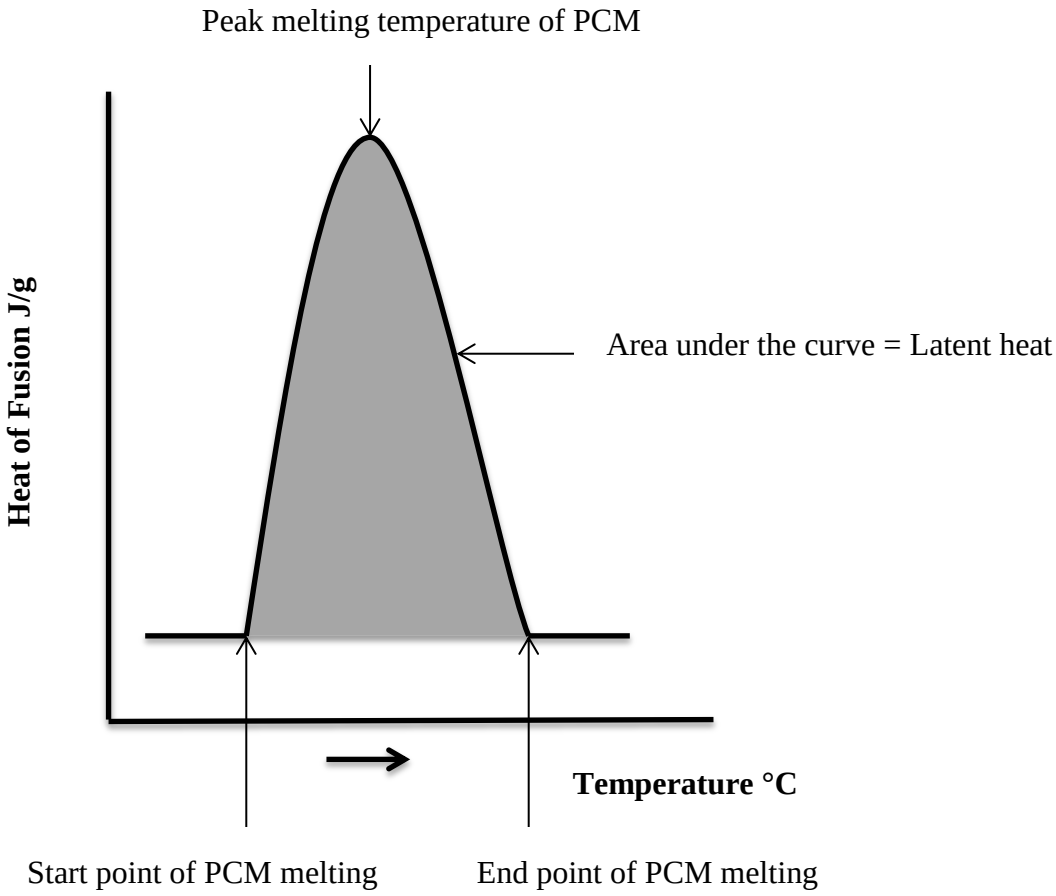

Figure 2.1 Phase change phenomenon of PCM

Chemical bonding is responsible for the above phenomenon as increase in temperature goes to break chemical bonding in the molecules of PCM material causes material to melt resulting in storing heat energy which is subsequently released during crystallization process restoring chemical bond [24].

2.1.2 *Types of PCM*

Phase change materials are theoretically able to change their phase at nearly constant temperature and are able to store large amount of energy [25]. More than 500 natural and synthetic PCMs are known in addition to water but they differ in their melting points and heat storage capacities [26]. The most common among all are paraffin which can be encapsulated and then either incorporated into fibre or applied via coating on

textiles. Some types of PCM with phase change temperature close to human skin temperature are described as follow.

Hydrated inorganic salt

Inorganic salts containing *'n'* water molecules can be used as PCM in thermoregulating textiles which usually have phase change temperature in the range of 20-40 °C. Glauber's salt ($Na_2SO_4.10H_20$) is very attractive and convenient because of its physical and chemical properties. It has a melting temperature of 32.4 °C which is very suitable for textiles and has large amount of latent heat of 254 J/g [27]. In the thermal energy system using Glauber's salt as a PCM, the thermal energy is produced by the chemical reaction between decahydrate crystal and water solution [28]. Hydrated salts are found useful in thermal energy storage system due to their high volumetric storage capacity, relative high thermal conductivity and lower cost as compared to paraffin. Glauber's salt which contains 44% of sodium sulphate and 56% of water by weight has been studied and investigated by Biswas [29] and Marks [30].

Linear long chain hydrocarbons

Long chain hydrocarbons are the by-product of oil refining containing general formula of C_nH_{2n+2}. They are suitable for various applications as they have wide range of melting temperature depending upon the number of carbon atoms. They are usually non-toxic, inexpensive and have large source of raw materials. By selecting the number of carbon atoms present in hydrocarbons, the required phase change temperature can be tailored for specific application. n-octadecane and Eicosane containing carbon atoms 18 and 20 respectively are suitable for textiles because their phase change temperature lies near the human skin temperature [31]. The phase change temperature and latent heat of some linear hydrocarbons are listed in Table 1 [32].

Table 2.1 Linear chain hydrocarbons with their phase change temperatures

Hydrocarbons	No. of C atoms	Latent heat (J/g)	Melting temperature (°C)
n-hexadecane	16	235.2	18
n-heptadecane	17	176.4	21.1-22.2
n-octadecane	18	244.8	28-30
n-nonadecane	19	177.6	32
n-eicosane	20	242	36-38

Polyethylene glycol (PEG)

PEG is another important type of PCM for textile applications. The repeating unit in PEG is oxyethylene (-O-CH_2-CH_2-) containing hydroxyl group on either side of the chain. The melting point of PEG depends on its molecular weight and is proportional as the molecular weight increases. The phase change temperature of PEG can be determined using differential scanning calorimetry [33]. PEG with degree of polymerisation 1000 has phase change temperature of 35 °C while PEG with degree of polymerisation 20,000 has melting temperature of 63 °C [34, 35].

2.2 Microencapsulation of PCM

Thermal management solution has always been a challenge where high temperature and heat is involved such as steel mills, glass factories and sports activities [36]. To overcome these problems, researchers have been working on smart textiles or intelligent textiles. Phase change materials are active smart materials which can sense and react to the environmental stimuli by storing and releasing heat energy [37]. Phase change materials cannot be applied directly on textiles because they melt by absorbing heat or crystallise by releasing the same heat. To prevent phase change materials from leakage, a process called microencapsulation or nanoencapsulation is used for durability and better application [11].

Microencapsulation is the process of covering core material such as PCM in a protective shell called capsule. Microcapsules define the particle size in the range of 1µm to 1000 µm while nanocapsules are used to describe the particle size less than 1 µm [38]. There are many techniques for microencapsulation such as complex coacervation [39], *in-situ* polymerisation [40], interfacial polymerisation [41] and spray drying [42]. *In-situ*

polymerisation is widely used among all of these synthesis techniques because of rapid wall formation and also strong capsule formation suitable for textile [11, 43].

Shin et al [44] synthesised microcapsules containing n-eicosane as core material and melamine formaldehyde as shell material by *in-situ* polymerisation. They determined that the latent heat of MPCM was 134.3 J/g with particle size of 1.89 μm. The maximum latent heat of thermo-regulating textiles after application was determined as 4.44 J/g. Sarier et al [45] used urea formaldehyde as shell material and different paraffin; n-hexadecane, n-octadecane and n-eicosane as core materials. The average particle size of microcapsules was found to be 69.1 μm with 51.7-54.8 J/g of latent heat. Fang et al [46] prepared microencapsulated phase change materials using silicone dioxide as encapsulating shell and paraffin as core material via Sol-Gel method. The differential scanning calorimetry results showed that the latent heat of microencapsulated paraffin was 165.68 J/g. Li et al [47] encapsulated n-hexadecane using urea formaldehyde as shell material. They studied the effect of surfactant on the process of nanoencapsulation and obtained the average capsule diameter of 270 nm. They determined that as the amount of surfactant increases, the particle size of nanocapsules decreases affecting the thickness of wall of particles; latent heat was found in the range of 114.6 J/g-143.7 J/g.

Salaun et al [48] prepared microcapsules using melamine formaldehyde as shell material and different paraffin as core material with their binary mixtures. They added 4% wt. tetra ethyl ortho-silicate to enhance latent heat of phase change material. Sanchez et al [49] microencapsulated paraffin wax from C_{19} to C_{27} sourced commercially as a mixture using polystyrene as shell material. The melting temperature of MPCM was from 40°C to 45°C. They coated 100% cotton fabric with prepared microcapsules using different commercial binders to characterise the thermoregulating effect of fabric and 7.6 J/g of latent heat was found on fabric containing 35% wt. of MPCM. The time duration for thermoregulating effect increases with the increase of the amount of latent heat (J/g) and hence more J/g is required where longer time duration of thermoregulating effect is required.

Nanoencapsulation has been paid attention by more researchers now a days because of narrow particle size and enhanced surface characteristics when they are applied on textiles for thermoregulating effect [38].

Sari et al [50] synthesised nanocapsules using PMMA (polymethyl methacrylate) as shell material and n-octacosane as core material for thermal energy storage. The melting temperature was measured as 50.6 °C containing latent heat of 86.4 J/g. The average diameter of the nanocapsules was 0.25 µm. In 2010, Kwon et al [51] developed NPCM with particle size less than 100 nm. They used polystyrene and PMMA as a shell material to encapsulate n-octadecane as PCM. The latent heat measured for polystyrene and PMMA based nanocapsules were 114 J/g and 120 J/g respectively. Nanocapsules of n-hexadecane with PMMA shell was made by Black et al [52] with the particle size between 100 nm and 280 nm. Alay et al [53] studied nanocapsules of PMMA shell containing n-hexadecane as core material with an average diameter of 260 nm and 148.05 J/g of latent heat at 17.23 °C. They incorporated nanocapsules into the PAN fibre during electrospinning and measured the heat of fusion which was 36.80 J/g.

More recently Karthikeyan et al [54] made NPCM containing urea formaldehyde as a shell and paraffin wax as PCM material using *in-situ* polymerisation technique; the average particle size was 256 nm. They applied nanocapsules on cotton fabric with 20% and 40% on weight of the binder using pad-dry-cure method and the latent heat was found 15.2 J/g and 19.1 J/g respectively.

The human is found to be thermally comfortable if the skin temperature is around 33 °C while in rest and less than 33 °C if any of the physical activity is involved. No research has been focussed until now on synthesising melamine formaldehyde NPCM in the range of 33 °C to target the skin comfort temperature. The synthesis of nanocapsules in this thesis focuses on the preparation of nanocapsules using melamine formaldehyde as shell material and mixture of n-octadecane and eicosane as PCM material. Moreover the developed capsules were in nano scale with narrow size distribution suitable for melt spinning process for synthetic filament production to overcome mixing and extrusion problems.

2.2.1 *General principle of microencapsulation*

Microencapsulation is the process of manufacturing polymeric particles in the range from nanometres to millimetres in which two main morphologies exist as microencapsulation and microspheres. Microsphere is the process in which active substance is enclosed within the polymeric network while microencapsulation exhibits the reservoir structure in which the active substance is surrounded by a polymeric wall called capsule shell. Microencapsulation technique was first used in 1950s by Green and

Schleicher for carbonless copying paper [55]. Microencapsulation techniques in textile field were utilised in 1990 in lab scale and then its application became popular even in industrial scale for added value of textiles [10].

There are many methods of microencapsulation described in literature and patents, the basic principle of all techniques is the same as enclosure of core material, formation of capsule particle and then hardening of capsules. The microencapsulation techniques are usually divided into main three groups:

- Mechanical methods;
- Physico-chemical methods; and
- Chemical methods.

The choice of method usually depends upon the cost of processing, chemical nature of shell material, capsule size requirement and the use of solvents especially when serious environmental issues are concerned. The physical methods give particle size greater than 100 µm but the particle size distribution among 20 µm to 40 µm are usually suitable for textile applications [56]. Capsules with small particle size usually ranging from 1 µm to 10 µm are preferably incorporated within textile fibres. According to Colvin capsules with small diameter around 1 µm or even less are suitable for fibre incorporation while the capsules with particle size of 100 µm are suitable for coating and foam application [57, 58].

The most suitable techniques are simple or complex coacervation in physico-chemical method and, *in-situ* polymerisation and emulsion solvent evaporation technique in chemical methods [42, 59-61]. In all of these methods, microencapsulation follows two steps: the emulsification step in which particle size and size distribution is affected and the capsule formation step. The emulsification step is usually influenced by stirring rate, volume ratio of the two phases, interfacial tension and the chemical composition of the two phases. The formation of capsules is greatly affected by the type and amount of surfactant which not only influences the dispersion stability of the emulsion but also determines the particle size of the microcapsule. The formation of capsule particle is also governed by the kinetic factors such as the ability of monomer or prepolymer to react or cross link [62-65].

2.2.2 *Methods of microencapsulation*

The shell material has been investigated by many researchers to improve the solid protection of core and to enhance shear and thermal stability of the capsules. Thus the interfacial polymerisation is used to obtain polyurea shells while PMMA and styrene shells are obtained using emulsion or suspension polymerisation and *in-situ* polymerisation is used to synthesise melamine derivative based microcapsule walls. Nowadays a new process called Sol-Gel has been widely used to produce the silica shell. The detailed chemical methods of encapsulation is described below[66].

Phase Coacervation method

Phase coacervation is the oldest method of microencapsulation which has two types of coacervation namely simple and complex coacervation. In simple coacervation technique one colloidal solute is used in aqueous polymeric solution; while in complex coacervation two oppositely charged colloids are used in a polymeric solution. The schematic diagram is shown in Figure 2.2 [66].

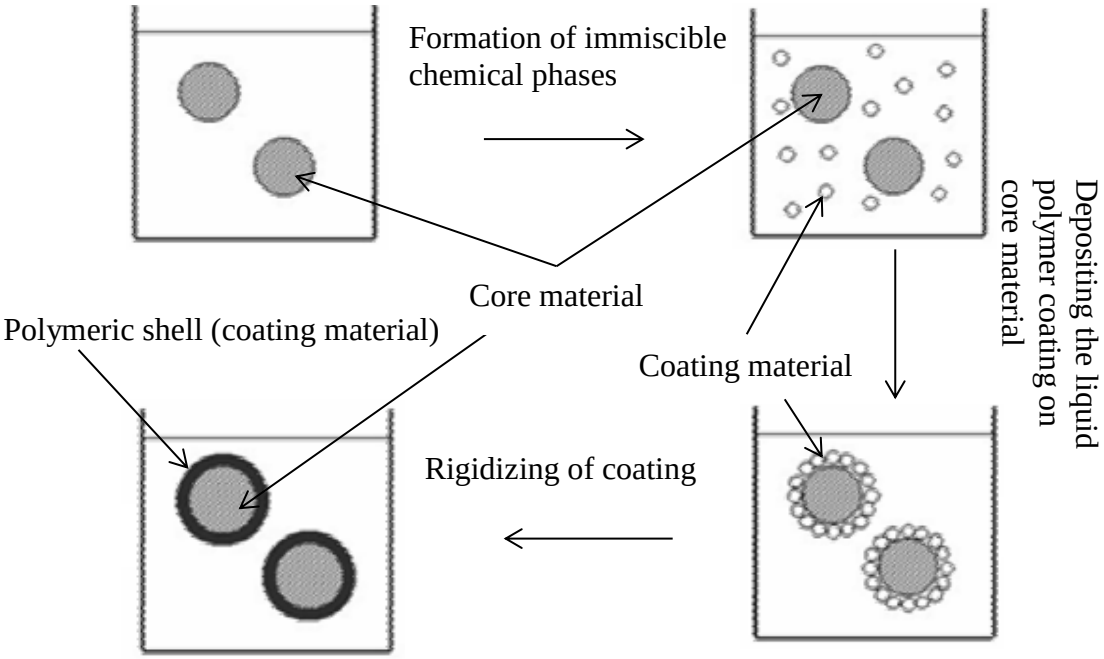

Figure 2.2 Various stages of microencapsulation process by coacervation method [66]

Figure 2.2 illustrates that initially two immiscible core and coating materials are dispersed in an aqueous phase. The coating material gets harder either by thermal or chemical cross linking to make solid capsules after it deposits on the core surface by decreasing the total free energy of the system.

The simple coacervation method was used by Uddin et al [39] in encapsulating paraffin wax. The objective of their study was to investigate the thermal performance of MPCM after cyclic operation and the latent heat measured was 56-58 J/g.

In complex coacervation method two oppositely charged polyelectrolytes are used such as gelatine/arabic gum [59] or silk fibroin /chitosan [67]. Thus the two electrolytes in acidic condition become oppositely charged to form liquid complex coacervate and deposit on the core materials forming primary capsule shell. The system is then cooled and formaldehyde is added for further cross linking reaction with amino groups present on the chain. The pH is then adjusted to 9-11 after cool down to get hardened capsules.

Onder et al [68] successfully produced microcapsules containing three paraffin waxes using complex coacervation method based on gelatin /gum arabic. They measured the enthalpy of n-hexadecane and n-octadecane which was 144.7 J/g and 165.8 J/g respectively.

***In-situ* polymerisation**

Urea formaldehyde (UF) and melamine formaldehyde (MF) based capsules are usually produced by *in-situ* polymerisation. The selection of UF and MF capsules is based on the fact that they are really thermal and shear stable. They also offer an advantage of being highly reactive resulting in the short processing of microcapsule formation with high loading content.

The microencapuslation process of MF polycondensation depends on the surface activity and the presence of resinous prepolymer in the interface, either it contains monomers like melamine and formaldhyde or methylated derivative of melamine [69]. The reaction mechanism is given in Figure 2.3.

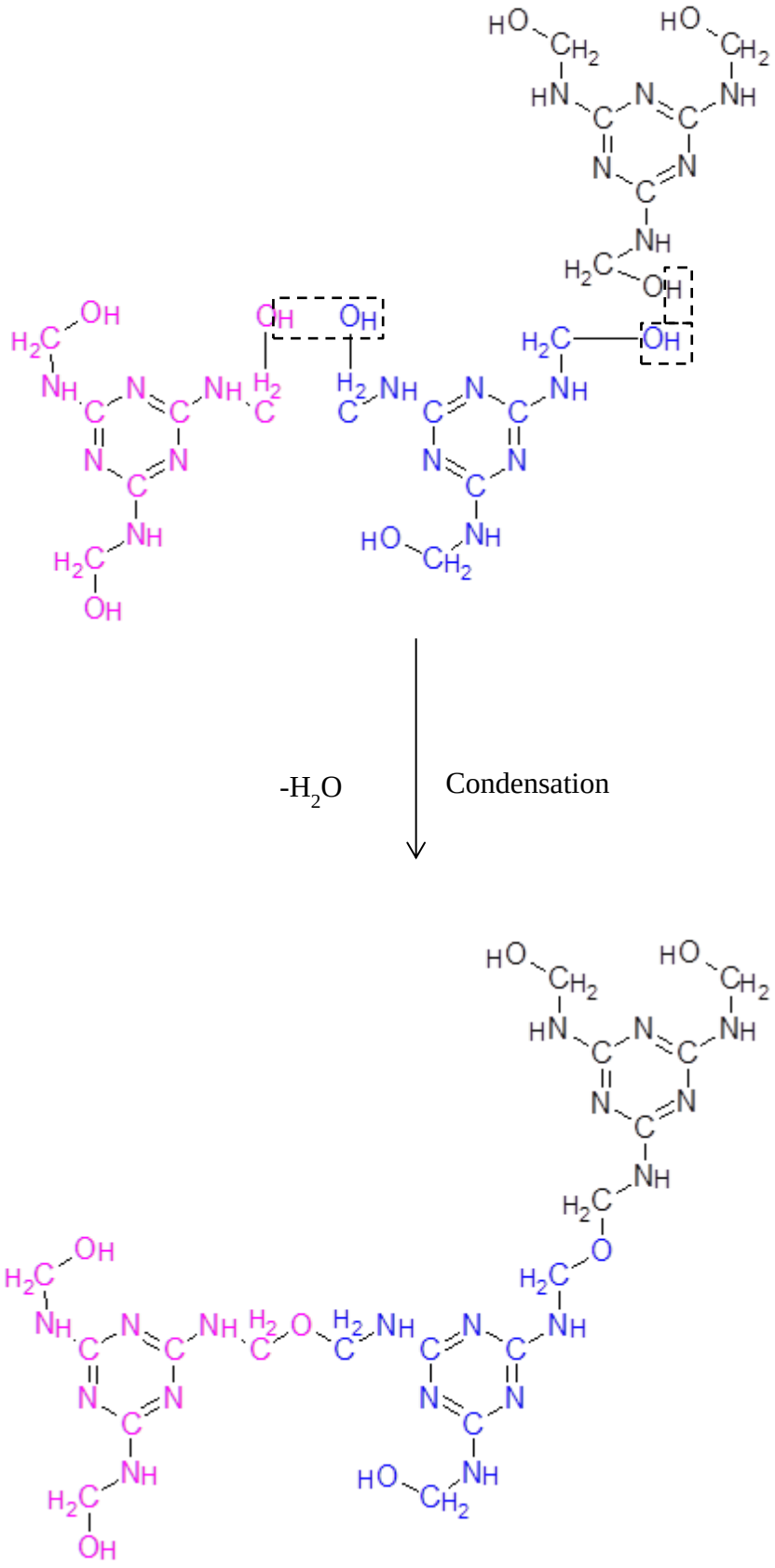

Figure 2.3 Melamine formaldehyde condensation reaction

Figure 2.4 describes the encapsulation process using *in-situ* polymerisation technique which consists of three steps. The first step is the preparation of oil in water emulsion

from the dispersion of melted phase change materials in an aqueous continuous phase by adding suitable surfactant under high stirring rate. The second step is the preparation of melamine-formaldehyde prepolymer by dissolving it in aqueous phase. The third step is the dribbling of prepolymer into the continuous phase to get the active core material encapsulated by the rotation of stirrer. Further the polymerisation occurs for 1-3 hours at 70-80 °C in acidic condition to complete the polycondensation reaction. The suspension is then filtered, washed and dried to get the desired MPCM in powder form.

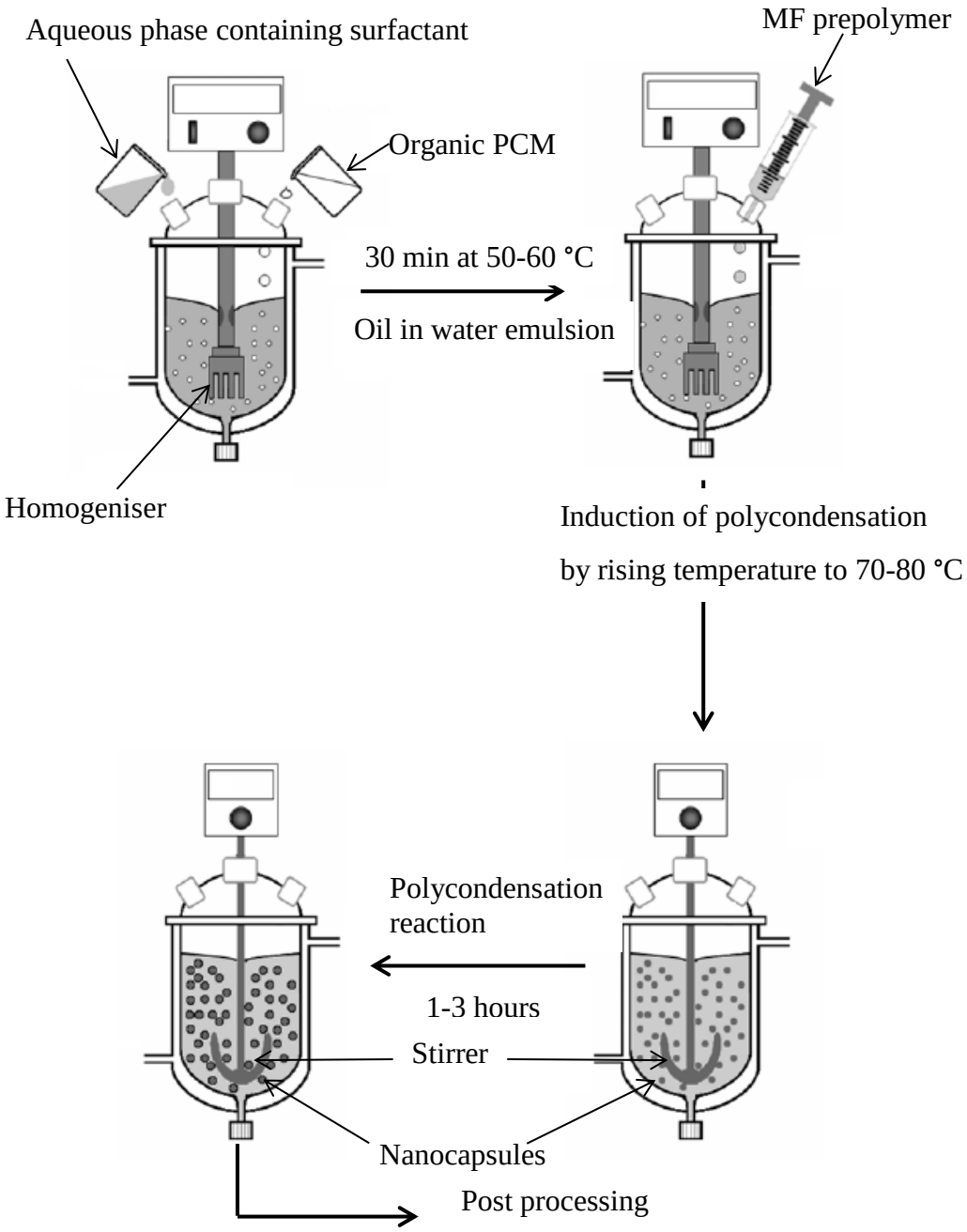

Figure 2.4 Schematic diagram of encapsulation process by *in-situ* polymerisation [66]

The study of literature shows that microencapsulation through melamine formaldehyde undergoes three consecutive stages [70]. The prepolymer is activated under acidic condition by protonation which results in the increase of ether linkages with decrease in hydroxyl group concentration. Due to decrease in the hydroxyl groups, the solubility of prepolymer decreases which results in the separation of material from the continuous phase in the form of relatively concentrated active prepolymer. In the second step the resinous prepolymer wets the core material droplets to form the primary wall around them. Due to the enhanced hydrophilic/lipophilic interactions, the concentration of resins around the wall is enhanced. The resin condensation at boundary phase proceeds much faster than the volume phase allowing a tough wall formation. It is possible to get the capsules in powder form from this step nevertheless the capsule wall is not yet thermally or mechanically stable but can collapse during drying and curing process. The final step precedes the Polycondensation reaction at the interface which results in the formation of thermo-mechanically stable capsule shell around the PCM.

Micro or nanocapsules using *in-situ* polymerisation produce high percentage yield. The shell of capsules prepared by melamine formaldehyde has better mechanical and thermal stability than those synthesised by other polymers [71]. The only disadvantage of this method is the presence of free-formaldehyde which may cause environmental and health problem. To solve the problem Li et al [72] proposed to increase the proportion of urea and melamine 3 times more than formaldehyde in prepolymer formation stage. Sumiga et al [69] suggested that the use of ammonia during the post processing of MPCM can decrease the formaldehyde content.

Emulsion/Solvent evaporation method

Preparation of capsules using solvent evaporation technique is widely used in the pharmaceutical industry. Different methods have been used in solvent evaporation technique for encapsulation and the choice of method depends on the hydrophilicity or hydrophobicity of the active ingredient to be encapsulated [73]. This method generally consists of four steps:

1) dissolution or dispersion of active ingredient in the organic solvent containing the polymer;
2) emulsification of this phase called dispersed phase in an aqueous phase called continuous phase;

3) extraction of solvent from dispersed phase accompanied by solvent evaporation forming droplets of dispersed phase into solid particles; and
4) post processing to get the solid capsules in powder form

However for extremely hydrophilic compounds, the aqueous phase is avoided due to the loss of active ingredients and the solid compounds are usually dispersed in solvents or polymer [74]. The reaction is preceded by addition polymerization usually initiated by an initiator. The schematic diagram of microencapsulation synthesis via solvent evaporation method is shown in Figure 2.5 [75]. In Figure 2.5 the active ingredient to be encapsulated is dispersed in organic solvent using ultrasonic homogeniser and then this dispersion together with a prepolymer dissolved in another solvent system are poured into a reaction flask. All the necessary chemicals to initiate the reaction are added in this stage. By gradual increase in temperature, solvent evaporates allowing the droplets to form into solid capsules. The obtained capsules are further filtered, washed and dried to get powder form of capsules.

In this method, solvent plays very important role which should have the following characteristics.

- be able to dissolve the polymer;
- has high volatility and low boiling point; and
- has low or no toxicity

Chloroform was an extensively used solvent in the synthesis of capsules before but now it is replaced by relatively low toxic solvent dichloromethane. Dichloromethane has low boiling point, high volatility and almost immiscible in water [74, 76, 77].

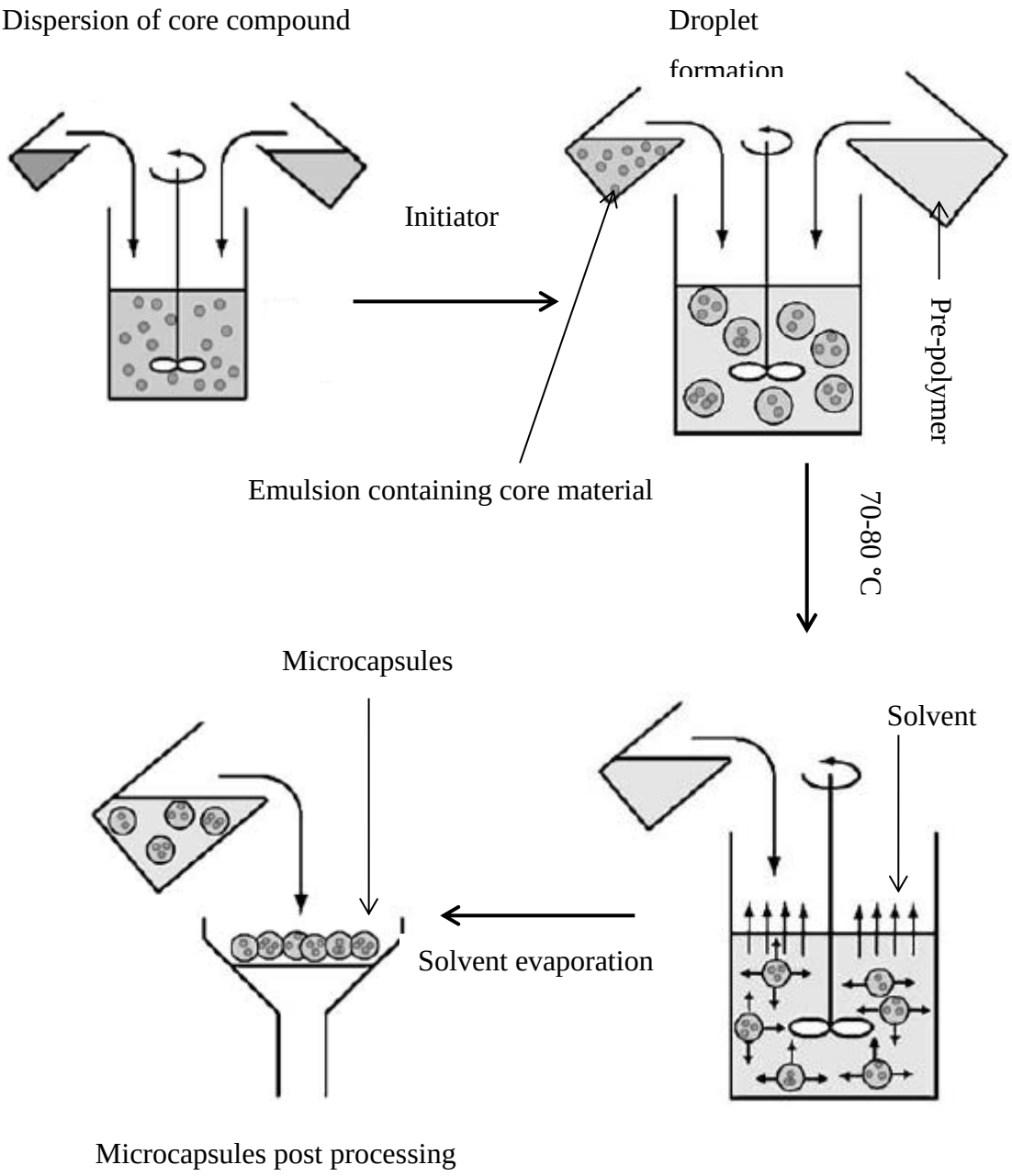

Figure 2.5 Emulsion/Solvent evaporation method [75]

2.3 **Textiles containing microencapsulated phase change materials**

There are five ways to produce thermoregulating textiles containing MPCM. The first method is called composite spinning in which PCM is directly mixed with melt spun or solvent spun polymers as core/sheath filament resembling sea-island structure [78]. This method gives the best thermoregulating effect because of the direct incorporation of pure phase change material in the core. However this method was not explored in the current research because of the facilities to do so were not available. The second method

is a hollow fibre spinning method in which hollow fibre is filled with PCM to make thermoregulating material [79]. The third method contains either melt spun or solvent spun incorporated with encapsulated PCM. This provides the PCM textiles with good chemical and thermal storage stability [80]. The fourth method is that MPCM are applied onto fabrics via coating or pad-dry-cure process with the help of binder to ensure the binding of capsules with fabric along with some ancillary chemicals. Different processes of coating like knife over air, knife over roll, dip coating and transfer coating are used to apply polymer matrix on textiles [11, 31]. The last method is the MPCM application through lamination process by thin polymer film or inner layer of fabric to make it thermo-physiologically comfortable. In some cases MPCM are applied on to fabrics by mixing with polyurethane foam through a lamination process. This foam has unique honeycomb structure which keeps air entrapped in it, making it insulating [81]. Two methods have been exploited in this research for the development of thermoregulating textiles; melt spinning technique to develop MPCM fibre and applying synthesised NPCM onto fabric through pad-dry-cure process.

2.3.1 *Incorporation of MPCM into fibre*

Microencapsulated phase change materials can be incorporated into fibre through conventional process. The microencapsulated phase change materials are first added to the fibre forming solution and extruded with conventional wet spinning and dry spinning or can be mixed with polymer prior to melt spinning to get thermoregulating melt spun filament yarn. Most of the work related to the incorporation of MPCM into fibre is patented and some literature is published about application via coating or pad-dry-cure techniques. Many researchers have tried to incorporate capsules containing phase change material into man-made fibres. In 1988, Bryant et al [82] succeeded in incorporating capsules containing eicosane as phase change material into viscose rayon and acrylic fibre by wet or dry spinning method and patented their work. These filament yarns gave thermo-regulating characteristics when subjected to heat and cold. Viscose rayon and acrylic successfully came into the market containing leak resistant capsules as shown in Figure 2.5 & 2.6 respectively.

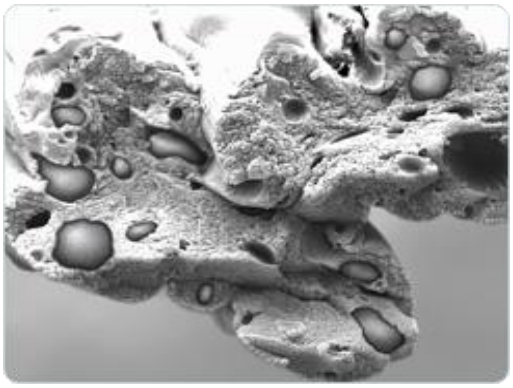

Figure 2.6: Viscose fibre (Outlast® Technologies) [83]

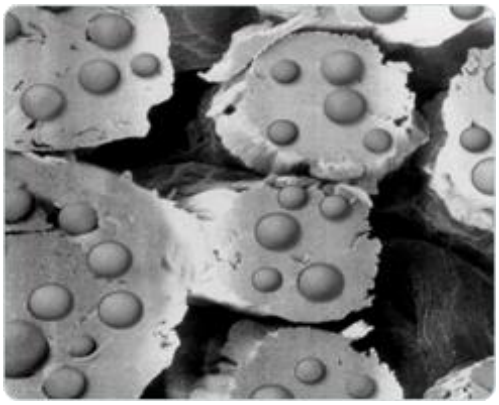

Figure 2.7: Acrylic fibre (Outlast® Technologies) [83]

Outlast Technologies assigned many projects to researchers to get fibre enhanced with reversible thermal properties. Hartman et al [23] developed viscose rayon fibre containing microencapsulated phase change materials and patented in 2010 which was the continuation of his previous work. The latent heat mentioned in his patent was from 1 J/g to 20 J/g in dependent of the different embodiments.

Zhang et al [84] in 2006 prepared flame retardant polyacrylonitrile-vinylidene chloride fibre through wet spinning containing n-octadecane as phase change material and urea-melamine-formaldehyde copolymer as shell. The amount of MCPM incorporated studied was 0-40% which explored the smooth spinning was up to 30%. The enthalpy of crystallization was determined by DSC from -20 to 320 °C with temperature gradient of 10 °C/min under nitrogen atmosphere showing 30 J/g and 44 J/g for fibre containing 30% and 40% of MPCM respectively. SEM result showed that the fibres which contain MPCM have rough surface, more density and cross sectional holes as compared to non-MPCM as shown in Figure 2.8.

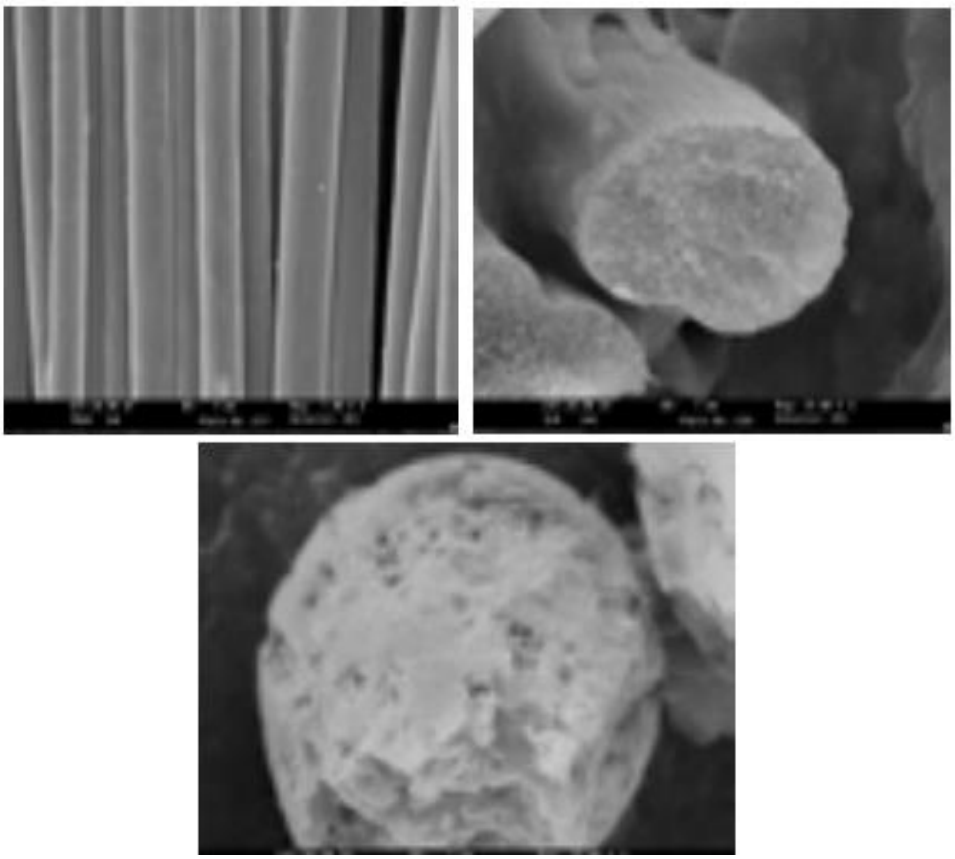

Figure 2.8: SEM images of PAN/VC fibre [84]

Incorporation of encapsulated phase change material into melt spun fibre is very problematic due to high temperature (200°C-380°C) and high pressure (3000 psi) used during the process. At such high temperature and pressure, normally phase change materials undergo thermally induced decomposition and oxidation. Factors affecting decomposition is temperature, pressure and duration of time during which phase change materials are exposed. This thermally induced decomposition leads to the formation of lower molecular products or isomers which not only reduce thermal regulatory properties but also impair melt spinning process [85].

Due to the thermal and shear stability, M/F capsules were used which cause some environmental issues during the preparation of capsules. Frank et al [86] published patent in 2001 about preparing M/F capsules through condensation process of melamine and formaldehyde and added urea as formaldehyde scavenger prior to curing of resin.

Later on, Li et al [87] manufactured MPCM using melamine-formaldehyde shell by putting aluminium chloride during the microencapsulation process to reduce the residual formaldehyde content. Outlast Technologies is anxiously waiting for melt spun thermoregulating fibre. Bryant [88] in his paper mentioned the problem related to melt

spinning filament yarns containing MPCM and suggested that the lower particle size preferably less than 10 µm are suitable for melt spinning filament yarns. Hartmann [85] prepared stabilised PCMs by mixing phase change materials with stabilizing agents consisting of thermal stabilisers and antioxidants that can be used in synthetic fibre manufacturing. The encapsulation of phase change material was done by incorporating PCM into hollow capsules containing phase change material alone or mixture of phase change material and stabilisers in the internal cavity and stabilizing agents in outer cavity.

In another patent Hartmann et al [89] mentioned the development of melt spinable concentrate pellets containing phase change materials either in microencapsulated form or non-encapsulated form absorbed into the carrier polymer. The polymer matrix was composed of one type of thermoplastic polymer or a combination of thermoplastic polymers. They claimed that these concrete pellets can be used with other thermoplastic polymers to form extrusion products including monofilament fibre but there was no filament made with such pellets.

In 2005, Magill et al [90] prepared a multi-component fibre containing phase change material by keeping the PCM in core and any thermoplastic or elastic fibre in the outer sheath using polyester, nylon, and many other polymers. They claimed in their patent that material contains 6.9 J/g and 8.4 J/g of latent heat in different embodiments of core/sheath yarn.

In 2009, Gao et al [91] prepared PAN containing MA (methyl acrylate) copolymer by melt spinning technique. The fibre was spun at 200°C containing 5-25% of MPCM. The enthalpies of crystallization of fibres containing 20% and 25% of MPCM were 21 J/g and 25 J/g respectively tested by DSC. The SEM analysis showed that the fibres containing MPCM are coarser while non-MPCM fibres are smooth and the fibres containing capsules contain micro-porous and defective structure as shown in Figure 2.9.

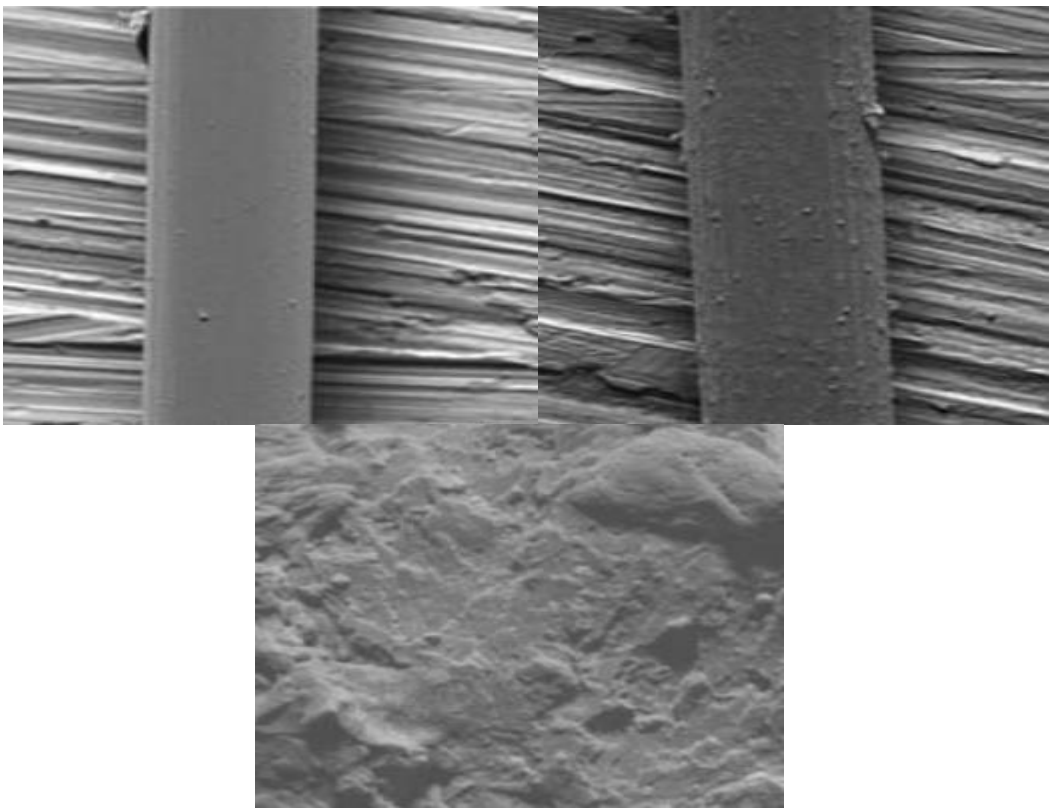

Figure 2.9: SEM images of PAN/MA fibre [91]

In 2010, Hagstrom [92] from Swerea IVF Sweden prepared core/sheath melt spun PA6 and PET fibre containing n-octadecane as phase change material in core as shown in Figure 2.10. It was found that to make a bicomponent fibre, PCM should be blended with viscosity modifier (e.g. HDPE) to make it close enough to the viscosity of sheath material. For suitable viscosity and high latent heat, 70% of PCM by weight is mixed in HDPE. Bicomponent yarns were successfully manufactured by different core/sheath ratios providing enthalpy of fusion up to 80 J/g.

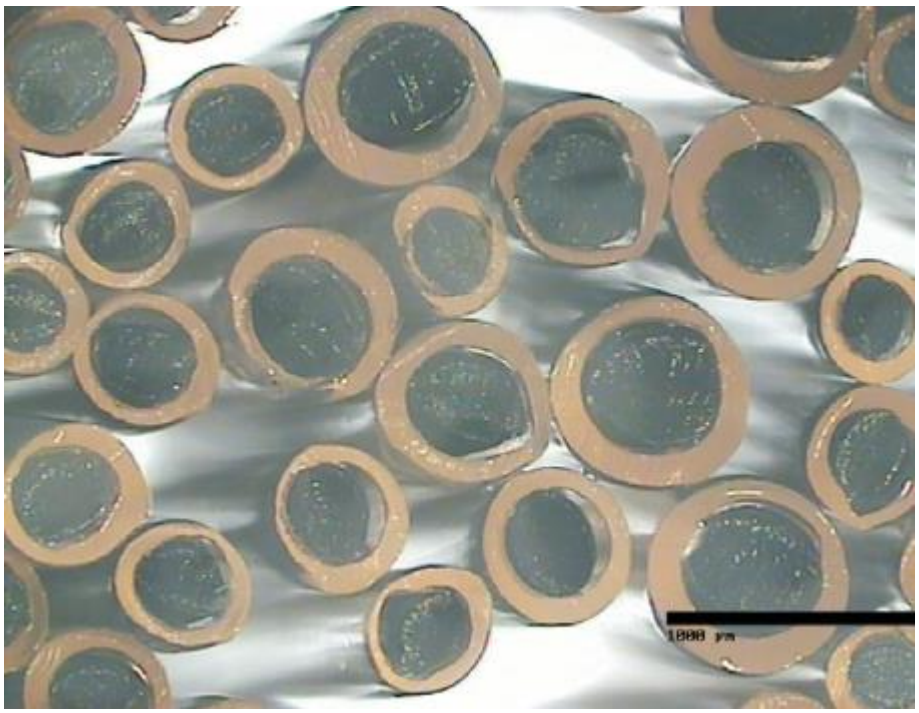

Figure 2.10: Melt spun fibre containing PCM in core [92]

Through extensive literature study the gap in the development of thermoplastic melt spinable filaments containing MPCM has been found and it is becoming a challenge for the researchers because of the stability of capsules during melt spinning process and the need of lower molecular size capsules. Melt spun monofilament and multifilament polypropylene yarns are developed in this research and will be discussed in chapter 4.

2.3.2 *Application of MPCM through pad-dry-cure*

Coating is an established field specially used in textiles for the purposes of high performance and technical textiles. The textiles made through coating process are used as water repellent, soil repellent, conductive and insulating textiles etc. In recent years, high performance sportswear that needs thermal insulation with water proof abilities has attracted the use of phase change materials through coating technique. However coating is not an appealing technique to the active smart textiles market where fabric breathability is the key characteristic to achieve. Hence discussion on coating does not fall in the scope of this research because the nanocapsules after synthesis were applied on cotton fabric via pad-dry-cure technique. Mostly researchers applied MPCM on textiles via coating and very little published work can be found in terms of applying MPCM on textile via pad-dry-cure technique.

In 2005, Shin et al [44] prepared M/F capsules containing eicosane by *in-situ* polymerization. The capsules were applied on polyester knitted fabric via pad-dry-cure method. MPCMs were bound with fabric using polyurethane binder and the amount of MPCM applied was 12.5, 25, 50 and 100% on weight of microcapsule slurry. The fabric was padded by two-dip-two-nip method and cured later at 130 °C for 10 min. The DSC analysis showed the latent heat of 0.91- 4.44 J/g depending upon the amount of MPCM used. Durability test showed that fabric retained 40% of its heat storage capacity after 5 launderings.

Later on Shin et al [93] extended their previous research and they applied MPCM on 100% knitted fabric of 197 gsm by pad-dry-cure method using polyurethane binder to study the thermal properties, air permeability, moisture vapour permeability, moisture regain and other mechanical properties of the MPCM fabrics. DSC results showed that as the percentage add-on increases, the amount of heat storage increases. Latent heat as 0.91 J/g, 2.15 J/g, 4.10 J/g and 4.44 J/g were determined against 5.3%, 11.1%, 18.1% and 22.9% of add-on respectively. Air permeability and moisture vapour permeability of the fabric containing 22.9% of MPCM decreased by 28% and 20% respectively. The moisture regain of fabric was increased by 22.8% with respect to the control fabric.

Khoddami et al [94] studied the effect of PEG (polyethylene glycol) as phase change material and the hydrophilic character on Polylactic Acid and PET fabric via conventional pad-dry-cure method. They used PEG along with DMDHEU (di-methylol di-hydroxy ethylene urea) to get PEG attached to fabric for durability purpose. Thermal analysis was done using DSC containing 5-6 mg of sample with heating rate of 10°C/min under nitrogen environment from -20 to 80°C. The maximum latent heat achieved was 43 J/g before washing.

2.4 **Fibre forming polymers and melt spinning technique**

A fibre is usually defined as the polymeric material which has length 100 times greater than its thickness while some of the fibres contain length thousand times more than the thickness. The general properties in textiles fibres which are desirable in synthetic fibres either individually or in combinations are as follows [95].

- Hydrophilicity or hydrophobicity
- Long chain and linear

- Capable of being oriented to impart strength
- Polymer system with high melting point
- Resistant to chemicals and microorganisms

Textile materials are generally classified into two main categories called natural and man-made fibres. The classification is shown in Figure 2.11 [96]. The man-made fibre synthesis began commercially in 1925 with the development of artificial silk called rayon. The type of polymer and process parameters involved in spinning process has great influence on the man-made or synthetic fibres [97]. Regenerated and synthetic fibre formation gives the option of blending and mixing of different polymers and incorporation of additive for high performance and smart applications. Melt spinning is the simplest and most economical technique of producing fibres [98, 99]. This process avoids the use of solvent and fibre solution forms through temperature and shear force acting on the polymer granules. The melt spun fibres have good temperature and chemical resistance and have higher specific strength than natural fibres [100]. The machine used to develop melt spun yarn is called extrusion machine and the working theory of extrusion machine is described in section 2.4.1.

2.4.1 *Extrusion Machine*

Polymers are fed to the extrusion machine either from the chemical reactor or in the form of chips and granules through hopper. Melt spinning machine simply can be defined by differentiating into the following processing parts: Polymer header, spin pack, quenches bath and winder. The schematic diagram of melt spinning is shown in Figure 2.11.

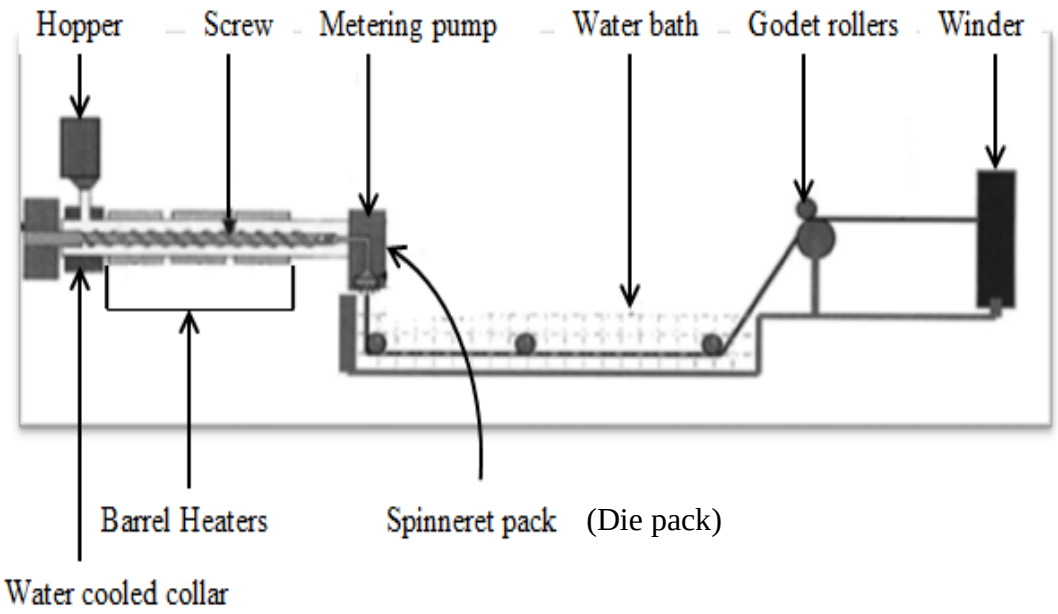

Figure 2.11 Melt spinning schematic diagram [101]

The polymer header transmits polymer to the metering pump which is heated by a jacket to keep the temperature uniform around the metering pump and this pump forces the melt through spinneret with tiny holes. The metering pump speed and the size of spinneret holes determine the filament denier. The extruder contains a screw which rotates in a heated barrel (cylinder) and pushes the material forward up to the die head (spinneret pack). The die head contains a die-pack which consists of a wire filter, a breaker plate (often called distributor), a copper seal and a spinneret [102].

Feeding zones

The screw in the barrel contains three zones: feed zone, compression zone and metering zone or melt zone as shown in Figure 2.12. The compression zone is also called transition zone because the polymer in this zone is in the phase of its glass transition. The length and the diameter of the screw are major factors which determine the volumetric capacity in transferring the temperature to the material from the heated barrel zones and by generating temperature from friction and shear with the walls of the barrel. Each extruder temperature zone has a heater which is controlled by individual thermocouple [103].

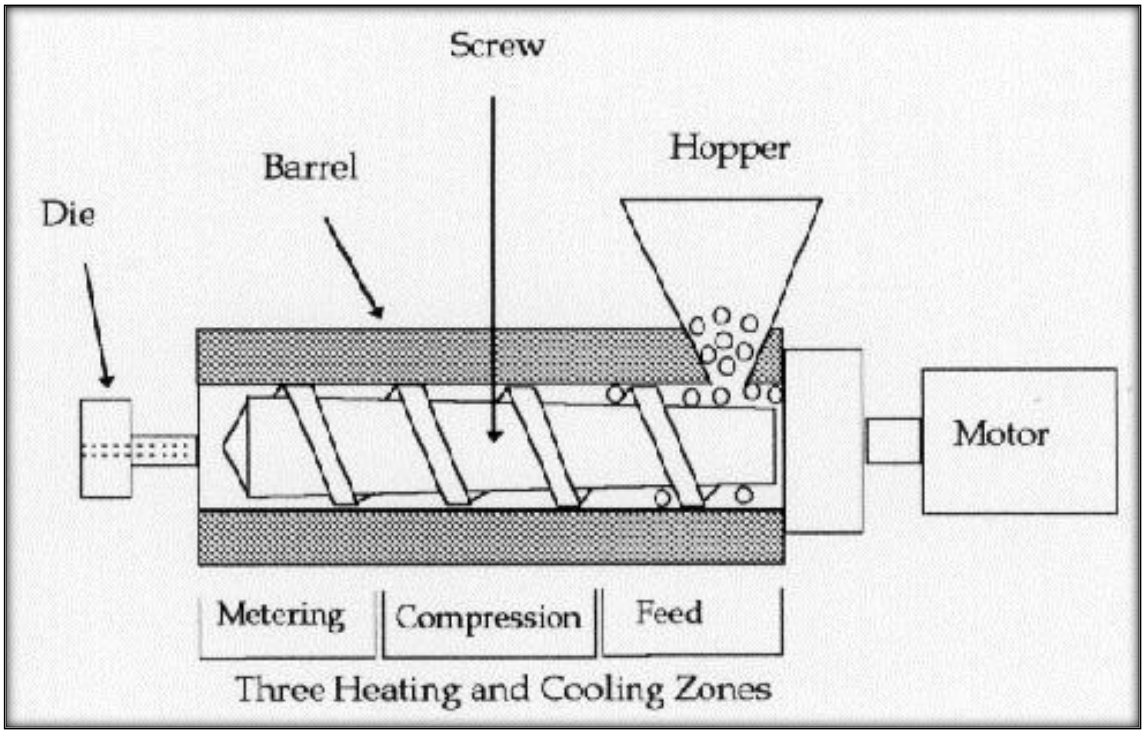

Figure 2.12 Heating zones of extruder [100]

The screw takes the material from hopper to the metering pump through heated barrel. The feeding zone is cooled with circulating water during the operation to facilitate the forward feeding of polymer granules and to prevent prior melting or sticking of the material to the feeding zone. Following the feeding zone the material is transferred to the compression zone which is the most critical area in the extruder because it helps drying of the material. In the compression zone the diameter of the rotating screw increases which facilitates the pushing of obstructed air in the material to the feeding zone and compacts the material [104]. The higher compression of the material in the compression zone gives more stable flow which is determined by the ratio of the space between barrel and screw root in the feeding zone to the space between barrel and screw root in the metering zone [105]. The third zone gives the material constant volume and pressure and passes the material to the die pack [106].

The material is heated by the hot barrel; the friction produced by material shear along the walls of the barrel is more than the friction between material and screw which helps in melting of the material. Decreasing the melt temperature leads to the increase in viscosity which increases the resistance to flow of material in the die and decreases leakage in the extruder [107]. The temperature rises due to friction can be controlled by the speed of the screw. By increasing the rotational screw speed, the shear force will be

increased while a low rotational speed can impair the homogeneity of the material affecting mixing of the material [108].

Figure 2.13 illustrates an example of screw design, the screw flight, flight land, screw root, flight lead including helix angle. Screw design not only controls the extrusion capacity but also determines the output of machines and controls the friction and shear applied to the material. A long screw gives better material heat transfer and larger length to diameter ratio for better consistency of the output [106].

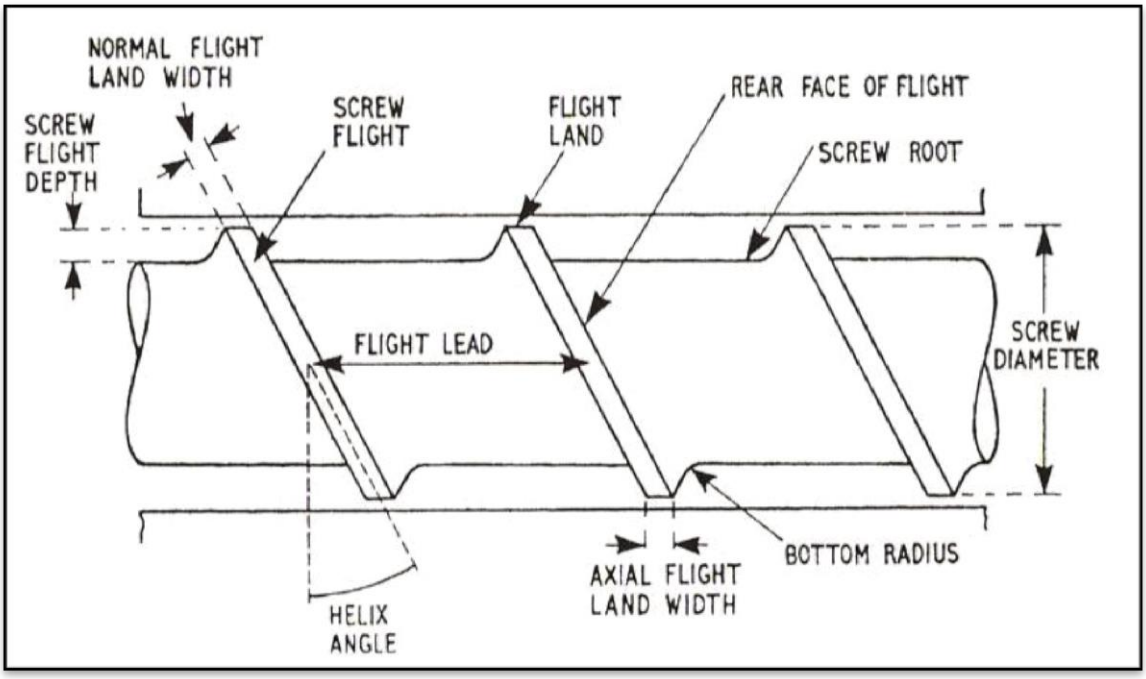

Figure 2.13 Screw design [100]

Some of the screws contain mixing head located just after the melt zone. The purpose of mixing head is to ensure the homogenous mixing of the polymer and sometimes additives to the polymers. Some types of mixing head are shown in Figure 2.14 [109].

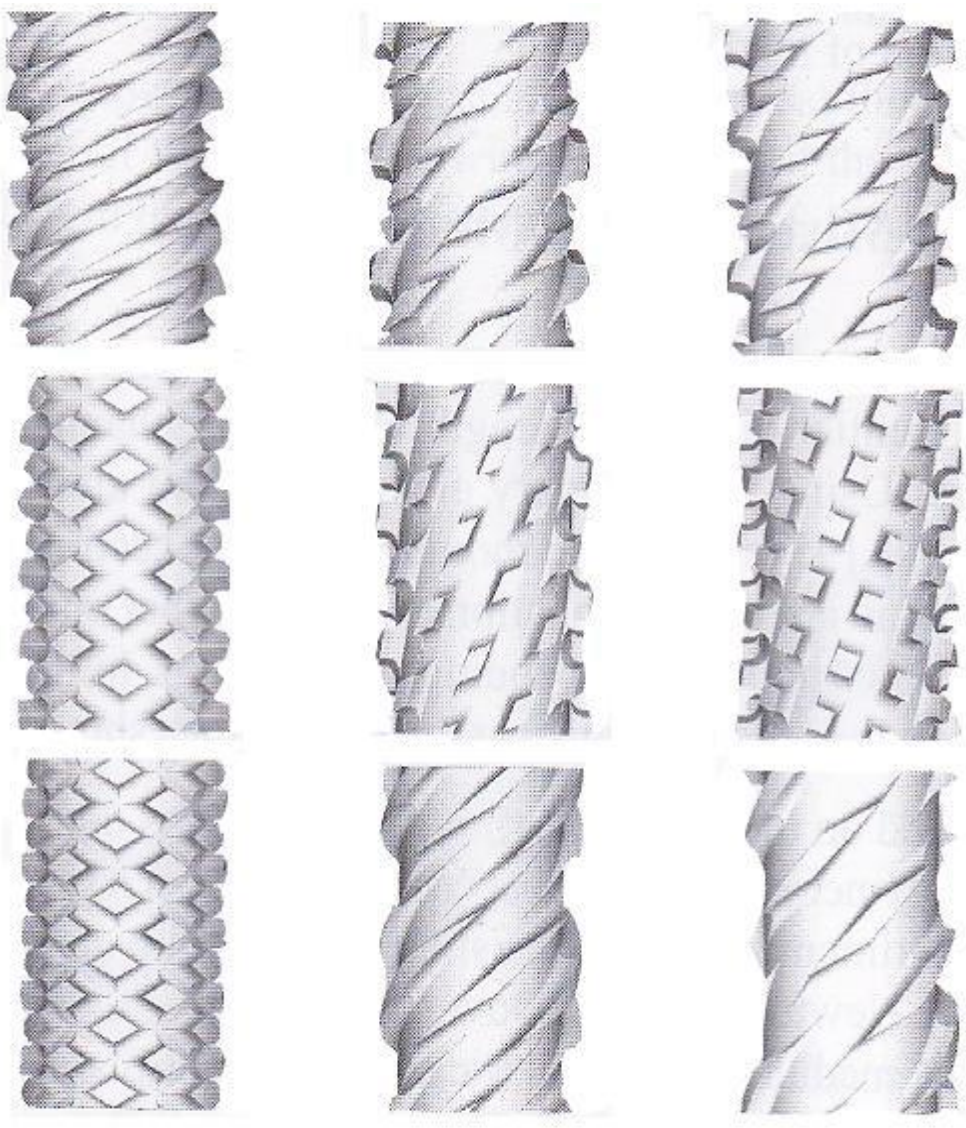

Figure 2.14 Types of screws used for extrusion [109]

Die assembly

Usually in extrusion machine a breaker plate (distributor) is used between the die assembly and barrel. The plate is thick metallic disc with narrowly spaced hole as shown in Figure 2.15. The main function of plate is to break the rotation flow of melt and convert it into straight path and build a die head pressure by mixing and distributing the material for consistent polymer melt flow. A woven wire filter is used in the pack to avoid any impurity, contamination and unplasticised material. The breaker plate also supports filter to sustain heavy extrude pressure and it also improves the heat transfer to the polymer melt by reducing the distance between die pack and metering channel eventually enhancing thermal homogeneity. The final part of the die pack is spinneret die which is the most important part and determines the polymer filament cross

sectional shape. Most of the times the die holes are circular but can adopt another shape according to the cross section of filament required. A die can be monofilament or multifilament according to the number of holes present in the die [110, 111].

Figure 2.15 Distributor for melt solution

The spinneret consists of large number of fine holes and the number of filaments is determined by the number of holes present in the spinneret. The filament takes the shape of the hole. The funnel shape entrance of the spinneret prevents the dead volume in the polymer path [112]. The spin finish is applied on the filaments during winding to impart proper friction and adherence and to avoid electrostatic charge during processing which can damage the fibre [113, 114].

2.4.2 *Fibre morphology in extrusion*

The fibre characteristics depend mainly on the structure morphology which is determined by the length, width, cross section shape and chemical composition of the polymers. Theoretically individual chemical units covalently bonded make the assembly of macromolecules which constitute the polymer fibre. There are three types of polymers as a result of fibre extrusion: homopolymers, copolymers and block polymers. The most common type is the homopolymers in which one molecular chain repeats itself to form the polymer. The copolymer consists of two or more types of monomers to constitute a polymer while in block polymers the block of homopolymers are repeated to form the polymeric chain. The fibre consists of two regions called crystalline region in which polymeric chains are closely packed and the amorphous region where polymeric chains are further apart. The degree of polymerisation is defined by how many times a monomer are repeated in the polymer chain. The fibres

containing high degree of polymerisation are stronger and require more force to break or elongate [115].

After the filaments leave the spinneret, it passes through the spin line which includes the control of extrusion temperature, take-up speed and medium of quenching. The filament undergoes stress by increasing the wind-up speed. The stress decreases with the increase of melt flow index while the draw and tension can be controlled by adjusting the speed of winder [107]. The orientation of fibre depends upon the temperature and the cooling rate while the cooling rate defines the amount of crystallinity in the polymeric structure [116]. The cooling must be done slowly to improve the crystallinity and crystal size in the fibre [117]. The high take-up speed is responsible for the uniaxial orientation of the polymeric chains within the fibre. The orientation can be increased by increasing the ratio between the take-up speed and extrusion speed but a mechanical drawing processes is needed to complete the orientation process [118].

The next critical part in the melt spinning processing is the fibre drawing which enhances the strength of the fibre and prevents unnecessary elongation in the subsequent use. The drawing process increases the orientation of the fibre improving the degree of crystallinity along the fibre axis, hence the strength of the fibre [119].

2.4.3 *Fibre Drawing*

Drawing is a process in which filament is stretched under tension to assign permanent deformation. If the drawing is done at a temperature near the glass transition temperature of the polymer then it is called hot drawing. As a result of stretching, the molecular chains slip over each other and become parallel along the fibre axis which improves the tenacity and modulus. The orientation phenomenon is shown is Figure 2.16.

Figure 2.16 Fibre orientation

During the extrusion process, the orientation occurs on the outer surface of the filament influenced by the edges of the spinneret hole which is called skin effect [120]. However the complete orientation of molecular chains is always achieved in drawing process but the crystallinity may either increase or decrease depending upon the drawing condition and the polymer involved. The following types of trend can occur [120, 121].

- The drawing process does not affect the proportionality of crystalline and amorphous region.
- Partial deformation occurs which can result in the decrease of crystallinity.
- Increase in orientation of the polymeric chains in drawing results in the increase of crystallinity.

The first effect occurs where polymer chains tend to become oriented in the amorphous region which does not lead to any crystalline formation. This trend is also seen in wet cellulose fibre where no changes occur in the crystalline region but some disruption occurs in amorphous or partially crystalline region as a result of swelling [122]. The second type of trend is observed where cold drawing is involved which results in the substandard crystalline structure. The degree of crystallisation decreases at lower temperature and plastic distortion occurs during the drawing process [123-125]. In the third trend, the molecular chain orientation increases by hot drawing process. The increased temperature assists in modifying the crystalline region with high draw ratio resulting in an increased degree of crystallization [126].

2.4.4 *Polypropylene*

Polypropylene can be polymerised in three stereo-isomeric forms; atactic, syndiotactic and isotactic as shown in Figure 2.17. In atactic form of polypropylene, the methyl groups are attached randomly around the main chain of polymer. In syndiotactic, the methyl groups are attached alternatively on the both side of polymeric chain while in isotactic, the methyl groups are attached on the same side of the main chain.

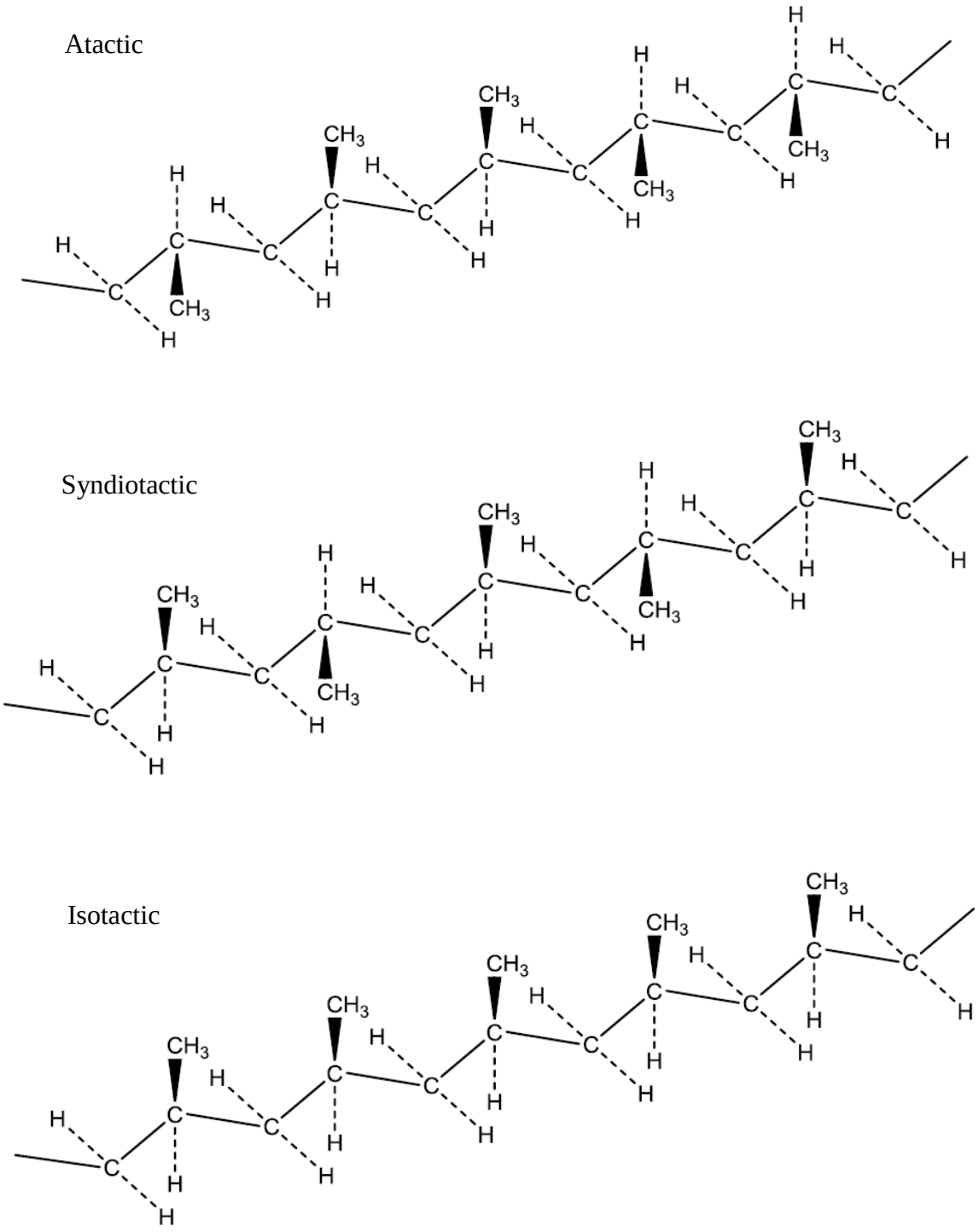

Figure 2.17 Stereo-isomers of polypropylene

The syndiotactic and isotactic have regular pattern and are crystalline while atactic is amorphous in nature. Complete syndiotactic and isotactic forms are not available and they are usually found with mixing of atactic. Isotactic in the crystalline region show helical conformation with either clock wise or anti-clock wise twist as shown in Figure 2.18. This stereo-isomeric form is considered as most favourable because the helical

conformation provides a balance between inter atomic repulsive force and vander Waals forces between methyl groups [127].

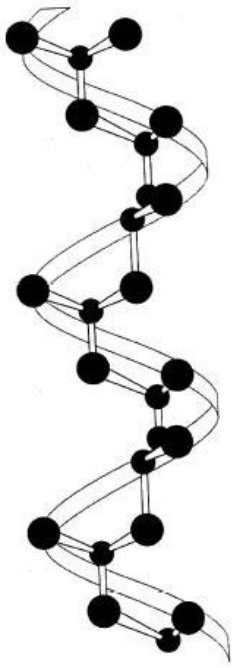

Figure 2.18 Helical arrangement of isotactic polypropylene [109]

2.4.5 *Polymerisation of polypropylene*

Polypropylene is made of propylene monomer which is obtained by cracking of petroleum products. Propylene is the basic ingredient in the C3 fraction and can be easily separated by fractional distillation. Polypropylene properties rely on the catalyst system used which is prepared by the reaction of titanium chloride with aluminium alkyl such as triethyl aluminium with naphtha under the nitrogen environment. This catalyst is called Ziegler-Natta catalyst.

Suspension polymerization was the first commercial method adopted for the polymerisation of polypropylene in which monomer is taken up in the pressure vessel and all the additives such as catalyst and naphtha are added separately as diluent. The reaction is completed at 60 °C, which is lower than the melting point of polymer, after 1- 4 hours and suspension is formed. The molecular weight of polymer can be controlled by chain transfer reaction with hydrogen using specific composition of catalyst, temperature and pressure in the vessel. After the polymerization reaction, atactic and isotactic polypropylene, solvent and catalyst are present in the reactor. The solvent along with atactic polymer (which is soluble in the solvent) are removed by centrifugation. The catalyst and residues are removed by dissolving them in methanol

solvent along with traces of hydrochloric acid. The polymer solution is then centrifuged, washed and dried at 80 °C [128].

Liquid and gas phase methods are also used which avoid the washing process and does not include the separation of residual impurities like catalyst, solvent and atactic polymer. This is also produced using metallocene catalyst in which the reaction is preceded under gas phase using methylaluminoxane catalyst. In this process a hemi-isotactic polypropylene is developed in which the isotactic units are configured alternatively. Using metallocene, copolymerization of polypropylene with cyclic and aliphatic olefin is also possible [128].

2.4.6 *Chemical reaction of polypropylene*

The synthesis of polypropylene involves free radical polymerization which is the most common type of addition polymerization. The addition of monomers takes place around the double bond of propylene in addition polymerization reaction as shown in Figure 2.19.

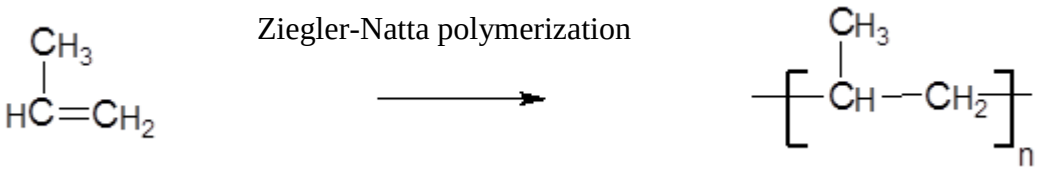

Figure 2.19 Polymerization of propylene

The free radical is usually a molecule with an unpaired electron which has tendency to gain an electron to complete its pair and thus is very reactive in such a way that it breaks the bond of another molecule (usually monomer) and steals an electron leading to molecule or monomer with unpaired electron which is another free radical. This newly formed free radical attacks another monomer and hence the process is repeated to grow a chain of polymer as shown in Figure 2.20. This stage is called propagation stage where a long chain polymer is formed.

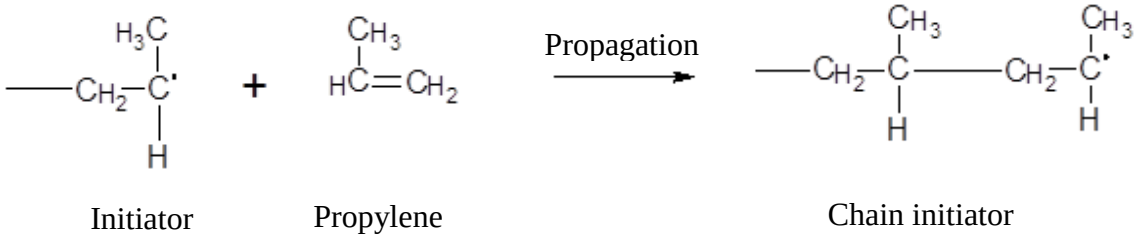

Figure 2.20 Reaction mechanism of polypropylene: Propagation

The propagation stops theoretically when the supply of monomer is exhausted and reaction stops. This step is called termination step as shown in Figure 2.21 in which two growing chains join together to form a single chain. R in this figure denotes the long chain hydrocarbons grown on both sides.

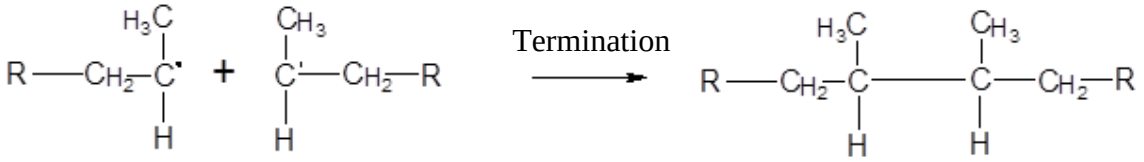

Figure 2.21 Reaction mechanism of polypropylene: Termination

2.4.7 *Properties of polypropylene*

The degree of crystallinity of polypropylene depends upon its stereo isomeric form. Atactic polypropylene is totally amorphous while isotactic is 100% crystalline. Commercially available polypropylene contains 60% to 70% of crystalline region and most filaments are smooth in surface and have waxy appearance. The tenacity of polypropylene filaments is normally 3-5 g/denier which can go up to 12 g/den in case of high tenacity yarn which is made of highly isotactic polymer [129]. The elastic properties of polypropylene depend on the type of polymer and processing conditions. For high tenacity polypropylene, the immediate recovery is 90% after 10% elongation.

The specific gravity of polypropylene is relatively lower among fibres as 0.85, 0.90-0.91 and 0.92-0.94 for amorphous polypropylene, commercial polypropylene and highly crystalline polypropylene respectively. Polypropylene is chemically hydrocarbon which does not absorb water at all and is considered as hydrophobic fibre. Water and steam does not affect the tensile properties of polypropylene fibre or yarn. Its softening

temperature is around 140-150 °C and melting temperature around 160-170 °C. The shrinkage of polypropylene depends upon the finishing process but if the polypropylene is kept in boiling water for 20 minutes, the monofilament can shrink up to 15-20% while multifilament and staple yarn can shrink up to 0-10%.

Polypropylene is a highly chemical resistant fibre. Acids and alkalis do not degrade polypropylene and organic solvents cannot solubilise polypropylene at room temperature. Polypropylene cannot be digested by insects and pests. The micro-organism such as bacteria and fungi do not affect polypropylene. Polypropylene has high electrical insulating properties and its electrical insulation remains constant even at high humidity level because of its hydrophobic character [109, 120].

2.4.8 *Polypropylene in active clothing*

Polypropylene fibre is becoming more and more important among the class of thermoplastic fibres because of its physical and chemical characteristics. Polypropylene fibre and filaments are widely used in ropes, cords, nets, woven bags, tents, upholstery and geotextiles [130]. Due to its excellent wicking properties and hydrophobicity it has attained the attention of researchers to use in active sportswear where thermal and physiological comfort is the key requirement [131]. The wicking properties can be enhanced by different means including modifying the cross sectional shape of filaments to provide wicking channel but inherently it depends on the degree of hydrophobicity which does not let the water to spread or absorb within the filaments. Polypropylene has the advantage on other fibres of providing insulation during wetting while the perspiration is transported away from the skin without being absorbed which makes this fibre ideal to be used in comfort clothing. Polypropylene is claimed to have good thermal properties owing to its low thermal conductivity and excellent hydrophobic nature and keeps the wearer cold in warm weather and warmer in cold weather [132].

The main requirements for comfortable clothing and active sportswear are light weight, thermal insulation, wicking and quick drying. Polypropylene is light weight and reusable material and is the best choice as comfortable clothing material as compared to other nature and synthetic fibres as it is 34% lighter than polyester and 20% lighter than nylon and its thermal conductivity is even lower than wool. The moisture transportation and wicking properties are even better than polyester because of its excellent hydrophobic nature [131-134]. Moreover it has excellent resistant to acids, alkali, bleaches, solvents and has good abrasion resistance and flexibility [135].

Babu et al [136] studied the moisture management properties of double layer knitted fabric made of cotton/polypropylene by varying the linear densities of cotton and polypropylene yarns. They reported that finer polypropylene yarn in the inner side of fabric has least spread area and transfers water quickly to the next layer. Lokhande et al [137] studied the moisture and wicking properties of bi-layered knitted fabric by combination of different hydrophilic and hydrophobic fibre. They found polypropylene was responsible for the best wicking and thermal properties. Abreu et al [138] investigated thermal comfort of three fabrics made of cotton, nylon, polyester and polypropylene in different combinations. It was found that fabric containing polypropylene possessed best thermal properties because of its highest thermal insulation.

It can be concluded that polypropylene is the fibre material which has good thermal and moisture management properties suitable for comfort clothes and sportswear. When wicking takes place in winter, wearer feels colder in that situation. While in summer, outdoor activity can increase the temperature of body which needs to be dissipated elsewhere. Thermal management solution is necessary to provide overall comfort to the wearer. There is no research reporting polypropylene based fibre materials to provide overall clothing comfort. This research will fill this gap to provide polypropylene fibre thermoregulating effect by incorporating MPCM through melt spinning technique. The incorporation of MPCM in polypropylene may also provide better wicking performance due to the rough surface of the filaments but this research only focuses on the thermal management solution.

2.5 **Modelling and simulation**

2.5.1 ***Geometric model of woven fabric***

Physical, chemical and thermal properties of fabrics depend upon the material properties and the structural properties of fabrics. Realistic geometric model plays very important role in the prediction of the properties of woven fabrics.

The first attempt to explain the geometric model of woven fabric was made by Peirce in 1937 [139] by considering yarn cross section as circular and yarn as absolutely flexible and incompressible. The woven geometric model explained by Peirce is shown in Figure 2.22 in which yarn path is defined by tangent line and arcs at cross over points. The limitation in this model is that the yarn is usually not circular especially in woven

fabrics and is flattened due to the sufficient pressure or forces acted upon during weaving process. Peirce later on presented modified model with elliptical yarn and replaced the circular cross section of yarn from his previous woven fabric model.

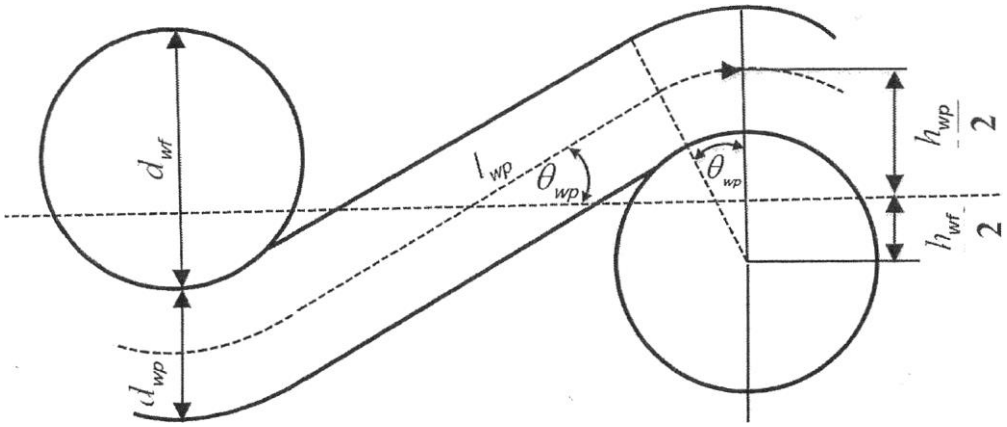

Figure 2.22 Peirce geometric model of woven fabric [140]

d_{wp} : diameter of warp yarn; d_{wf} : diameter of weft yarn; Θ_{wp}: maximum angle of the warp axis to plane of cloth in radians; Θ_{wf} : maximum angle of the weft axis to plane of the cloth in radians; h_{wp} : warp crimp height; h_{wf} : weft crimp height; l_{wp}: length of the warp axis between planes containing the consecutive cross threads; l_{wf} : length of the weft axis between planes containing the consecutive cross threads.

Kemp in 1958 [141] modified Peirce model by replacing circular or elliptical cross section of yarn by racetrack cross sectional shape which is composed of rectangle with two semicircle of each side as shown in Figure 2.23. The limitation of this model is that the yarn in woven fabric is, most of the times, flattened therefore racetrack model does not simulate actual yarn cross section. Later on in 1978, Shannan and Hearle [139] proposed a woven geometric model with lenticular cross section shape of a yarn as shown in Figure 2.24 which gave more realistic yarn geometry where flattened cross section is required.

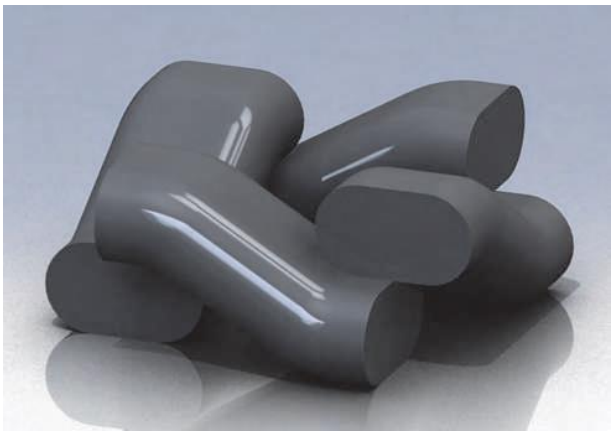

Figure 2.23 3D representation of Kemp's woven geometric model [141]

Figure 2.24 lenticular cross section

Lin and Newton [142] developed a method to define the yarn path in three dimensional plain woven fabrics using cubic B-spline curves. They assumed the cross section of yarn as circular. Hofstee et al [143] proposed a three dimensional woven geometric using fibre bundles through the yarn cross section and assumed that the relative location and packing fraction of fibre within the yarn was constant throughout the cross section.

Gong et al [144] developed realistic yarn model based on new algorithms from the real fabric images using synchrotron technique. They analysed and traced the yarn image using ImagePro and converted the line into coordinate by Matlab. In their research they found that the elliptical shape fitting was more suitable in case of cotton yarn and more significantly, the yarn cross sectional shape was variable along the yarn path.

However fabric geometry is very complicated and the measurement of geometric parameters is a difficult task. The consideration of yarn cross section in a woven geometric model is difficult because it depends on many factors such as twist per inch in yarn, the forces induced during weaving process and sometimes the inaccuracy of measuring yarn parameters. Even one factor can lead to different cross section e.g. high twisted yarn is more resistant to force which flatten yarn and less twisted yarn can be flatten up to single fibre thickness.

The geometric model in this research is developed using TexGen which is general public licensed software and developed at the University of Nottingham by Textile Composite Research group. The geometric model of woven fabric can be generated in TexGen using parameters such as yarn height and width of the cross section, yarn spacing and fabric thickness.

2.5.2 *Finite element method*

The finite element method is the numerical method of solving the problems of engineering and mathematical physics involving the areas of structural analysis, heat transfer, fluid flow, mass transport and electromagnetic potentials. In engineering problems, where complicated geometries, material properties and loadings are involved,

it is not possible to obtain the solutions using analytical mathematical expressions in which ordinary and differential equations are used for the solutions. Hence engineers rely on numerical method such as finite element method which uses the system of algebraic equations for solution rather than differential equations. The advantages of this method over other methods are the accurate representation of complex geometry, inclusion of dissimilar properties and easy representation of the total solution. This numerical method yields approximate values of unknown variables at discrete number of points by dividing a body into equivalent system of smaller bodies called finite elements interconnected with each other by nodes and this process of division is called discretization [145].

General steps of finite element method

Finite element method involves the modelling of structures containing finite elements connected through boundary lines or surfaces and nodes, and a displacement function or temperature function is associated with each element in case of stress analysis or heat transfer analysis respectively. The general steps involved for finite element analysis were described in details by Logan [145] and are presented below from step 1 to 6.

Step 1, involves the discretising of model and selecting the element type. The selection of appropriate element type and size are made. The elements should be small enough to produce useful and accurate results yet should be a compromise with the computational cost. The choice of the appropriate element type for a particular problem is one of the major tasks which should be carried out. In some cases, the model geometry restricts the selection of element type and suggestion is made by computational software. For three dimensional problems usually tetrahedral and hexahedral element types are used. Tetrahedral type of element as shown in Figure 2.25 is mostly used in textiles because this shape fits best to lenticular and elliptical yarns and spherical capsules.

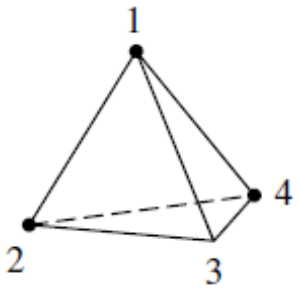

Figure 2.25 Tetrahedral elements used for 3D problems

In step 2, displacement or temperature function within the element is selected which is defined using the nodal values of the element. Linear and quadratic are most commonly used functions in finite element formulation.

In step 3, heat transfer equations are derived for heat transfer finite element analysis. Heat transfer based on conduction follows the Fourier's law of heat conduction. According to the conservation of energy:

$$E_{in} + E_{generated} = \Delta U + E_{out} \tag{2.1}$$

$$q_x A dt + Q A dx dt = \Delta U + q_{x+dx} A dt \tag{2.2}$$

where E_{in} is the energy entering the body in joules (J) or kW,

ΔU is the change in stored energy in kW.h,

q_x is the heat flux at surface edge x conducted into the body in kW/m^2,

q_{x+dx} is the heat flux at surface edge $x + dx$ out of the body,

t is time in h,

Q is the internal heat source (heat generated per unit time per unit volume) in kW/m^3, and

A is the cross sectional area in m^2.

Fourier's law of heat conduction is:

$$q_x = -K_x \frac{dT}{dx} \tag{2.3}$$

where, k_x is the thermal conductivity in x direction in kW/m.°C,

T is the temperature in °C, and

dT/dx is the temperature gradient in °C/m.

In equation 2.3 minus sign is presented by convention which indicates that heat flow is positive in the direction opposite to the direction of temperature increase. Therefore equation 2.3 can be written in the form of gradient as:

$$q_{x+dx} = -K_x \frac{dT}{dx}\Big|_{x+dx} \tag{2.4}$$

Any general function *f(x)* according to Taylor's expansion can be expressed as

$$f_{x+dx} = f_x + \frac{df}{dx}dx + \frac{d^2f}{dx^2}\frac{dx^2}{2} + \cdots \tag{2.5}$$

Using first two terms of Taylor series, equation 2.4 becomes

$$q_{x+dx} = -\left[K_x \frac{dT}{dx} + \frac{d}{dx}\left(K_x \frac{dT}{dx}\right)dx\right] \tag{2.6}$$

The change of stored energy can be expressed by:

ΔU = density x specific heat x temperature change

$$= c(\rho A dx)dT \tag{2.7}$$

where c is the specific heat in kWh/kg°C and ρ is the density in kg/m3. Substituting equations 2.3, 2.6 and 2.7 into equation 2.2 and simplifying, the heat conduction can be expressed as:

$$\frac{\partial}{\partial x}\left(K_x \frac{\partial T}{\partial x}\right) + Q = \rho c \frac{\partial T}{\partial t} \tag{2.8}$$

For steady state problem the differentiation with respect to time is zero, so Eq. 2.8 becomes:

$$\frac{d}{dx}\left(K_x \frac{dT}{dx}\right) + Q = 0 \tag{2.9}$$

In step 4, stiffness matrix and related equations are derived. There are different methods used to derive the stiffness matrix which depend on the type of analysis used. In heat transfer analysis usually Galerkin's method is used to derive the equations to solve the behaviour of elements and these equations are expressed in the form of matrix as mentioned in Eq. 2.10.

$$\begin{Bmatrix} f_1 \\ f_2 \\ f_3 \\ . \\ . \\ f_n \end{Bmatrix} = \begin{bmatrix} K_{11} & K_{12} & K_{13} & \dots & K_{1n} \\ K_{21} & K_{22} & K_{23} & \dots & K_{2n} \\ K_{31} & K_{32} & K_{33} & \dots & K_{3n} \\ . & & & & . \\ . & & & & . \\ K_{n1} & K_{n2} & K_{n3} & \dots & K_{nn} \end{bmatrix} \begin{Bmatrix} t_1 \\ t_2 \\ t_3 \\ . \\ . \\ t_n \end{Bmatrix} \tag{2.10}$$

Equation 2.10 can be expressed in compact form:

$$\{f\} = [K]\{t\} \tag{2.11}$$

where *f* is heat flux or heat source, *K* is the element stiffness matrix and *t* is the unknown nodal temperature of element.

Step 5 involves the assembly of element equations to get the global nodal equilibrium equations and applying boundary conditions. After final assembly the global equation can be written in the form shown below.

$$\{F\} = [K]\{t\} \tag{2.12}$$

where *F* is the total heat flux, *K* is the global stiffness matrix and *t* is the total unknown nodal values.

Step 6 involves the solution of equations to get unknown nodal values and interpret the results. Post processing in computational software can be used for detailed analysis and further prediction of some of the characteristics.

2.5.3 ***Simulation of textiles containing PCM***

The main objectives for the incorporation of PCMs in textiles are to get thermal insulation and comfort properties. PCMs possess the ability to change their state from solid to liquid or vice versa within a certain temperature range. The PCMs absorb energy during the heating process as phase change occurs and the same amount of energy is being transferred to the wearer or environment during reverse cooling process [146].

Heat transfer analysis on textiles containing PCMs has been investigated by different researchers. Lamb et al [147] determined heat loss through fabrics by ventilation with and without phase change additives. They claimed that incorporation of PCMs at the proper location of layered garment can significantly enhance the insulating properties of fabrics. Pause [22] in 1995 investigated the development of heat and cold insulating membrane structures containing PCMs and claimed the substantial improvement in the thermal insulation of the material. But in their investigation, there was no numerical simulation. Nuckols[148] established an analytical model for diver dry suit with comfortemp® foams containing MPCM and studied the thermal performance of fabric. He concluded that microencapsulated octadecane gave better thermal protection against microencapsulated hexadecane due to higher melting temperature than hexadecane. Shim et al [149] quantified the effect of PCM in clothing to investigate the thermal performance of fabric. They claimed that heating and cooling effect could last for 15 minutes depending on the number of PCM garment layers and combination of garments. Junghye et al [150] developed thermostatic fabrics treated with microcapsules containing n-octadecane and compared the thermal storage/release properties with untreated fabric.

In 2004 Ghali et al [151] experimentally and numerically investigated the effect of PCM on clothing during periodic ventilation. They claimed that heating effect could last for approximately 12.5 minutes in fabric treated with MPCM depending on the amount of MPCM and outdoor temperature conditions. Li and Zhu [152] developed a mathematical model of coupled heat and moisture transfer with PCMs and simulated the thermal buffering effect of PCM in fabrics. They numerically computed the temperature distribution and moisture concentration in porous textiles with and without PCM and validated their model with experimental results. Fengzhi et al [153] developed a mathematical model of heat and moisture transfer in hygroscopic textiles containing microencapsulated PCMs. They further used the model to investigate the effect of fibre hygroscopicity on heat and moisture transfer properties of textile with MicroPCMs. They claimed on the basis of results from their proposed model that fibre hygroscopicity not only has influence on the distribution of water vapour concentration in the fabrics and water content in fibres but also on the effect of MPCM in delaying fabric temperature variation during environment transient periods.

In 2009, Fengzhi [154] did numerical simulation work to investigate the effect of MPCM distribution on heat and moisture transfer in porous textile materials and

claimed that the total heat loss from body is the lowest when PCMs are located in the outer layer of fabrics. Ying et al [155] used finite difference volume method to numerically simulate the heat and moisture transfer characteristics on multilayer PCM incorporated textile assemblies. Bendkowska et al [24] studied the thermoregulating behaviour of nonwoven incorporated with MPCM and determined the amount of latent heat per unit area of nonwoven fabrics. They reported that distribution of MPCM in fibrous substrate and position of PCMs layer in garments has significant effect on thermoregulating behaviour of the garments. Alay et al [156] studied the thermal conductivity and thermal resistance of fabrics containing MPCM under steady state conditions. Yoo et al [157] studied the effects of the number and position of fabric layers coated with nanosilver nonadecane PCM in the influence of thermoregulating properties of a four layer garment. They used Human-Clothing-Environment simulator for the evaluation of temperature changes in the air layers of microclimate within clothing. Their research showed that outer layer containing PCM in garment assembly gives good thermoregulating properties.

In 2013, Hu et al [158] developed a mathematical model based on finite difference technique to investigate the heat flow in protective clothing embedded with PCM for fire fighters. They simulated the temperature variation by comparing different thickness and position conditions of PCM in protective clothing as well as melting phase of the PCM in protective clothing for firefighters using one dimensional mathematical model. More recently Siddiqui and Sun [159] investigated thermal conductivity of MPCM coated woven fabrics made of cotton, wool and Nomex® using finite element method. They evaluated thermal conductivity of fabrics in two steps by generating the two separate unit cell models for coating portion only and the coated composite fabrics.

The finite element heat transfer analysis on PCM textiles has been reported in literature using PCM as a composite coated layer on fabric substrates mentioned above. No theoretical research work has yet been reported in the effect of heat transfer behaviour of yarns and fabrics incorporated with MPCM and how to inform the yarn and fabric engineering in practice. The aim of the FE modelling and simulation in this thesis is to investigate the heat transfer properties of woven fabric constructed by multifilament polypropylene yarn incorporated with MPCM developed through an extrusion process. A geometrical model was developed based on actual geometry of fabric as well as shell and core part of the MPCM. The heat transfer simulation is done using finite element

method under Abaqus environment. The further prediction of thermoregulating effect on fabric based on the validated model will be discussed in chapter 5.

Chapter 3 Research Methodology

This chapter describes the techniques used for the research to characterise the developed monofilament, multifilament and nanoencapsulated PCM. Furthermore this chapter also elaborates the objectives of the project in order to provide linkages among the next chapters. The types of work undertaken in chapters 4-6 describe the experimental as well as numerical methods of thermoregulating studies of textiles and their characterisation.

Textiles containing microencapsulated phase change materials can be developed using different techniques as described in detail in Section 2.3 of Chapter 2. The incorporation of MPCM in the filament through man-made fibre spinning can provide permanent thermoregulating effect. In man-made spinning, the wet and dry spun fibres incorporated with PCMs have already been commercialised but the gap in melt spinning still exists. Chapter 4 will focus on the development of melt spun filaments incorporating commercially available MPCM to fill this gap.

It is important to obtain some necessary information before manufacturing textiles containing MPCM and show the thermal behaviour in different environments. This can be obtained using finite element method in ABAQUS environment to predict the time dependent thermal regulating effect of MPCM fabric. The heat transfer study of MPCM fabric using FEM will be discussed in chapter 5. Chapter 5 contains the theoretical heat transfer analysis of fabric made of MPCM multifilament yarn described in Chapter 4.

The particle size is an important factor while incorporating encapsulated PCM in a melt spun filament. The nano scaled capsules may provide better continuous filament during extrusion process and enable the capsules to settle within the filament rather than exposed on the surface of the filament. For this purpose, NPCM was synthesised and was incorporated into the filament to compare the latent heat of MPCM and NPCM incorporated multifilament. The synthesis and application of NPCM paraffin and Glauber's salt on cotton fabric by pad-dry cure method will be described in Chapter 6.

3.1 **Differential Scanning Calorimetry (DSC)**

Differential Scanning Calorimetry (DSC) is used to identify the thermal characteristics of material by measuring the amount of heat absorbed by the material in comparison to the reference material. After absorbing heat, the material undergoes to physical or chemical change and DSC indicates phase change of that material by measuring the change in enthalpy to the specific temperature range.

A Mettler DSC 12 E instrument as shown in Figure 3.1 was used in this study to evaluate the latent heat of monofilament and multifilament yarn incorporated with MPCM and in house synthesized nanoencapsulated PCMs. For the filaments, they were cut into fine small pieces with sharp blade to spread them evenly on the surface of aluminium crucibles. The crucible was filled with 5-10 mg of sample and was weighed on Mettler TG50 Thermobalance which measures up to the accuracy of 0.0001mg.

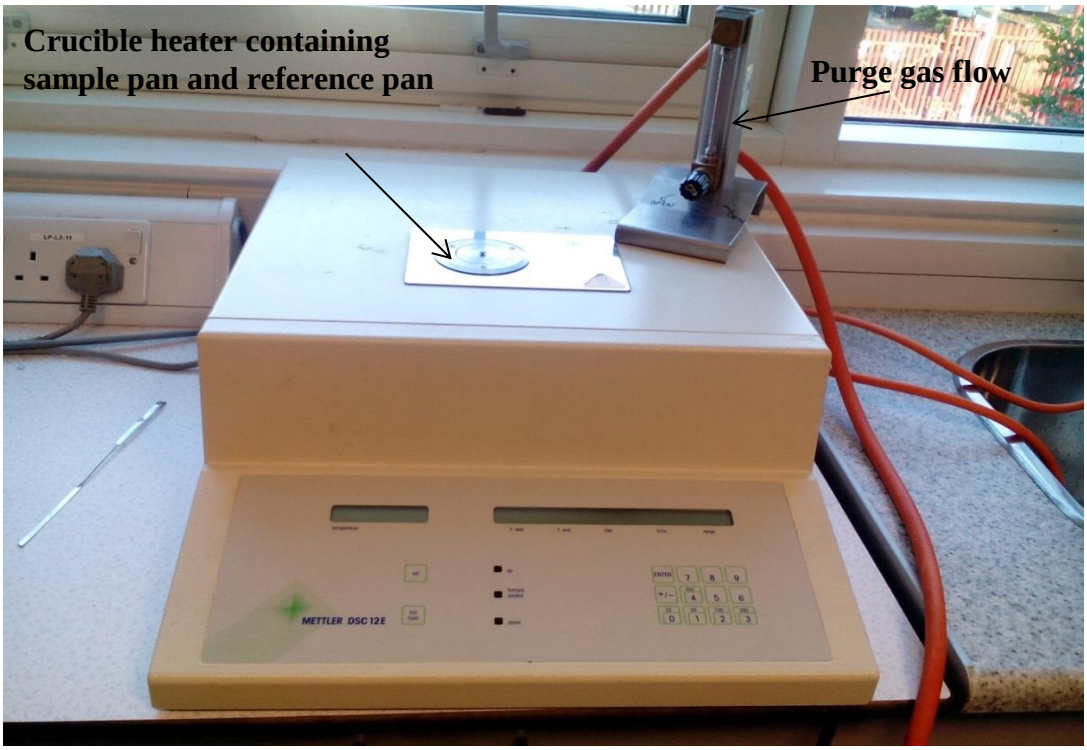

Figure 3.1 Differential Scanning Calorimetry

3.2 **Scanning Electron Microscopy (SEM)**

SEM was used to analyse the incorporation of MPCM into the polypropylene monofilament and multifilament, Hitachi S-4300 Field Emission Scanning Electron

Microscope, as shown in Figure 3.2 was used. The in-house synthesized NPCM was also studied by taking images from SEM. The actual fabric geometry used for modelling was also studied using SEM instrument.

Figure 3.2 Hitachi S-4300 SEM

For analysis, the sample was placed on stub and sputter coated with gold before SEM examination using a Polaron SC7620 Sputter Coater. Sputter coating showed good results by providing a protective layer to the samples under high voltage of SEM. The instrument was controlled by computer and scanned image was monitored on screen. In this machine, the electrons are sourced by field emission tungsten tip fixed in the gun assembly. The electron column in the chamber was kept under vacuum all the time to avoid any air interruption. For exchanging samples, the chamber was disconnected from SEM by closing the electron column. Sample was screwed to an exchanging rod and electron column was then connected to SEM by creating a vacuum. The sample position was ensured straight and electron column was closed after the stub was inserted in to the sample holder inside the electron column. The images were captured after adjusting to the working distance and required magnification with the help of controller.

3.3 **Tensile strength of MPCM yarn**

Instron 3345K7484 was used to determine the tenacity and modulus of monofilament and multifilament yarn as shown in Figure 3.3. The testing procedure was adopted as

described in BS EN ISO 2062:2009. The method describes how to determine the single end breaking force and elongation at break of a yarn. The linear density of monofilament and multifilament was determined by following the procedure described in BS EN ISO 2060-1995.

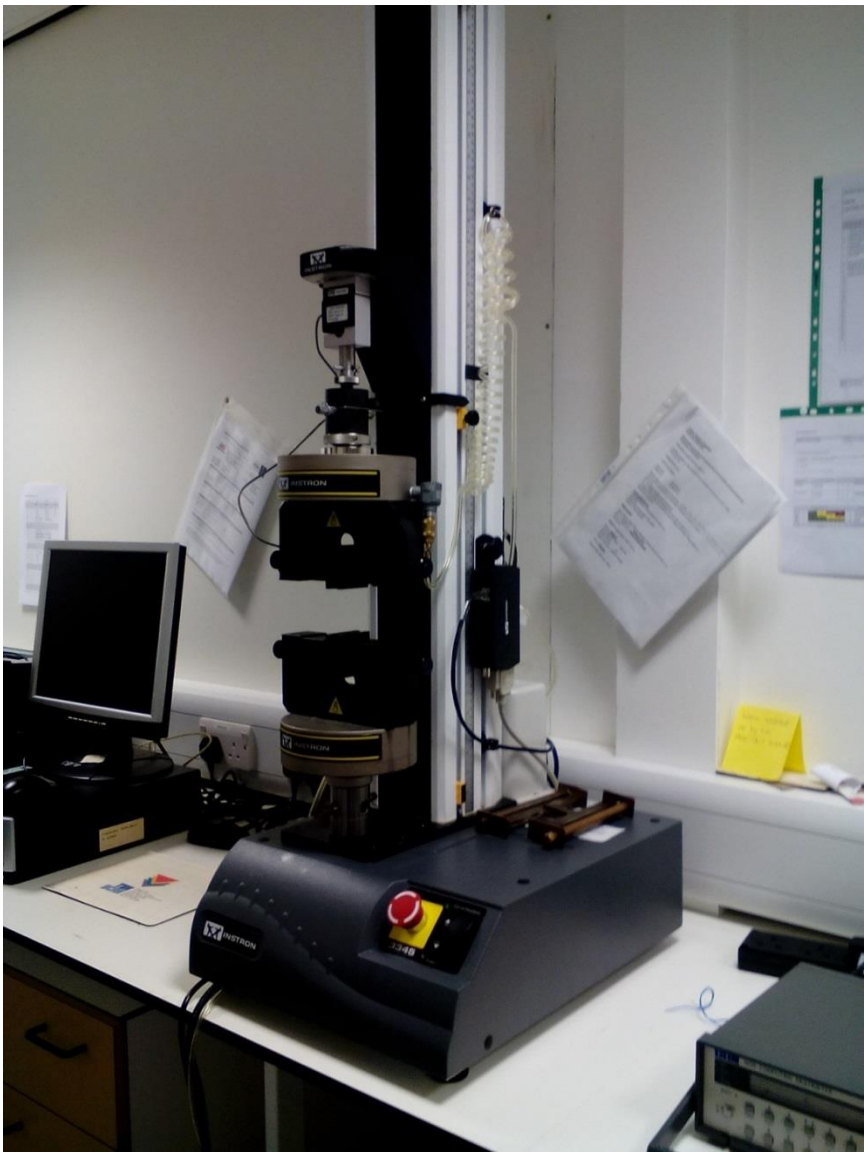

Figure 3.3 Instron tensile tester

Tenacity is the mechanical property and shows the strength of the yarn which is defined as the breaking force divided by the linear density of yarn. This is measured in cN/Tex, where Tex is the linear density of the yarn, measuring the weight of yarn in grams per 1000 meters of length. Figure 3.4 exemplifies the extension of yarn after the application of load. It shows that load is applied to the yarn which causes extension in the yarn. At certain point where the extension in yarn reaches maximum, load causes the yarn to break. This breaking of yarn determines the strength of yarn.

Yarn tenacity can be calculated by:

Tenacity (cN/ Tex) = load at break (cN)/Tex of yarn

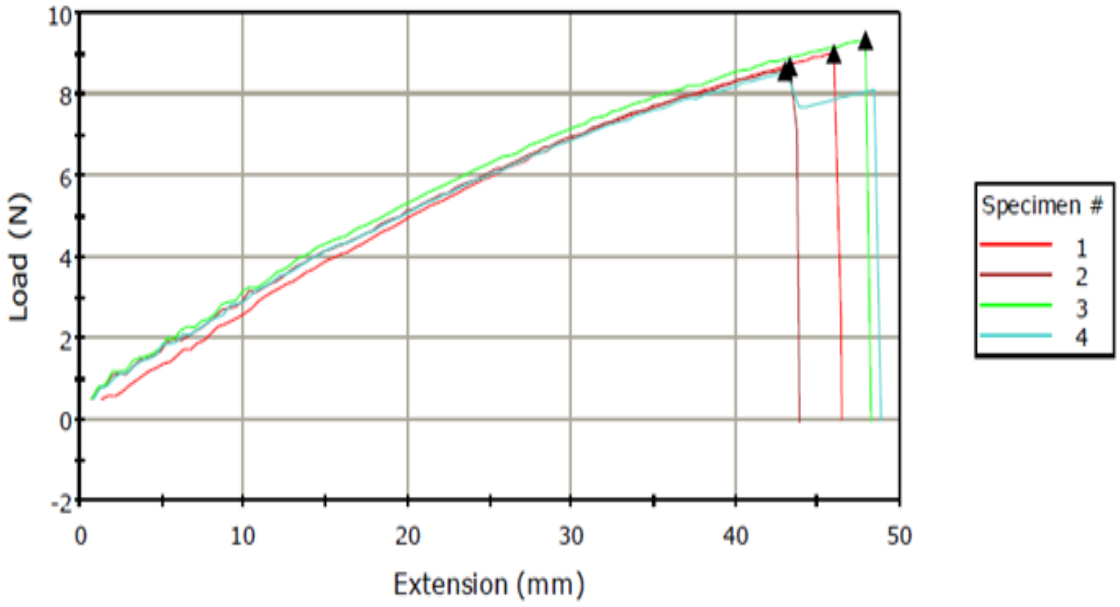

Figure 3.4 Load vs extension in tensile testing of yarn

3.4 **Infra-Red thermography**

The surface temperature of any surface can be measured using infrared thermography with high precision without surface contact. The technique enables non-destructive evaluation of the product. All of the objects emit radiation energy according to the surface temperature although human eyes are not able to capture them if they are not in visible region. Human eyes can recognize the temperature during heating of metal when it changes from red (720 ^{o}C) to white (1350 ^{o}C). For low temperature radiations, infrared camera provides us with artificial eyes to see and capture the invisible images. An infrared (IR) system includes a camera, a computer and a series of changeable optics. The core of the camera is infrared detector which absorbs the infrared heat radiation by the object and converts them into electrical voltage or signals.

In this research FLIR E60 infrared thermal camera provided by FLIR® System was used to evaluate the thermal insulation effect of fabric constructed by MPCM incorporated yarn. The efficiency of thermal insulation usually depends upon the heat storage capacity of PCM and their incorporated quantity within the yarn or textiles. The thermal

effect was evaluated by heating the fabric containing incorporated PCM and without PCM up to a temperature higher than their phase change temperatures. The aim was to measure the time increase against the temperature rise for fabrics with and without MPCM in order to evaluate the thermoregulating effect of the fabric with MPCM.

3.5 **Heat transfer measurement**

The thermal property of the fabric was tested using an in house developed heat transfer testing device [140]. The results were used for model validation of the developed FE models. The entire test was performed under standard conditions at room temperature of 20±2 °C and relative humidity 65±2 %. The samples were cut in 50x50 mm dimension and conditioned for 24 hours before testing.

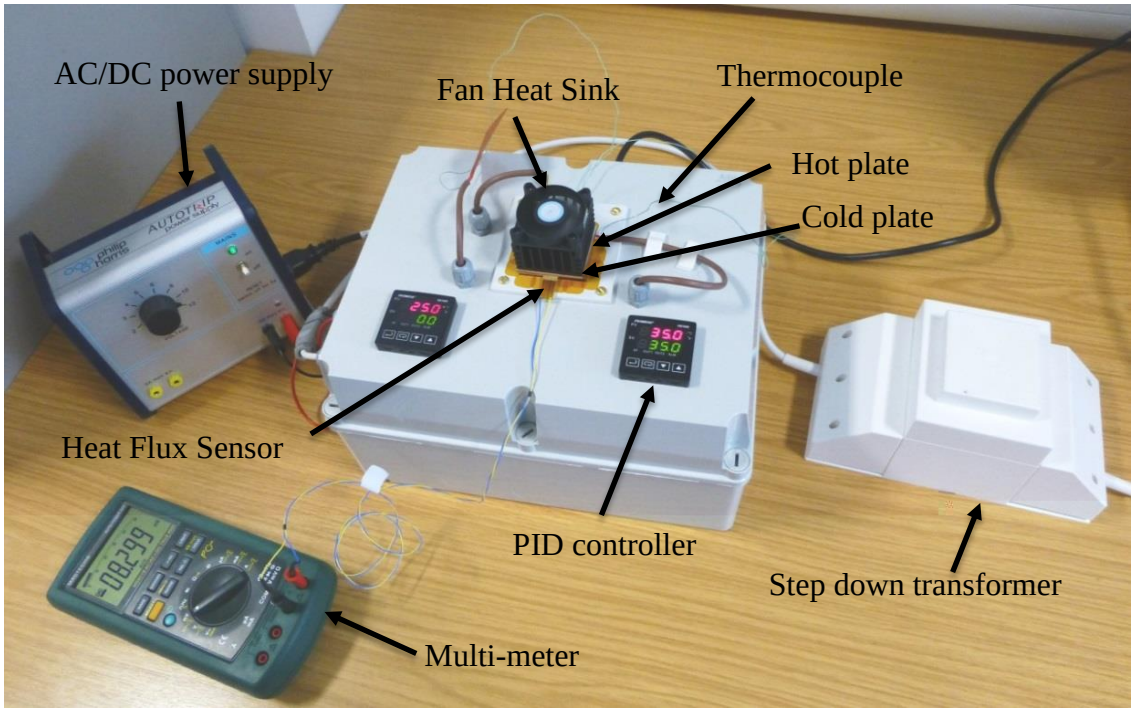

Figure 3.5 Experimental setup of heat flux instrument [140]

Figure 3.5 shows the experimental setup where the hot plate temperature was maintained by a PID controller at 35 °C because this temperature is within the range of normal body temperature and suitable for heat transfer analysis of MPCM fabrics. The heat flux sensor was connected with a cold plate to measure the amount of heat flow through MPCM fabric. The sensitivity of flux sensor was 16.8 µvolt/ (W/m^2). To measure the temperature difference across the MPCM fabric, the temperature sensors were connected with hot and cold plates. The data obtained from the heat flux sensors

in millivolt can be converted into heat flux by dividing the voltmeter value with the sensitivity of heat flux sensor as shown in Equation 3.1.

$$Q = \frac{V}{S} \tag{3.1}$$

where *V* is the output of heat flux sensor (multi-meter) and *S* is heat flux sensitivity.

The main components of the device are hot and cold plates, a heater, a heat flux sensor and a fan heat sink as shown in Figure 3.6. The fabric sample under investigation was placed between cold and hot plates where the lower hot plate heated by a controlled heater. Thermocouples are attached to the plates to sense and monitor the temperature (T_1) and (T_2). The temperature difference between the hot and cold plates allows the heat to transfer through the back side of the fabric sample to the face side of the fabric. The heat flux sensor is attached to the upper plate and cooled down by the fan heat sink. This instrument was validated by Siddiqui [140] for heat transfer experiment with commercially available Togmeter, Alambeta and DTC-25.

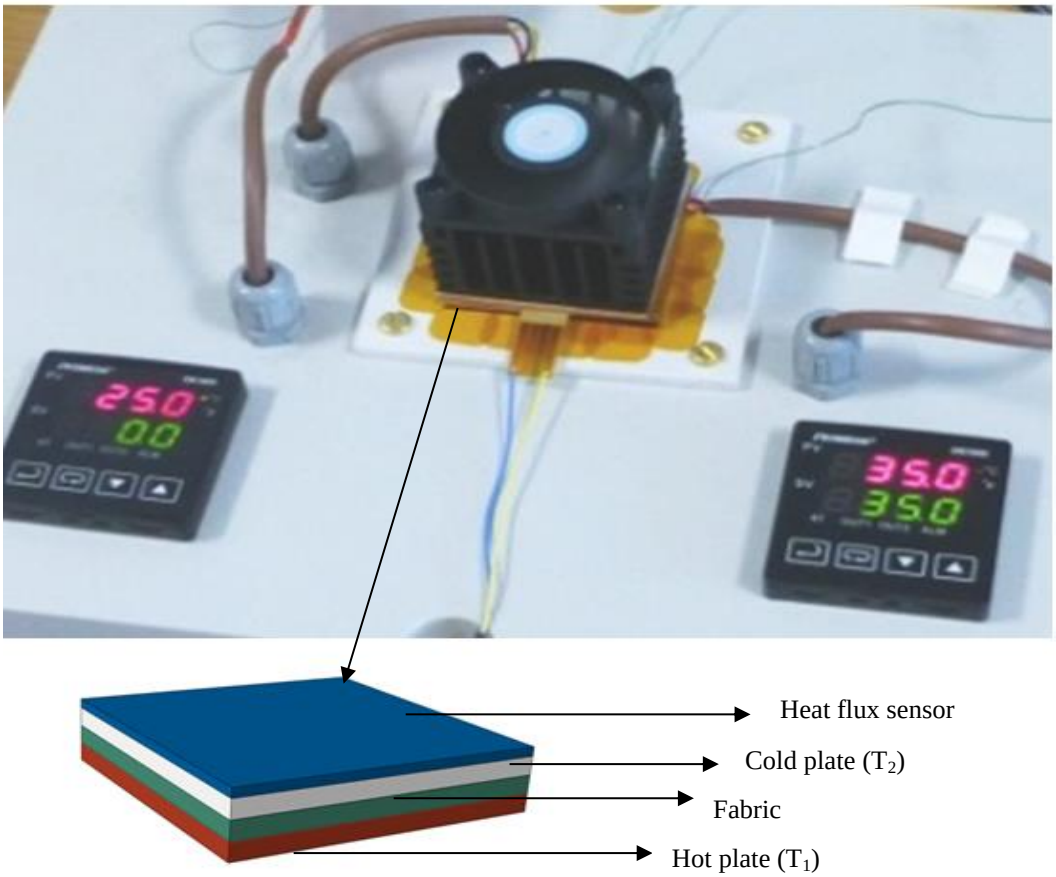

Figure 3.6 Heat flux measuring instrument

Chapter 4 Mono and multifilament polypropylene yarn incorporated with MPCM

This chapter explains the development, characterisation and analysis of melt spun monofilament and multifilament polypropylene yarns incorporated with MPCM.

4.1 Materials and methods

This section explains the materials and processes used for the development of monofilament and multifilament yarns incorporated with microencapsulated PCM.

4.1.1 *Microencapsulated Phase Change Material (MPCM)*

Microencapsulated phase change material under the commercial name of MPCM 28-D was purchased from American company Microteklab Laboratories Inc. Capsules were composed of n-octadecane as phase change material in core and Melamine Formaldehyde as shell material. The capsules are in the form of dry powder and are claimed to be extremely stable and have less than 1% leakage when heated to 250°C. The melting point of n-octadecane was 28°C containing enthalpy of fusion 180-190 J/g which is claimed by the supplier. The tested result of enthalpy of fusion of MPCM by DSC is 150-170J/g. Mineral oil was used to enhance the mixing of MPCM powder with polymer granules.

4.1.2 *Fibre grade polypropylene*

Fibre grade polypropylene under the name Moplen HP561R supplied by Basell Polyolefins was used to make monofilament and multifilament polypropylene yarn. The polypropylene polymer was purchased in the form of granules which were ready for extrusion.

4.1.3 *Benchtop Extrusion*

The benchtop extrusion machine was used to extrude the monofilament and multifilament MPCM yarn. This machine is also called screw extrusion because a screw is used inside the barrel. The line diagram of benchtop melt spinning machine is shown in Figure 4.1. On one side of the screw, the hopper is installed where material is fed while on the other end a die pack is installed where die head is situated. The function of

the screw is to transport the material from feeding section to the die head performing homogeneous melting and mixing. Metering pump is used to regulate the amount of molten material to reach the die head and its speed is controlled by the electronic panel. The die head consists of a filter which prevents the foreign particle, a breaker plate which distributes the material and a spinneret.

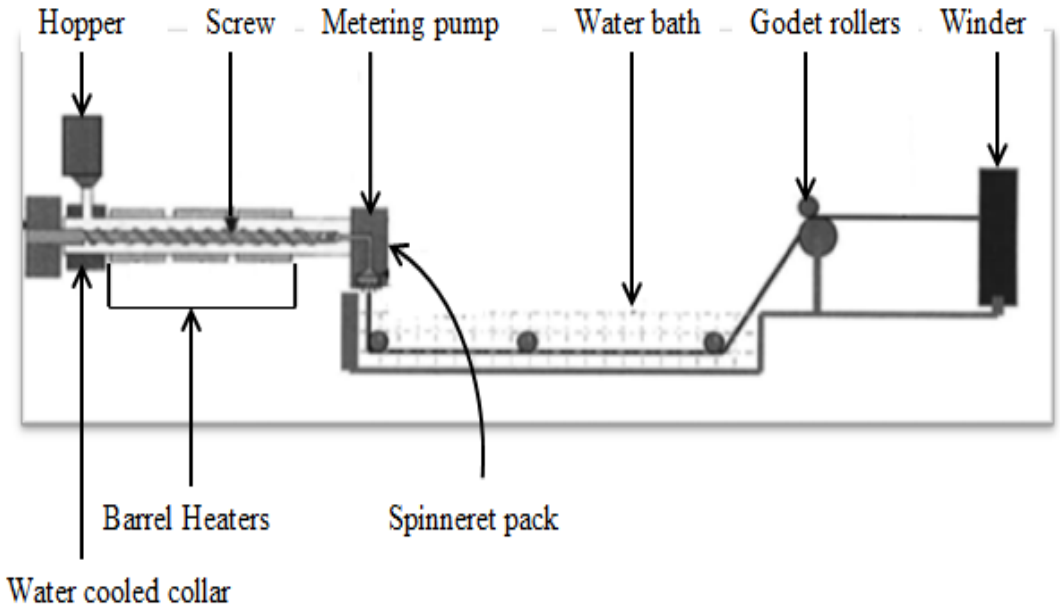

Figure 4.1 Benchtop extrusion line diagram

The screw used in this machine contained a mixing head to ensure better mixing of the material and any additives used during the process. The MPCM powder was mixed with polymer granules using very little amount of mineral oil which helps the powder to stick with the granules. The further mixing was obtained with the screw mixing head. The benchtop extrusion machine provided by Extrusion Systems Ltd. Leeds, England is shown in Figure 4.2.

Figure 4.2 Benchtop extrusion machine

4.1.4 *Drawing of yarn*

Hot drawing of filaments was carried out on pilot scale drawing machine installed in the extrusion lab provided by Extrusion System Limited (ESL) as shown in Figure 4.3. The machine consists of four rollers and three hot plates of which first three rollers were used for hot drawing. The temperature of rollers was adjusted accordingly to soften the filaments so that polymer chains have enough mobility to stretch. The stretching is done by the different speeds of the preceding roller from the following roller. The filaments were wound on a package followed by the cooling roller. The polymer molecules become more linearly orientated along the fibre axis, as a result, the fibre diameter decreases due to the stretch, but its strength considerably increases after drawing.

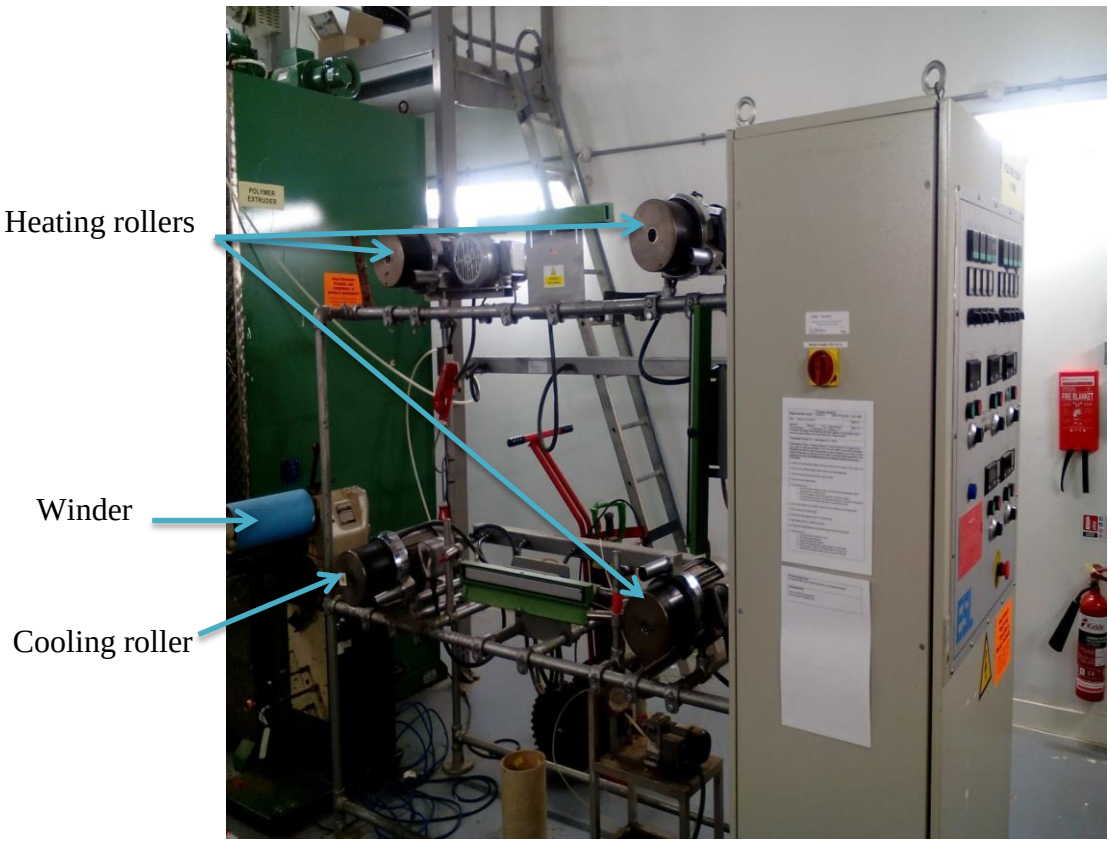

Figure 4.3 Filament drawing machine

4.1.5 *Twisting of yarn*

The machine used for twisting was J.T. Boyd twisting machine in which twisted yarns is taken up downward rotating on spindles through ring-spinning system. Twist was applied on multifilament polypropylene yarn at room temperature. 3 twists per inch (TPI) were inserted by setting the dragging roller speed while the spindle rotates with constant speed of 316 rpm. High TPI was not inserted because the purpose of twist was to bind yarn rather than to impart strength. Figure 4.4 shows the bobbin on spindle which rotates with constant speed and the filaments are twisted together with the difference of rotational speed of spindle and delivery roller.

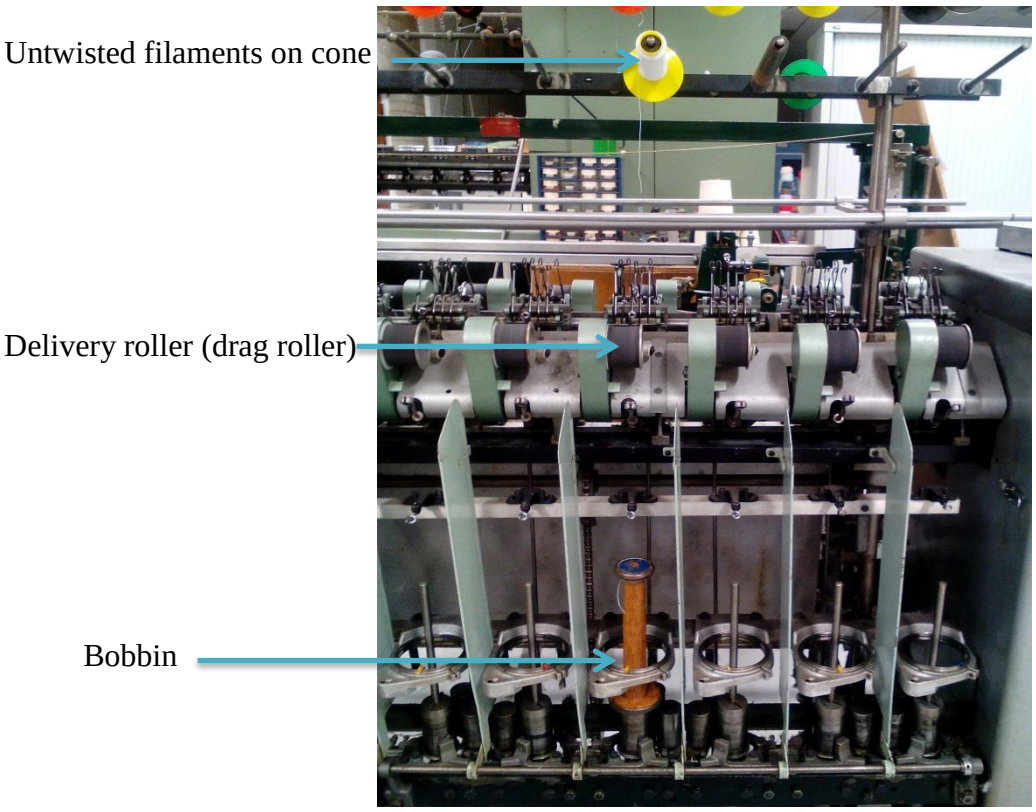

Figure 4.4 Twisting of multifilament yarn

4.2 **Development of monofilament polypropylene yarn**

The Monofilament polypropylene yarns were made with different percentage of MPCM by varying the processing parameters. The most important processing parameters observed were temperature, metering speed and the extruder speed. They had to be set differently due to the different amount of MPCM incorporated in a yarn. The extruded filament was collected by a winder through a water bath. After spinning, the filaments were drawn on a drawing machine to enhance the strength and get the appropriate fineness of the filament. MPCM were mixed with PP granules from 2% to 12% on the weight of polymer in a container and well shaken manually with mineral oil to get homogenous mixing of capsules with granules.

4.2.1 ***MPCM monofilament input variables and response***

Table 4.1 shows the experiment details containing input and output (response) variables. The experiments were run at 235 °C maintaining the temperature of feeding zone at 170 °C to avoid pre melting of the polymer. For drawing of filaments, the temperature for the first three drawing rollers were set at 80 °C, 100 °C, 100 °C respectively in all cases and the speeds were adjusted to get different Tex of filaments. The difference of

proceeding roller from previous roller can be twice, three times or more depending upon the required Tex. Table 4.1 shows the yarn count measured according to BS EN ISO 2060-1995 and latent heat tested using DSC. The measured tenacity and modulus of MPCM monofilament were measured according to BS EN ISO 2062:2009 are also presented in Table 4.1.

Table 4.1 Input variables and response for the development of MPCM monofilaments

MPCM %	Yarn count (Tex)	Latent heat (J/g)	Tenacity (cN/Tex)	Modulus (cN/Tex)
2	50	1.12	42	450
3	71	2.1	27	251
4	82	2.23	22	172
5	97	3.3	19	150
6	92	4.09	19.5	149
8	90	6.14	18.5	140
10	43	7.9	48	404
12	95	9.2	15	132

4.2.2 *SEM observation*

Scanning electron microscopy images show the presence of microcapsules in MPCM incorporated polypropylene filaments. Figure 4.5 clearly indicates the difference between filaments with and without MPCM. Very rough surface was observed in filaments incorporated with MPCM while filaments without MPCM showed smooth surface.

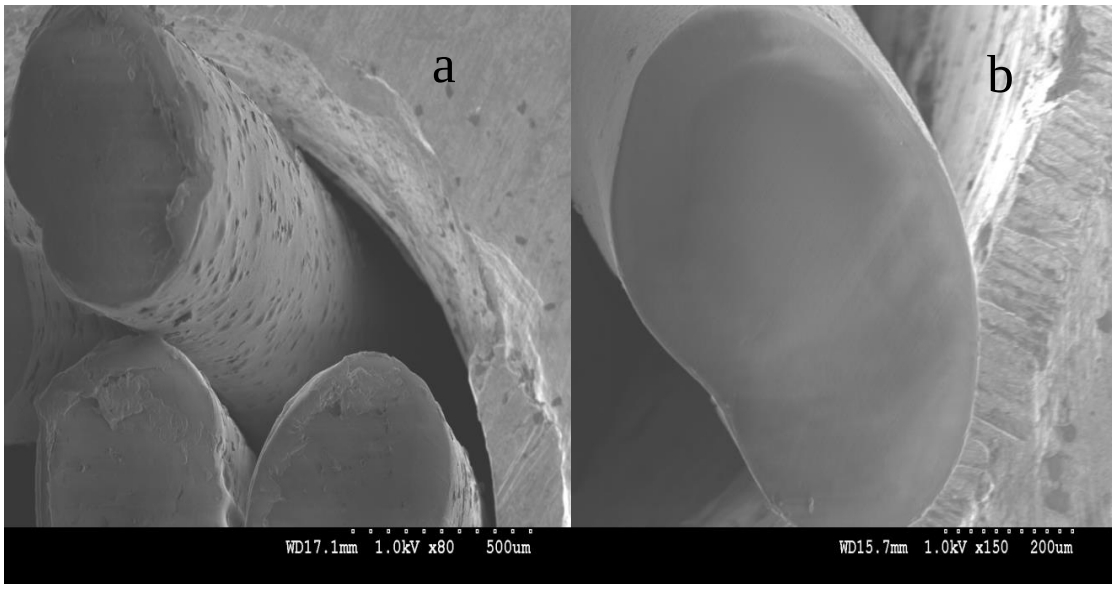

Figure 4.5 SEM images of PP filaments (a) with MPCM (b) without MPCM

The presence of MPCM within the monofilament yarn was observed as presented in Figure 4.6. The sample was prepared by cutting the filament cross sectional-wise in order to see the incorporated MPCM contained in the filament. The images were taken at different magnifications and can be seen in Figure 4.6 how they are incorporated as an integral part of filament.

Figure 4.6 Monofilament with MPCM

4.2.3 *Latent heat in MPCM incorporated yarn*

The peaks in DSC graph shown in Figure 4.7 indicate the latent heat contained in the MPCM incorporated yarns against different percentages of MPCM. All fibres from 2% to 12% have been evaluated, and for those filaments with MPCM the peak of curve increases with the increase of the percentage of MPCM in the filament, indicating increase in the latent heat with increasing the amount of MPCM. The time duration of thermoregulating effect depends on the amount of latent heat; the more latent heat contained in a yarn the longer thermoregulation effect of the fabric made of such yarn.

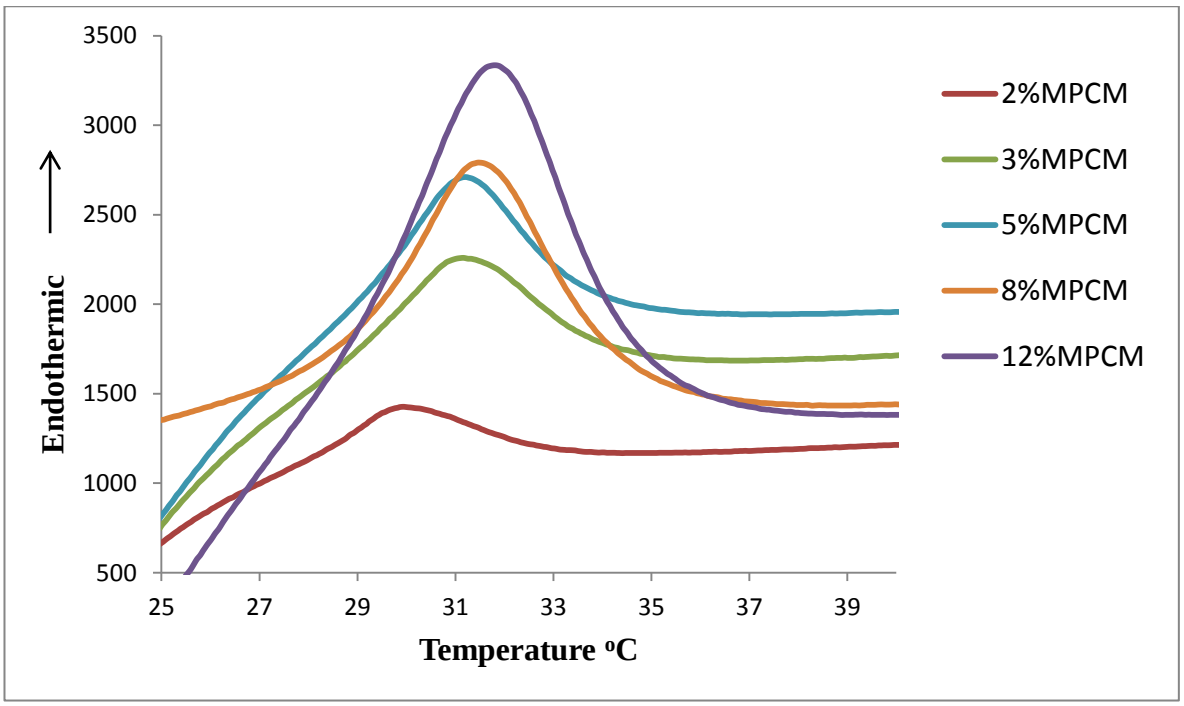

Figure 4.7 DSC graph showing latent heat of monofilaments containing MPCM

4.2.4 *Response Surface Analysis for MPCM monofilament*

Response surface analysis (RSM) was used to better understand the relation between the input and output variables and the effect of one variable on others. The design of experiment was not made in RSM because of some limitations when combining all of the processing parameters. The possible combination of processing parameter by RSM was not desirable and impossible to run on Benchtop extruder. The other reason was that, the processing parameters to develop monofilament yarns incorporated with different percentage of MPCM vary and cannot be determined by random combination of processing parameters. Therefore the input processing variables and output properties were manually inserted in Minitab worksheet to analyse the response surface design for the study of statistical model. The RSM analysis generated the p-values based on the input and output variables from which significance of factors in the model can be described.

Table 4.2 shows the coefficient of determination in terms of p-value. If p-value is less than the α-value (0.05 at 95% confidence interval), it means that the specific parameter has a statistically significant effect on model. The p-value for latent heat, modulus and tenacity are presented in Table 4.2. The p-values of MPCM factor and yarn count factor (in Tex) for the response latent heat are 0.000 and 0.152 respectively which means that

the percentage of MPCM has significant effect on latent heat while yarn thickness does not. This can be explained that latent heat is thermal energy storage which only depends upon the amount of MPCM incorporated in the material.

For modulus the p-values are 0.001 for MPCM and 0.000 for filament thickness while in case of tenacity the p-values are 0.006 and 0.000 for MPCM and filament thickness respectively. These p-values indicate that both factors i.e. MPCM and filament thickness have significant effect on the output factors modulus and tenacity. The reason can be explained as tenacity and modulus of filament depend upon the orientation in polymeric chains and this orientation in filaments increases with increasing drawing of filament which results in lower yarn count Tex. Hence yarn count controls the modulus and tenacity of yarn. The reason of MPCM effects on modulus and tenacity can be explained by the same phenomenon. The orientation or straightening of polymer chains is interrupted by the presence of additives like MPCM which can cause reduced strength or tenacity of filament. Therefore MPCM and Tex have significant effect on the modulus and tenacity.

R^2 and adjusted R^2 represent the proportion of variation in the response that could be explained by the model (R^2 is also called the coefficient of determination). The predicted R^2 represents how well the developed model can be used for property prediction. The R^2 values for latent heat, modulus and tenacity are 99.58%, 97.02% and 96.36% respectively showing high coefficient of determination. The values for R^2 (pred) show that the model can predict the response up to 98.69% for latent heat, 93.60% for modulus and 83.56% for tenacity as shown in Table 4.2.

Table 4.2 Coefficient of determination of model showing p-values

	Model Predicted Coefficient of Regression							
Response	Latent Heat		Modulus			Tenacity		
Factors	MPCM	Tex	MPCM	Tex	Tex*Tex	MPCM	Tex	Tex*Tex
p-value	0.000	0.152	0.001	0.000	0.014	0.006	0.000	0.005
R^2	99.58%		97.02%			96.36%		
R^2 (adj)	99.43%		95.95%			95.06%		
R^2 (pred)	98.69%		93.60%			83.56%		

4.2.5 *Interaction effect of studied parameters*

An interaction plot is a plot of means for each level of a factor with the level of a second factor held constant. Interaction is present when the response at a factor level depends upon the level of other factors. If the lines are parallel in the graph this indicates absence of interaction which means the level of one particular factor does not depend on the level of other factors. If the lines are not parallel then the interaction exists between the levels of factors. The greater the departure of the lines from the parallel state, the higher the degree of interaction will be. Figure 4.8 shows the interaction plot for latent heat and all the combination of levels are parallel which indicates the absence of interaction between the levels of two factors. Hence when latent heat is desired, the levels of yarn count do not affect the latent heat and only the amount of MPCM contained in the filament should be considered because yarn count does not contribute to the latent heat storage capacity.

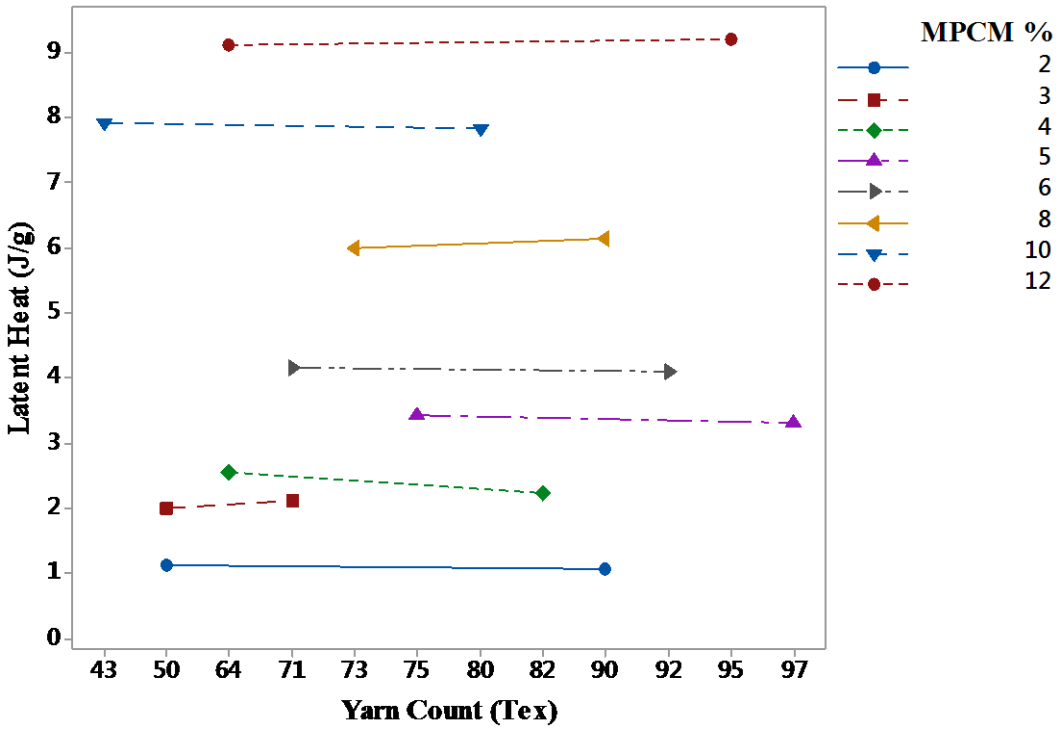

Figure 4.8 Interaction plot for latent heat (J/g)

Similarly the quantitative value (p-value) for interaction of latent heat was found 0.557 from model as shown in Table 4.3 and is greater than the α-value showing no significant interaction between the levels of Tex and MPCM when latent heat is required.

Table 4.3 ANOVA table showing significance of model terms

	Response		
	Latent Heat	**Modulus**	**Tenacity**
Linear	p=0.000	p=0.000	p=0.000
Square	p=0.820	p=0.044	p=0.010
Interaction	p=0.557	p=0.025	p=0.273

In the interaction plots for modulus and tenacity the lines are not parallel in both cases, as shown in Figure 4.9 which indicates the presence of strong interaction between all levels of the factors MPCM amount and yarn count (Tex). This graph helps in realizing that all the levels of both factors are responsible for optimum tenacity and modulus.

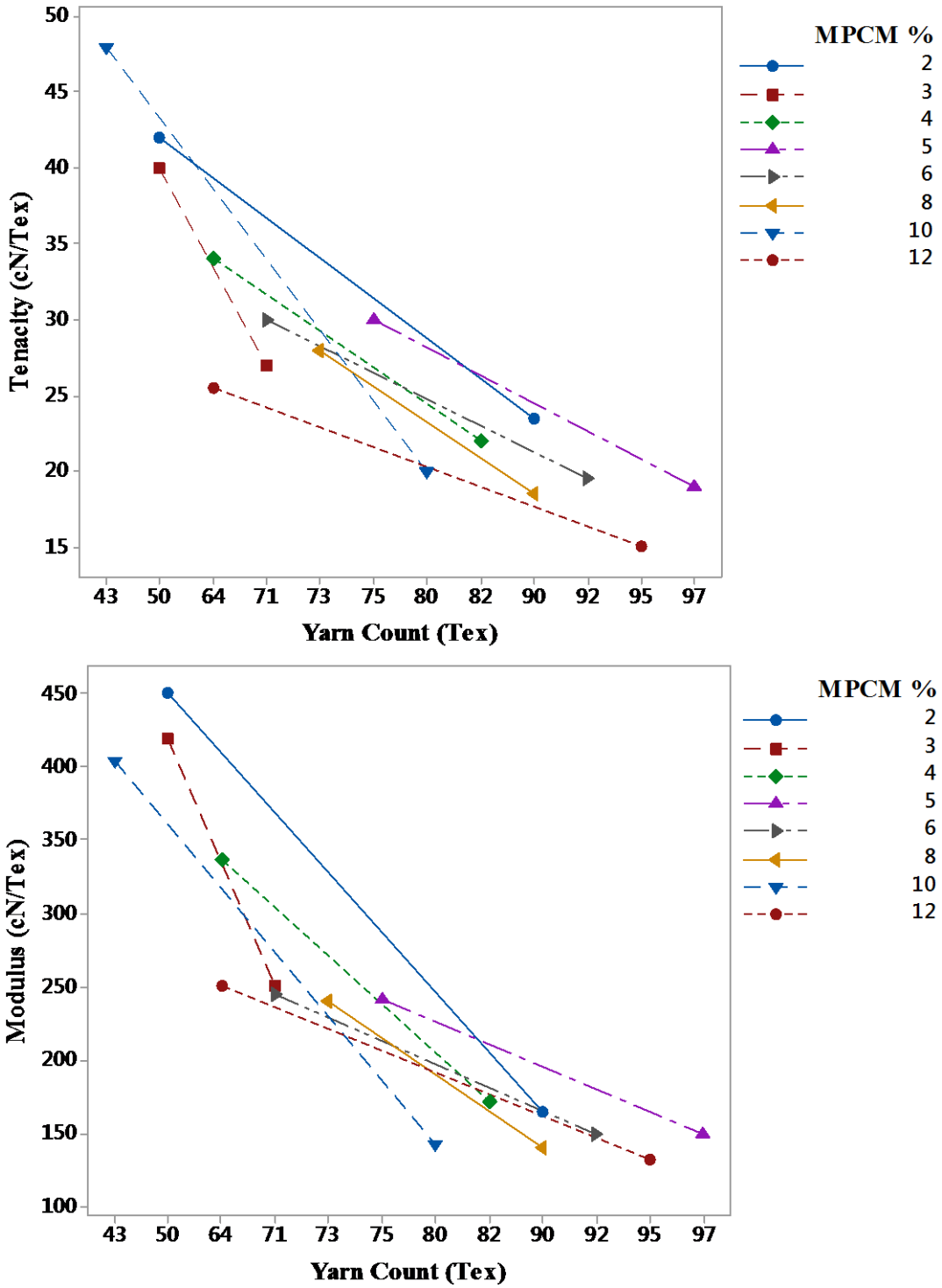

Figure 4.9 Interaction plots for tenacity and modulus

4.2.6 *Residual plots*

Residuals generally explain the difference between observed values in the time series and fitted values. The residual plots of the fibre properties are shown in Figures 4.10-4.12. For latent heat, modulus and tenacity, the residuals generally appear to follow a straight line. There does not exist any evidence of non-normality and outliers. In versus

fitted and versus order graphs, the residuals appear to be randomly distributed and scattered around zero axis for latent heat, modulus and tenacity, showing no evidence for non-constant variance, missing terms and correlation of error terms.

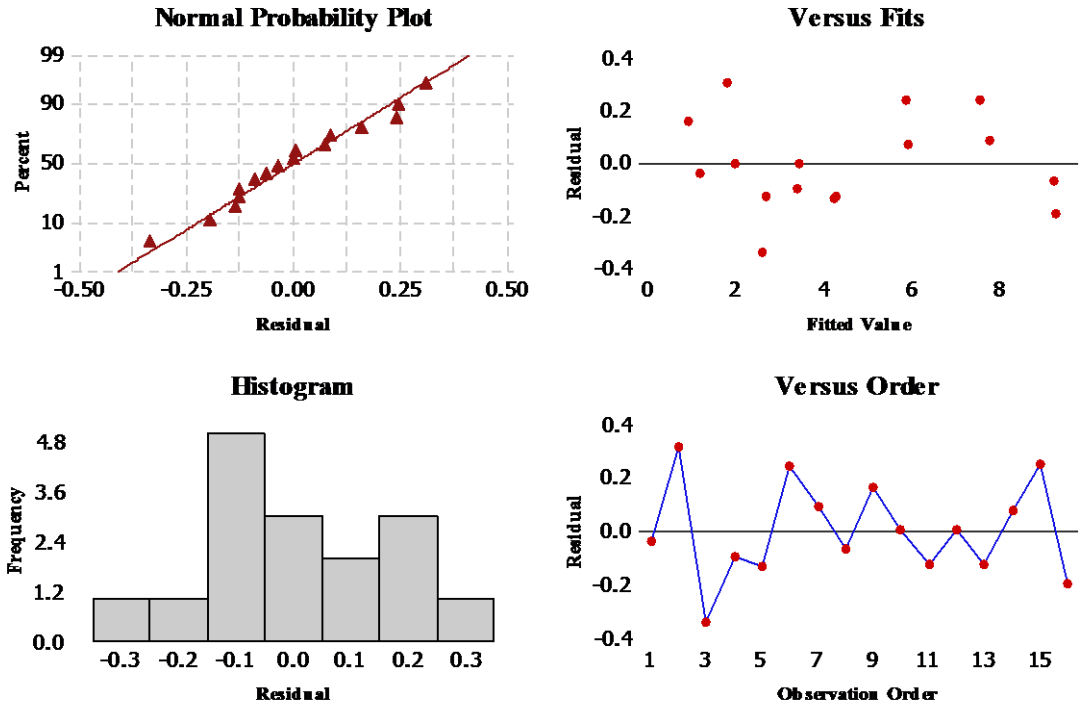

Figure 4.10 Residual plots for latent heat J/g

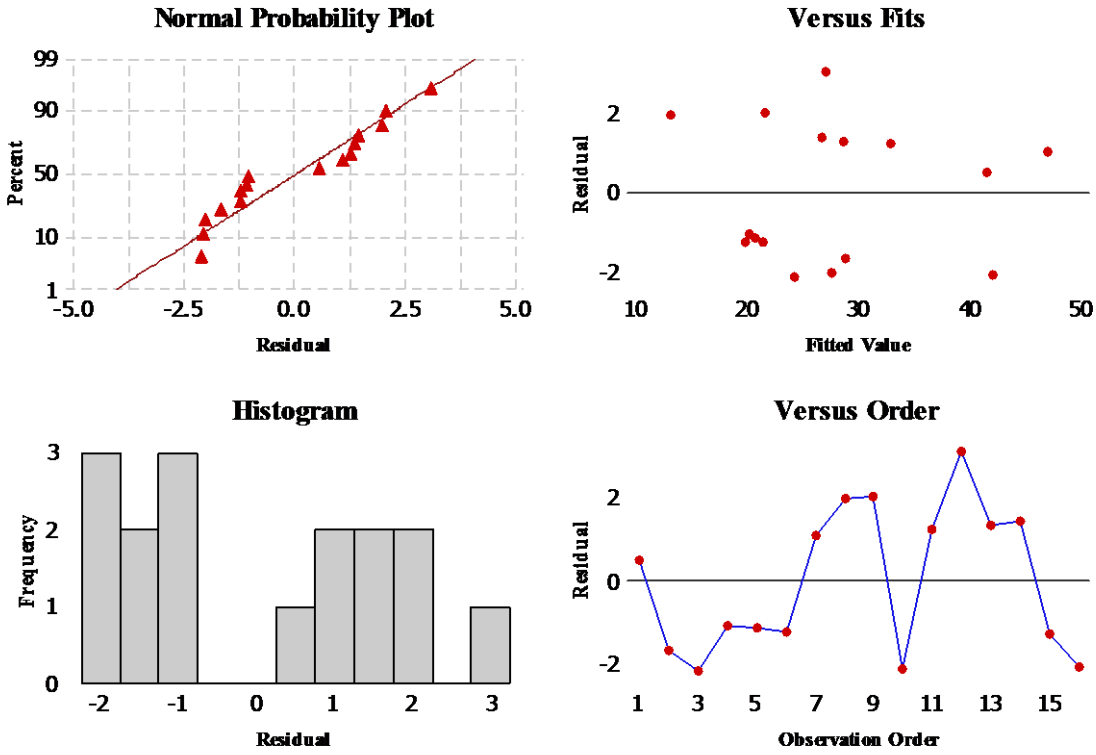

Figure 4.11 Residual plots for tenacity cN/Tex

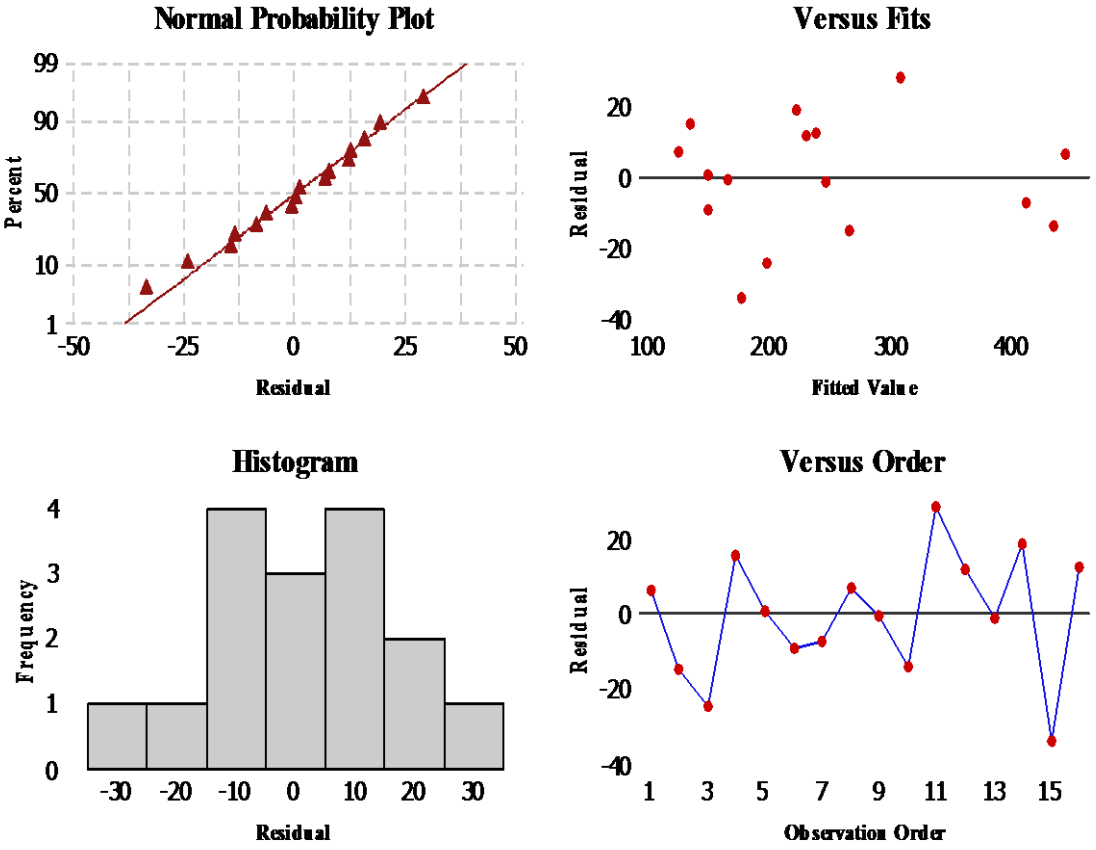

Figure 4.12 Residual plots for modulus cN/Tex

4.2.7 *Contour Plots*

The contour plot in Figure 4.13 shows that latent heat increases directly with the increase of the amount of MPCM in the monofilament while yarn count does not have any effect on latent heat. Figure 4.14 show that modulus depends on both MPCM percentage and Tex and both factor values should be kept minimum to get high modulus.

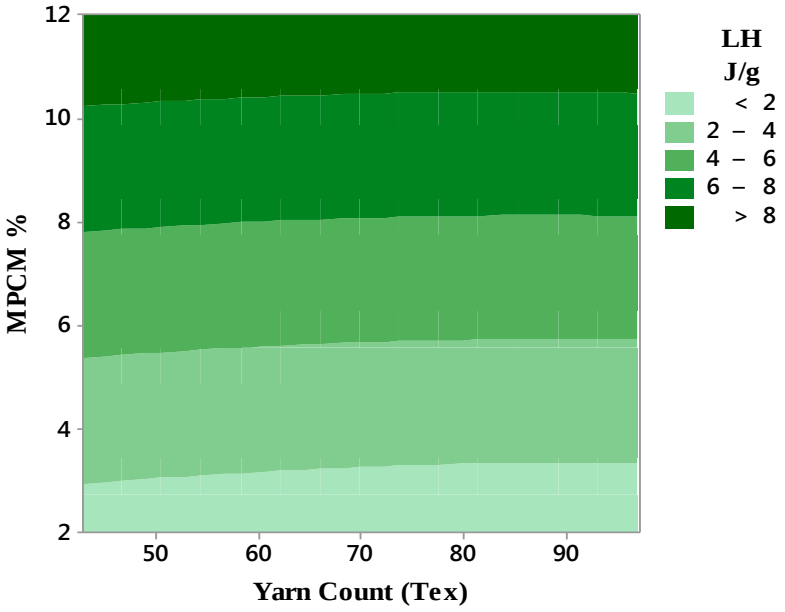

Figure 4.13 Contour plot of latent heat J/g vs. MPCM%, Tex

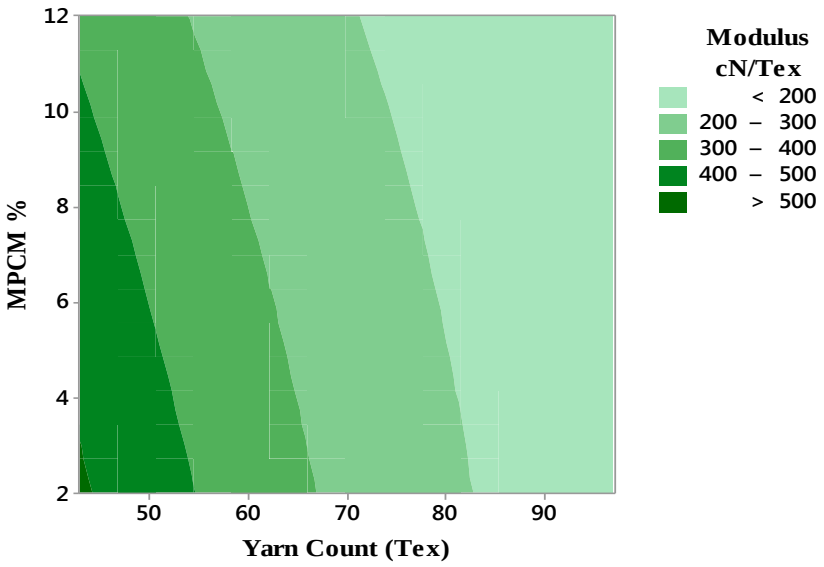

Figure 4.14 Contour plot of modulus cN/Tex vs. MPCM%, Tex

Figure 4.15 explains the dynamic relationship of yarn strength (tenacity), yarn thickness and the amount of MPCM contained in filament. It can be seen that the higher tenacity can be obtained with lower yarn count shown in dark green colour in the contour graph. The incorporated amount of MPCM does not affect tenacity significantly if the yarn count is kept lower. However if yarn count goes higher, the MPCM amount should be maintained at lower level to control the strength of yarn.

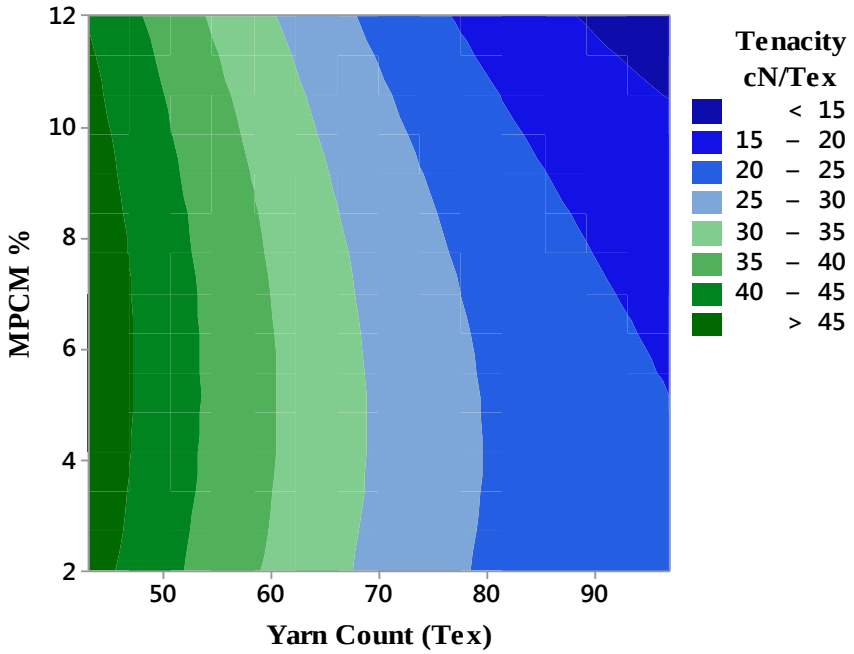

Figure 4.15 Contour plot of Tenacity cN/Tex vs. MPCM%, Tex

4.2.8 *Statistical model for latent heat, modulus and tenacity for monofilament yarn*

Equations (1) - (3) are statistical models for latent heat, modulus and tenacity. They are developed in Minitab in accordance with the results from experiments, where X is the amount of MPCM contained in filament, in %, Y is fibre count, in Tex.

$$\text{L.H. (J/g)} = 0.279703 + 0.832129\,X - 0.0219239\,Y - 0.00244207\,X^2 + 9.74289E\text{-}05\,Y^2 + 0.000513071XY \quad (13)$$

$$\text{Modulus (cN/Tex)} = 1064.43 - 17.7730\,X - 14.7934\,Y - 0.296939\,X^2 + 0.0524250\,Y^2 + 0.216460\,XY \quad (2)$$

$$\text{Tenacity (cN/Tex)} = 90.4268 + 1.78041\,X - 1.32445\,Y - 0.113053\,X^2 + 0.00599395\,Y^2 - 0.00961094\,XY \quad (3)$$

4.2.9 *Model Validation of monofilament yarn*

Model validation was made by comparisons between the data collected from practical tests and predicted data obtained by the above three equations. The models were tested using data collected from practical tests to the two new developed filaments with 7% (SET 1) and 11% (SET 2) MPCM respectively, which were not made previously for model generation. The response from model and experiments against input variables are compared and shown in Table 4.4. It shows that there is 0.6% and 0.8% difference

between models predicted and tested results for latent heat against SET 1 and 2 respectively. For SET 1, the difference between obtained and predicted values of tenacity and modulus are 1.28% and 4.5% respectively. For SET 2, the modulus and tenacity difference is found to be 8.3% and 2.3%, respectively.

Table 4.4 Validation of model

Factors			Latent Heat (J/g)		Modulus (cN/Tex)		Tenacity (cN/Tex)	
SET	PCM%	Tex	Obtained	Predicted	Obtained	Predicted	Obtained	Predicted
1	7	73	5.2	5.165	246.81	235.53	28.05	27.69
2	11	52	8.48	8.5545	359.44	329.29	37.31	38.17

4.3 **Development of multifilament MPCM polypropylene yarn**

For the development of multifilament yarn an innovative spinneret was engineered after performing couple of trials based on the literature study for the uniformity of the extruded filaments. The experiments were performed on a benchtop extruder made by Extrusion System Limited to incorporate MPCM into yarn. Multifilament MPCM polypropylene was made successfully with different percentages of MPCM by the newly designed spinneret. The processing parameters such as temperature, metering speed and extruding speed were optimized. The multifilament yarn was further undergone a drawing process to increase its strength by getting molecular chains in the filament orientated. Following the drawing process, the loose filament yarns were twisted on a yarn twisting machine.

4.3.1 ***Design of spinneret for multifilament yarn***

The problem related to the uniform extrusion of multifilament polypropylene yarn through orifices was faced while incorporating phase change microcapsules. Due to the high processing temperature in melt spinning, the long stay of microcapsules in extruding chamber can cause damage and rupture of the shell of microcapsules. To decrease the time period of microcapsules in extruding chamber, the screw speed needs to be increased. This increase in speed can cause the increase in melt flow pressure

through spinneret die. A low pressure was required at the exit of spinneret to reduce any leakages. Zhao et al [160] reported that the spinneret with less number of holes with each hole had larger diameter provided low pressure and better processing than the spinneret containing more number of holes with lesser diameter. However their design was not conical from the top surface of the holes as can be seen in Figure 4.16.

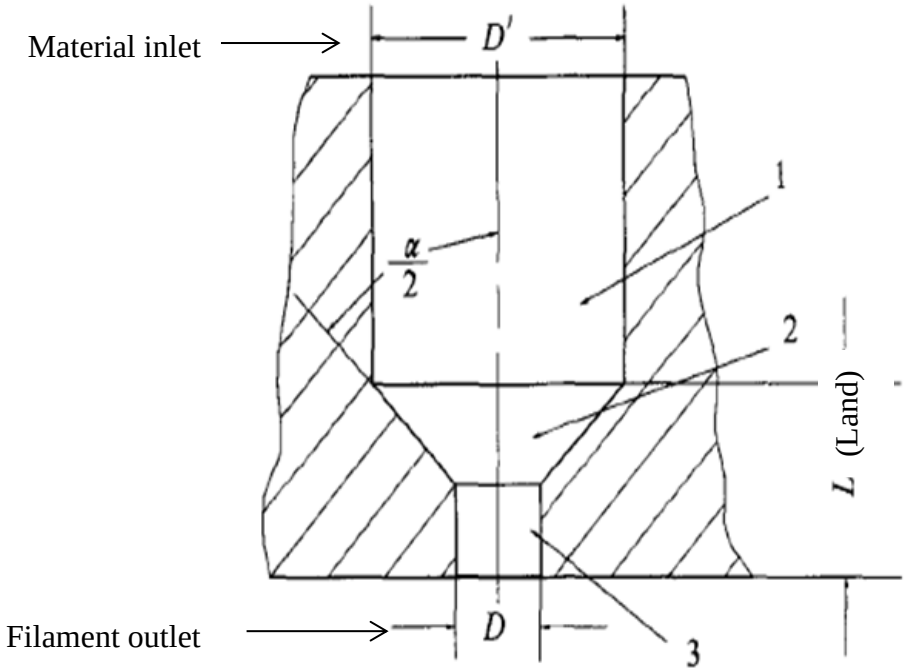

Figure 4.16 Cross section of spinneret hole as made by Zhao et al[160]

In order to minimize the pressure, the length or land is usually longer than the diameter of holes. The plate is usually kept thicker to withstand the upstream pressure. The conical sections on the top of the hole as shown in Figure 4.17 will also provide pressure drop as well as orientation of filaments [161].

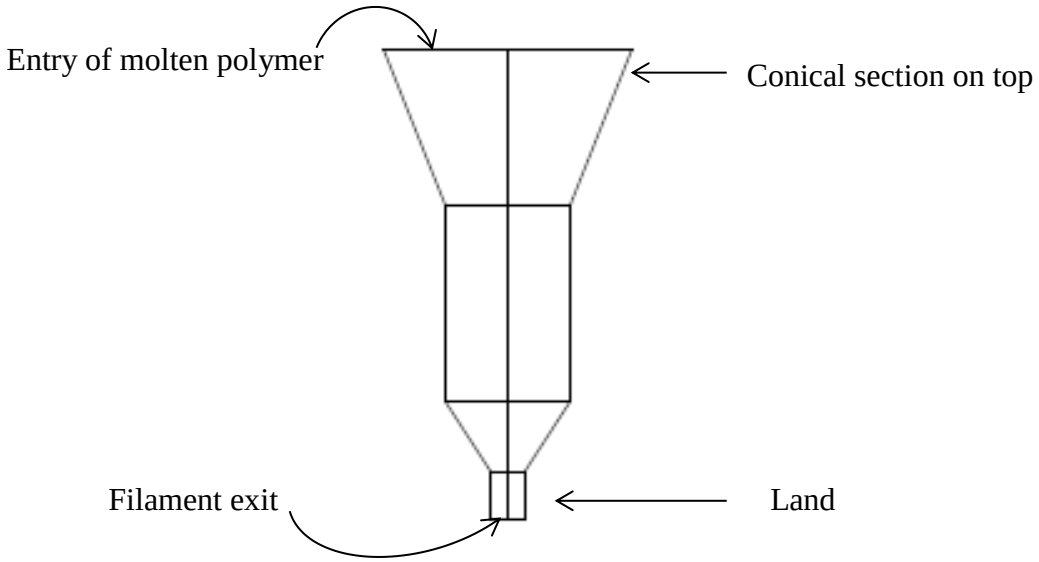

Figure 4.17 Improved cross sectional view of hole with conical top

Based on the above concept, a new spinneret was designed containing fewer holes with larger diameter. Different spinnerets with different orifices diameter and land sizes were designed and experimented for yarn extruding. It was found that the spinneret with 28 mm PCD (pitch circle diameter) and 7 holes on it was able to successfully produce MPCM multifilament yarns, shown in Figure 4.18.

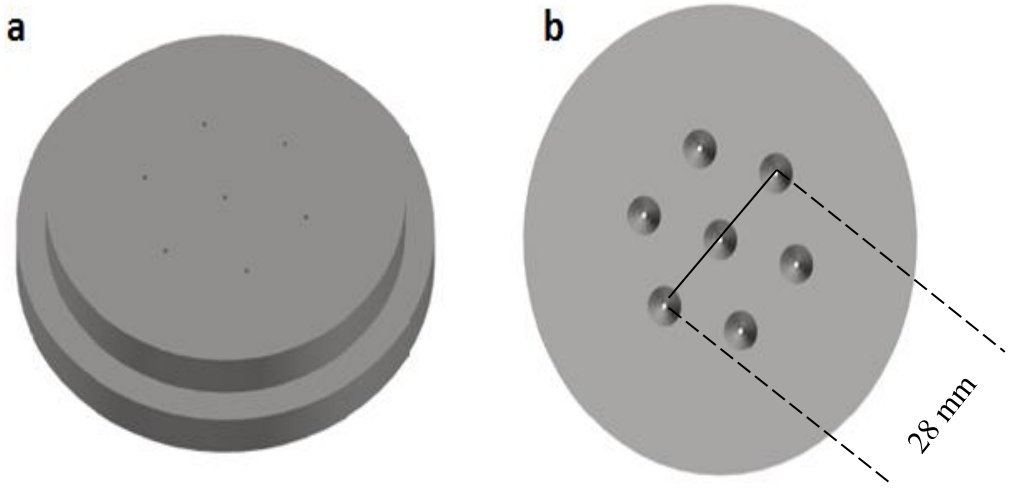

Figure 4.18 3D view of spinneret to show exit (a) and entry (b)

The geometry and dimension of the spinneret was designed in AutoCAD 2015, shown in Figure 4.19 and Figure 4.20 respectively. Figure 4.19 shows the cross sectional dimension of the spinneret in 2D and 3D shapes. The distance between all the holes was

kept constant as 14mm and the depth of spinneret was 12 mm. Figure 4.20 shows the dimension of spinneret hole having a land of 1.2 mm and the hole diameter of 0.8 mm.

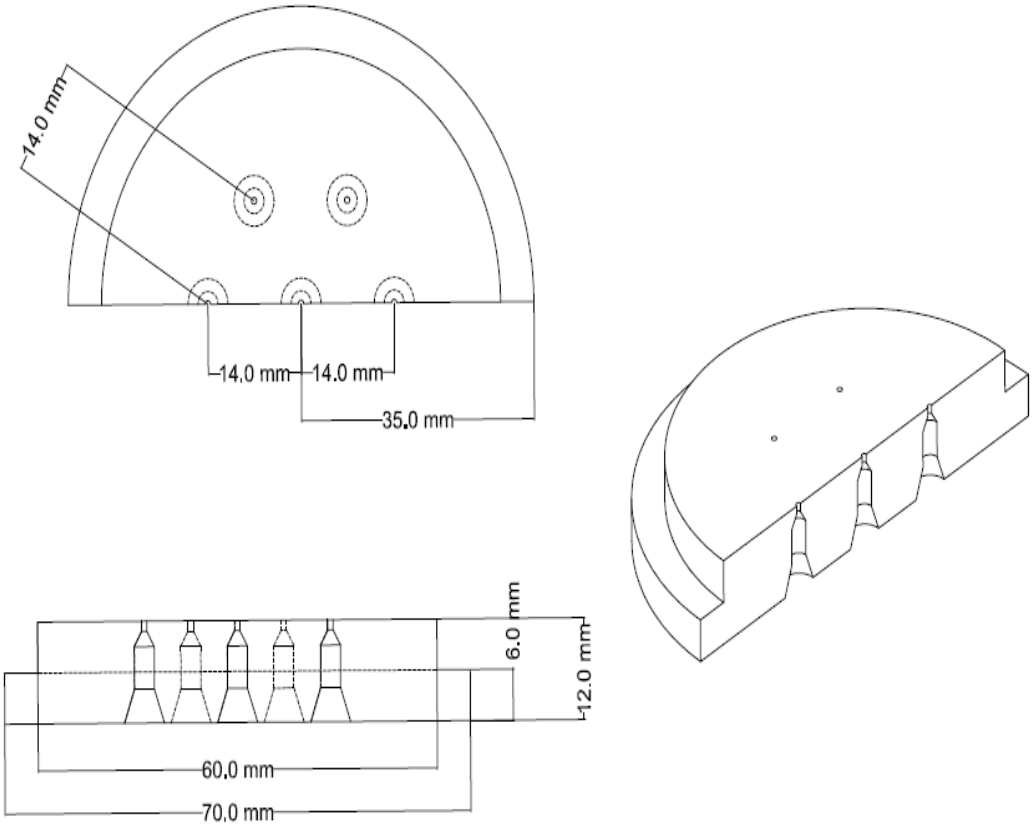

Figure 4.19 2D and 3D images showing geometry of Spinneret

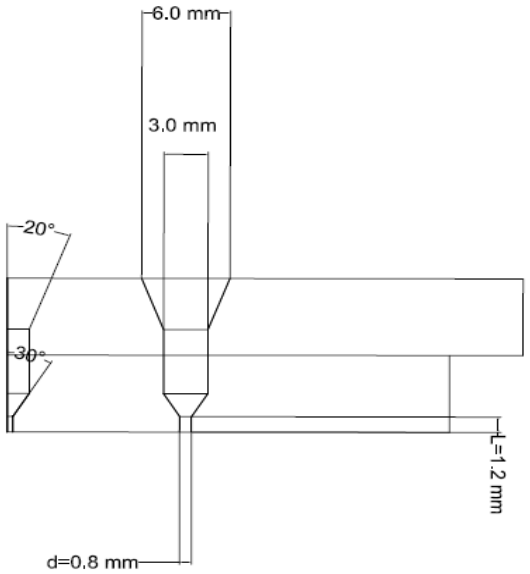

Figure 4.20 Dimension for the spinneret hole

Figure 4.21 shows the twisted yarn containing 7 filaments which is a result of successful uniform extrusion using the newly designed spinneret. The manufactured twisted yarn can be used for MPCM containing fabrics and temperature regulating garments.

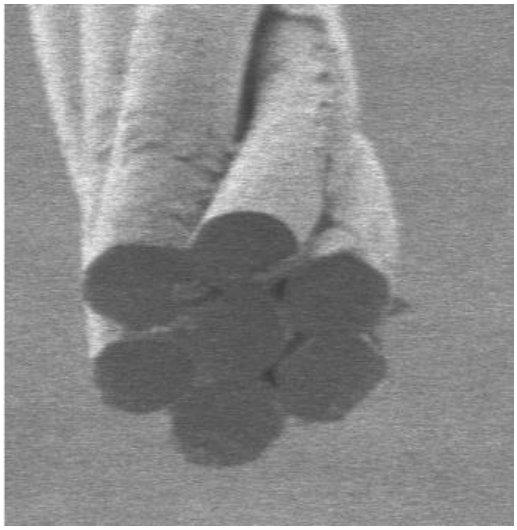

Figure 4.21 Twisted multifilament yarn containing MPCM

4.3.2 *MPCM multifilament input variable and response*

Table 4.5 shows the values of input variables used for the development of MPCM multifilament and the response obtained. These parameters were used to study the effect of factors on response and behaviour of response with different combination of factors. The drawing temperatures were set at 80 °C, 110 °C, 115 °C for roller 1,2 and 3 respectively and 4^{th} roller was used as cold roller to cool down the filaments. The roller speeds were adjusted to 60 rpm, 160 rpm, 180 rpm and 182 rpm for rollers 1, 2, 3 and 4 respectively.

Table 4.5 Input variables and response for the development of MPCM multifilament

	Input variables		**Response**	
MPCM %	Extruder Speed (m/min)	Temperature (°C)	Modulus (cN/Tex)	Tenacity (cN/Tex)
0	12	230	270	32.41
2	13.8	233	186	26.14
4	15.4	238	165	25.23
6	17.2	242	148	24.46
8	21.4	248	100	19.89
Note: The temperature of feeding zone was maintained at 170 °C to avoid pre melting of the polymer in all trials.				

4.3.3 ***SEM Observation***

SEM images of multifilament yarn incorporated with MPCM are shown in Figure 4.22. The images show that the MPCM were successfully incorporated in the multifilament yarn. The images were taken at higher magnification due to the small size of microcapsules. The microcapsules MPCM can be found in yarn either in mono-molecular form or in agglomerated form as can be seen in Figure 4.22.

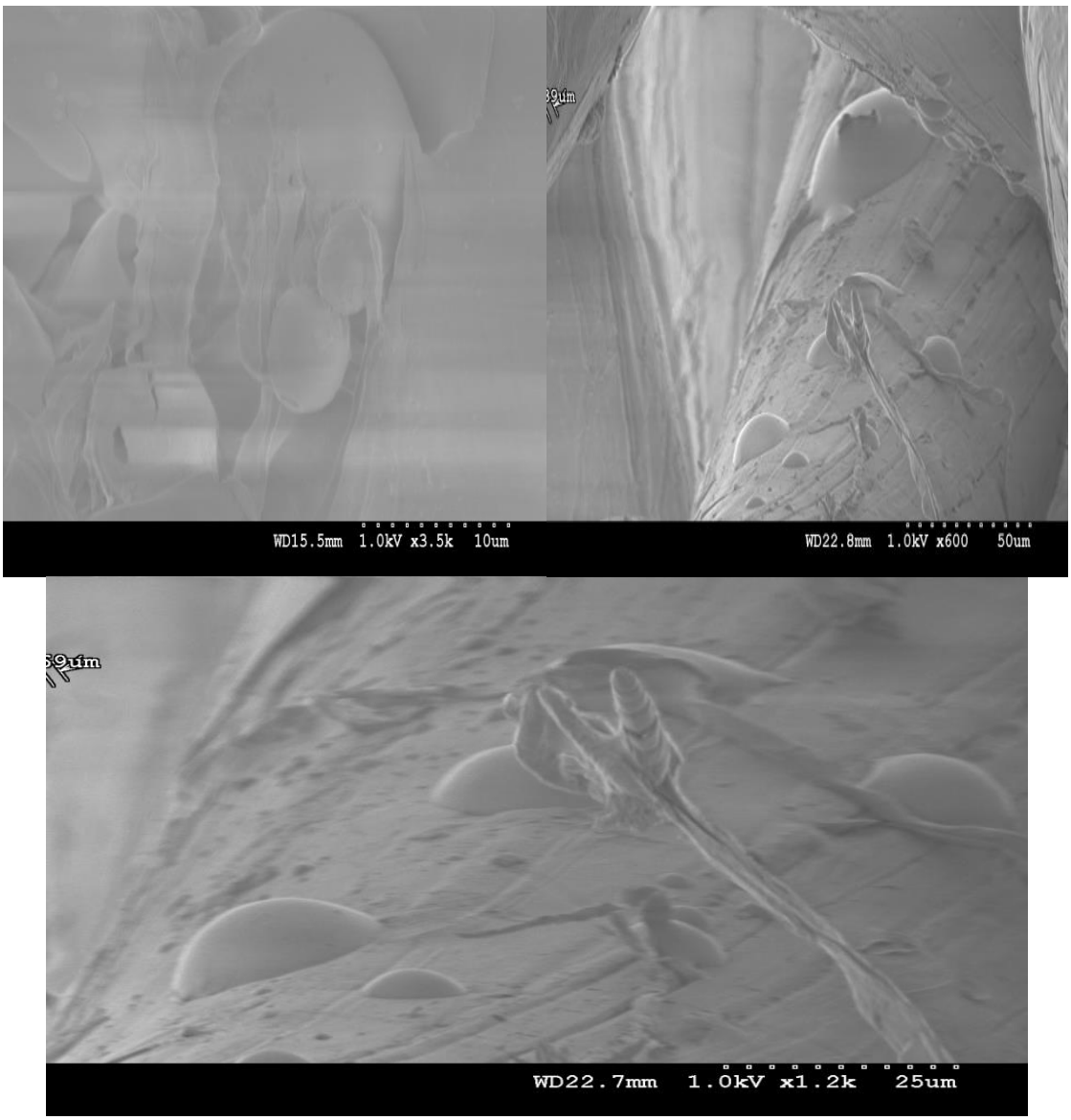

Figure 4.22 Presence of MPCM in multifilament yarn

4.3.4 *Latent heat*

DSC analysis was performed on the developed multifilament yarn. The latent heat curve showed the presence of MPCM in the multifilament yarn. Four levels of MPCM were selected to develop the yarn with the designed spinneret. The levels selected were 2%, 4%, 6% and 8 % of MPCM to incorporate in the yarn. The curve presented in Figure 4.18 shows the latent heat indicated by the area under the curve. The latent heat (the area covered by the curve) in J/g can be calculated from DSC against the specific amount of yarn tested (in grams). As the latent heat depends on the amount of PCM contained in the yarn, small variations in weight of yarn and percentage of MPCM can make change to the amount of latent heat. The amount of latent heat in multifilament

containing yarn with 8% of MPCM was 8.08 J/g as shown in Figure 4.23. Figure 4.24 shows the DSC results for all the multifilament yarns with and without MPCM. It can be seen that it is a straight line for the yarn having no MPCM meaning that the yarn cannot provide latent heat when needed. It is clear that the amount of latent heat contained in the MPCM-containing yarns increases with the increase of the percentage of MPCM. A yarn having more latent heat would be able to offer better thermo-regulating characteristic.

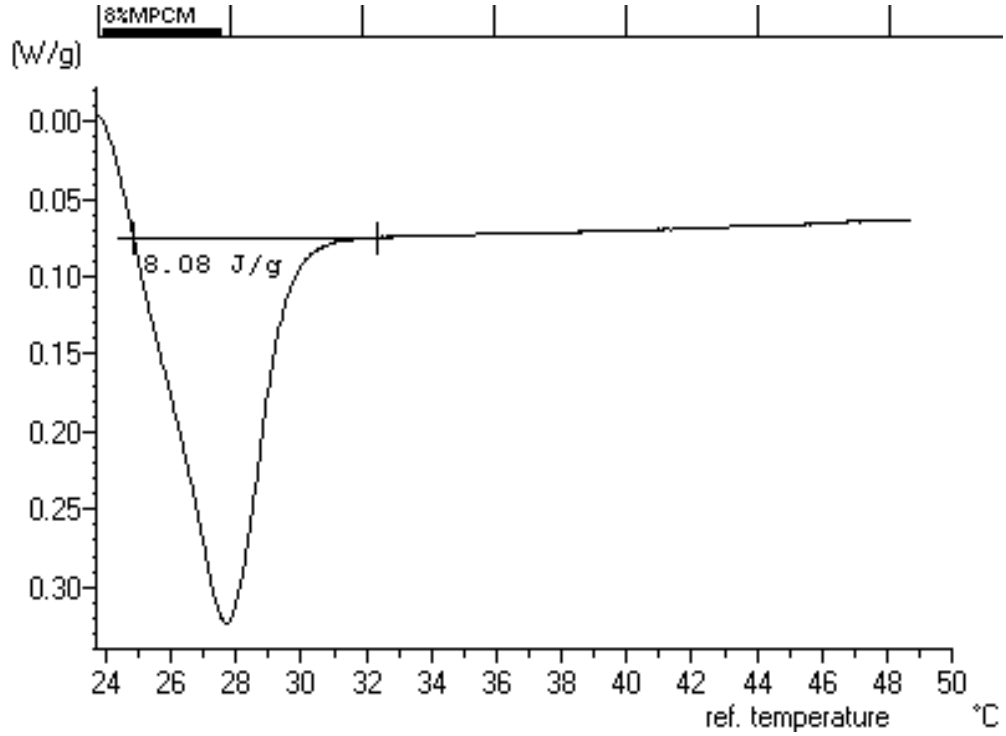

Figure 4.23 Amount of Latent heat in Multifilament Yarn having 8% MPCM

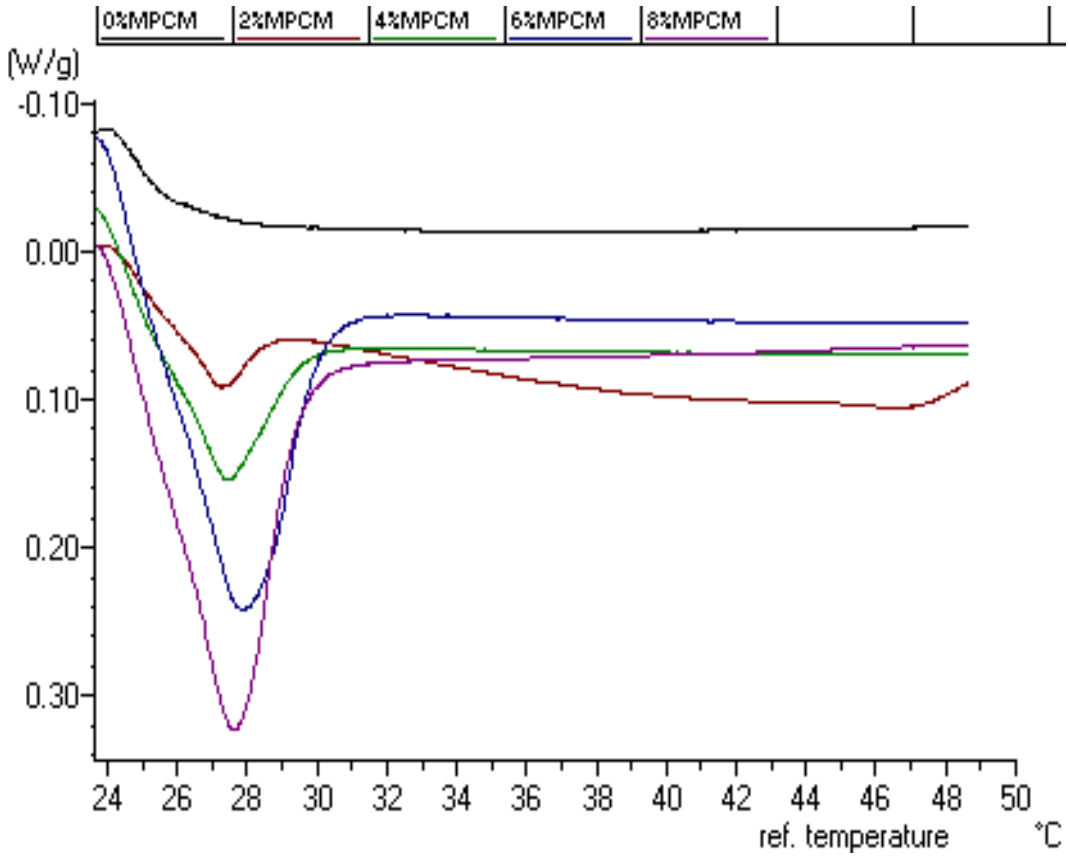

Figure 4.24 Multifilament Yarns containing different amount of MPCM

4.3.5 ***Surface diagram***

In extrusion machine, temperature and extruding speed were found as crucial parameters for the manufacture of multifilament yarn. As the percentage of MPCM in the yarn changes, the parameters change due to the following reasons. First of all the temperature and extruding speed were set for plain multifilament 100% polypropylene yarn without any MPCM. When MPCM was added with increasing percentage, more pressure was required to push the raw material to extrude in order to form homogeneous filament yarns. The pressure on spinneret holes also increases which can be controlled by the diameter and land size of the holes. For this purpose the new spinneret was designed. Due to increase in extruding speed, the stay of polymer in the extrusion chamber reduces which causes insufficient melt of raw materials. The workable solution was found to increase the temperature to certain degrees. The control of these parameters is presented in Figure 4.25, as a surface diagram.

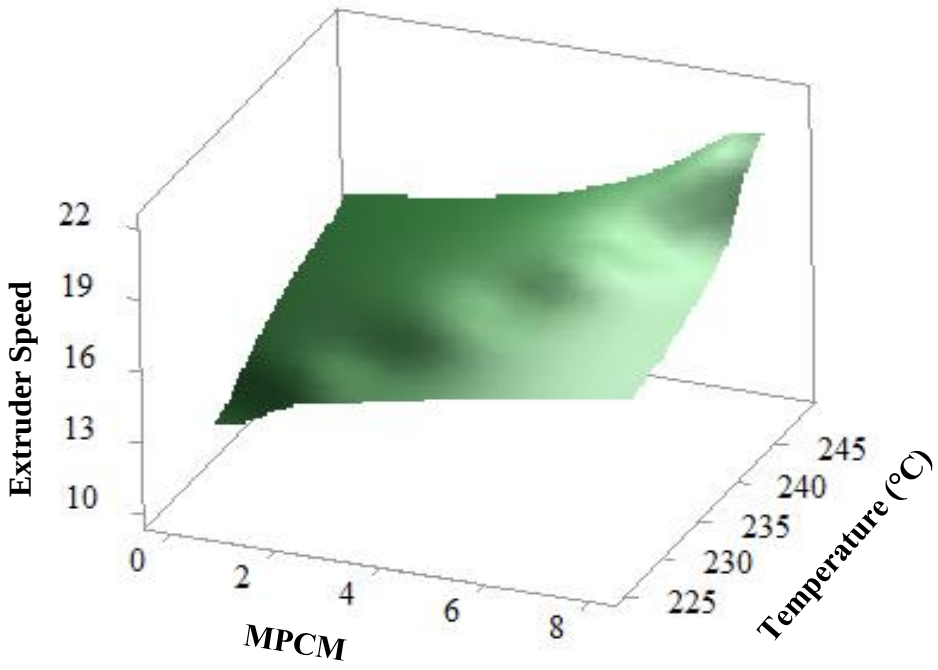

Figure 4.25 Surface diagram for MPCM, Extruder Speed and Temperature

Figure 4.25 illustrates how the temperature and extruding speed is controlled with respect to the amount of MPCM contained in thermoregulating yarn. As the percentage of MPCM increases in the yarn, processing temperature and extruding speed also increase for getting the multifilament MPCM yarn. The graph clearly shows that if higher percentage of MPCM is required, the extruding speed and temperature should be kept at higher level. As the amount of MPCM increases, more pressure is required to push the polymer material homogenously through the spinneret holes which causes the increase in extruding speed. The higher speed results in the short stay of polymer within the extrusion chamber, therefore the temperature has to be increased to compensate the short stay for getting proper melt of the polymer.

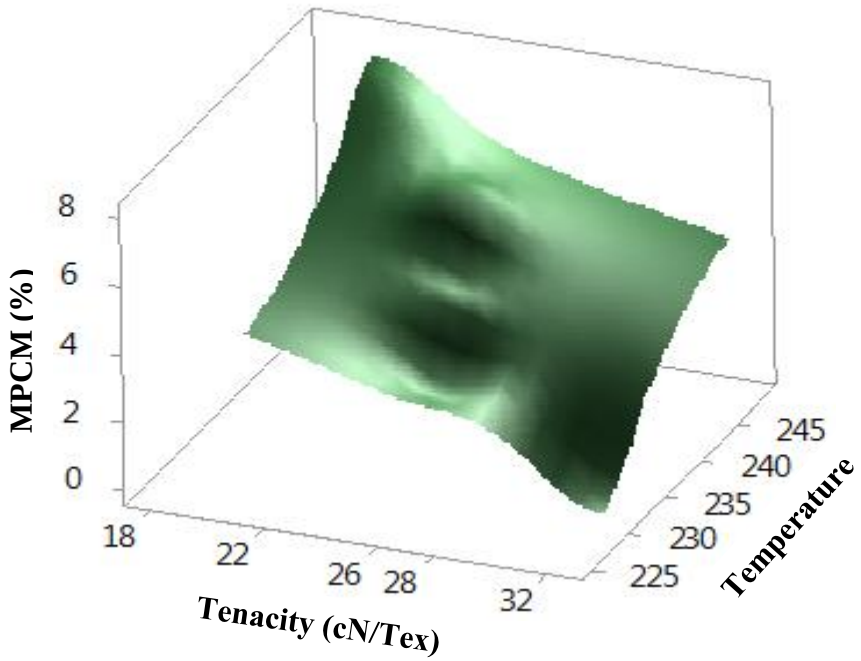

Figure 4.26 Surface diagram for MPCM, Tenacity and Temperature

The surface diagrams in Figure 4.26 and 4.27 indicate the tenacity as a function of the amount of MPCM contained in yarn, extruding temperature and speed. It shows that the strength of yarn decreases with the increase of the amount of MPCM contained in the yarn. The strength of yarn depends on the orientation of molecular chains in the filaments of a yarn. When MPCM are incorporated into yarns, gaps are created in the molecular chains, resulting in reduced strength of the yarn.

The graph in Figure 4.27 clearly indicates that higher strength of yarn can be achieved at lower temperature with low percentage of MPCM. Higher extruding speed creates higher pressure which causes more shear force and disturbing of molecular chains. Furthermore higher feeding speed and pressure do not allow polymer in the conical section of the spinneret to get aligned due to short period stay which causes decrease in molecule orientation and yarn strength [162].

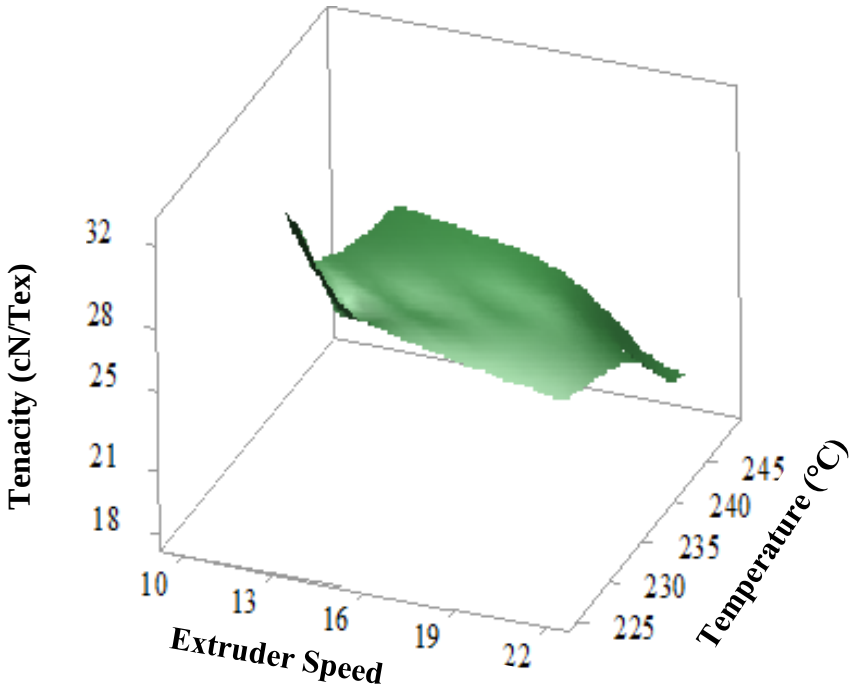

Figure 4.27 Surface diagram between Tenacity, Temperature and Extruder Speed

4.3.6 *IR thermography*

Infrared Thermal Camera has been used to study the thermal characteristics of the engineered fabrics. Two fabrics were made with plain weft knitting structure because woven fabric process is lengthy and requires high amount of filaments. One fabric was made by combination of cotton and the developed multifilament yarns containing MPCM, the other made by cotton and PP only. The blend ratio used was 43/57 (PP/Cotton). The specifications of plain weft knitted fabrics are given in Table 4. 6.

Table 4.6 Plain weft knitted fabric specifications for IR thermography

Fabric	Yarn count (Tex)	Gauge	Stitch cam setting
Without MPCM	37+50 (PP + Cotton)	10	12
With MPCM	37+50 (MPCM PP+ Cotton)	10	12

Both fabrics were carefully placed on the pre-heated knob with temperature of 33°C. The time delay was videoed and recorded for both of the fabrics. The fabric with MPCM containing yarn showed delay to reach the same temperature (30°C) as compared to the fabric without MPCM. The rise in temperature was noted frame by frame based on time which is shown in Figure 4.28. It clearly shows that the

temperature of thermoregulated fabric does not exceed to 29°C even after 30 seconds while the fabric without MPCM reach the same level in less than 10 seconds. Figure 4.29 shows the thermal images of the fabrics with and without MPCM. The temperature of fabric with and without MPCM on spotted area exactly above the heat source has been shown after 40 and 6 seconds respectively. The evaluation clearly shows that the fabric incorporated with MPCM gives better thermo-regulating behaviour. The thermal regulating effect for the fabric with MPCM lasts a very short period because the amount of MPCM in filament is 4% which is randomly distributed within the filament. The thermal regulating effect decreases further when the fabric is exposed to a higher temperature of 45 °C because heat is transferred quicker through the fabric at higher temperature.

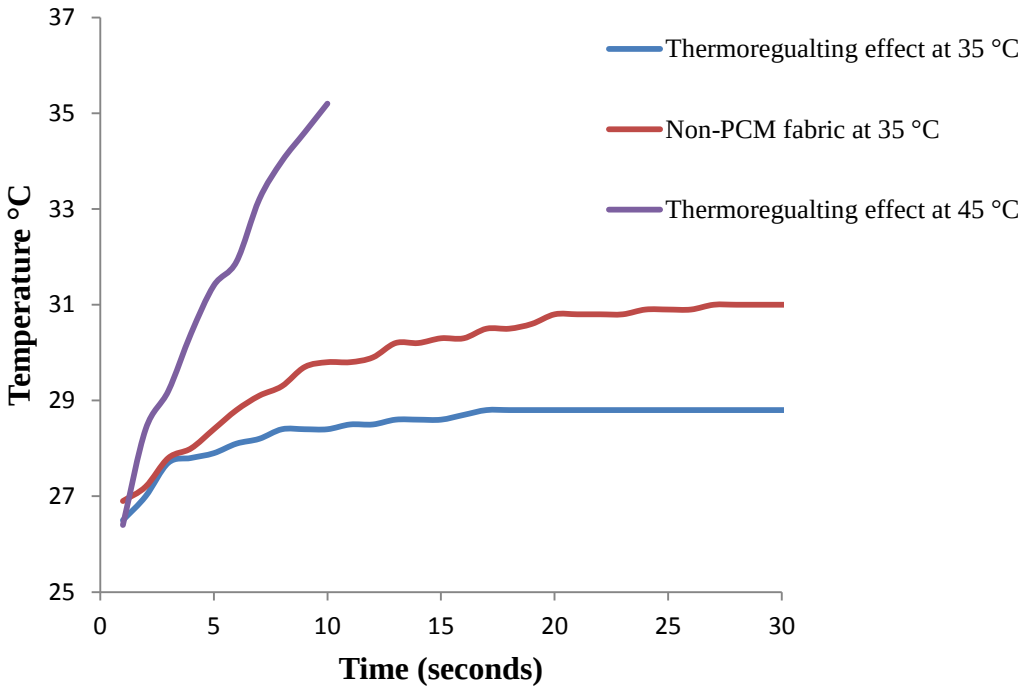

Figure 4.28 Time delay of fabrics with and without MPCM

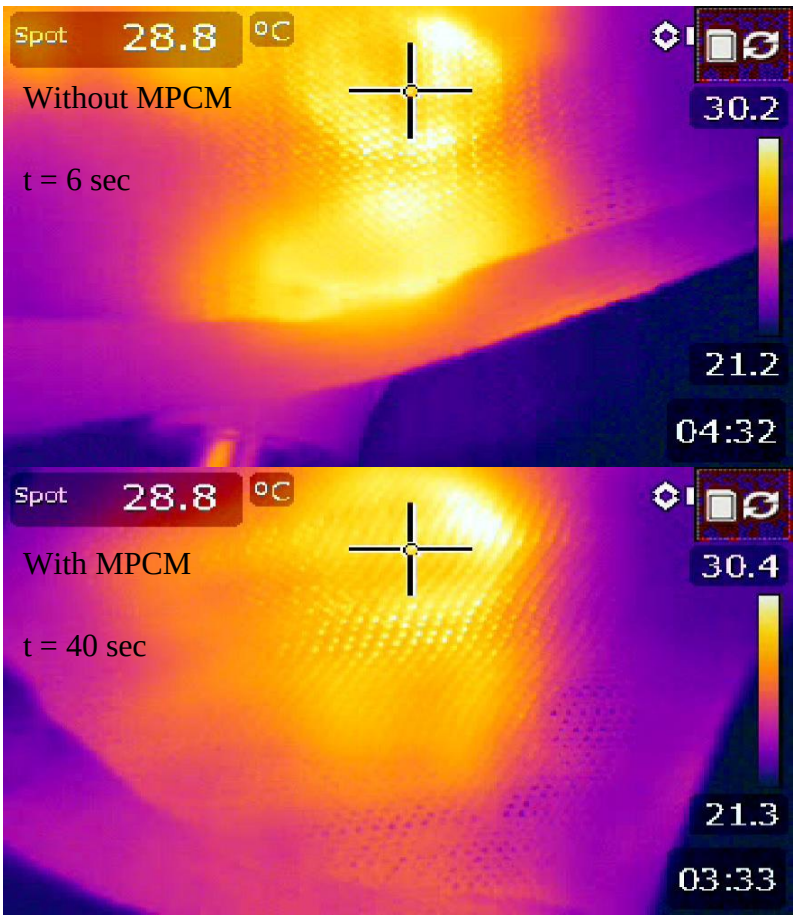

Figure 4.29 Thermal images for fabrics with and without MPCM

Chapter 5 FE thermal analysis of yarn and fabric containing MPCM

This chapter describes the finite element (FE) simulation of fabric incorporated with MPCM for heat transfer analysis using a commercial software ABAQUS. The thermoregulating effect based on the validated FE models is predicted and discussed accordingly. In this study the heat transfer analysis of plain woven fabric was performed using FEM. The purpose of the study was to investigate thermoregulating effect of fabric containing MPCM rather than to study the effect of fabric structures on thermal properties. The knitted structure has already been studied in Chapter 4, therefore the developed MPCM multifilament was woven into fabric for further study of the heat transfer experimentally and to validate the simulation results.

5.1 **Methodology**

Finite element (FE) method has been used to study the heat transfer characteristics of MPCM fabric theoretically. For that purpose commercial software ABAQUS was used for simulation and prediction of thermal regulating effect of the MPCM fabric.

5.1.1 ***Geometric model generation***

Geometric model of fabric was created using TexGen. TexGen is used to generate 3D textile geometry at the level of unit cell in this study. TexGen is flexible designed software and can be used to model many types of textile structures such as woven, knitted and composites. Yarn path, the cross section of the yarn, yarn spacing are the important parameters to be considered when creating yarn and fabric geometries. Figure 5.1 shows a unit cell of plain woven fabric structure developed in TexGen. The actual yarn cross section, yarn spacing and yarn path can be obtained by SEM images.

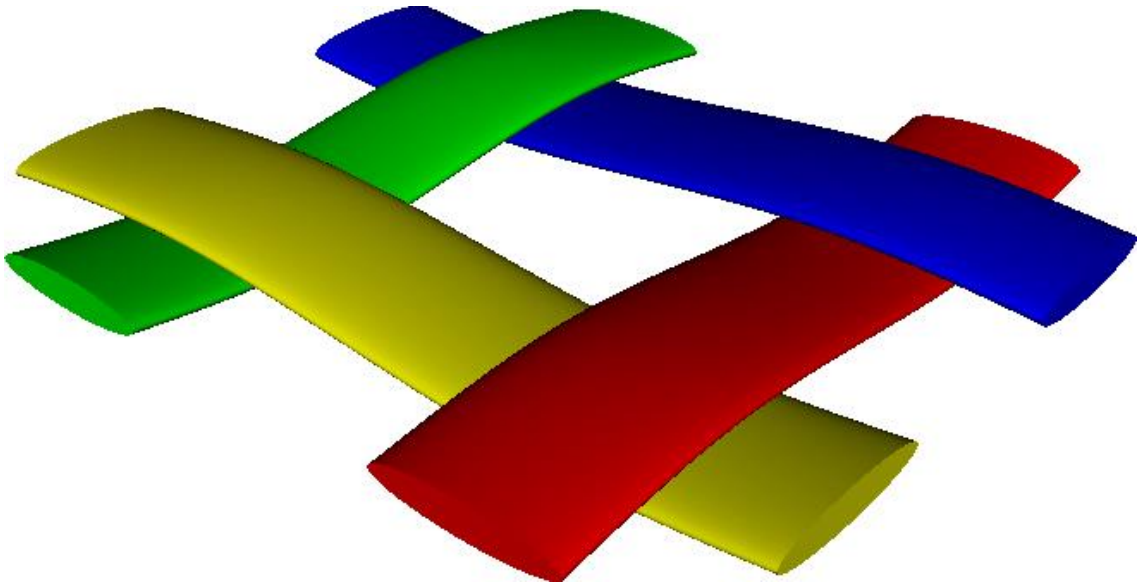

Figure 5.1 Unit geometry of woven fabric by TexGen

The basis of TexGen is the description of yarns using a centreline and superimposed cross section as shown in Figure 5.2. The shape and size of the cross sections can be changed locally using exploited functions in the software where the unit cell of textile can be modified according to geometric considerations to avoid any interpenetration of yarns. When the yarn cross section changes the total amount of fibres within the textile remain constant which means that the total volume fraction or mass does not change. TexGen has automated routines to discretise the model, assign material orientations and properties. The geometric model generated in TexGen was exported to ABAQUS where boundary conditions, material properties etc. can be applied to enable post-processing and analysis.

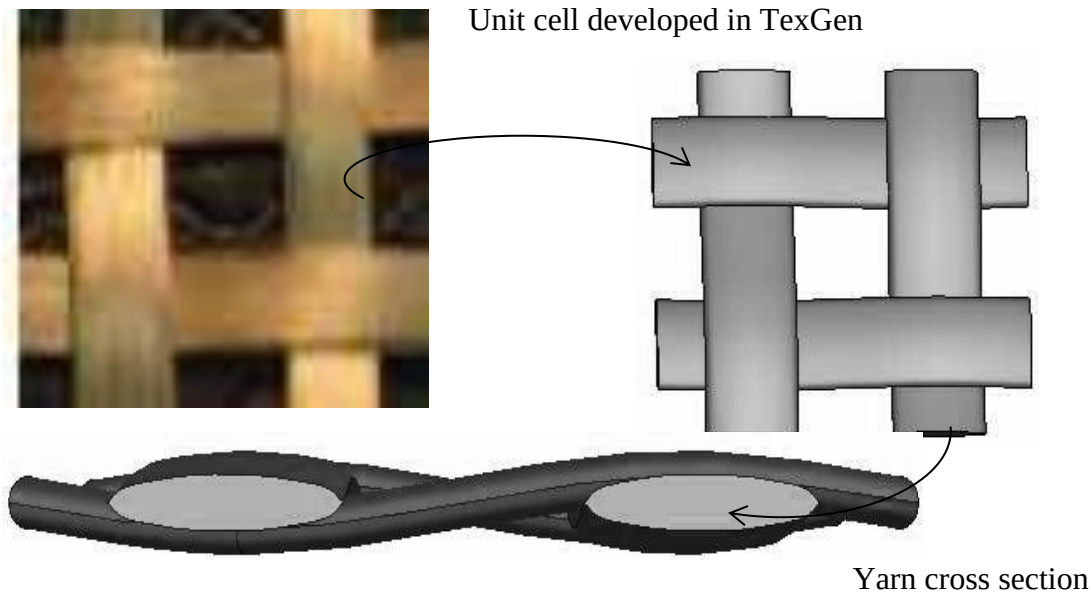

Figure 5.2 TexGen yarn model path and cross section

5.1.2 ***Simulation steps***

Commercial software ABAQUS was used to conduct simulation for the heat transfer study of the yarns and fabrics. The yarn geometric model was developed in ABAQUS while the fabric geometric model was developed using TexGen and was imported in ABAQUS. The MPCM were incorporated within fabric in ABAQUS by creating parts, translating and assembling them. All the parts were then merged together as one model by merging boundary nodes together to create natural contact. The material properties, discretization, and boundary conditions were assigned to the model followed by job submission for post-processing analysis. The basic steps involved in ABAQUS are shown in the flow chart in Figure 5.3.

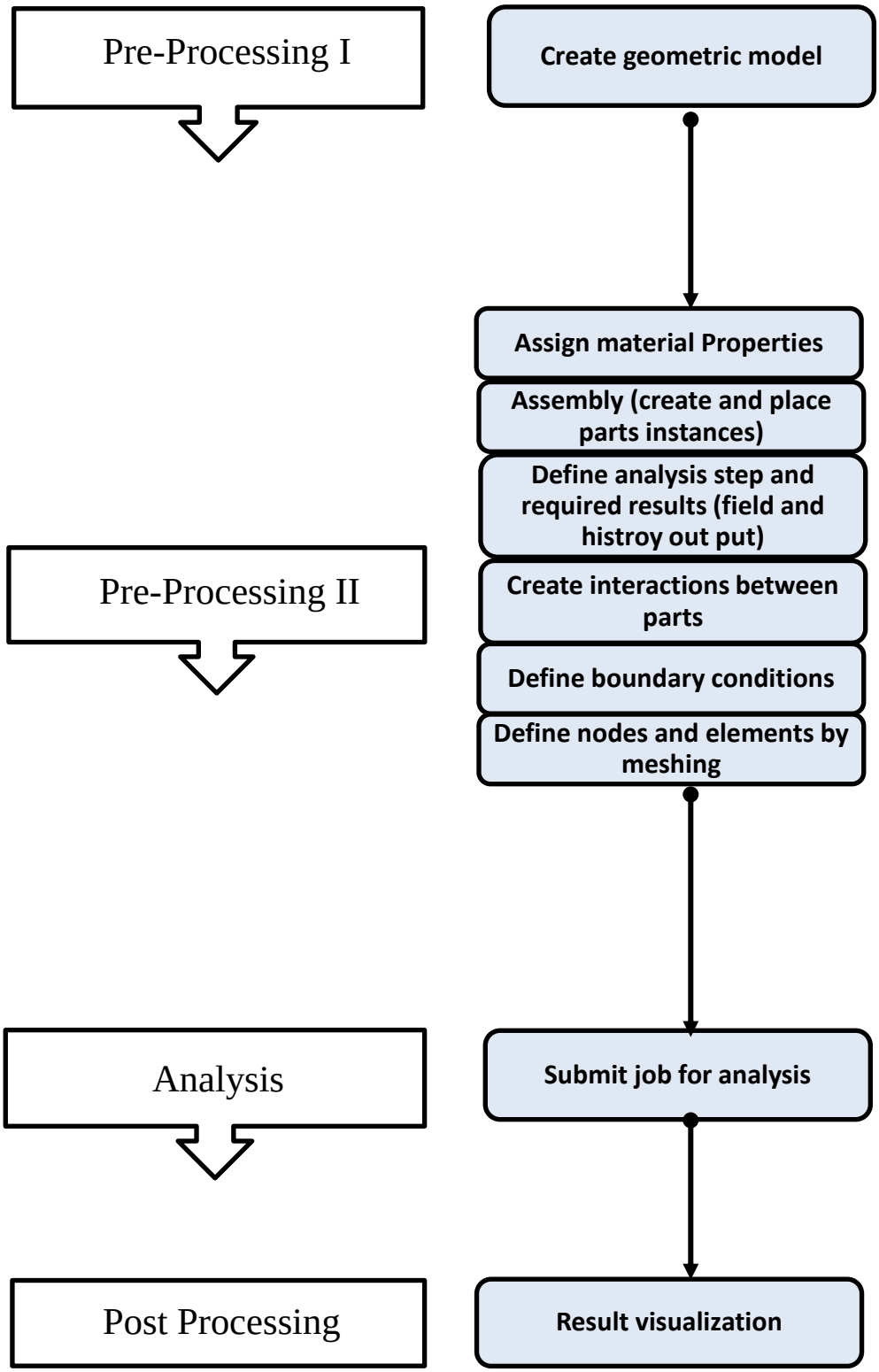

Figure 5.3 Methodology adopted for simulation

5.2 **FE analysis of PCM fabric**

This section describes the heat transfer of woven fabric constructed by MPCM polypropylene filaments. A FE model consisting of a geometrical model has been developed based on the actual fabric made of multifilament polypropylene yarn incorporated with 4% MPCM. The thermoregulating behaviour of the model was investigated based on the validated model. Furthermore fabric made of core (PCM)/ sheath (polypropylene) yarn was studied to predict the thermoregulating zone based on absorbed energy in the form of latent heat. The heat transfer simulation was performed using finite element method under ABAQUS environment.

5.2.1 ***Phase change phenomenon of MPCM fabric***

Heat transfer through conduction follows Fourier's law of heat conduction which is described in equation 5.1.

$$H = k\frac{\Delta T}{\Delta x} \tag{5.14}$$

H is the heat flux, k is the conductivity, Δx is the thickness of the material and ΔT is the temperature gradient.

The heat transfer mechanism can be explained in a model as described in equation 5.2 [163].

$$\int_{V_0}^{V} \rho U dV = \int_{S_0}^{S} q dS + \int_{V_0}^{V} r dV \tag{5.2}$$

Equation 5.2 is the basic energy balance for heat transfer where V is a volume of material with surface area S, ρ is the density of the material, U is the internal energy, q is the heat flux per unit area flowing into the body and r is the heat supplied externally into the body per unit volume.

The above relation is usually written in terms of specific heat as equation 5.3.

$$c(t) = \frac{dU}{dt} \tag{5.3}$$

For latent heat where phase changes involved, the effect is shown in terms of solidus and liquidus temperature indicating area under the curve as latent heat shown in Figure

5.4. The line showing specific heat is linear over the temperature gradient whereas in case of phase change materials the curve makes peak between solidus and liquidus temperature to store energy in terms of latent heat. The area under the curve with blue shaded region is the amount of latent heat or stored energy during phase change.

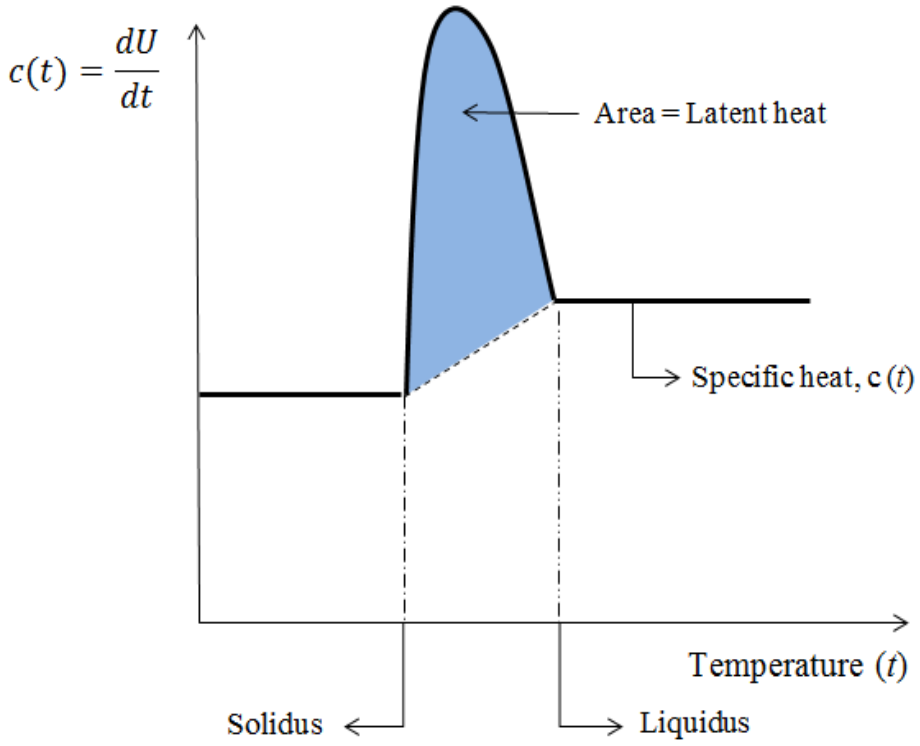

Figure 5.4 Principle of phase change

5.2.2 *Geometric model generation*

Geometric model of woven fabric incorporated with MPCM was developed for heat transfer analysis using finite element method. For geometric model generation, TexGen was used for 3D model generation and the generated 3D geometrical model was exported to ABAQUS for finite element simulation. The shell and core of the microcapsules were generated in ABAQUS and were translated within the yarn of the fabric model. For the calculation of the number of capsules based on 4% of MPCM within the volume of modelled fabric, the length of yarn was determined. Due to the crimp in the yarn the length of yarn in woven fabric is difficult to be determined. A method was developed to determine the length of yarn in a unit cell of woven fabric as shown in Figure 5.5. Furthermore the number of capsules was calculated for crimped yarn length.

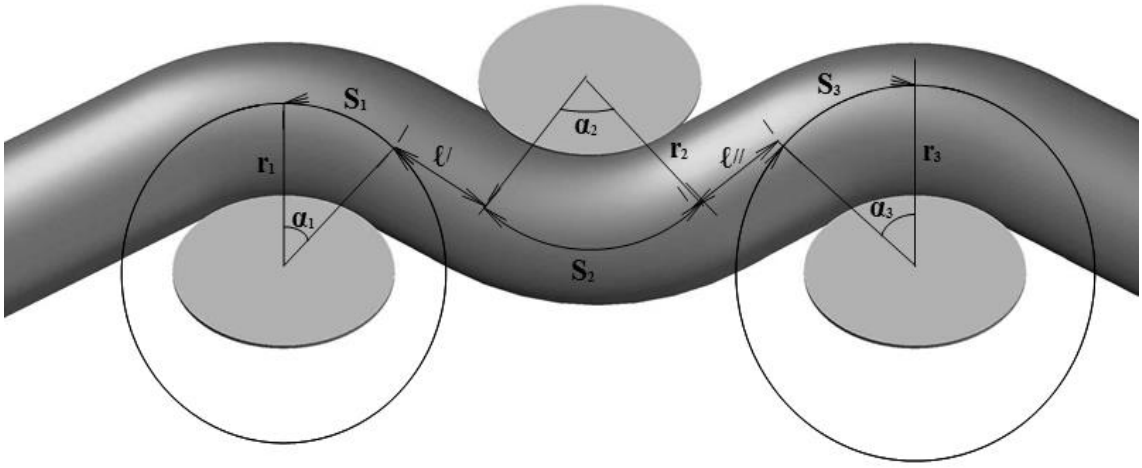

Figure 5.5 Determination of crimped yarn length

The yarn length in a repeat unit of woven fabric can be calculated by equation 5.4.

$$L = S_1 + \ell' + S_2 + \ell'' + S_3 \tag{5.4}$$

where L is the total length of a single yarn in a unit cell and ℓ', ℓ'' are the straight portion of yarn, the arc length S can be calculated by using the relation shown in equation 5.5.

$$S = r\alpha \tag{5.5}$$

where r is the radius of the circular loop and α is the angle of arc. Based on this length, the volume of yarn was calculated and number of capsules within the yarn against the percentage was obtained accordingly.

The above developed method was validated by ImageJ analysis as shown in Figure 5.6. The correlation between the predicted length by numerical method and result from ImageJ was found to be 98.62% showing very high agreement. The values calculated by numerical method and ImageJ software are shown in Table 5.1.

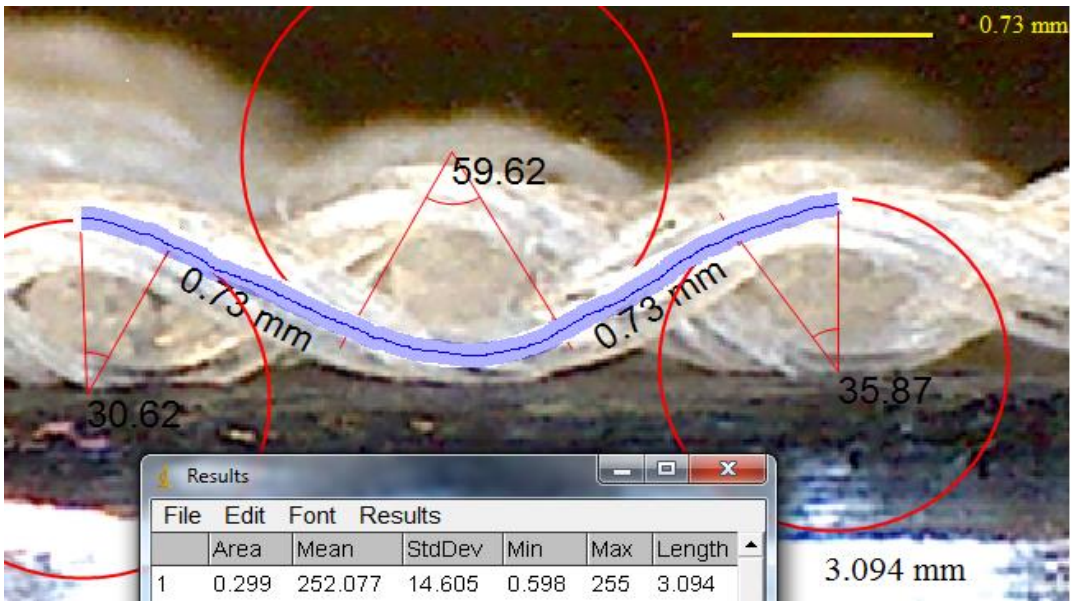

Figure 5.6 Crimped yarn length made in Image Analysis

Table 5.1 Validation of length of crimped yarn

Numerical Method	ImageJ	Relative Error
3.0514 mm	3.094 mm	1.38%

For geometric model of MPCM, the shell thickness of microcapsule was calculated using equation 5.6 [164].

$$T = R\left(1 - \sqrt[3]{\frac{P \times \rho_S}{\rho_C - P \times \rho_C + P \times \rho_S}}\right) \tag{5.6}$$

where T is the thickness of shell, R is the radius of capsule, P is the content of core material, ρ_c is the density of core material and ρ_s is the density of solid shell material.
And the content of the core material can be found by using the following relation as shown in equation 5.7 [165].

$$\text{PCM core content } \% = \frac{\Delta Hcap}{\Delta Hpcm} \times 100 \tag{5.7}$$

where ΔHcap is enthalpy of MPCM and ΔHpcm is the enthalpy of phase change material (core material).

The parameters used for the generation of the geometric model of woven fabric are listed in Table 5.2.

Table 5.2 Specifications of actual fabric to generate geometric model

Warp/Weft major diametre (mm)	0.366
Warp/Weft minor diametre (mm)	0.299
Fabric thickness (mm)	0.860
Total width of unit cell (mm)	0.860
Total length of unit cell (mm)	2.730
Unit cell volume (mm^3)	2.019

The geometric model contains the following parts:

- a unit cell of woven fabric which was modelled in TexGen and exported to Abaqus CAE;
- MPCM consisting of inner part core and outer part solid shell; and
- air to fill the gaps among the yarns.

The geometric model parts are shown in Figure 5.7, consisting of yarn, MPCM and air. The magnified and cross sectional image of MPCM is shown in Figure 5.7 where green part shows the core part comprising of PCM and the encapsulating shell part in dark peach colour.

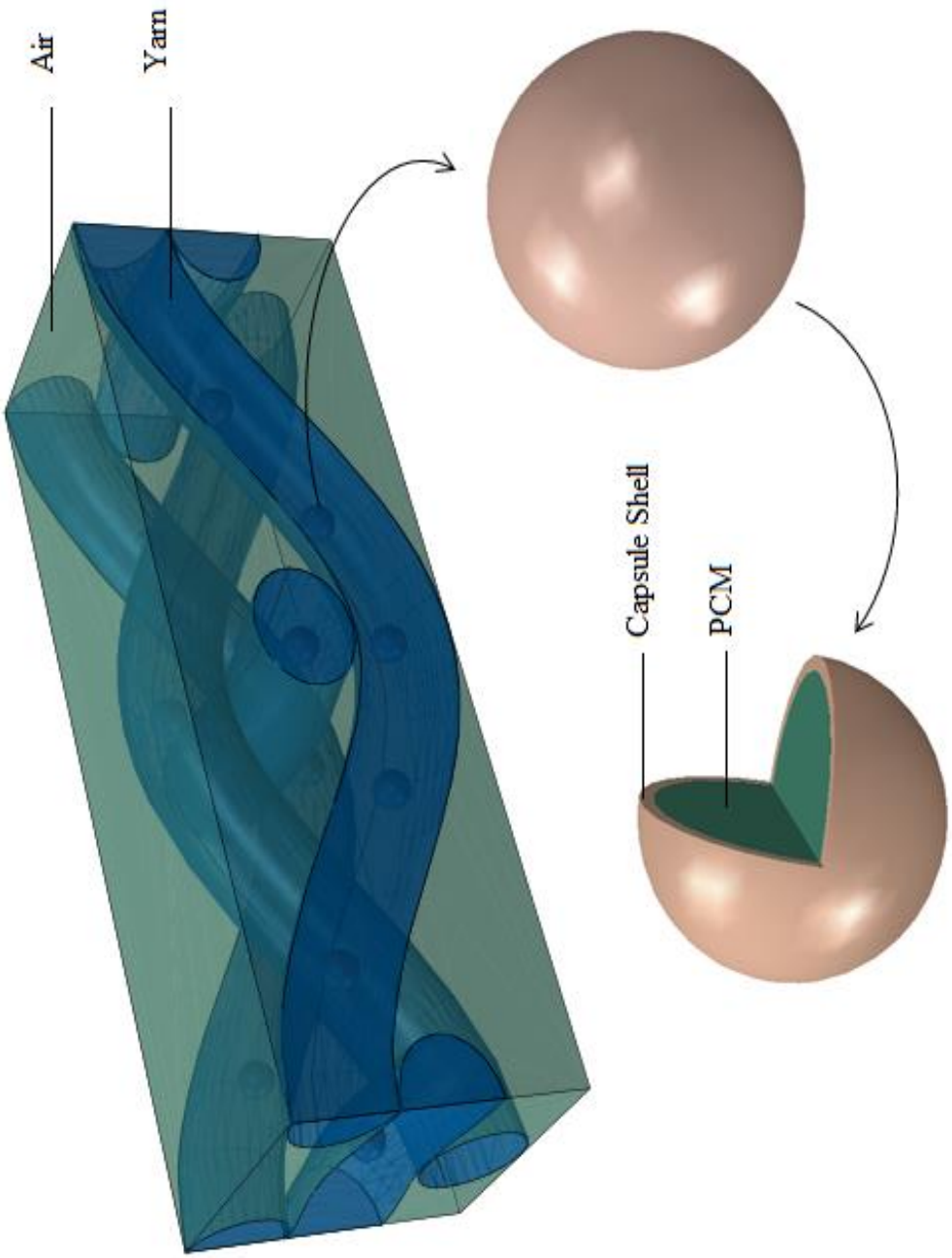

Figure 5.7 Geometric model of fabric made of MPCM yarn

5.2.3 *Material Properties and Interaction*

For theoretical heat transfer analysis the material properties were assigned to all the parts of the MPCM fabric as shown in Table 5.3 and 5.4. The geometry of MPCM was created as 5 times bigger than the actual MPCM capsule size (20 µm) to decrease the number of capsules for optimum mesh density and cost effective simulation. All the steps mentioned in section 5.1.2 were followed to execute the simulation.

Table 5.3 Physical properties of MPCM

Properties of MPCM	
PCM	n-octadecane (C_{18})
Capsule Material	Melamine Formaldehyde
Particle size (µm)	17-20
Melting Point (°C)	28.2
Latent heat (KJ/Kg)	170-190

The thermo-physical properties of materials are shown in Table 5.4 which was used for transient phase change heat transfer analysis. As filament was composed of three materials; polypropylene as fibre base material, melamine formaldehyde and n-octadecane as shell and core materials of MPCM capsules respectively.

Table 5.4 Thermo-physical properties of materials used in the model of MPCM fabric

Property	n-octadecane	Melamine Formaldehyde	Polypropylene
Density (kg/m^3)	777	1500	910
Specific heat (KJ/Kg °K)	1.9	1.2	1.925
Thermal conductivity (W/m°K)	0.3	0.5	0.137
Latent heat of fusion (KJ/Kg)	238		

The complete geometric model comprises of four materials including air, yarn (polypropylene), capsule (melamine formaldehyde) and phase change material (n-octadecane).

For finite element analysis the following assumptions were taken into consideration:

- yarn is considered as uniform solid;
- effect of radiation is neglected due to small gradient of temperature;
- effect of convection is neglected; and
- no change in PCM density over change in temperature;

For simulation, all different parts brought together to make a single part model. For the purpose, interaction among all different parts created by merging them into a single part to induce thermal contact.

5.2.4 *Model discretisation and boundary conditions*

Four-node linear tetrahedral DC3D4 was used for meshing the model and the mesh density with 1387523 elements was obtained. The initial condition was used for the whole model and boundary condition was assigned to the one side of the fabric as done in real experiment. The sides of the fabric were considered as completely insulated. Two temperature boundary conditions are used as follow:

$T_{(1)} = T_1$

$T_{(2)} = T_2$

T_1 is the initial temperature of the fabric while T_2 is the boundary temperature of the fabric.

5.2.5 *Experimental study of fabric thermal property*

The heat flux of the fabric was tested using an in house developed heat transfer device [159]. The main components of the setup consist of hot and cold plates, a heater, a heat flux sensor and a heat sink fan as shown in Figure 5.8. The fabric sample under investigation was placed between the cold and hot plates where the lower hot plate was heated by a controlled heater. Thermocouples are attached to the plates which sense and monitor the temperature (T_1) and (T_2). The temperature difference of hot and cold plates allows the heat to transfer from one side of the fabric sample to the other side. The heat flux sensor is attached to the upper plate and cooled by heat sink fan and gives the value of heat flux by dividing the value on multi-meter with flux sensor's sensitivity.

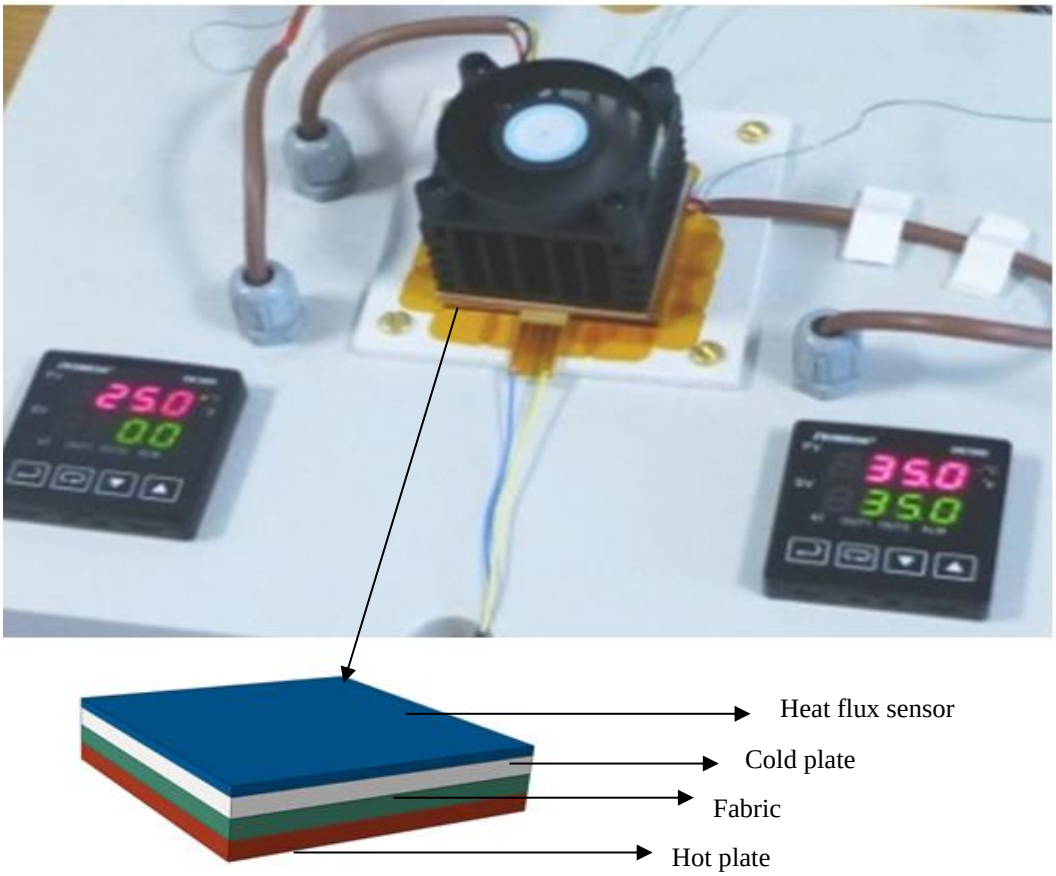

Figure 5.8 Experimental setup

5.2.6 *Validation of simulated model*

Figure 5.9 shows the simulation results of heat flux contour and temperature contour values for the fabric containing 4% MPCM.

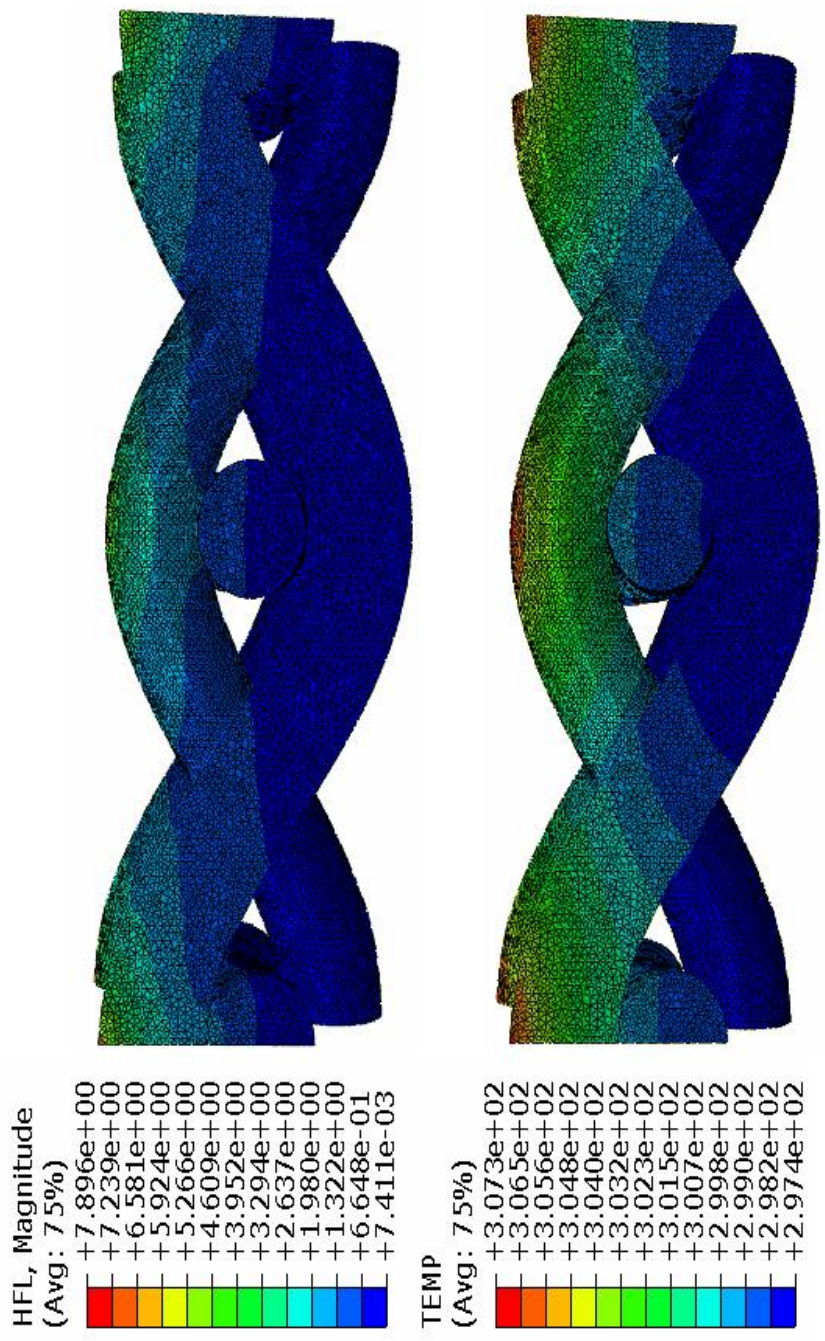

Figure 5.9 Heat flux and temperature contour

Figure 5.10 shows the translucent visualization of fabric model after simulation. The model is shown as a single part containing MPCM inside of yarn and distributed evenly. The magnified image shows the heat transfer through the fabric and MPCM.

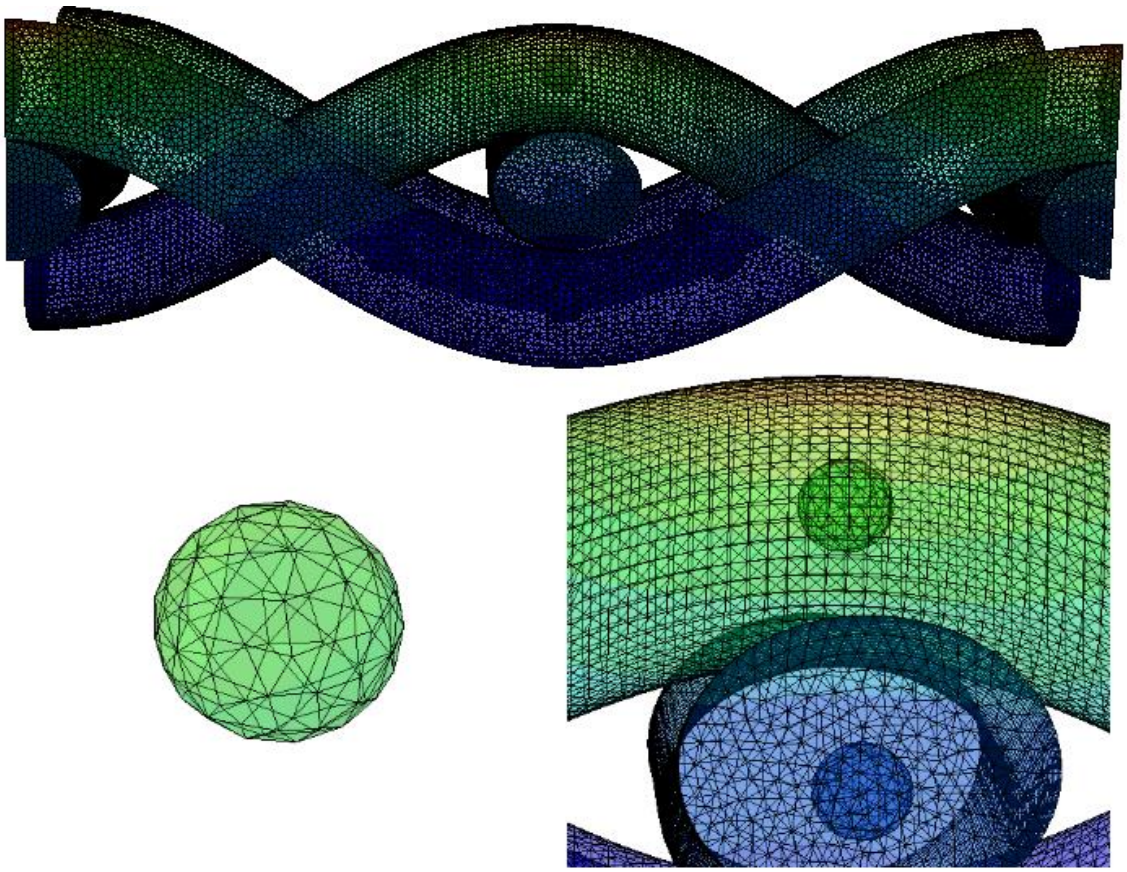

Figure 5.10 Visualization of fabric model containing MPCM

Table 5.5 shows the heat flux values obtained experimentally and predicted from FE model post processing in ABAQUS. The agreement between the two is 91.02% which shows that the model is successful and can be used for further study of heat transfer characteristics of MPCM fabric. The heat flux measured experimentally was 583.33 W/m^2 which is less than the predicted value 635.70 W/m^2. This is due to the traces of air present between the multifilament yarns in actual fabric whereas in FE model, the multifilament yarns were assumed as a solid material. The presence of air provides insulating effect hence decreases the amount of heat flow in the yarn. This methodology adopted in the model can be used to analyse heat transfer of different textiles incorporated with MPCM and fabrics containing different amount of MPCM.

Table 5.5 Results comparison between FE model and experiment

Obtained from experiment (W/m^2)	Predicted from simulation (W/m^2)	Relative Error
583.33	635.70	8.98%

5.2.7 *Prediction of thermoregulating effect*

Prediction of thermoregulating effect was conducted with the fabric containing 4% MPCM, 10% MPCM and PCM in core against the control fabric without any MPCM. Figure 5.11 shows the images of fabric containing PCM in core and the meshed fabric made of core/sheath yarn.

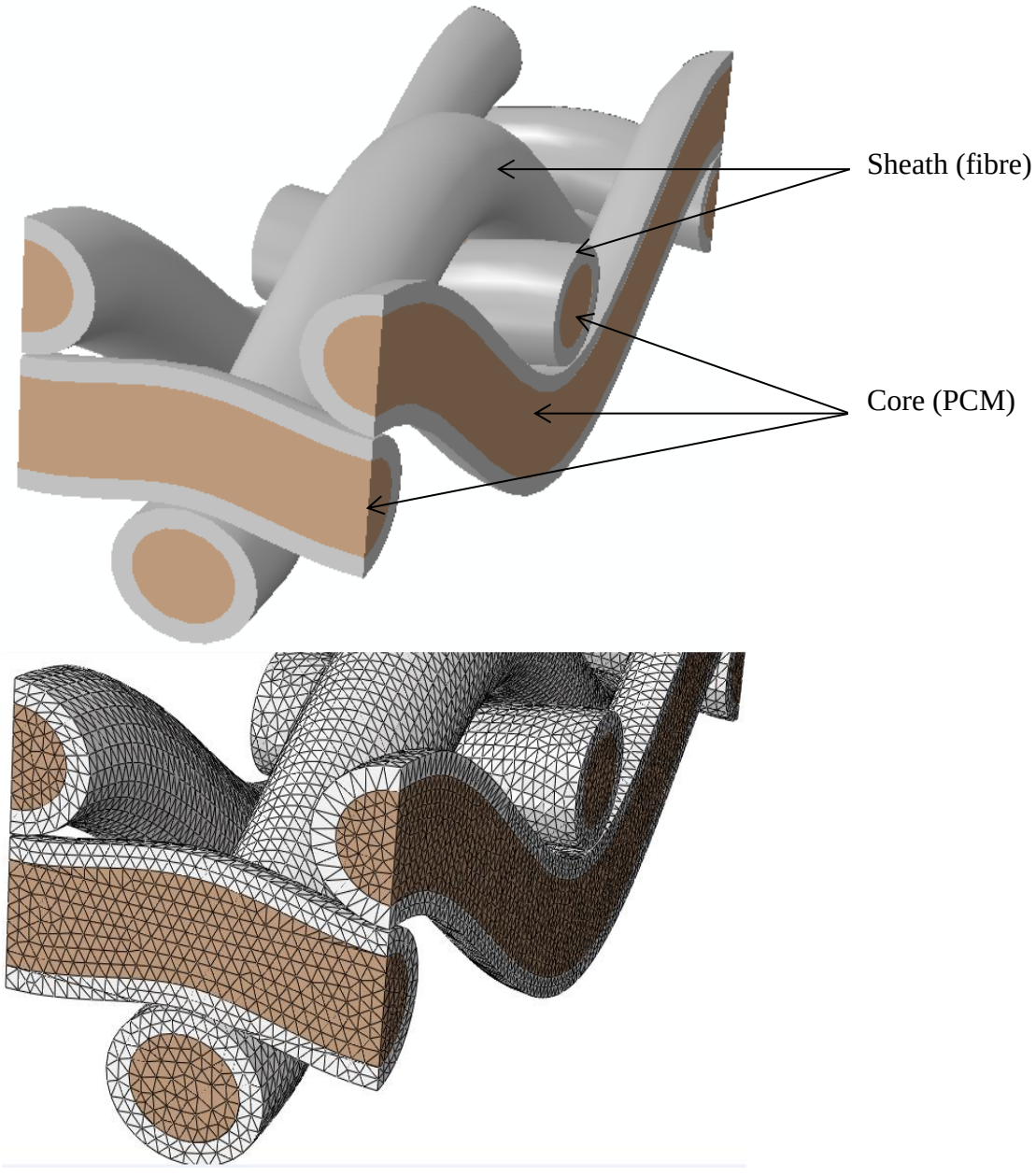

Figure 5.11 Core/Sheath fabric containing PCM in core of yarn

Figure 5.12 shows the cut view of fabric with and without MPCM from z-axis at time interval t=2000 second for both fabrics with and without MPCM. The temperature where MPCM are not present, the fabric reaches around 39 °C in grey colour as shown

in Figure 5.12. The same area where capsules are present in the fabric containing MPCM shows the temperature around 27 °C which enables the thermoregulating effect of MPCM within the fabric. Even the places where phase change capsules are not present in the fabric containing MPCM also show the grey colour indicating the maximum temperature of 39 °C.

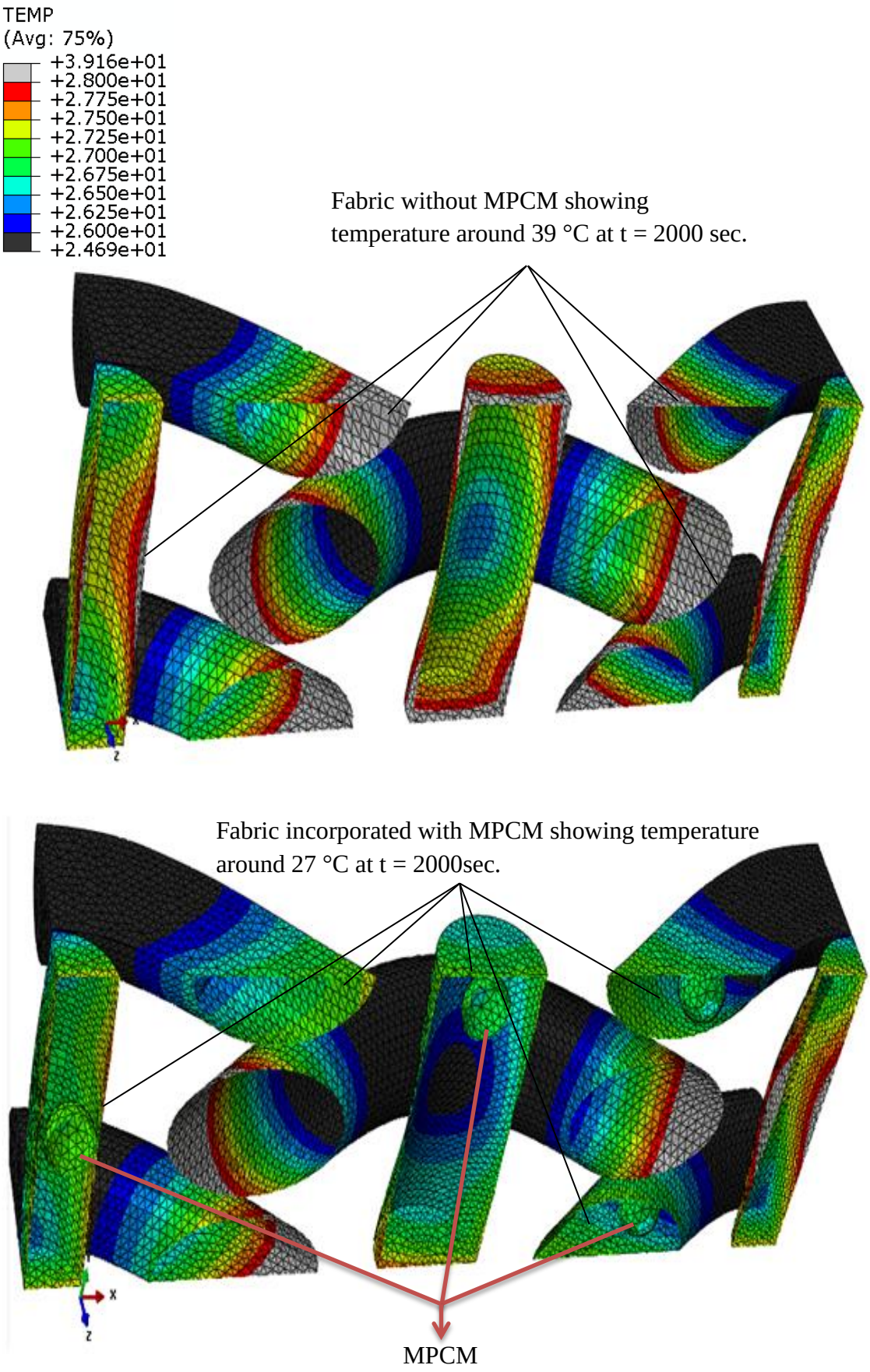

Figure 5.12 Cut view of Fabrics with and without MPCM from Z-axis

Figure 5.13 shows the cut view of fabric made of core sheath yarn with PCM in the core against the control fabric without PCM from z-axis at time interval t= 2000sec. The temperature in the fabric without PCM reaches around 39 °C at the specific area in grey colour shown in Figure 5.13. The same area in the fabric containing PCM in core shows the temperature around 23-25 °C which confirms the thermoregulating effect of PCM within the fabric. This lowest temperature can be seen in the whole fabric with blue colour as a result of the PCM present in the whole area of the fabric.

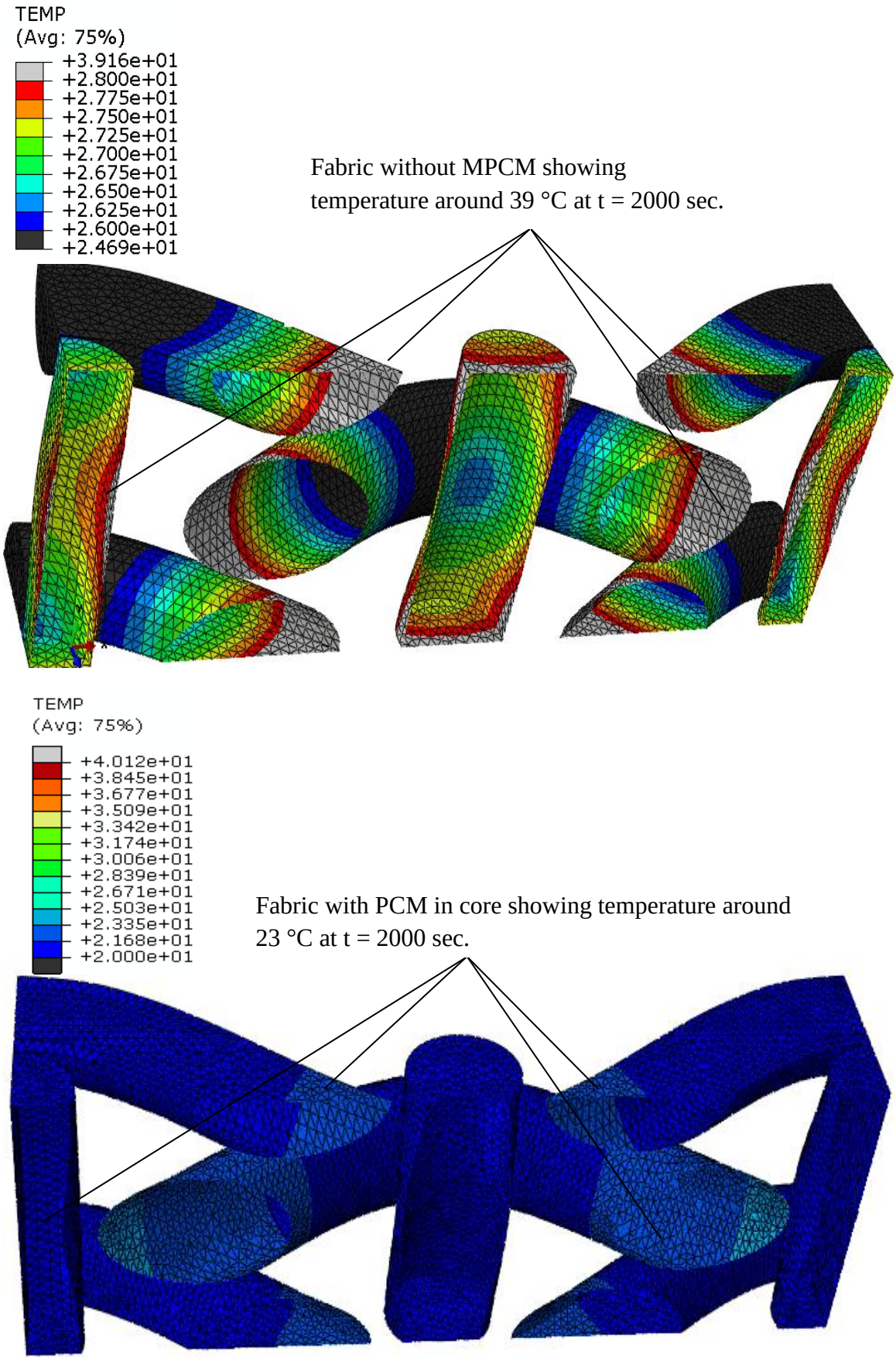

Figure 5.13 Cut view of fabric without MPCM and PCM in core from z-axis

5.2.8 *Time dependent thermoregulating effect*

PCM starts melting at its melting temperature and stores energy in the form of latent heat. The constant supply of heat does not allow the temperature to rise near the melting point of PCM and makes delay in temperature increase for certain period of time depending on the amount of PCM used. This delay in temperature increasing characteristic of PCM with time is difficult to determine experimentally. This thermoregulating property has been predicted using post processing in ABAQUS based on the validated model as determined for the case of yarn described previously.

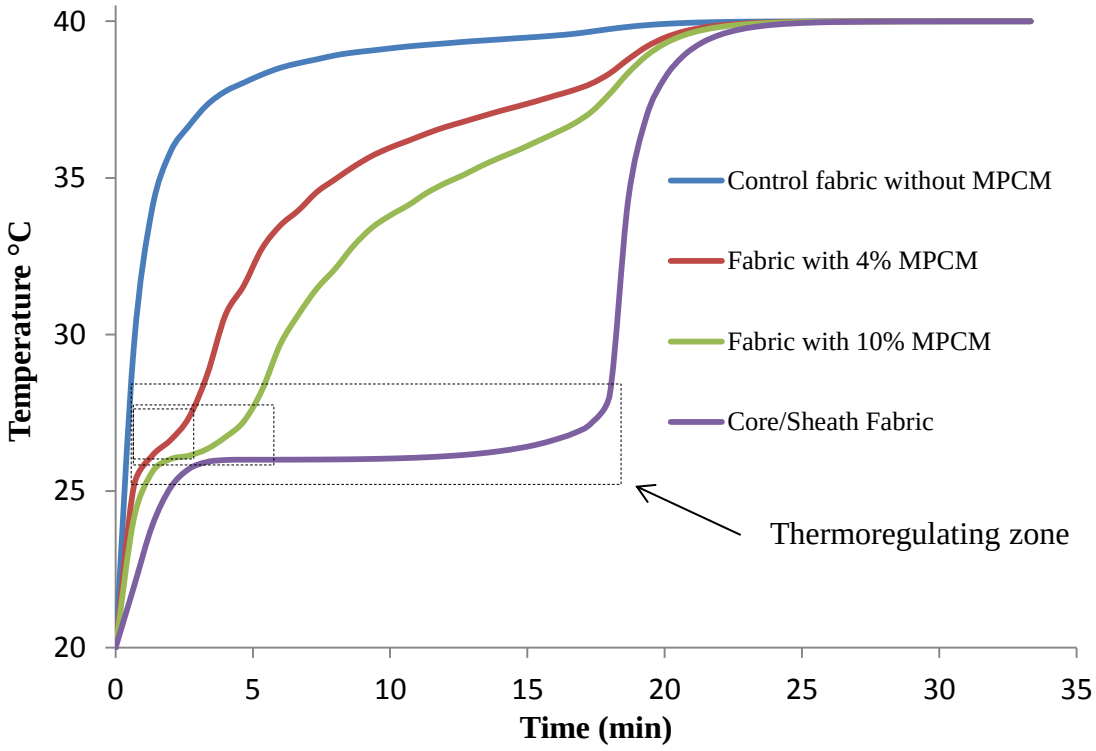

Figure 5.14 Time dependent thermoregulating effect at 40 °C

Figure 5.14 shows the time dependent temperature change for the four fabrics: without MPCM, with 4% MPCM, with 10% MPCM and the PCM in core of yarn in the fabric. Overall the temperature increases as the time increases. However for the fabrics containing phase change materials, the graphs near the phase change temperature proceed parallel to the time axis showing latent heat storage, resulting in the delay in temperature increase. The maximum effect can be seen in fabric made of core/sheath yarn where the amount of PCM is 70% showing that as the amount of PCM increases in the fabric from 4% to 70%, the thermo-regulating effect is enhanced. The thermoregulating zone is shown by dashed boxes for all the fabrics in Figure 5.14.

There is no thermoregulating zone for the fabric without MPCM. For the fabric with 4% MPCM the thermoregulation effect lasts for 2 minutes and for the fabric with 10% MPCM the effect lasts for around 5 minutes. While for the fabric containing 70% PCM in core of yarn the effect lasts even longer for around 17 minutes.

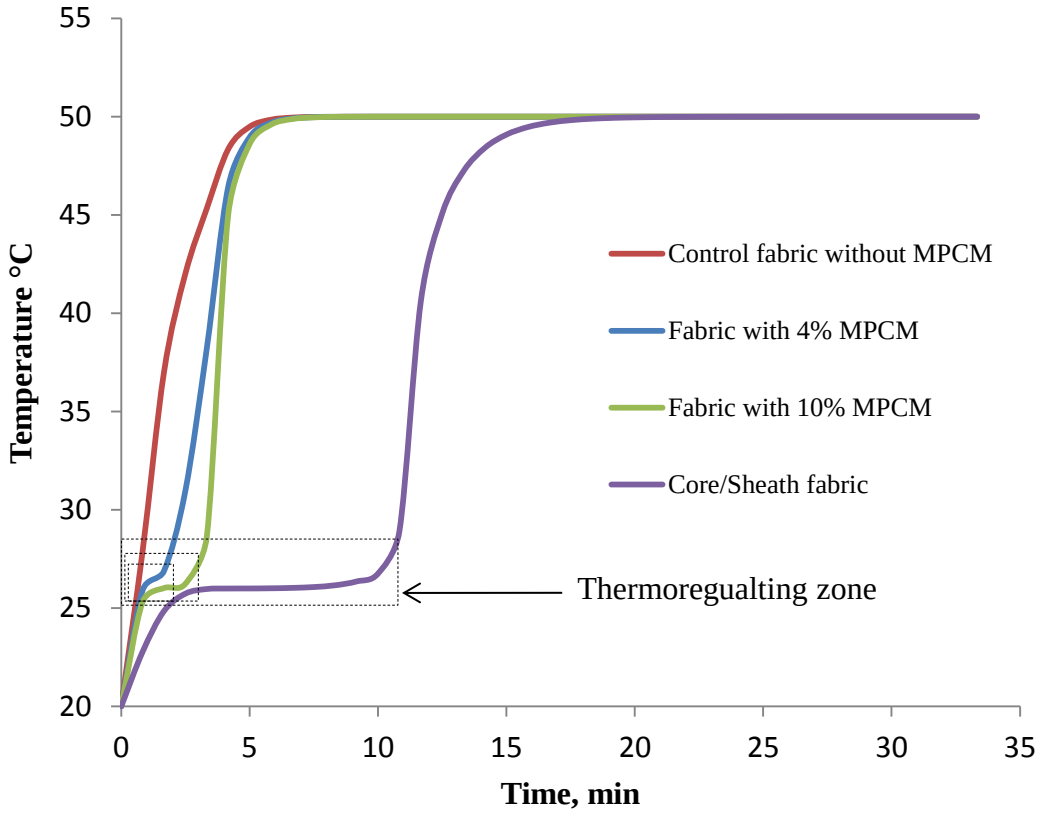

Figure 5.15 Time dependent thermoregulating effect at 50 °C

In certain regions the day temperature can raise up to 50 °C which may be able to affect the thermoregulating environment due to high amount of heat. The thermoregulating effect of all above fabrics is also predicted by raising the temperature of fabric up to 50 °C. The thermoregulating effect decreases by increasing the temperature to the higher level as shown in Figure 5.15. The fabrics containing MPCM also delay the temperature rise and this effect increases as the amount of MPCM increases. The comparison of thermoregulating fabric at 40 °C and 50 °C is shown in Figure 5.15.

Figure 5.16 shows the comparison of temperature delay of fabric made of core/sheath yarn at 40 °C and 50 °C. The temperature delay can be seen in both cases as the time proceeds but the thermoregulating effect decreases as the analysis temperature increases. The thermoregulating environment for the fabric at 40 °C lasts for around 17

minutes while for the fabric at 50 °C, it only last for 10 minutes. This may be caused by the amount of heat increase at higher temperature which causes the heat to transfer quickly at higher temperature as compared to the fabric exposed to lower temperature.

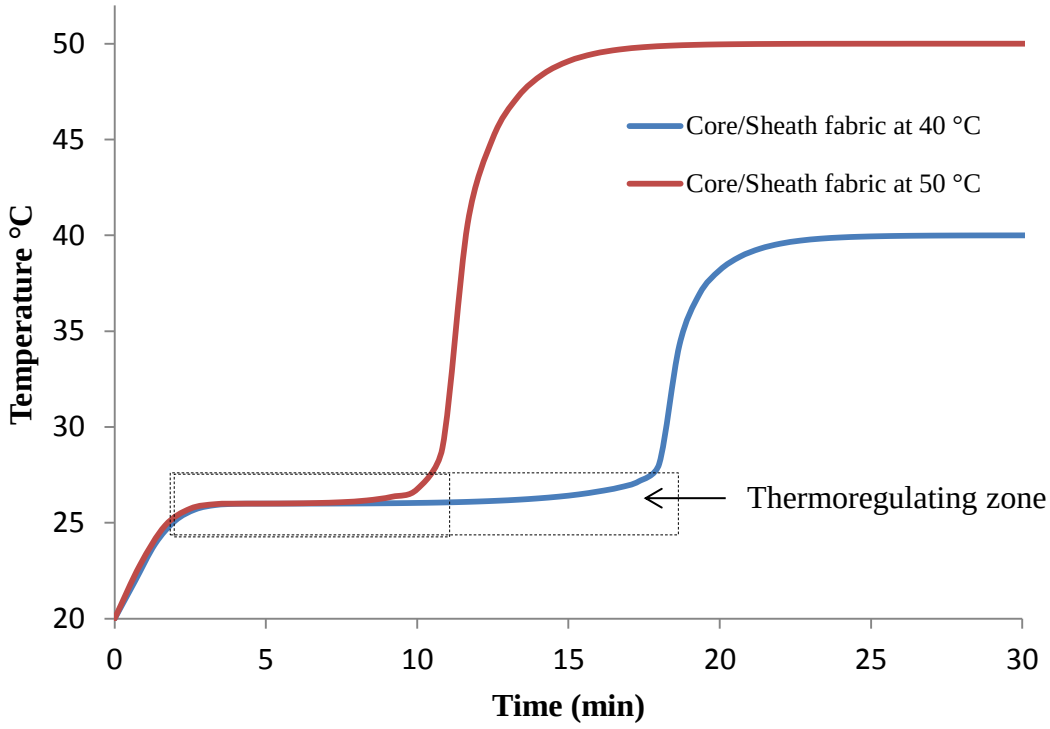

Figure 5.16 Comparison of core/sheath fabric at 40 °C vs 50 °C

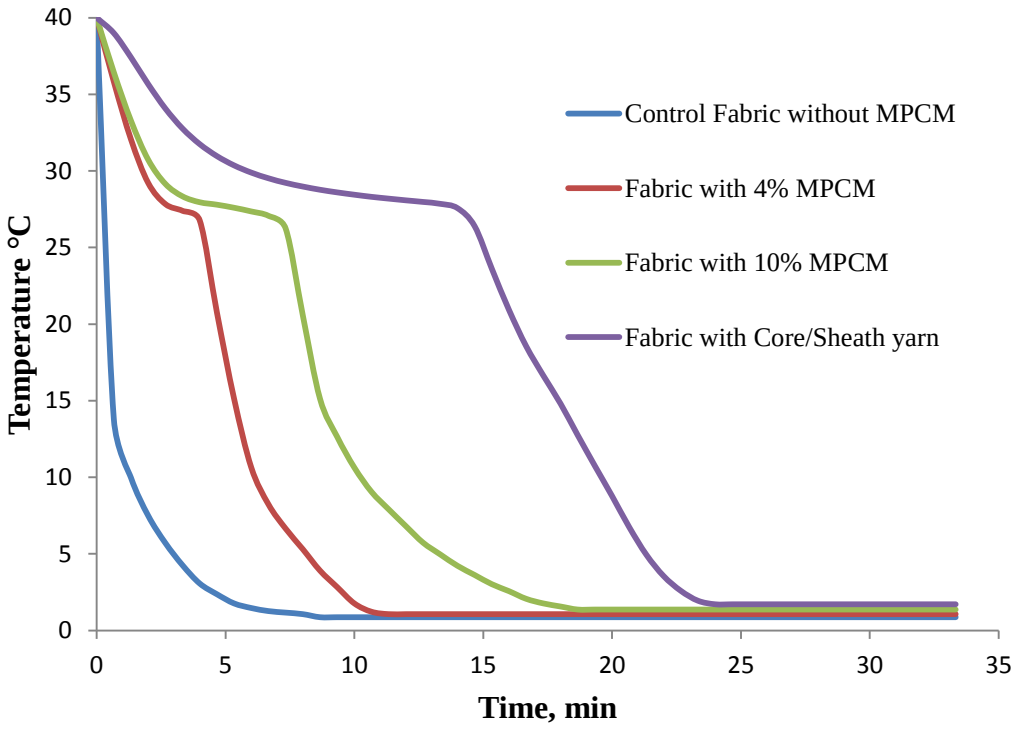

Figure 5.17 Thermoregulating effect against cold temperature

Figure 5.17 shows the thermoregulating effect against cold temperature of simulated fabrics containing 4% MPCM, 10% MPCM and PCM in core with control fabric without MPCM. The effect is simulated from 40 °C to 0 °C to predict the thermoregulating effect against the cold weather. The thermoregulating effect can be seen in Figure 5.17 near to the phase change temperature 28 °C. PCMs are reversible materials therefore the phase change process is exactly reversible which solidifies PCM upon cooling and releases absorbed energy providing thermoregulating effect.

Figure 5.18 shows the comparison of heating and cooling of fabrics containing PCM in core of yarn. The thermoregulating zone is shown in Figure 5.18 which illustrates that when fabric temperature goes from 20 °C to 40 °C during heating, the thermoregulating effect lasts for around 17-18 minutes while upon cooling from 40 °C to 0 °C, the effect lasts 15 minutes because the temperature difference in this process is more compared to heating effect. The 0 °C temperature is simulated for winter season to investigate the thermoregulating effect.

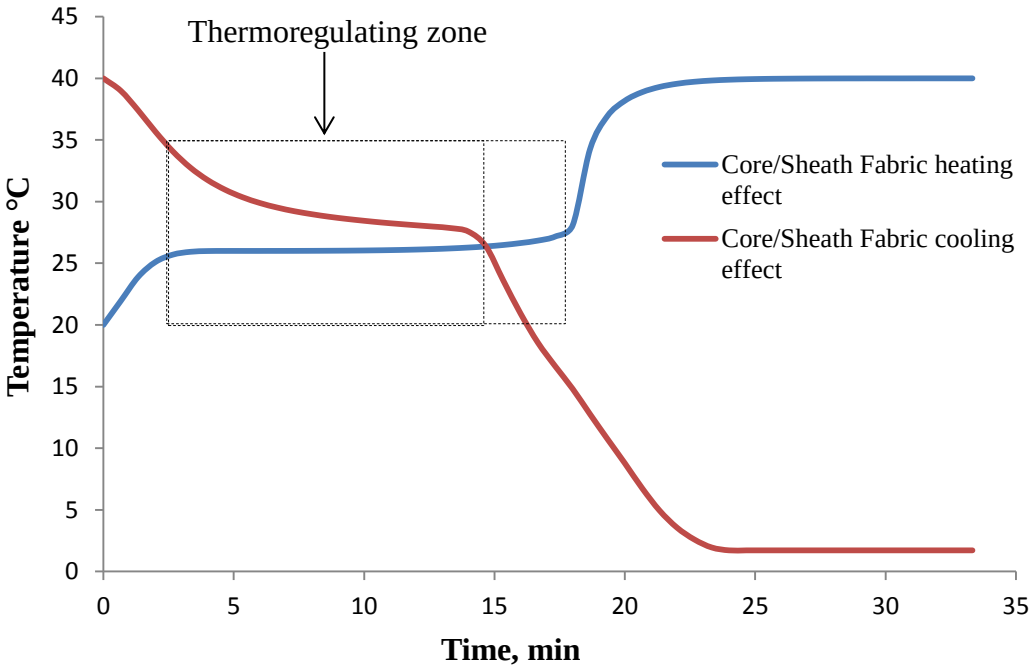

Figure 5.18 Comparison of heating and cooling of Core/Sheath fabric

In certain environment, the temperature can be severe up to freezing and hence it is important to predict the thermoregulating effect of textiles containing phase change materials. Figure 5.19 shows the thermoregulating effect of fabric containing 10% MPCM and PCM in the core of yarn against the control fabric without MPCM. The thermoregulating zone is indicated by dashed boxes. The thermal arrest for the fabric made of core/sheath yarn continues for 6 minutes while for fabric containing 10% MPCM, thermal arrest is quite short.

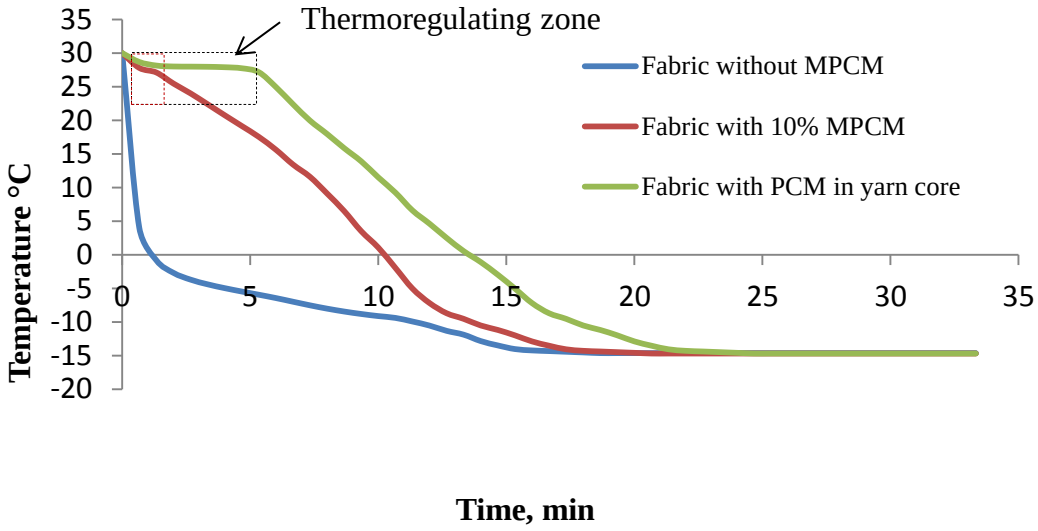

Figure 5.19 Cooling of thermoregulating fabrics to freezing temperature

The comparison of fabrics containing PCM in core of yarn is shown in Figure 5.20 to study the thermal behaviour of fabric under extreme low temperature. The fabric exposed to -15 °C provides less thermoregulating effect (6 min for the core/sheath yarn made fabric) because of the severe cold condition as compared to the fabric exposed to 0 °C. Therefore when the environment is severe, it is suggested to use multilayer fabrics with each layer made of PCM core/sheath yarn to increase the thermal arrest of fabric providing more thermoregulating effect to wearers. The thermal arrest time can be doubled or tripled using two or more layers of fabrics. For instance people working in chiller room can wear garments developed by PCM which can provide the thermoregulating effect for 16 minutes as shown in Figure 5.20 whereas people working in freezer room can use two or three layer fabrics made of core/sheath yarn that would be able to keep the wearer in a micro comfort environment for more than 12 minutes.

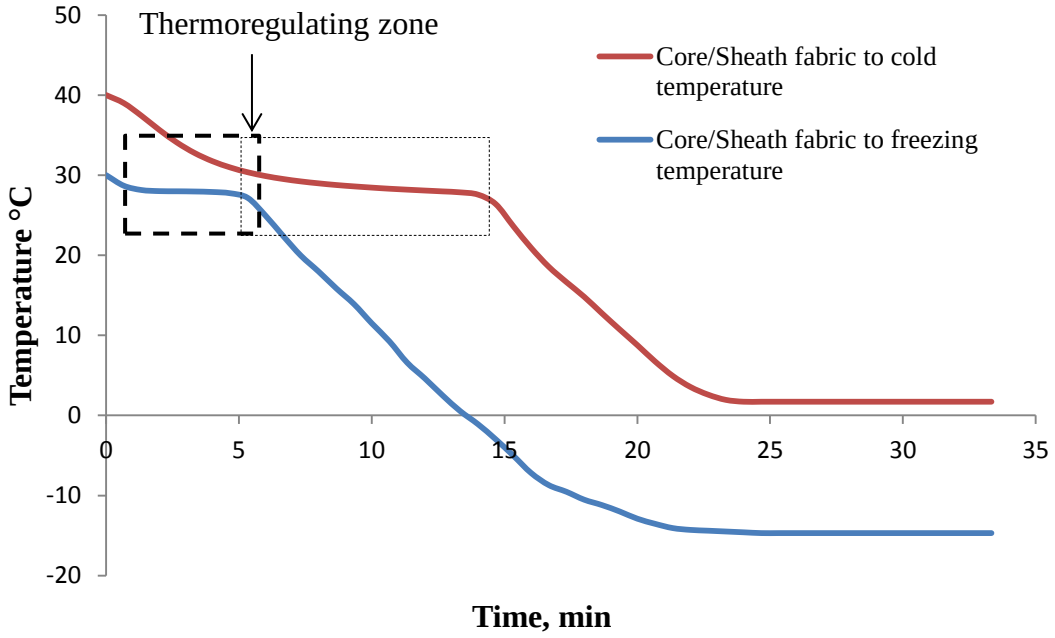

Figure 5.20 Comparison for the cooling of Core/Sheath fabrics

Chapter 6 Synthesis and characterisation of nanoencapsulated phase change materials

This chapter describes the nanoencapsulation of two PCM materials: paraffin with combination of n-octadecane and eicosane, and Glauber's salt. The chapter also discusses the characterisations of two types of NPCM (nanoencapsulated PCM) using DSC, SEM and FTIR. Furthermore the incorporation of NPCM paraffin into melt spun polypropylene yarn and the application of NPCM paraffin and Glauber's salt on cotton fabric have also been described.

6.1 Materials for NPCM paraffin and NPCM Glauber's salt

This section describes the materials and techniques used for the synthesis of nano paraffin and hydrated salt.

6.1.1 *Melamine and formaldehyde*

Melamine and formaldehyde were purchased from Alfa Aesar® and used as raw materials to synthesize MF (melamine formaldehyde) shell material. MF forms shear and thermal stable shell and that's why it was selected in this study. Formaldehyde purchased was 37% w/w in aqueous solution. The structures of melamine and formaldehyde are shown in Figure 6.1.

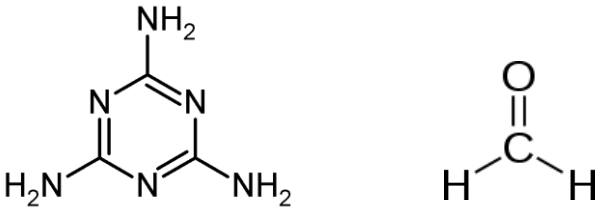

Melamine Formaldehyde

Figure 6.1 Structure of melamine and formaldehyde

6.1.2 *Paraffin*

Paraffins are inexpensive material which can store high amount of latent heat and that's why they were selected as core materials for the synthesis of NPCM paraffin. Eicosane

and n-octadecane purchased from Alfa Aesar® were used as PCM core material. The melting temperature of n-octadecane is 28 °C containing 18 carbon atoms in straight chain and the melting temperature of eicosane is 36-38 °C containing 20 carbon atoms. The chemical formulas of n-octadecane and eicosane are presented in Figure 6.2.

n-octadecane Eicosane

Figure 6.2 Structure of n-octadecane and eicosane

6.1.3 *Surfactant*

Surfactants are the auxiliary chemicals which help to make and stabilise the emulsion. Sodium dodecyl-benzene-sulfonate (SDS) was used as emulsifying agent and polyvinyl alcohol (PVA) was used as stabilizer. As paraffin is water insoluble therefore to make the emulsion in water, SDS was used. The emulsion usually remains stable as long it is under the high stirring rate. To keep it stable for later stage, PVA was used. The structures of SDS and PVA are shown in Figure 6.3 where "n" indicates the degree of polymerisation.

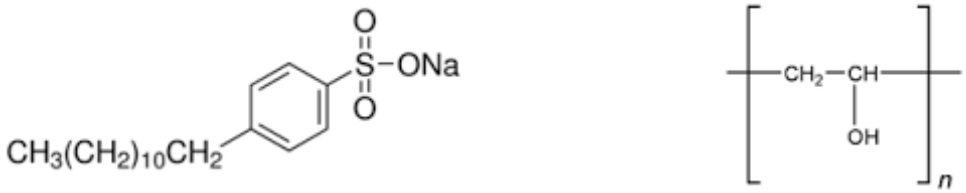

Sodium dodecyl-benzene-sulfonate Polyvinyl alcohol

Figure 6.3 Structures of SDS and PVA

6.1.4 *MMA and EA*

MMA (methyl methacrylate) and EA (ethyl acrylate) were purchased from Alfa Aesar® and were used as raw materials to prepare PMMA (polymethylene methacrylate) capsule shell via solvent evaporation method. PMMA is more appropriate shell material used in the solvent evaporation method and was selected as a shell material in this research for the synthesis of NPCM Glauber's salt. This pre-polymer shell material was

used to encapsulate the sodium sulphate decahydrate (Glauber's salt). The structures of methyl methacrylate and ethyl acrylate are shown in Figure 6.4.

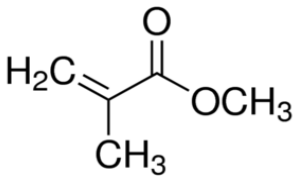

MMA

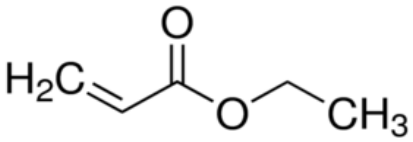

EA

Figure 6.4 Structures of MMA and EA

6.1.5 ***Solvents***

To encapsulate Glauber's salt using PMMA shell by solvent evaporation method, toluene and dichloromethane were used as solvents. Toluene was selected because of its high boiling temperature and dichloromethane was selected because of its less toxicity and more volatile nature. Toluene was purchased from Rathburn Chemicals and dichloromethane was purchased from Fisher Scientific. Toluene was used as a solvent to make emulsion of Glauber's salt while dichloromethane was used as a solvent for the PMMA pre-polymer. The structures of toluene and dichloromethane are shown in Figure 6.5.

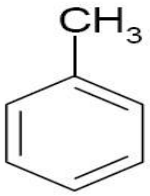

Toluene

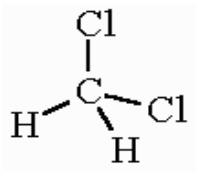

Dichloromethane

Figure 6.5 Structures of toluene and dichloromethane

6.1.6 ***Glauber's salt***

Glauber's salt ($Na_2SO_4.10H_2O$) was used as a core PCM material which has a melting point 32.4 °C. The Glauber's salt was purchased from Alfa Aesar®. Glauber's salt was selected as a PCM material because its melting temperature is closer to human skin comfort temperature and contains higher amount of latent heat.

6.1.7 *Reaction ingredients*

Dibenzoyl peroxide (wet with 25% water) was used as initiator to start the polymerization reaction for PMMA shell formation. 4-methoxy phenol was used as inhibitor which terminates the reaction when required. Both chemicals were purchased from Alfa Aesar®. Sodium salt of polyacrylic acid purchased from Sigma Aldrich was used as reaction stabilizer which helps in controlling the reaction. Their structures are shown in Figure 6.6.

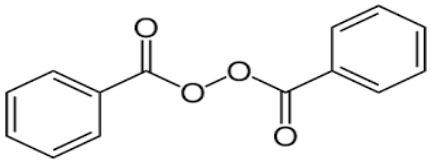

Dibenzoyl peroxide

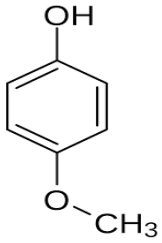

4-methoxy phenol

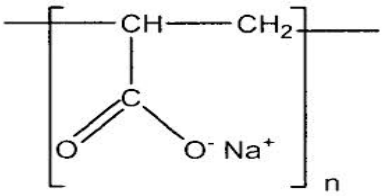

Sodium salt of polyacrylic acid

Figure 6.6 Structures of dibenzoyl peroxide, 4-methoxy phenol and sodium salt of polyacrylic acid

6.1.8 *Nanoencapsulation technique*

Two different methods were explored for the encapsulation of paraffin and Glauber's salt respectively. Interfacial polymerization was used for the nanoencapsulation of paraffin using melamine formaldehyde as shell material. The detailed procedure for both methods will be discussed in sections 6.2.1 and 6.3.1. Figure 6.7 shows the process flow chart of paraffin encapsulation via interfacial polymerization method.

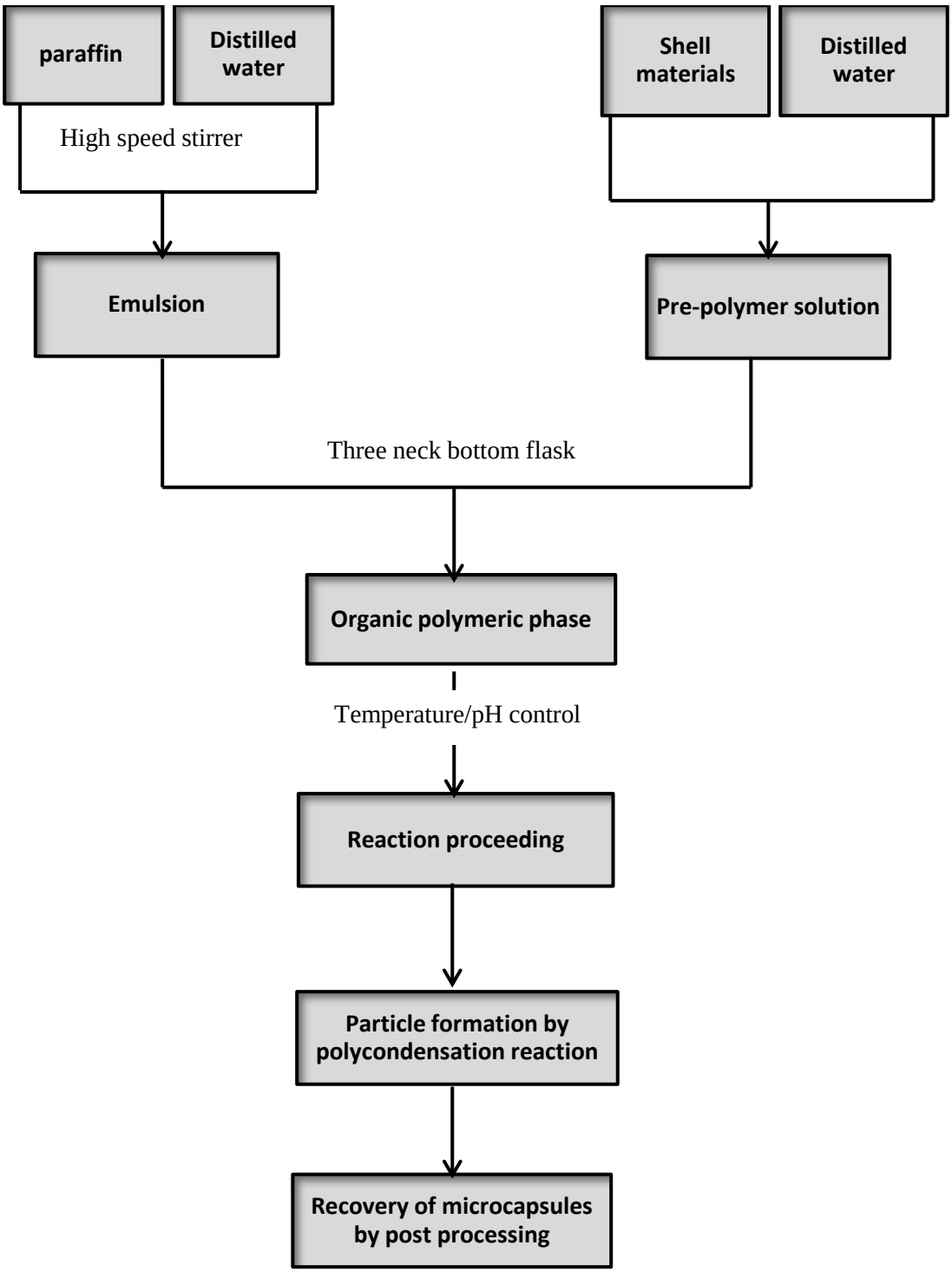

Figure 6.7 Flow chart of encapsulation by interfacial polymerization

Solvent evaporation method was explored for the encapsulation of Glauber's salt and Figure 6.8 shows the process flow chart for the encapsulation of Glauber's salt via solvent evaporation method.

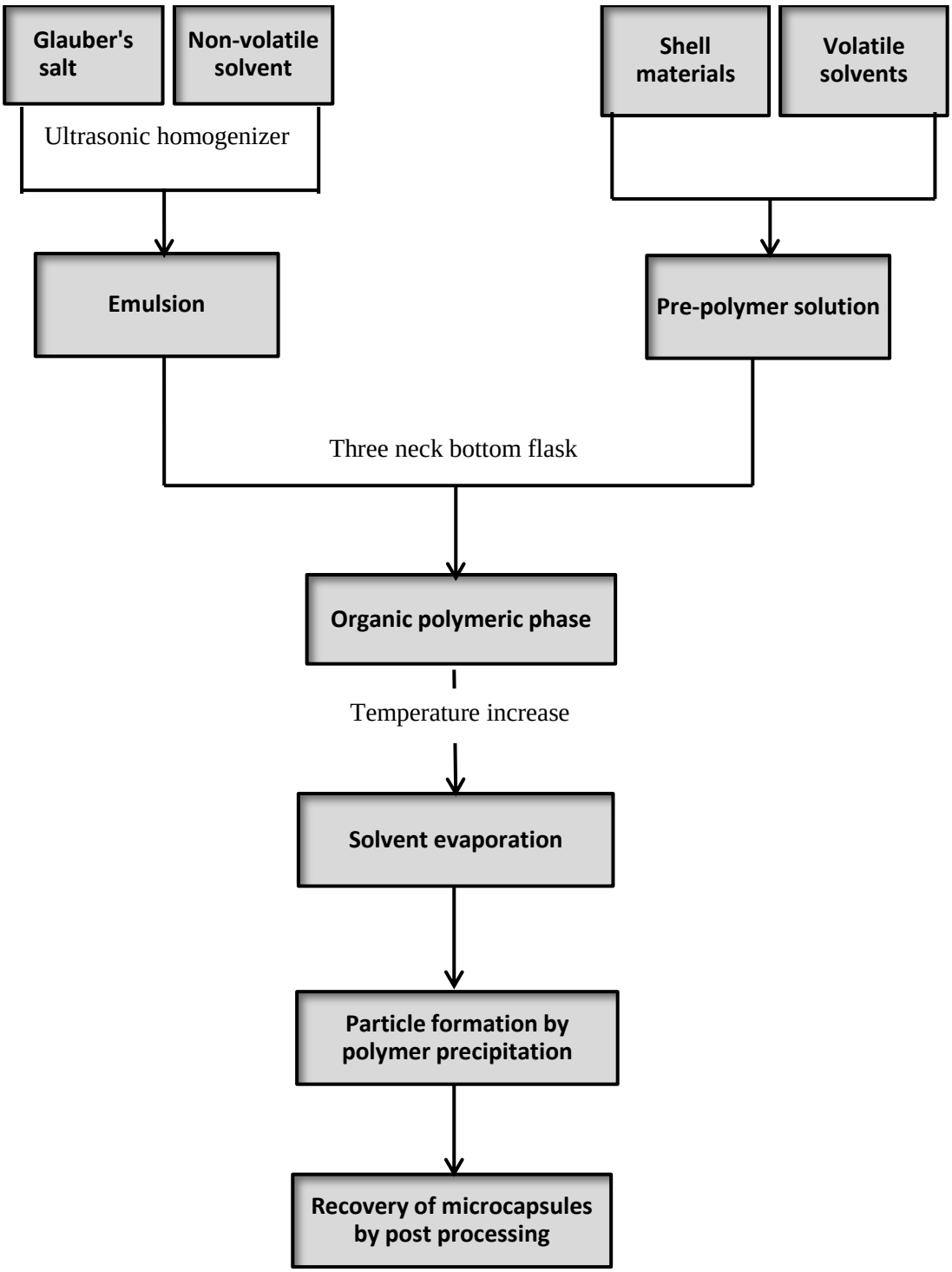

Figure 6.8 Flow chart of encapsulation by solvent evaporation technique

6.2 NPCM paraffin encapsulation, characterization and its application on textiles

This section describes the synthesis of NPCM paraffin, its characterisation, incorporation in polypropylene yarn through melt spinning process and its application

on cotton fabric via pad-dry-cure technique. The experiments were designed using Minitab and the effect of factors on response has also been studied.

6.2.1 *Design of experiment (DOE)*

DOE aimed to identify the processing conditions, parameters and product components that affect the quality of nanoencapsulation and optimise those factors for the best result. DOE helps to investigate the effects of factors (input variables) on response (output variables) at the same time. The designed experiments were composed of series trials where different levels of input variables were used. Data was collected for each trial in the form of output variables.

A response surface design is a set of advanced DOE techniques that helps to better understand and optimise the response. Response surface design methodology is often used to refine models after the important factors affecting the response have been defined. Response surface design has two types called central composite design (CCD) and Box-Behnken design.

The Box-Behnken design of experiment was selected for nanoencapsulation to determine the effect of levels of different factors on response. Box-Behnken design usually has fewer design points than central composite design thus it is less expensive to run with the same number of factors. Box-Behnken design is very useful especially when the safe operating zone of a process is known. CCD usually has axial points outside the cube as shown in Figure 6.9 and these points may not be in the region of interest or may be impossible to conduct because they are beyond safe operating limits. Box-Behnken design does not have axial points and all design points fall within the safe operating zone. Box-Behnken design always has 3 levels per factor unlike CCD which has up to 5 levels per factor because of the axial points in the design. The axial points were not desired in the current research therefore Box-Behnken design was adopted.

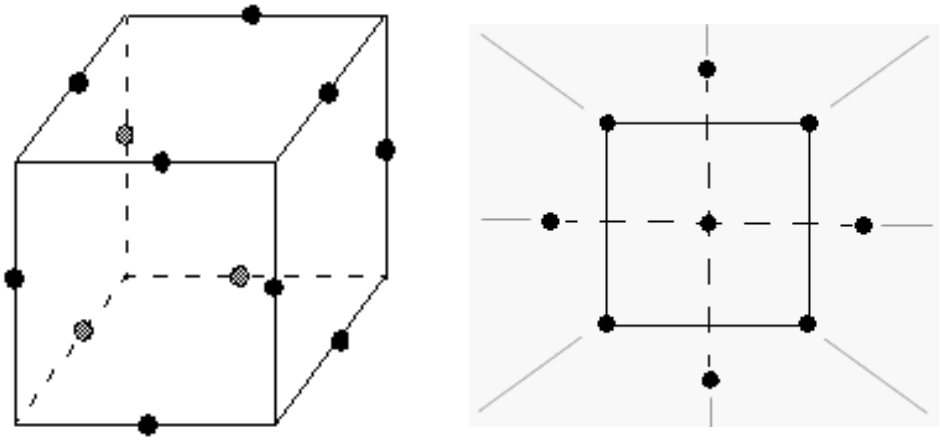

Box-Behnken Design Central Composite Design

Figure 6.9 Response surface design

For the design of experiment, Box-Behnken method was adopted using response surface design of experiment. The response surface optimiser uses two methods called CCD and Box-Behnken. The difference in CCD and Box-Behnken is that CCD uses two levels of each factor and makes extra three levels by taking axial and centre point of the levels provided. On the other hand Box-Behnken only makes one level extra by defining centre point of the given levels and reduces the number of experiments if axial levels are not required. Box-Behnken was used because axial levels were undesired in this case.

Melamine and formaldehyde were used as raw materials for the synthesis of capsule shell. Eicosane and n-octadecane were used in combination as phase change materials in core to bring the melting temperature closer to the skin comfort temperature. Sodium dodecyl benzene sulfonate (SDS) and PVA were used as emulsifier and stabilizer respectively. Acetic acid and NaOH were used as pH controllers.

Table 6.1 shows the three factors and their levels which were used to study the particle size of NPCM. Using the above lower and upper levels of each factor, experiments were designed using Box-Behnken response optimiser. The estimated range of upper and lower levels was selected based on the knowledge and experience to attain the desired response. Table 6.2 shows 15 designed experiments in different combination of levels with each factor. All the experiments were randomised by default and were performed according to the run order. The last column shows the particle size against each experiment as outcome.

Table 6.1 factors and levels for DOE

Factors	Lower level	Upper level
Emulsifier (g)	0.7	1.2
Emulsion speed (rpm)	5000	10000
Encapsulation stir speed (rpm)	400	800

Table 6.2 Design of experiments

		Factors			Response
Std. order	**Run order**	**Emulsifier (g)**	**Emulsion stir speed (rpm)**	**Encapsulation stir speed (rpm)**	**Particle size (nm)**
15	1	0.95	7500	600	610
6	2	1.20	7500	400	1500
5	3	0.70	7500	400	1505
13	4	0.95	7500	600	611
11	5	0.95	5000	800	1398
9	6	0.95	5000	400	1505
1	7	0.70	5000	600	1836
3	8	0.70	10000	600	700
4	9	1.20	10000	600	1168
10	10	0.95	10000	400	589
2	11	1.20	5000	600	2261
12	12	0.95	10000	800	318
14	13	0.95	7500	600	620
8	14	1.20	7500	800	1467
7	15	0.70	7500	800	743

Encapsulation procedure

In-situ polymerization method was used for the nanoencapsulation process. For oil in water emulsion, 20g of octadecane and 10g of eicosane were taken in 150ml of distilled water containing SDS and 0.1g stabilizer. The amount of SDS (emulsifier) and emulsion stirring rate were used in different combination and has been shown in the

experimental design. The emulsion was prepared under high stirring rate using high speed homogeniser at 70 °C for 30 to 40 min. as shown in Figure 6.10.

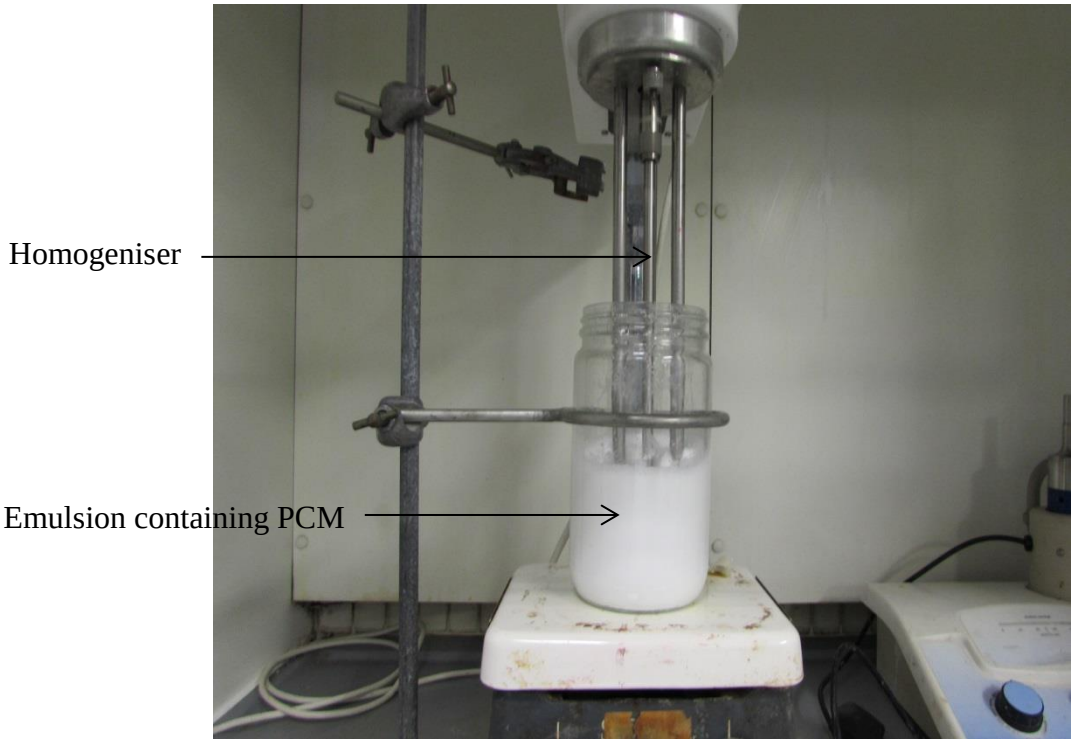

Figure 6.10 O/W emulsion using high speed homogeniser

The prepolymer solution was prepared by adding 10g of melamine and 20g of formaldehyde in 50g of distilled water and mixed at 60-65 °C as shown in Figure 6.11 (a) until a clear solution was obtained as shown in Figure 6.11 (b).

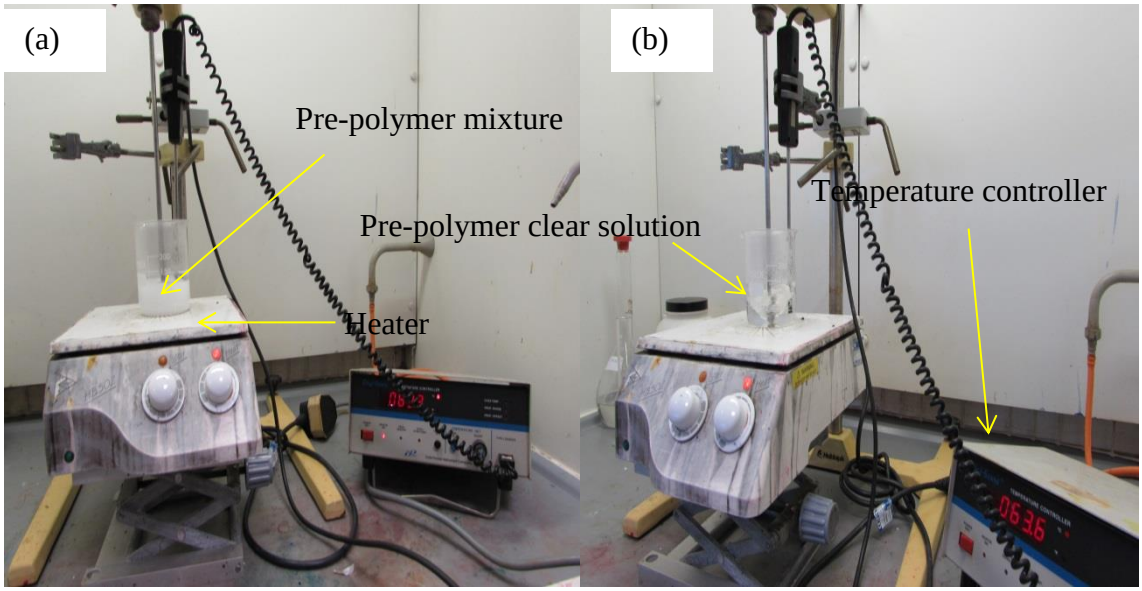

Figure 6.11 Pre-polymer formation using melamine and formaldehyde

For nanoencapsulation, the emulsion was poured into three neck flask and prepolymer solution was dribbled into the emulsion drop wise as shown in Figure 6.12. The temperature of the mixture was increased gradually up to 80 °C while controlling pH in the range of 4-4.5 using acetic acid. The mixture was under stirring using different rpm speed as shown in experimental design. The process was held under controlled parameters allowing polycondensation reaction to complete and nanocapsules were washed, filtered and dried to get NPCM paraffin powder as shown in Figure 6.13.

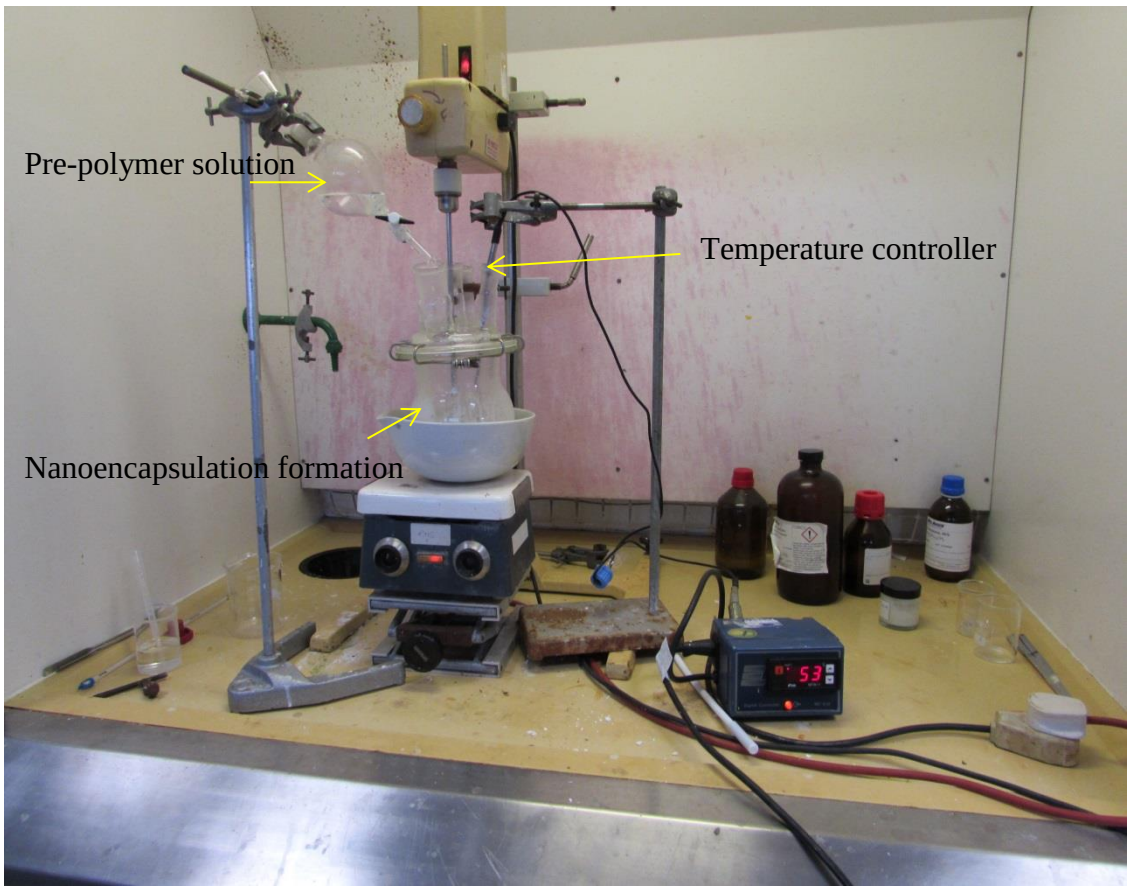

Figure 6.12 Microencapsulation of NPCM paraffin in reaction flask

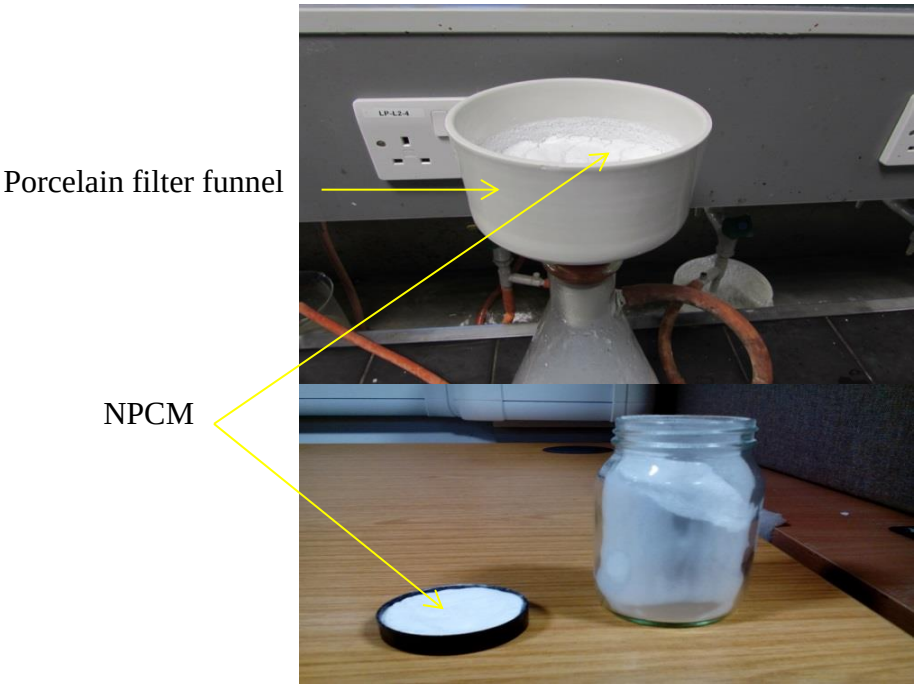

Figure 6.13 NPCM after filtration and drying

Reaction mechanism

The first step is the direct reaction between melamine and formaldehyde forming methylolamine prepolymer as shown in Figure 6.14.

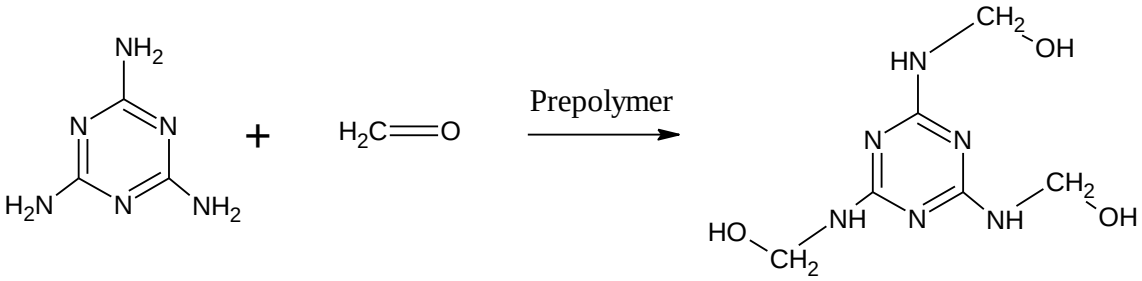

Melamine Formaldehyde Methylolamine

Figure 6.14 Formation of methylolamine

The second step shown in Figure 6.15 is called the condensation reaction step in which methylolamine combines together to form three dimensional network of cross linked melamine formaldehyde with methylene bridges. The condensation reaction takes place between the methylol groups of neighbouring methylolamine with the elimination of water molecules which cross link in three dimensions. The water molecules are shown in Figure 6.15 by dashed boxes which are eliminated during the polymerization reaction.

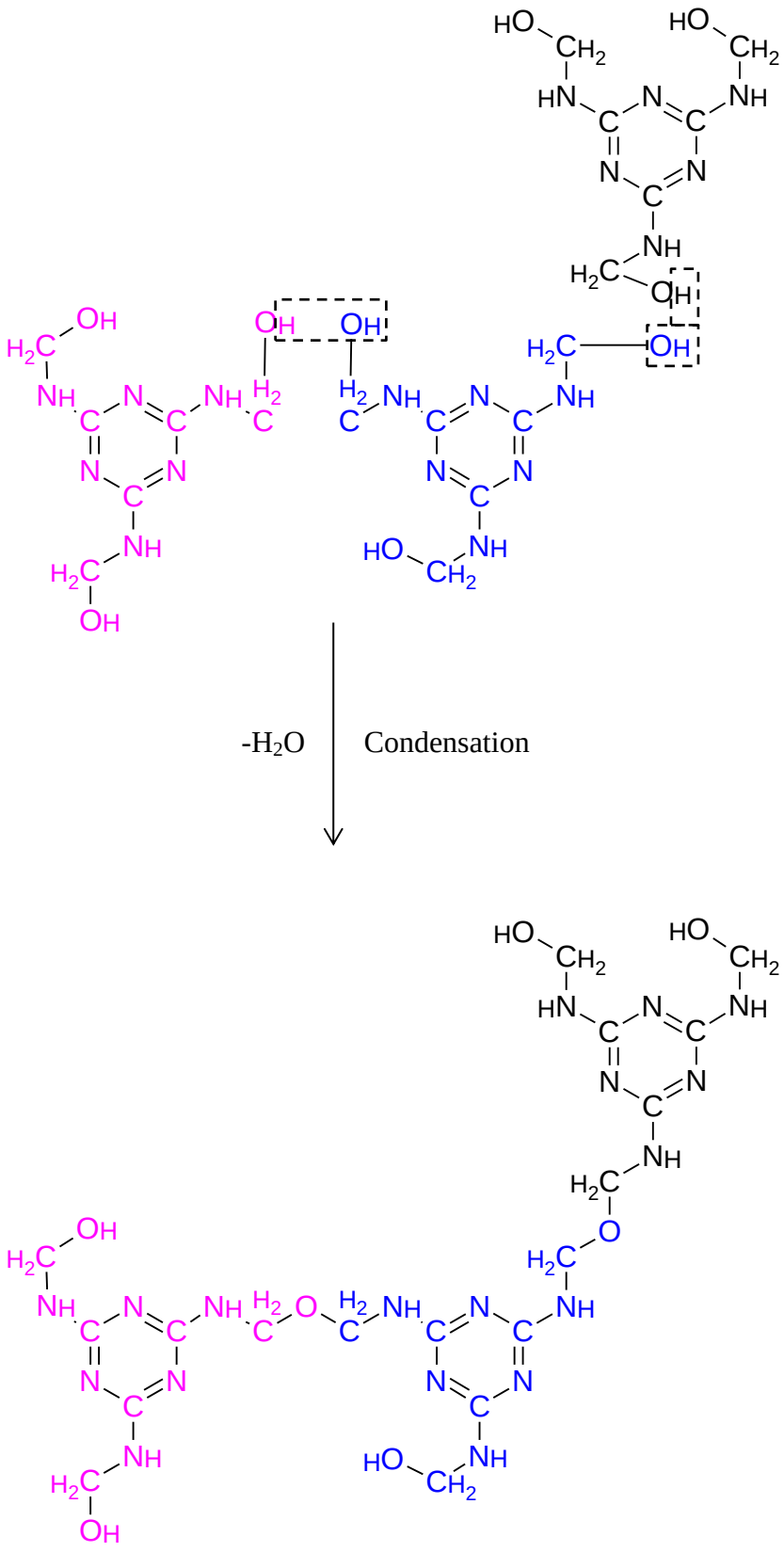

Figure 6.15 Condensation reaction of melamine formaldehyde

6.2.2 *Characterisation of NPCM paraffin*

SEM micrographs for NPCM paraffin

The images of nanocapsules were analysed using scanning electron microscopy. The images of NPCM paraffin are shown in Figure 6.16 which indicates that all the images are very consistent in their particle size. The images shown in Figure 6.16 were taken at lower magnifications to show the aggregates of nanocapsules with narrow size distribution. The images taken at 8000 and 20000 magnification in Figure 6.16 indicates that nanocapsules are very consistent in size and are spherical in shape.

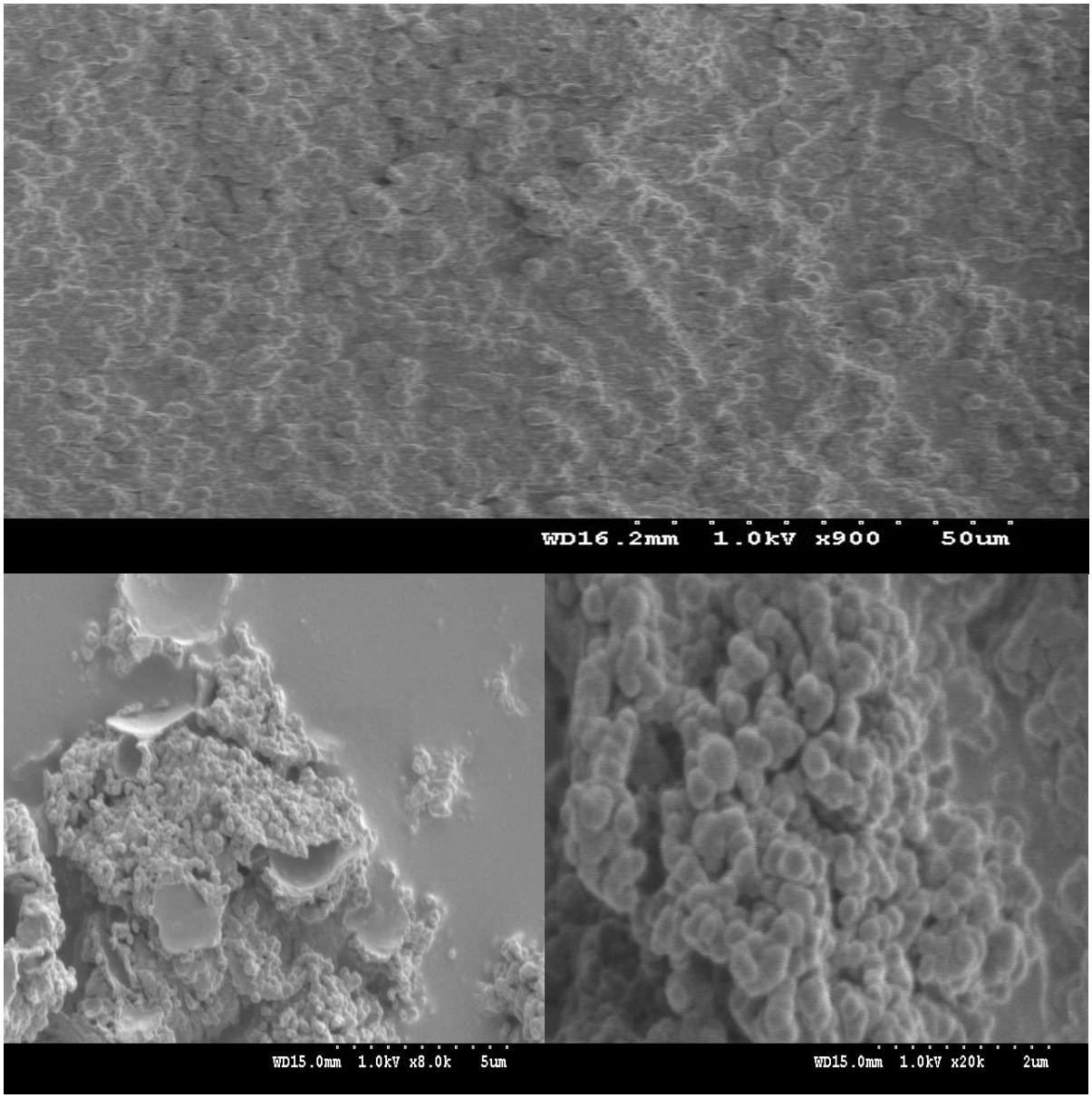

Figure 6.16 SEM images of NPCM paraffin

Figure 6.17 shows the SEM images at higher magnification of 40K and were used to measure the size of nanocapsules. The size of nanocapsules of one sample measured through SEM was from 300 nm to 326 nm as shown in Figure 6.17.

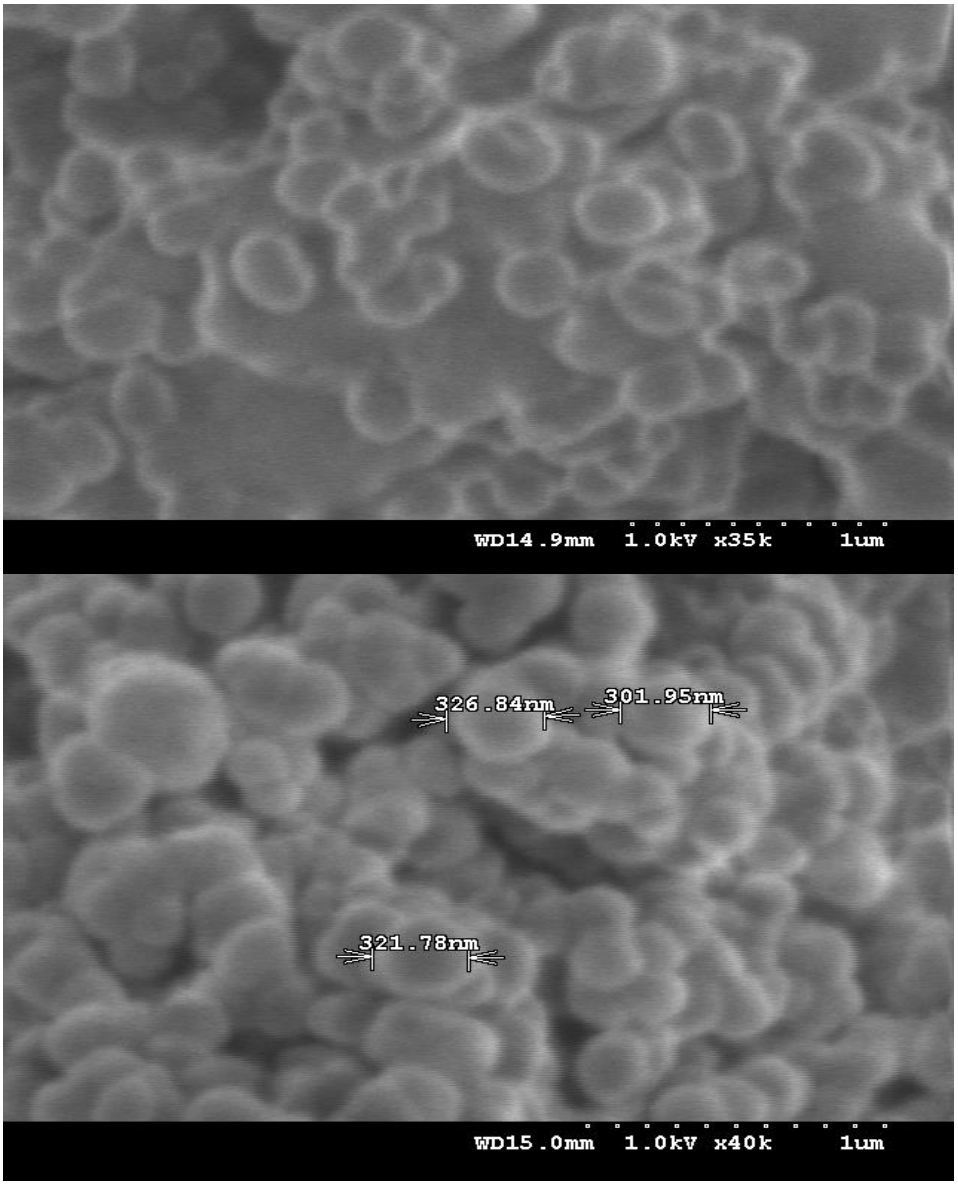

Figure 6.17 SEM images at higher magnification

DSC study of NPCM paraffin

The result of latent heat from DSC shows the presence of paraffin in NPCM. The melting temperature of NPCM paraffin was found near the human skin comfort temperature i.e. 33 °C. Figure 6.18 shows the curves of MPCM 28 (from supplier) and NPCM synthesized in this research. The peak melting temperature of both curves shows clearly that the phase change temperature of the newly developed NPCM is closer to

human skin comfort temperature although the curved areas are almost the same. The latent heat of NPCM paraffin is 144 J/g as shown in Figure 6.18.

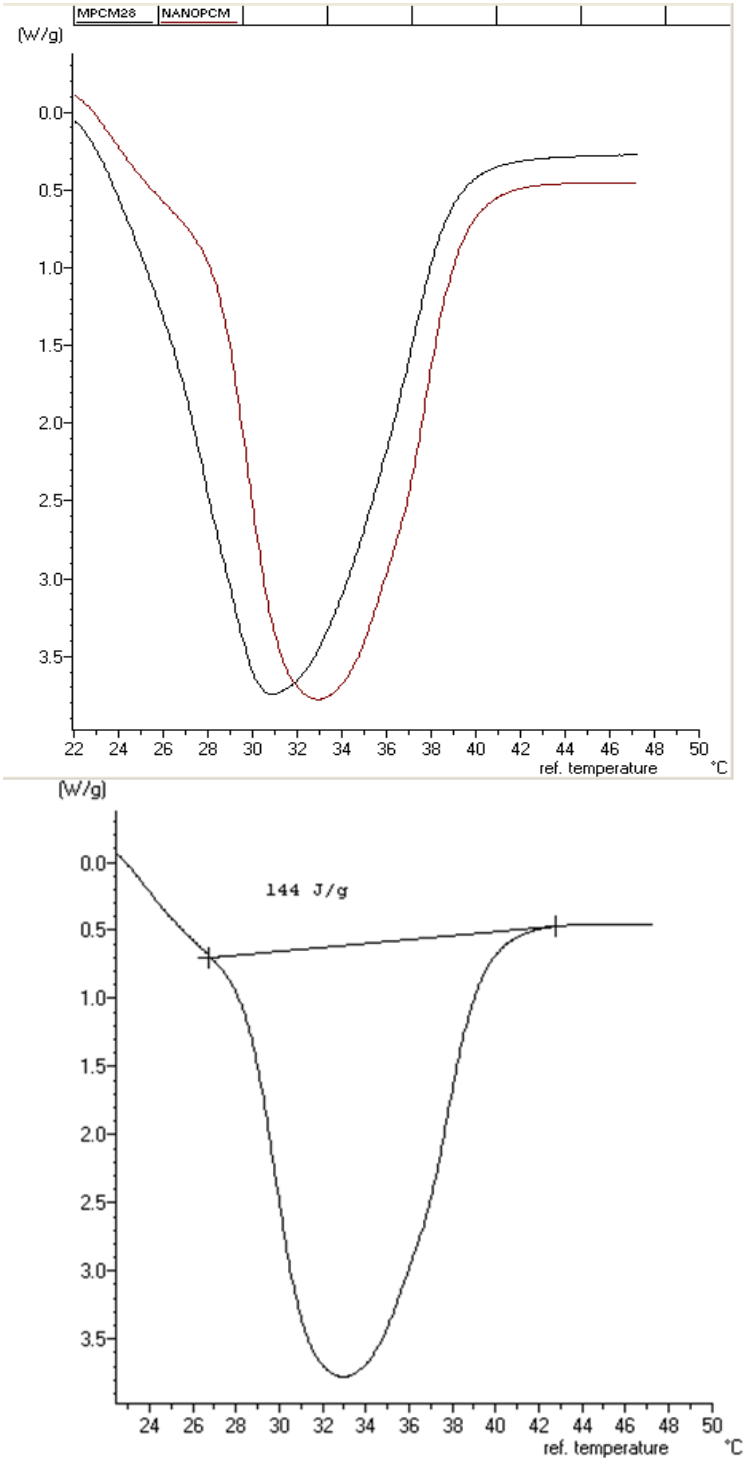

Figure 6.18 DSC curves for MPCM 28 and NPCM paraffin

Structure of NPCM paraffin

The FTIR spectra of NPCM paraffin is presented in Figure 6.19. The spectrum shows a strong absorption band at 2850-2930 cm^{-1} attributing to the stretching vibration of aliphatic C-H group of the paraffin. The N-H stretching can be observed at 3300 to 3400 cm^{-1} and N-H bending can be seen at 1320 cm^{-1}. The C-N stretching in the triazine ring can be seen at 1550 cm^{-1} and triazine ring bending is presented by a very sharp peak at 810 cm^{-1}. This proves that the developed nanocapsules indeed are composed of paraffin as core and melamine formaldehyde as shell materials.

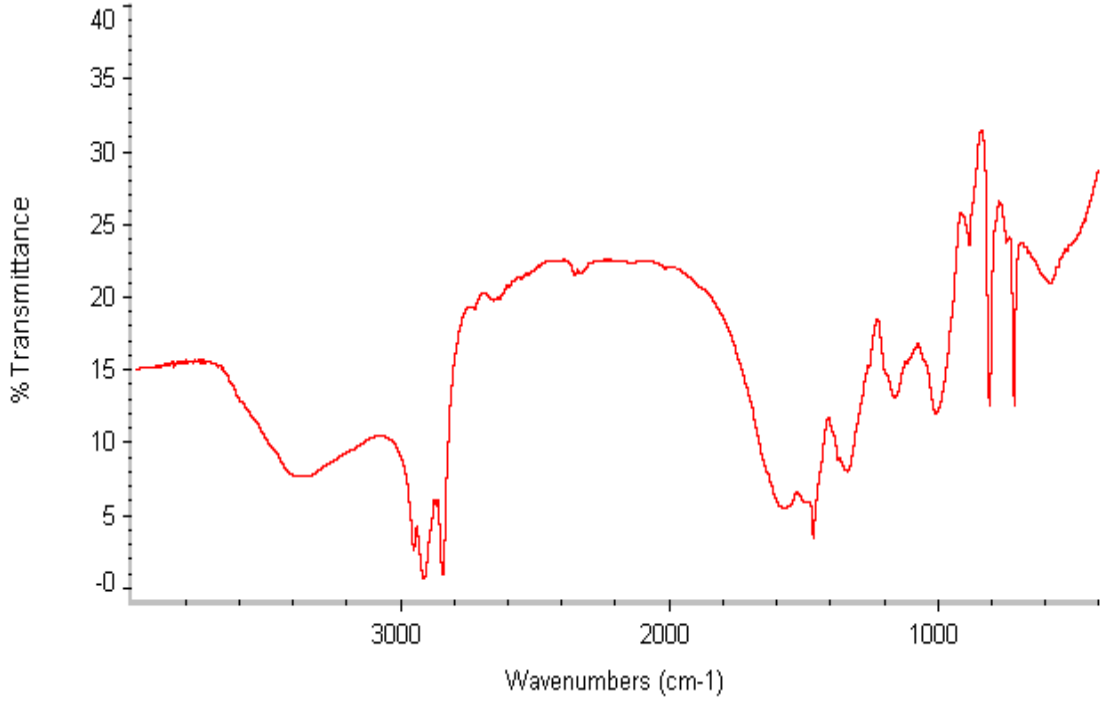

Figure 6.19 FTIR for NPCM paraffin

6.2.3 *Effect of factors on response of particle size*

Main effect plots for particle size

Three parameters called the amount of emulsifier, emulsion stirring speed and encapsulation stirring speed were studied to investigate the effect of nanocapsules particle size. The main effect plot for particle size is shown against each parameter individually in Figure 6.20. The graph shows that particle size decreases as the amount of emulsifier increases up to a certain level, then increases when further increasing the amount of emulsifier. This is caused by emulsifier which has functionality of enhancing the emulsification process by linking its hydrophobic tail to the oily paraffin. As the

amount of emulsifier increases, the emulsification increases hence the droplet size decreases. After the saturation takes place, any addition amount of emulsifier starts agglomeration among the individual mono-molecular droplets which affect the efficiency of emulsification process by increasing the droplet size in the form of agglomerate. Hence the amount of emulsifier is important to ensure the formation of nano-emulsion.

The second factor in the graph is emulsion stirring speed which plays the main role in the particle size. The graph clearly indicates that increase in rpm decreases the droplet size which helps in getting nano size capsules. The reason can be described as the stirring creates physical agitation which keeps the emulsion in mono molecular form and even become more severe when the stirring rate is increased.

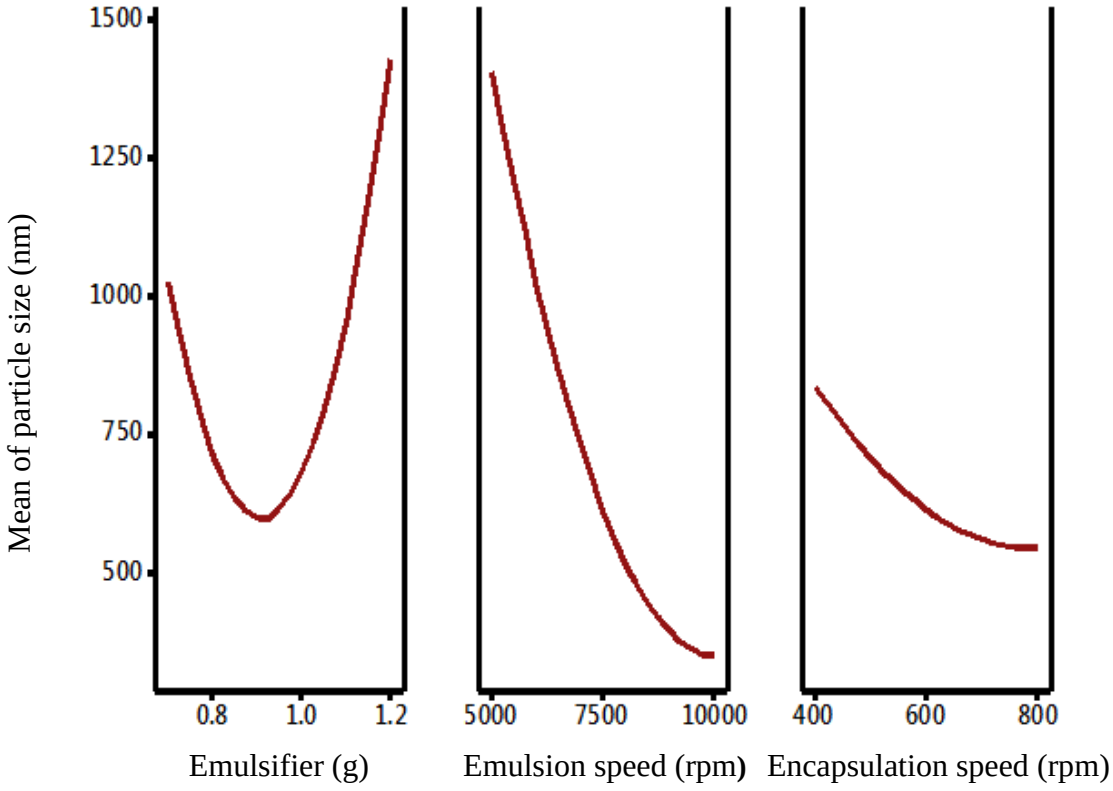

Figure 6.20 Main effect plots for particle size

The third parameter was stirring speed during encapsulation process. Figure 6.21 shows that the stirring speed during nanoencapsulation also affects the particle size of NPCM. The effect of encapsulation stirring speed on particle size is less drastic than emulsion stirring speed. The optimum stirring speed is found to be 600 rpm for the encapsulation. As the encapsulation speed increased up to 800 rpm, the nanocapsules were found

ruptured because of severe agitation and shear force of the stirring blades acting on capsules as shown in Figure 6.21.

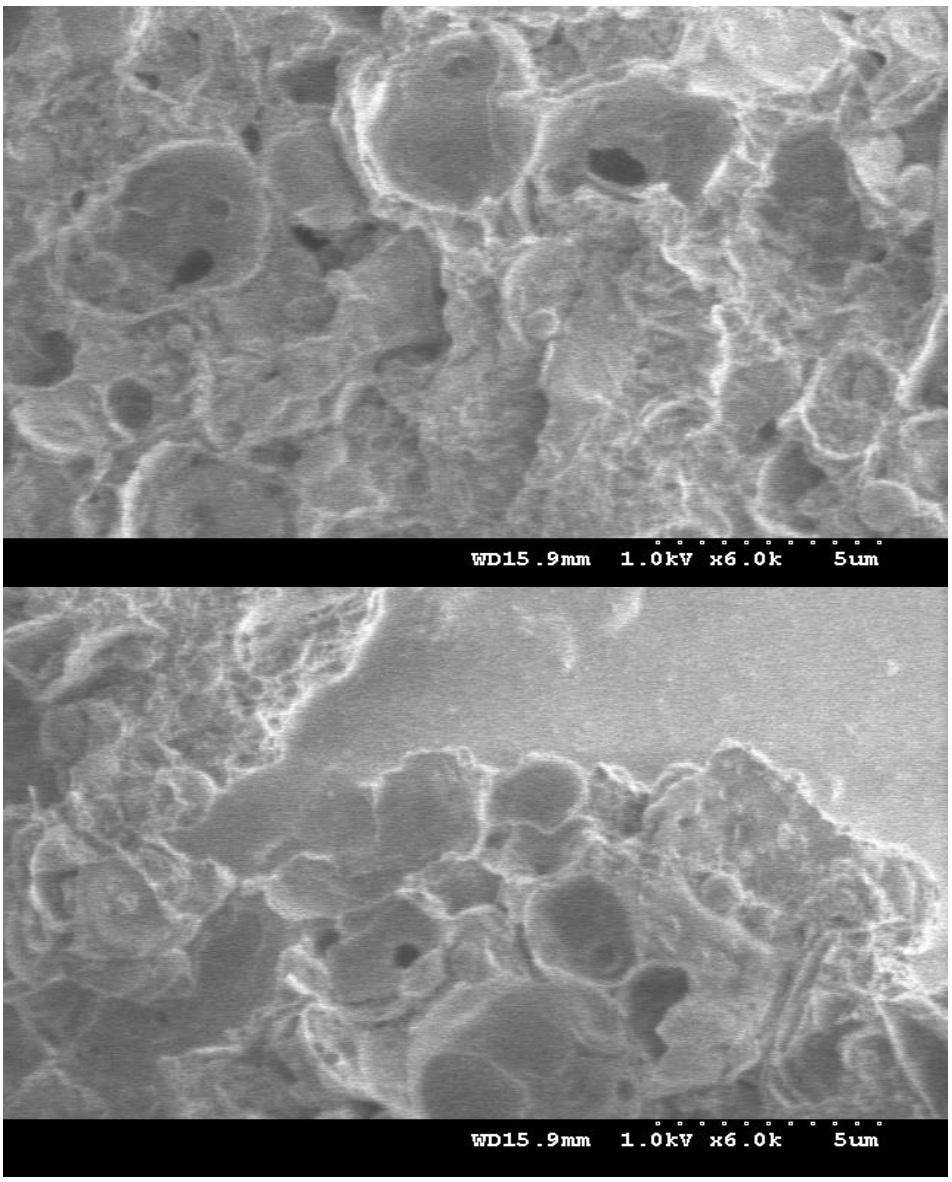

Figure 6.21 Ruptured capsules with higher encapsulation speed

Contour plots for particle size

The contour plot shows how a response factor relates to the two continuous variables during experimentation. With the help of contour plots, the relationship between outcome and variables (parameters) can be determined. The contour plot in Figure 6.22 shows how emulsion stirring speed and the amount of emulsifier influence on the size of the nanocapsules. The contour plot also helps in determining desirable response values against the value of each factor. The particle size of 500 nm of NPCM paraffin can be achieved by using 0.9g emulsifier and around 8000 rpm emulsion speed as

shown in Figure 6.22. The above parameter values were taken by setting the value of third factor (encapsulation speed) at 600 rpm.

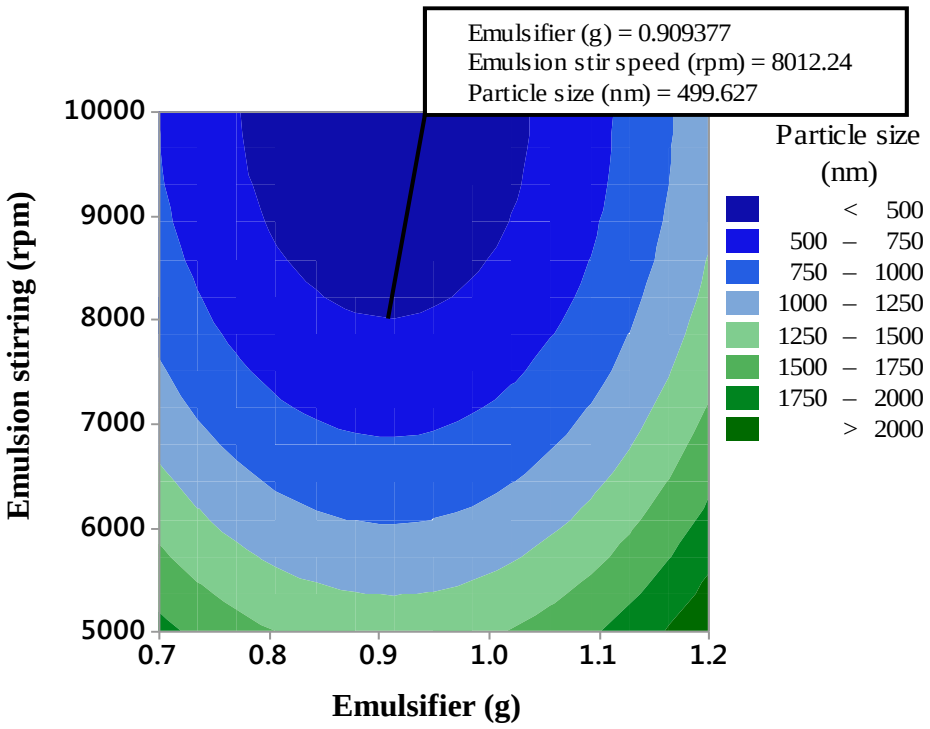

Figure 6.22 contour plot of particle size with emulsifier vs emulsion stir speed

Figure 6.23 shows the effect of emulsion speed and encapsulation speed on the particle size of NPCM paraffin. The flag in Figure 6.23 shows the desired outcome of nanocapsules by setting the emulsifier value at optimum level. If the size of particle is required for instance 500nm, then the emulsion and encapsulation speed would be required around 8000 rpm and 600 rpm respectively.

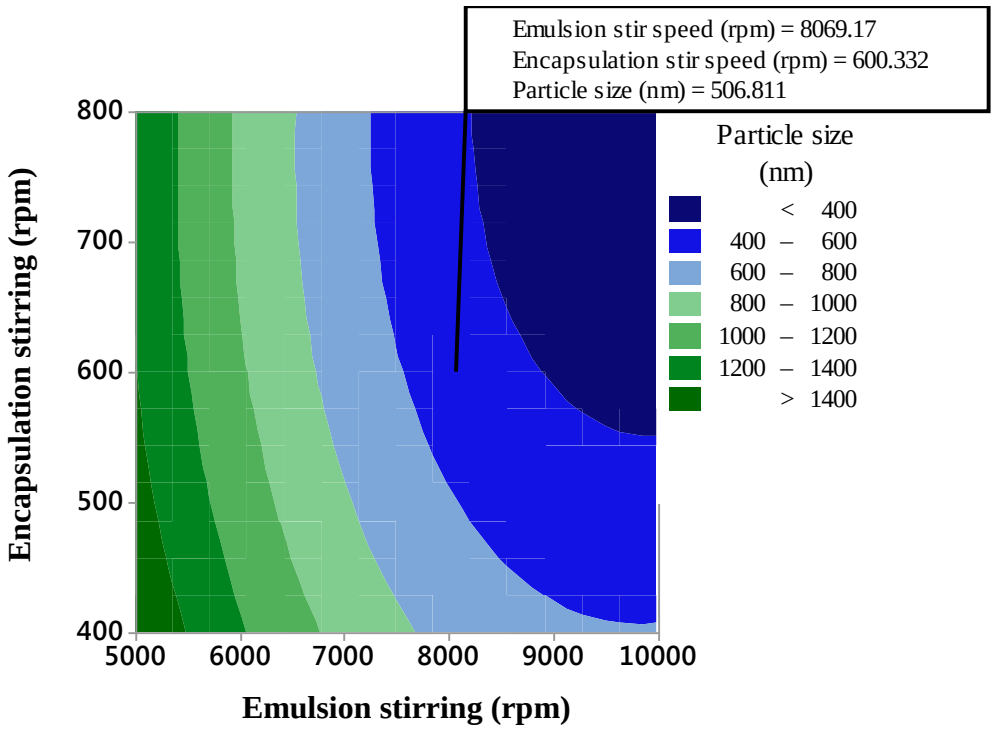

Figure 6.23 Contour plot of particle size with emulsion vs encapsulation stir speed

6.2.4 *Incorporation of NPCM paraffin in filament*

The monofilament polypropylene yarn containing 4% NPCM paraffin was developed to study the sustainability of nanocapsules in the filament. The developed filament was analysed using SEM and DSC and was compared to the previously developed polypropylene monofilament incorporated with 4% MPCM 28.

SEM of NPCM paraffin incorporated filament

The SEM images are shown in Figure 6.24 which ensures the incorporation of NPCM within the filament. The filament was cut diagonally cross-section wise in order to have better chance of capturing nano capsules and images of nanocapsules were captured at different magnifications. It is very clear from the images that the filament surface at its cross section is quite rough because of the presence of nanocapsules within the filament. The image taken at higher magnification shows the presence of nanocapsules scattered randomly.

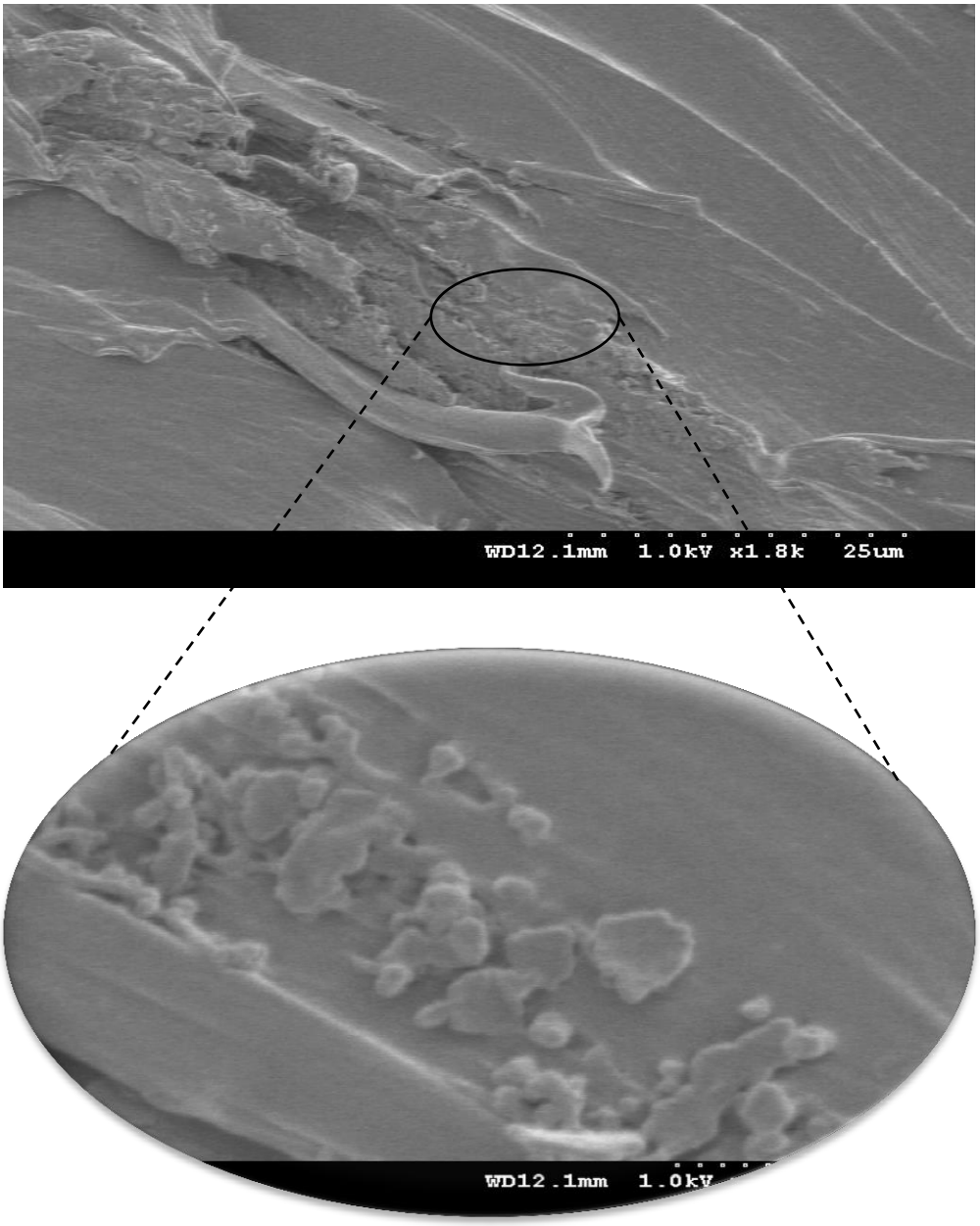

Figure 6.24 Nanocapsules within the yarn at higher magnification

DSC study of NPCM paraffin incorporated filament

Latent heat for the filaments incorporated with 4% MPCM 28 and NPCM paraffin were tested using DSC and shown in Figure 6.25. The latent heat determined was 2.31 J/g and 3.24 J/g for filaments with MPCM 28 and NPCM paraffin respectively. The reason for more latent heat in yarn incorporated with NPCM paraffin can be described as the NPCM paraffin capsules are smaller as compared to that of the MPCM 28 which increases the incorporation of nanocapsules resulting in enhanced thermal characteristics. The larger the size of capsules, the more difficult would be for capsules

to be incorporated into the filaments during extrusion process. Secondly during extrusion process surface deposition of microcapsules occurred resulting in the capsules adhered to the surface of the filaments to be removed easily in the subsequence drawing process. On the other hand, the nanocapsules are prone to incorporate inside the yarn and even because of the smaller size they make integral part of the surface which is not removed significantly during the subsequent process of drawing.

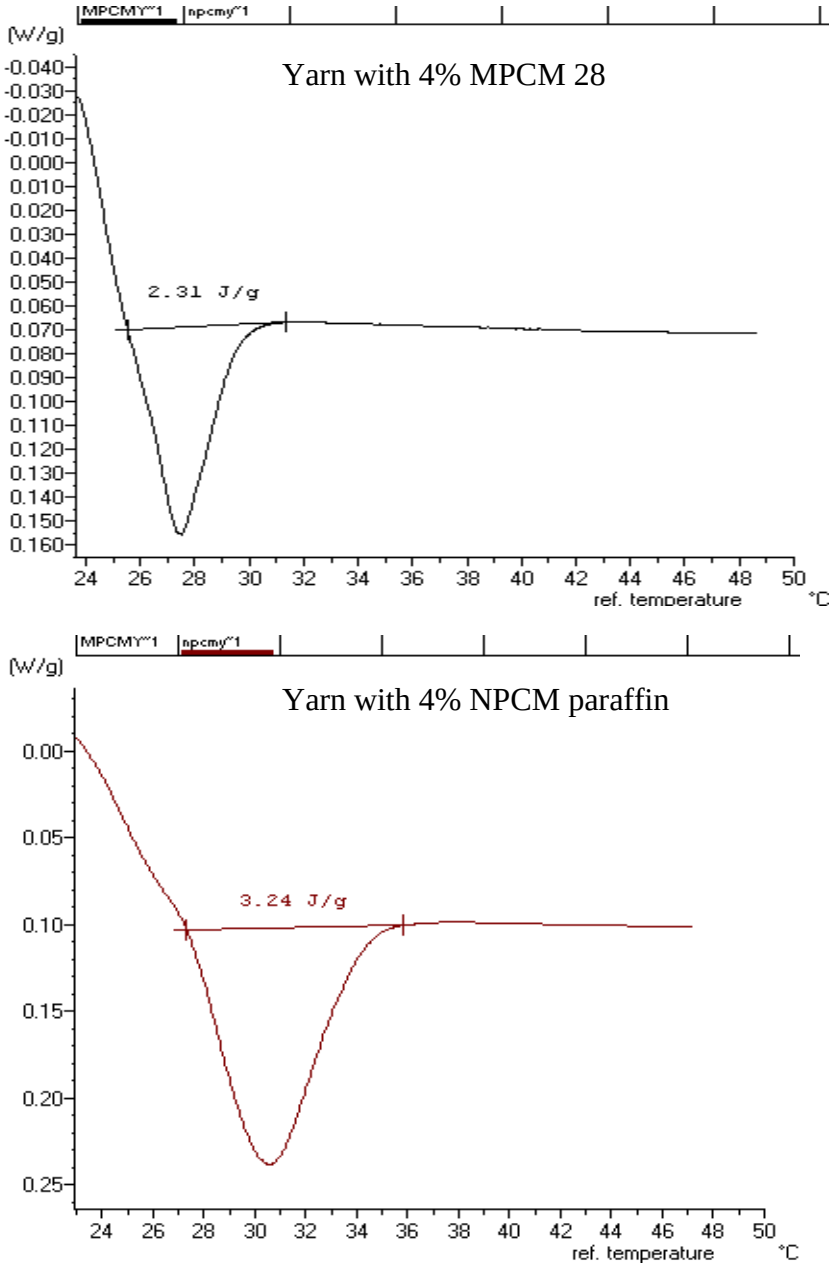

Figure 6.25 Latent heat of 4% yarn containing MPCM 28 and NPCM paraffin

6.2.5 *Application of NPCM paraffin on cotton fabric via pad-dry-cure technique*

MPCM 28 and NPCM paraffin were applied on plain woven fabric made of 100% cotton by pad-dry-cure technique. The coating method was not adopted because it

makes the fabric stiffer and adversely affects the breathability of fabric which is not ideal for the active smart textile market. The padding solution contained: 60 g/l of polyurethane binder ARRISTAN EPD; 50 g/l of REAKNITT ZF which is dimethyl-dihydroxyl-ethylene urea, formaldehyde free cross linking agent which enhances the cross linking of binder; 50g/l of TUBINGAL RGH softener which is modified polysiloxane and 8g/l of CHT CATALYST AD, a modified inorganic salt; and MPCM 28 and NPCM paraffin were used 30% of the weight of binder. The fabric was padded with the pressure of 2 bars between the mangles with speed of 2 m/min. using two dip two nips. The fabric was then dried at 100 °C then cured in a stenter at 150 °C for 3 minutes.

Each sample was then taken for washing (1 wash and 5 washes) to study the durability of the applied PCM capsules. British Standard BS EN 26330: 1994 program 15, 6A 40 °C was followed to perform the washing of samples. SEM and DSC were used to characterise the washed fabrics as comparison to the untreated.

SEM for NPCM paraffin treated cotton fabric

Figure 6.26 shows the images of fabric finished with MPCM 28 before and after washing. The microcapsules are spread all over the fabric after pad application and attached to the surface with the help of binder. The images of the same fabric after 1st and 5 washes show that microcapsules are still present but not in large amount especially for the fabric after 5 wash. When the capsules are in large size, most of the capsules are attached on the surface of yarn and fabric but would not sustain after severe washing. Only those capsules bound firmly to the yarns and fabric with the aid of binder would not be washed off.

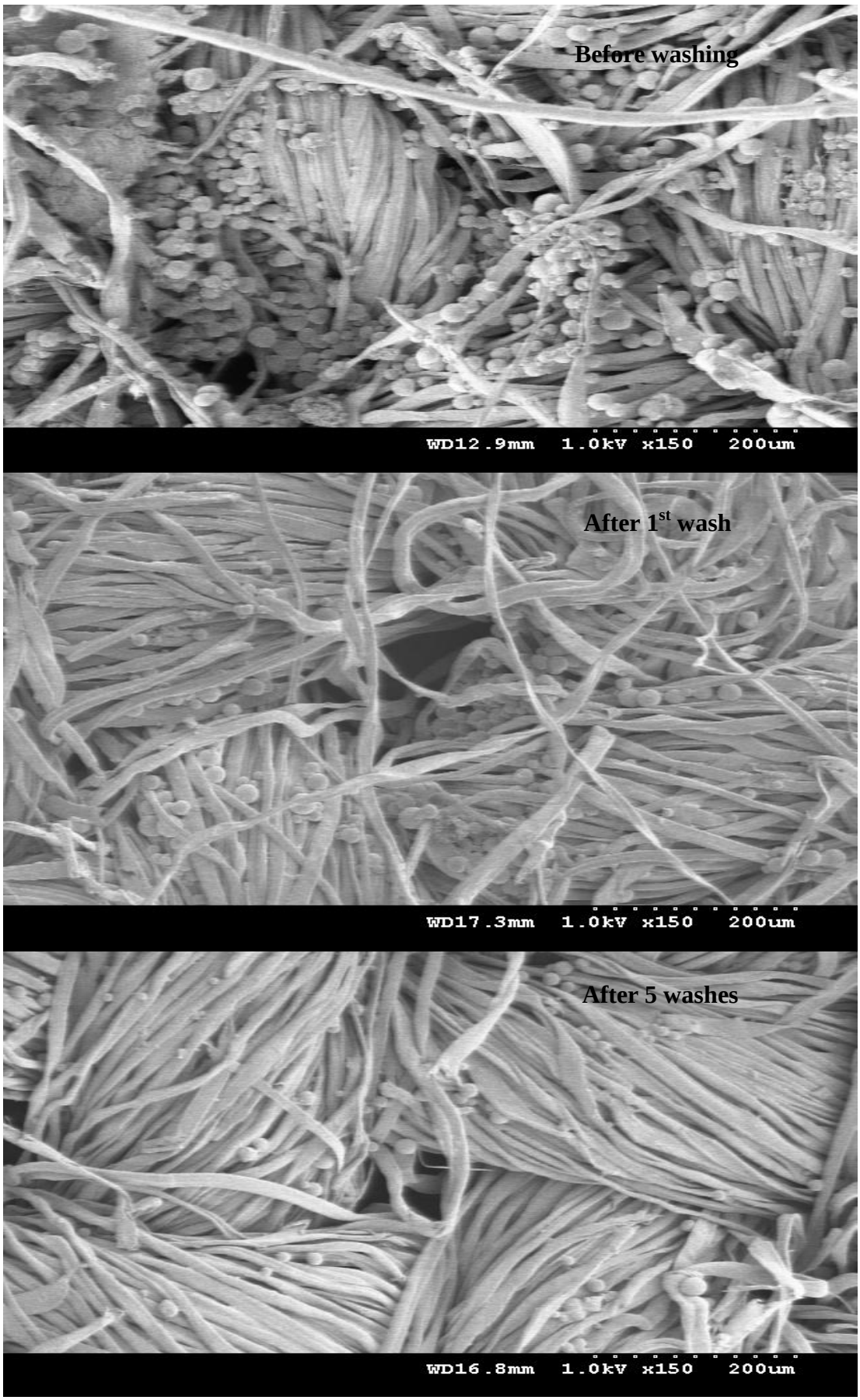

Figure 6.26 Fabric treated with MPCM 28 before and after washing

Figure 6.27 shows the images of fabric treated with NPCM paraffin before washing. It is clear from Figure 6.27a that large amount of nanocapsules are bound on the yarns of fabric. Figure 6.27c is a magnified image which even more clarifies that nanocapsules are firmly bound to the yarn surface and not just adhered to the fabric as was seen for the case of MPCM 28 treated fabric.

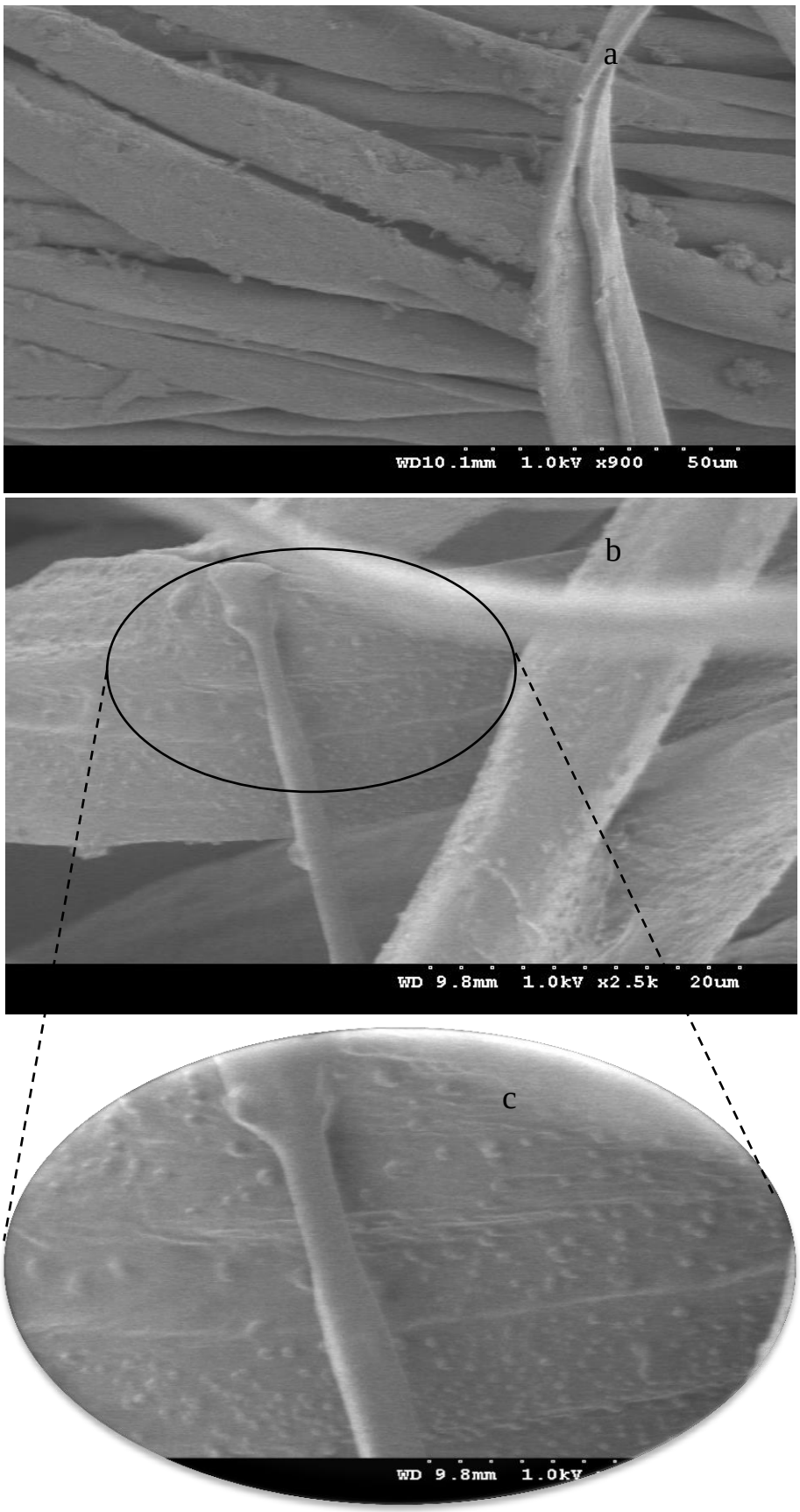

Figure 6.27 Fabric treated with NPCM paraffin before washing

Figure 6.28 shows the SEM images of treated fabric after one wash. The nanocapsules are attached to fibre level in comparison to microcapsules which are attached to yarns of the fabric; they are more firmly attached and perform better resistance to washing. The image in Figure 6.28 is magnified to show how nanocapsules are mixed within the resinous material of binder.

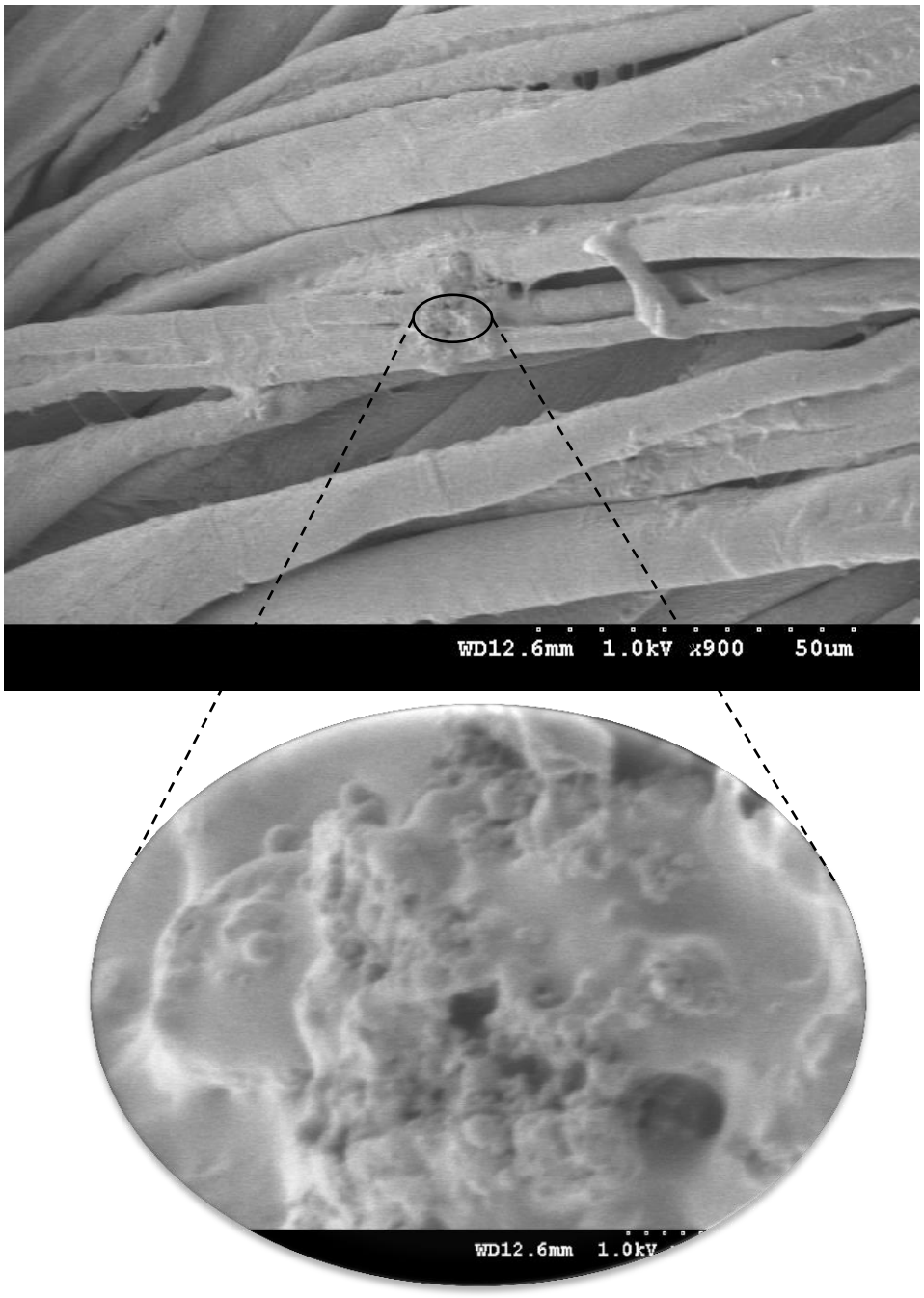

Figure 6.28 SEM for fabric treated with NPCM paraffin after 1st wash

Figure 6.29 shows the images of fabric treated with NPCM paraffin after 5 washes. The nanocapsules are still present in large amount on the surface of yarns up to the fibre level along with binder because of the nano scale size.

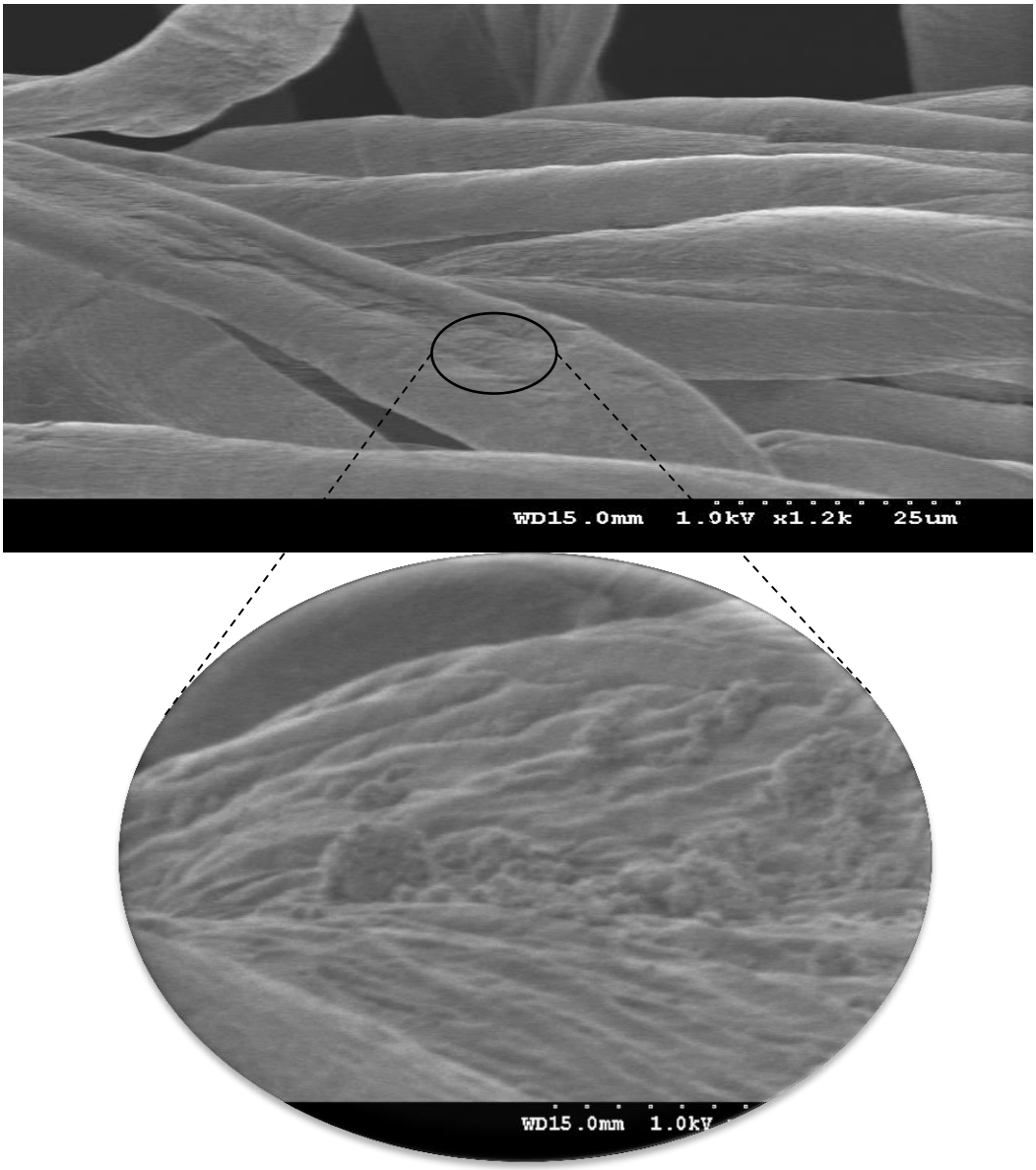

Figure 6.29 Fabric treated with NPCM paraffin after 5 washes

Figure 6.30 shows the comparison of images of fabric treated with both MPCM 28 and NPCM paraffin in one bath. This is clear from the images that microcapsules with MPCM 28 are attached to the surface of the filaments while the newly developed nanocapsules are bound to the fibre as its integral part with the help of binder. As long as binder is present, the nanocapsules are difficult to be removed. In Figure 6.30 larger capsule is magnified showing that a significant amount of nanocapsules is spread even

on the surface of microcapsule; this means if nanocapsules are used instead of microcapsules, they can enhance the thermal characteristic of the treated fabric.

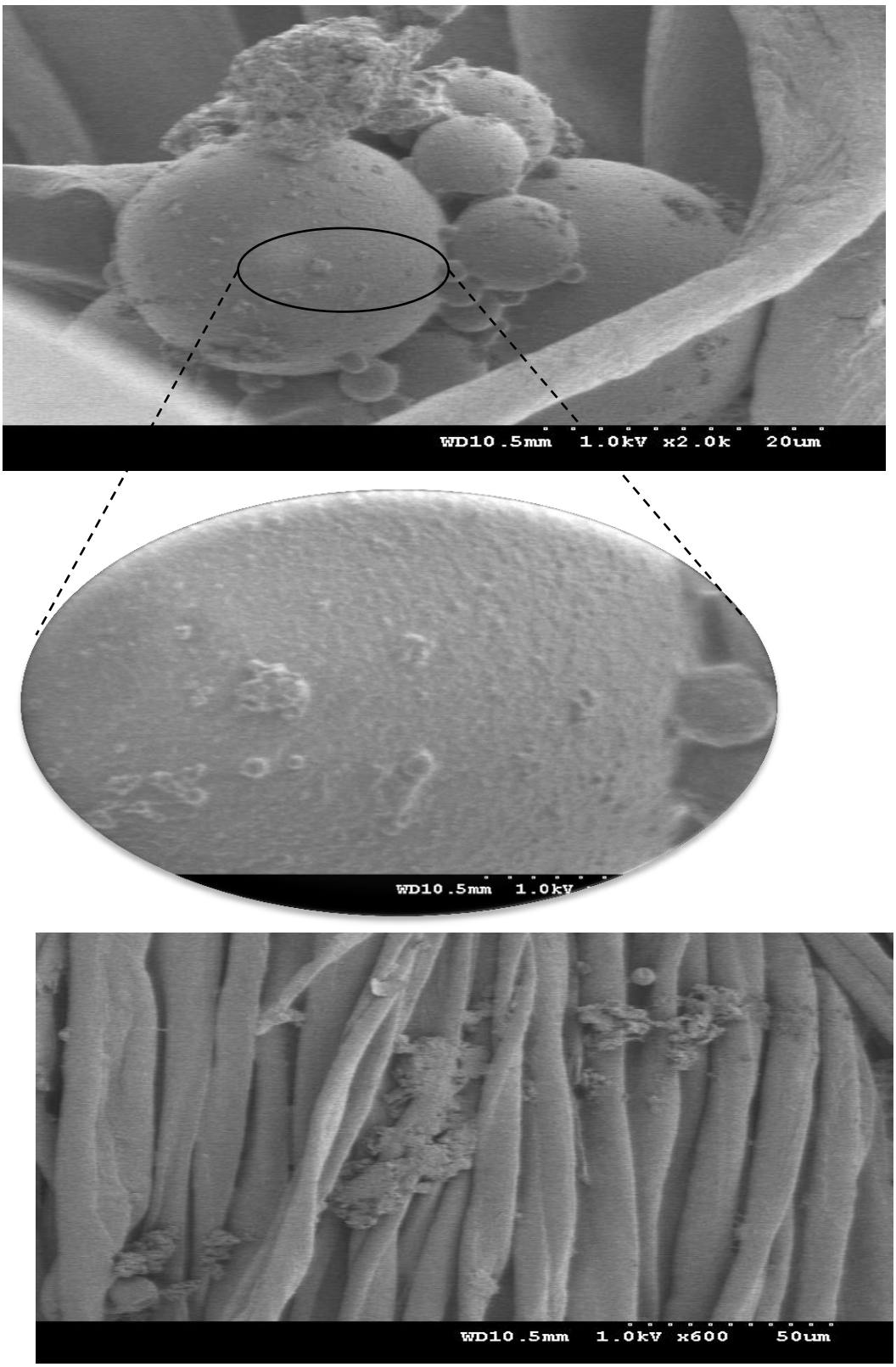

Figure 6.30 Comparison of MPCM 28 and NPCM paraffin in one bath

DSC study of NPCM paraffin treated fabric

DSC was performed for all fabrics treated with MPCM 28 and NPCM paraffin before and after being washed. The lines were drawn manually to measure the area of the curves by joining the onset and offset temperature. Although this manual process of drawing lines can lead to variation in measuring latent heat and for this study it was ±1.5% of the actual value, it is negligible. Figure 6.31 shows the DSC curves of treated fabrics with MPCM 28 after one wash and after five washes in comparison to the original. This is clear from Figure 6.31 that after washing the latent heat of the fabric decreases 60% and 83.4% for the fabrics after one wash and five washes respectively.

Figure 6.32 shows the DSC curves of fabrics treated with NPCM paraffin before washing, after one wash and five washes. The latent heat of the fabrics decreases 32.2% and 62.8% after one wash and 5 washes respectively, which is much less compared to fabrics treated with MPCM 28. The reason is that nanocapsules are difficult to be removed as they bind well with filaments in the fabric due to the nano scale of the particles.

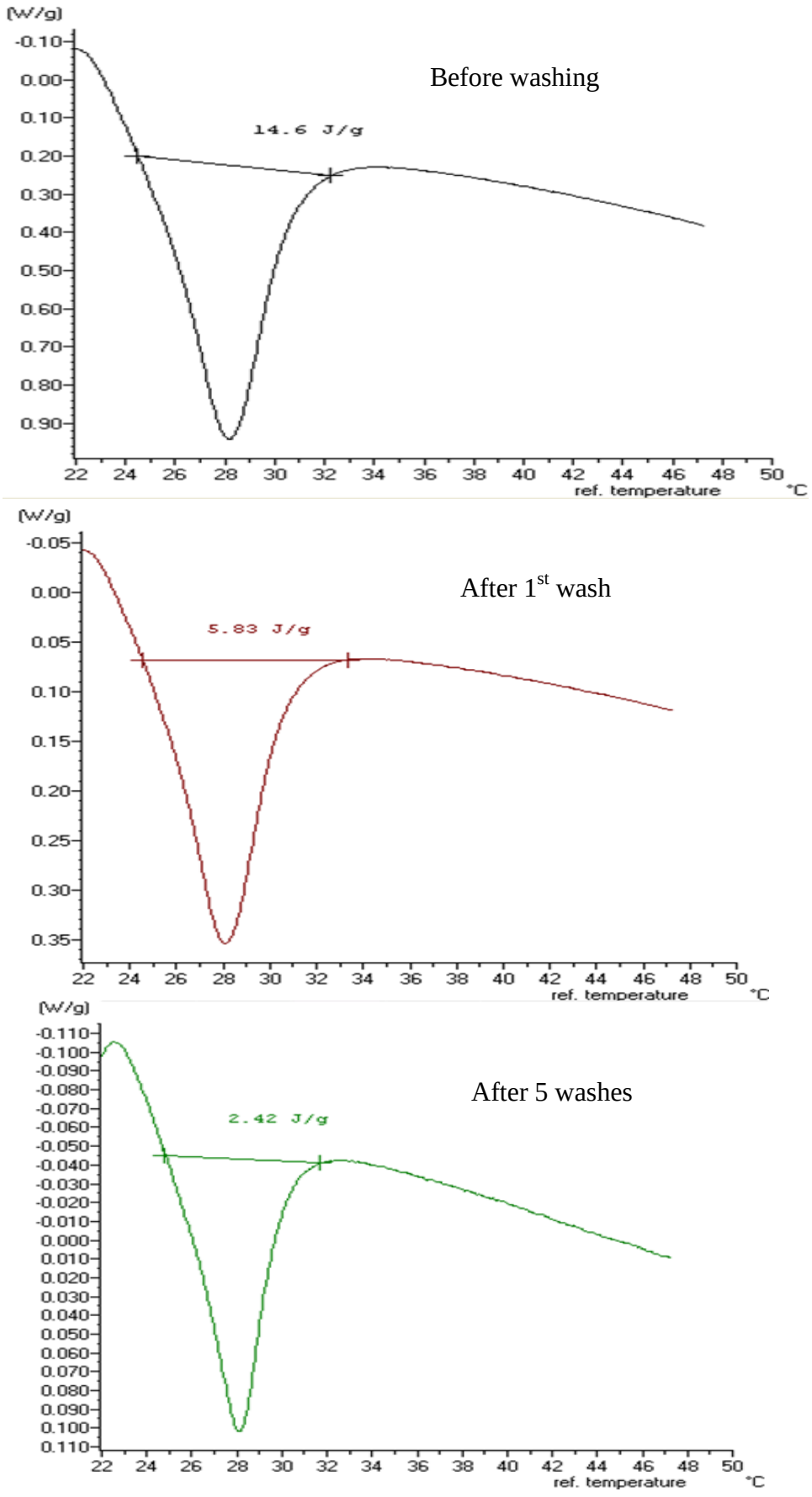

Figure 6.31 Changes of latent heat after washing for fabric treated with MPCM 28

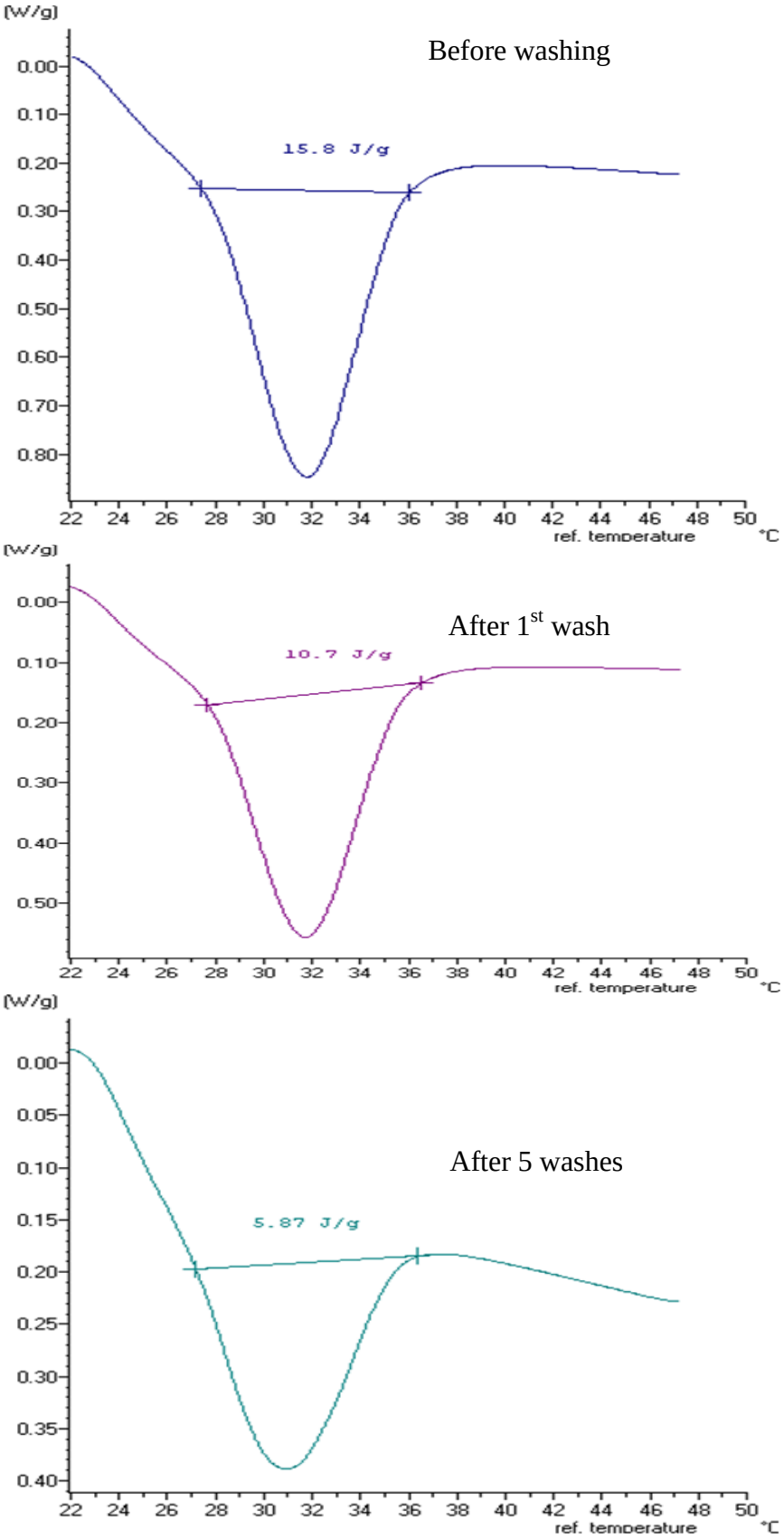

Figure 6.32 Changes of latent heat after washing for fabric treated with NPCM paraffin

Figure 6.33 illustrates the comparison for the latent heat of fabrics treated with MPCM 28 and NPCM paraffin before and after washing. The decrease of latent heat is attributed to washing but this is obvious as shown in Figure 6.33 that the smaller the size of capsules, the more firmly it bound to the filaments in fabric. The developed nanocapsules are more durable to washing as compared to commercially supplied microcapsules.

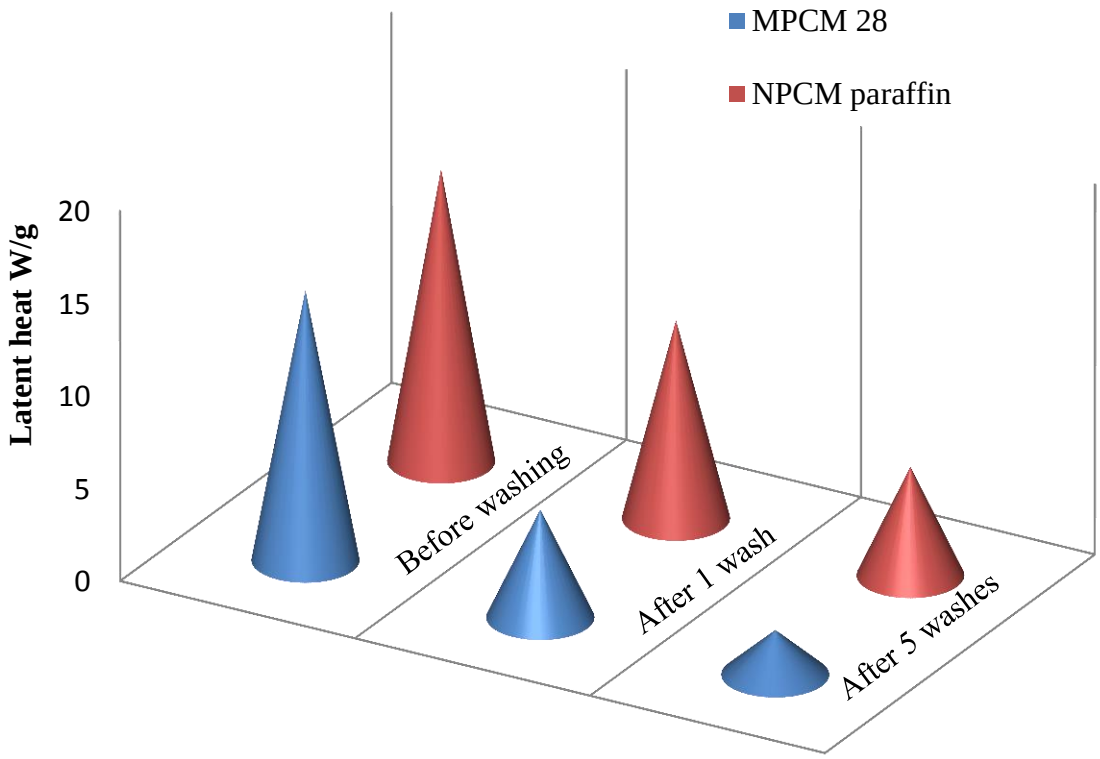

Figure 6.33 Comparison of latent heat of fabrics treated with MPCM 28 and NPCM paraffin

6.3 Encapsulation, characterisation and application of NPCM Glauber's salt on fabric

This section describes the synthesis of NPCM Glauber's salt, its characterisation and application on cotton fabric via pad-dry-cure technique.

6.3.1 *Encapsulation procedure*

Glauber's salt $Na_2SO_4.10H_2O$ was used as core material and was encapsulated by shell containing PMMA. Because of the hydrophilic nature of hydrated salt and its low melting temperature, the non-volatile solvent was used to prepare the emulsion.

Toluene and dicholoro-methane were used as non-volatile and volatile solvents respectively. Tween® was used as an emulsifier and polyvinyl alcohol was used as emulsion stabilizer. Dibenzoyl peroxide was used as initiator and 4-methoxy phenol was used as inhibitor. All above chemicals were supplied by Alfa Aesar®.

The emulsion of Glauber's salt was made by adding 20g of Glauber's salt in an organic solvent containing 80ml of toluene and emulsifying agent using ultrasonic homogeniser for 5 min at 30 °C. 5mg of PVA was added as stabilizer to keep the emulsion in stable form. The prepolymer solution was made by mixing 12g of MMA and 2g EA in a 50 ml of volatile solvent dichloromethane and was stirred at room temperature until the clear solution was obtained. Half of the Emulsion was poured into three neck flask bottle and prepolymer solution was dribbled into the emulsion slowly. Meanwhile, initiator and stabilizer were added into the emulsion to initiate the reaction. The initiator was added in two steps to ensure the controlled and proper polymerization reaction. As the temperature was gradually increased to 60 °C, the rest of the emulsion was added in the reaction flask and initiator was added as well. The temperature was raised up to 80 °C under the stirring rate of 600 rpm until the solvent was evaporated. Finally the post processing was done by adding inhibitor to stop the further polymerization reaction and the sample was filtered and washed with diethyl ether and dried in an oven.

Reaction mechanism

The reaction of PMMA shell formation is shown in Figure 6.34 which indicates the polymerization of MMA in the presence of initiator. The free radical polymerization also occurs between the MMA and EA forming modified PMMA as shown in Figure 6.35. The Ethyl acrylate is more prone to initiate in the presence of initiator due to the presence of ethyl group which is less stable and helps the system to propagate for the polymerization reaction.

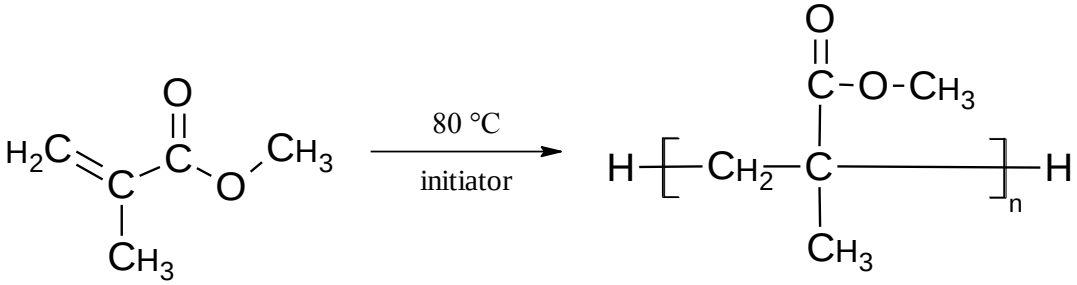

Figure 6.34 Reaction of PMMA shell formation

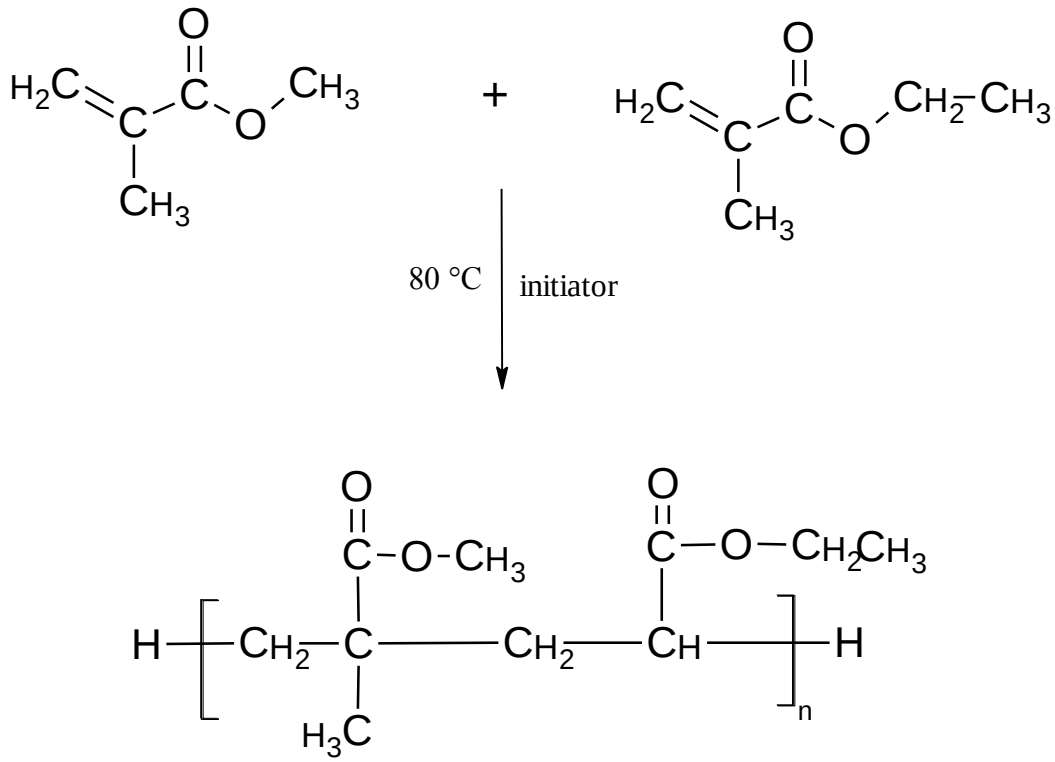

Figure 6.35 Copolymerization forming modified PMMA shell

6.3.2 *Characterisation of NPCM Glauber's salt*

SEM micrographs of NPCM Glauber's salt

Figure 6.36 shows the image of newly developed NPCM Glauber's salt before washing and the images in Figure 6.37 show NPCM Glauber's salt after washing with diethyl ether. Before washing, the capsules are visible but seem as they are within resinous bed. After washing with diethyl ether, the capsules are well separated and quite visible. The images are captured at higher magnification in order to show the spherical shape of capsules.

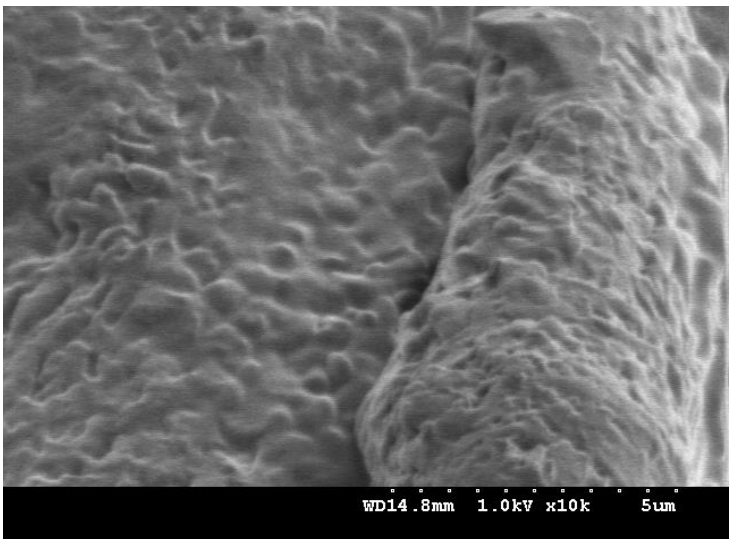

Figure 6.36 NPCM Glauber's salt before washing

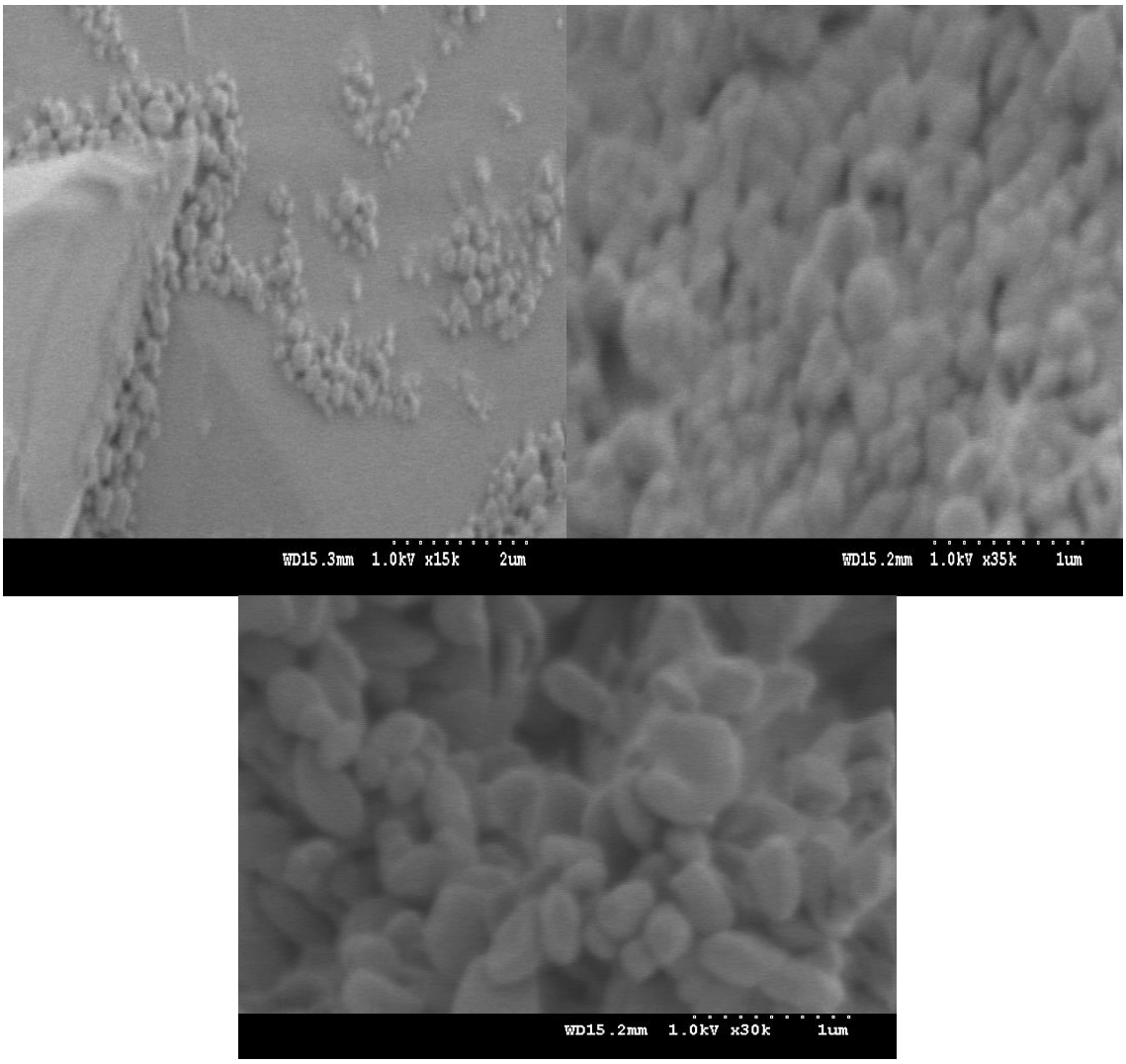

Figure 6.37 NPCM Glauber's salt after washing with diethyl ether

DSC study of NPCM Glauber's salt

Differential scanning calorimetry was used to determine the latent heat of the newly developed NPCM Glauber's salt. The image taken from DSC is shown in Figure 6.38 which indicates the curve changes as the temperature changes. The slope on the curve with two perpendiculars indicates the melting range. The melting of NPCM Glauber's salt starts at 32.4 °C and ends at 41.1 °C.

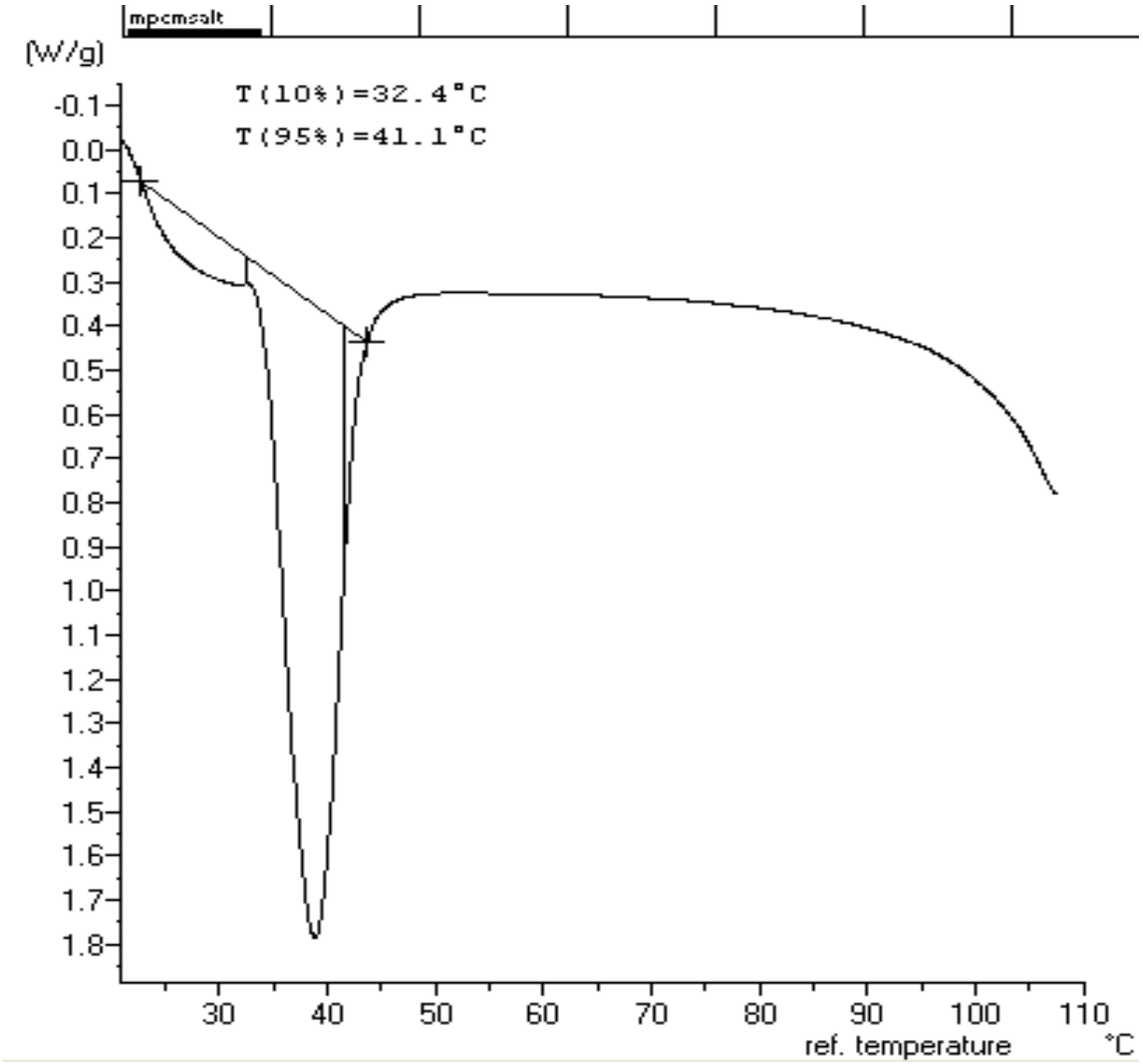

Figure 6.38 Latent heat for newly developed NPCM Glauber's salt

Structure of NPCM Glauber's salt

Figure 6.39 shows the FTIR image of nanoencapsulated Glauber's salt. The absorption band at 3400-3550 cm^{-1} shows the presence of –OH group of water attached to Glauber's salt. The broader peak at 1060 cm^{-1} shows the existence of $SO_4^{=}$ group in Glauber's salt. The band at 1750 cm^{-1} shows the presence of acrylate carboxyl group.

The two bands from 2800-2900 cm^{-1} can be assigned to the C-H stretching vibration of $–CH_3$ and $–CH_2$ groups. The peak at 2100 cm^{-1} can be attributed to $CH-CH_2$ stretching vibration of PMMA. Hence the above spectrum shows the synthesis of nanocapsules composed of Glauber's salt and PMMA shell.

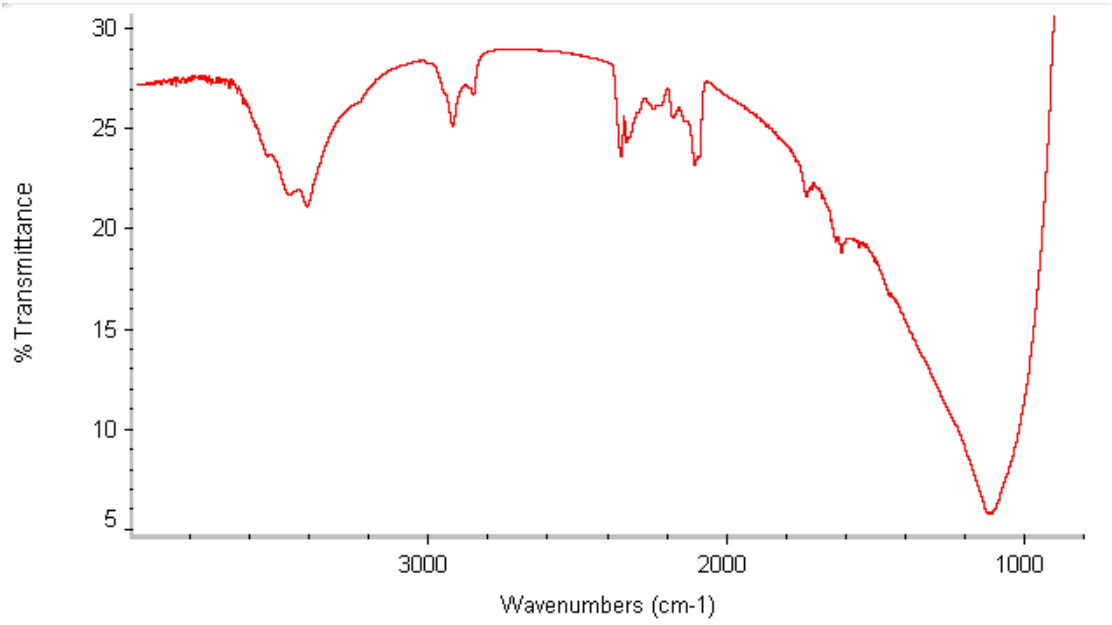

Figure 6.39 FTIR of NPCM Glauber's salt

6.3.3 *Application of NPCM Glauber's salt on fabric via pad-dry-cure technique*

The newly developed NPCM Glauber's salt were applied onto plain woven fabric made of 100% cotton through padding in the same manner as MPCM 28 described in the section 6.1.5 and comparison made between fabrics treated with the two types of capsules. The padding solution was prepared in water containing 60 g/l of polyurethane binder ARRISTAN EPD, 50 g/l of REAKNITT ZF which is dimethyl-dihydroxyl-ethylene urea, formaldehyde free cross linking agent which enhances the cross linking of binder, 50g/l of TUBINGAL RGH softener which is modified polysiloxane and 8 g/l of CHT CATALYST AD, a modified inorganic salt, and NPCM Glauber's salt accounted for 30% of the weight of binder. The fabric was padded with a pressure of 2 bars between the mangles with 2 m/min using two dip two nips. The fabric was then dried at 100 °C and was cured in a stenter at 150 °C for 3 minutes.

Each sample was then taken for washing (1 wash and 5 washes) to study the durability of the applied PCM capsules. SEM and DSC were used to characterise the washed fabrics as comparison to the untreated.

SEM study of NPCM Glauber's salt treated cotton fabric

Figure 6.40 shows the images of cotton fabric treated with NPCM Glauber's salt. The nanocapsules attached to the filaments in fabric with the help of binder can be seen clearly and are present in large amount while in Figure 6.41, the images of treated fabric after 1st washing shows the presence of nanocapsules present on the surface of fibre or yarns in fabric.

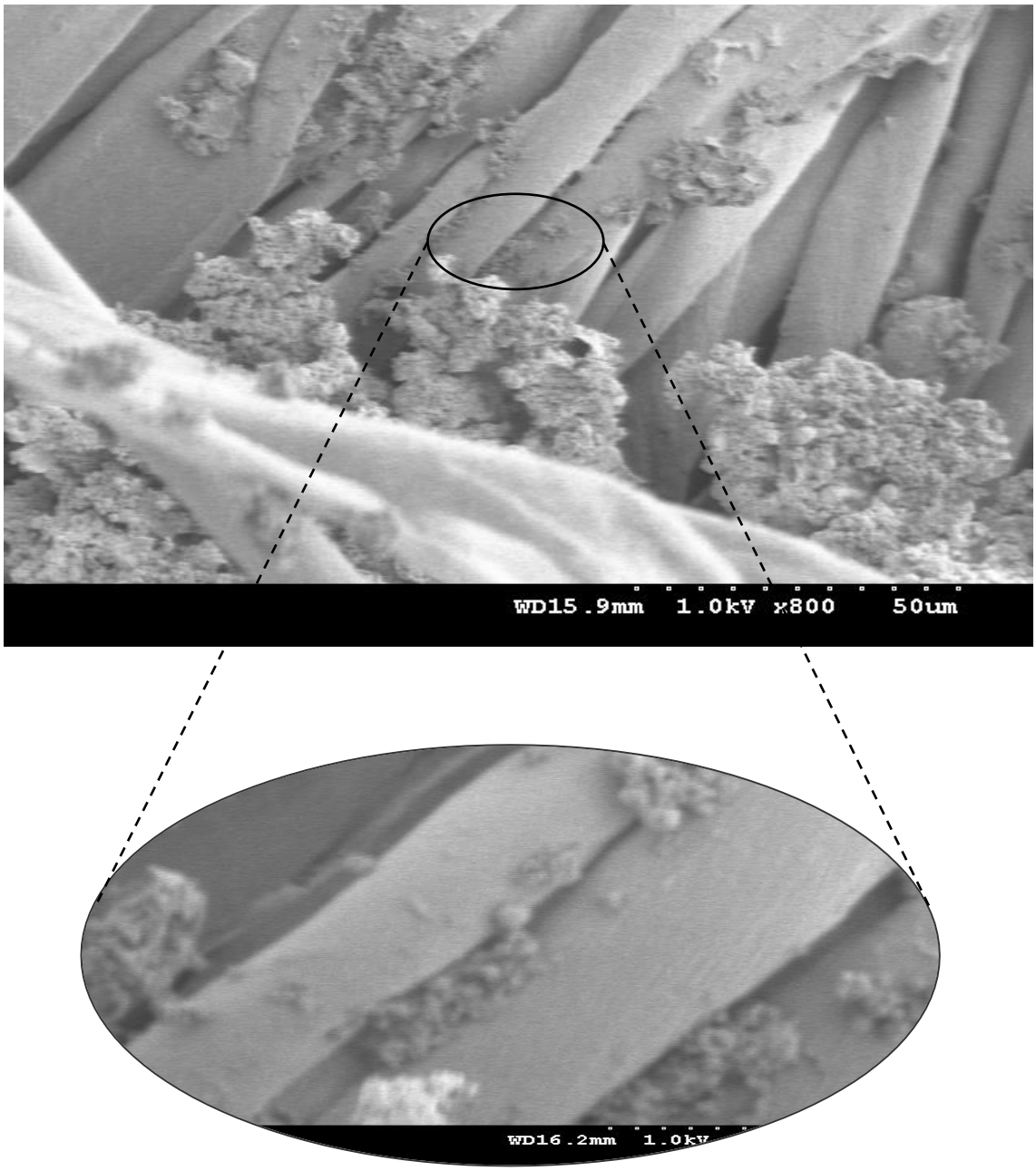

Figure 6.40 Fabric treated with NPCM Glauber's salt before washing

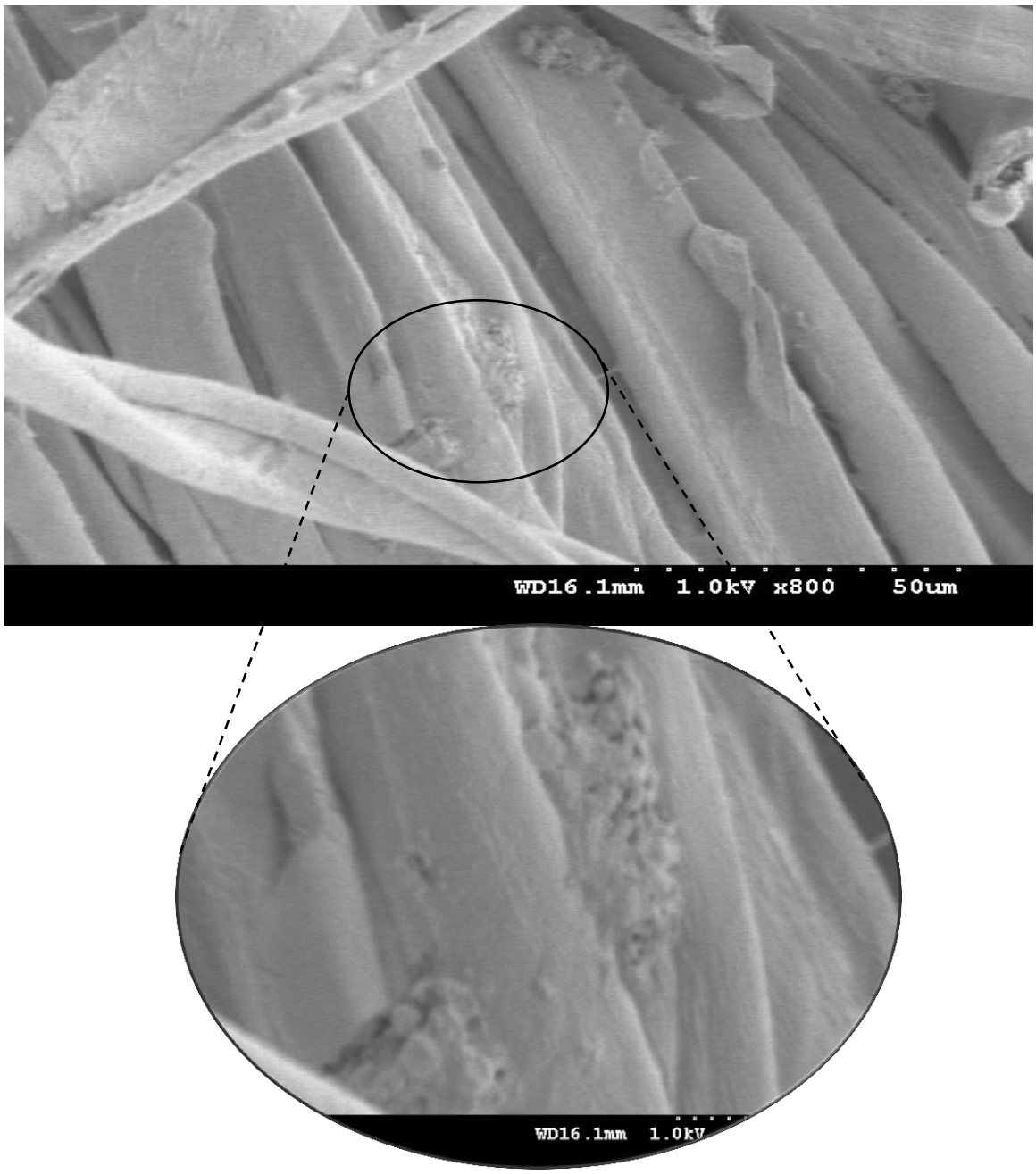

Figure 6.41 Fabric treated with NPCM Glauber's salt after 1st wash

Figure 6.42 shows the images of the fabric which was treated with NPCM Glauber's salt after 5 washes. The nanocapsules are present in fewer amounts as can be seen and image was further magnified to show the presence of nanocapsules. The nanocapsules are firmly bound with the help of binder up to the fibre level.

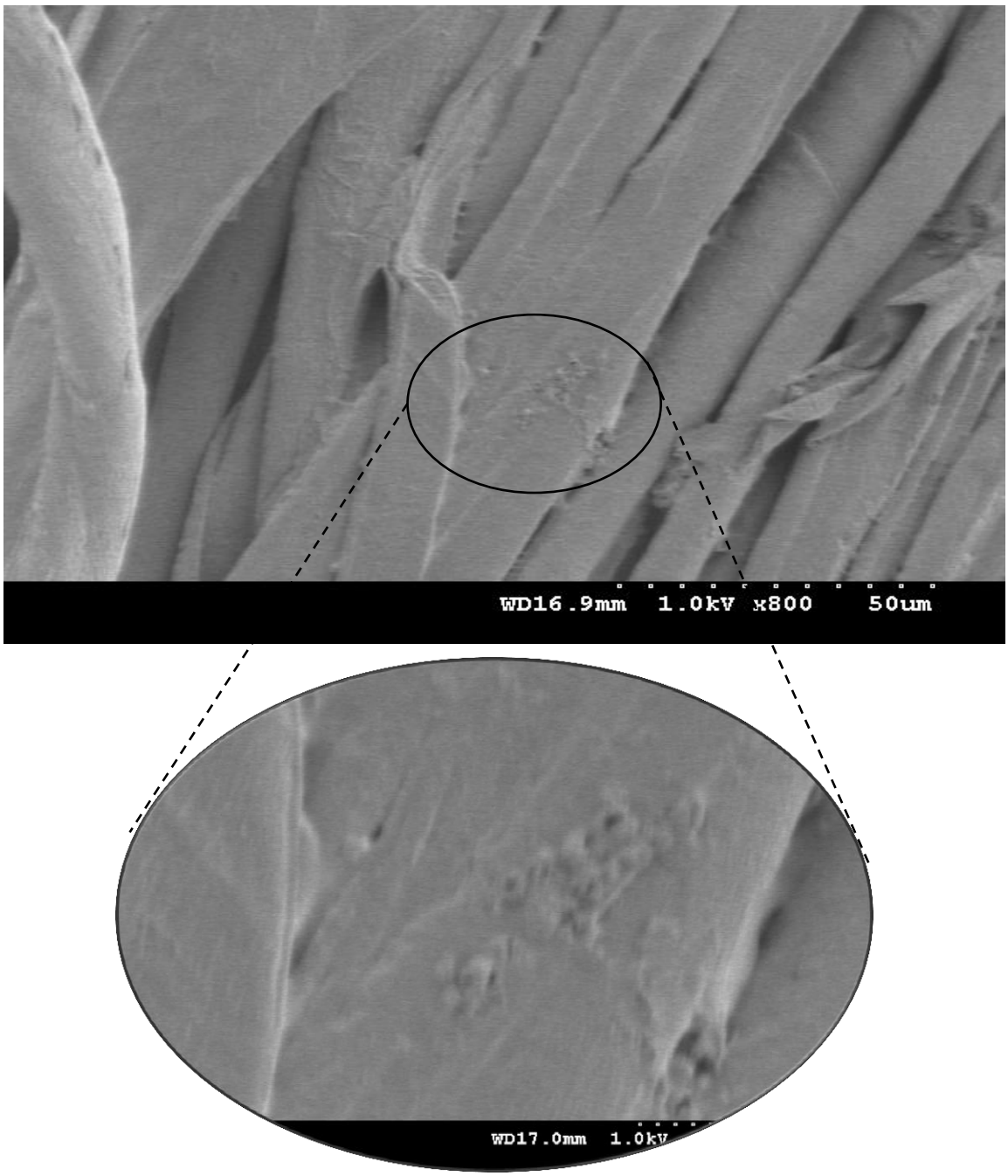

Figure 6.42 Fabric treated with NPCM Glauber's salt after 5 washes

DSC study of NPCM Glauber's salt treated cotton fabric

DSC was performed for fabrics treated with MPCM 28 and NPCM Glauber's salt before and after washing. Latent heat for the fabrics treated with MPCM 28 has already been shown in Figure 6.31 before washing, after 1 wash and 5 washes. Figure 6.43 shows the latent heat for the fabrics treated with NPCM Glauber's salt. The treated fabrics show latent heat of 12.3 J/g before washing and decreases 24.3% and 62.2% after 1 wash and 5 washes respectively.

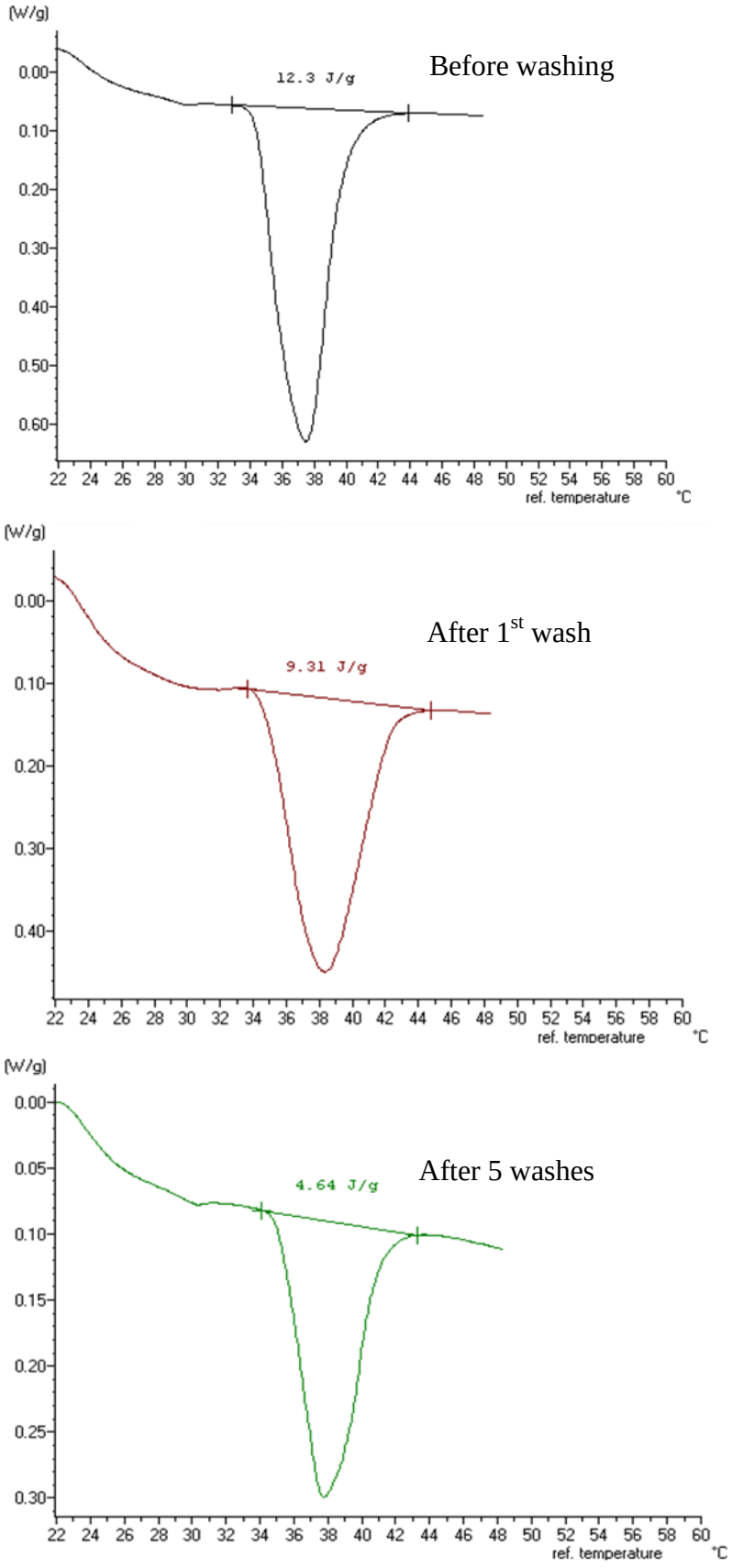

Figure 6.43 Change of latent heat of fabric treated with NPCM Glauber's salt after washing

Figure 6.44 shows the comparison of the latent heat of fabrics treated with MPCM 28 and the newly developed NPCM Glauber's salt before and after washing. The decrease in latent heat is because the loosely attached capsules leave the fabric as a result of washing. This is clear from Figure 6.44 that the latent heat after washing is less in case of MPCM 28 because of the microcapsules are larger as compared to NPCM Glauber's salt, which are in nano scales. The nanocapsules are more durable to washing and attached to fibre and yarns in fabric firmly as an integral part of binder as compared to microcapsules.

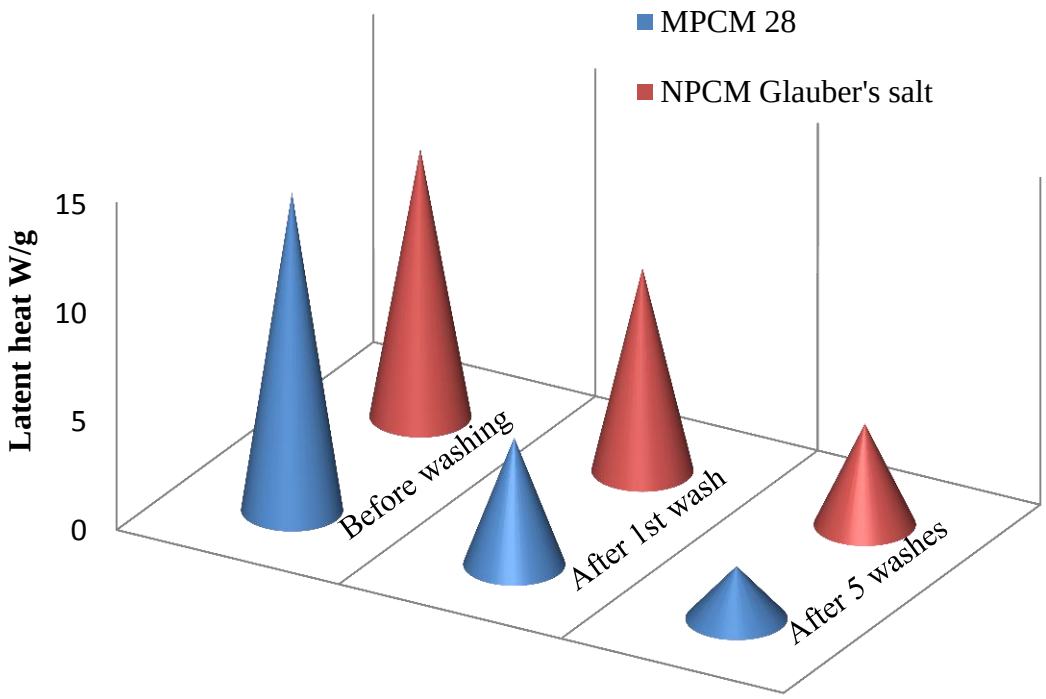

Figure 6.44 Comparison of latent heat of treated fabrics with MPCM 28 and the NPCM Glauber's salt

From the above analysis it is clear that incorporation of NPCM and its application through finishing process on fabrics provide better thermal characteristics as compared to MPCM. The capsules bound with fabric in fibre level when they are in nano scale showing better resistance to washing as compared to capsules with larger size though the permanent effect can be achieved by incorporating NPCM into the filaments.

Chapter 7 Conclusions and Future work

7.1 Conclusions

This research investigated thermoregulating textiles containing phase change materials through experimental and theoretical studies, and the development of nano scaled phase change capsules suitable for PCM fibre extrusion and production. The research led to the following conclusions.

7.1.1 *Monofilament polypropylene incorporated with MPCM*

One of the objectives of this research was to develop thermoregulating melt spun filament incorporated with MPCM which has been successfully developed with different percentages of MPCM. SEM and DSC confirmed the presence of microcapsules in the filament. The important processing parameters were found to be temperature, metering speed and the extruder speed. They were required to be set differently due to the different amount of MPCM contained in a yarn. SEM and DSC results confirmed the presence of MPCM in the developed monofilament. Furthermore the statistical models were developed for the prediction of the latent heat, modulus and tenacity of MPCM incorporated filaments. The reliability of the models was further verified by the high correlation between the predicted results and the experimental results tested on a new developed filament.

7.1.2 *Multifilament polypropylene incorporated with MPCM*

Another objective of the research was to develop multifilament yarn containing MPCM through melt spinning process. MPCM containing multifilament yarns have been successfully developed using a newly designed spinneret to overcome the problems of extrusion. SEM and DSC results confirmed the presence of MPCM within the multi filament yarn and up to 8% MPCM is incorporated in the multifilament with continuous extrusion. Further investigations of this part of research reveal the following findings.

- By decreasing the spread of holes of spinneret and increasing the L/D (land/diameter) ratio of spinneret, the uniformity of fibre can be increased during extruding process.

- Extrusion parameters such as temperature and extruder speed were optimised for continuous filament production and it was found that they were dependent on the amount of MPCM used during filaments manufacture.

7.1.3 *Heat transfer analysis of yarn and fabric incorporated with MPCM using FEM*

The heat transfer analysis of yarn and fabric incorporated with MPCM was studied using finite element method in ABAQUS. The results of simulated models were compared with experimental results for model validation. The thermoregulating effect for the protection of wearer against extreme weather was predicted against different amount of PCM. The following conclusions are made from this part of research:

- The yarn model containing 4% MPCM was successfully developed and heat flow property was investigated through ABAQUS to compare with DSC heat flow for model validation. Further models were developed containing larger amount of PCM to study the time dependent thermoregulating effect and this provides useful information in yarn design to meet effective thermal regulation for a required period of time.
- A woven fabric model was successfully developed with multifilament yarn containing 4% MPCM; it was validated by experimental results. The study of plain woven fabrics containing different percentages of PCM revealed that PCM enhances the thermoregulating effect up to several minutes depending upon the amount of PCM used in the fabrics. The further investigation reveals that the duration of thermoregulating effect is decreased when PCM incorporated yarn or fabric are exposed to extreme temperature conditions.

7.1.4 *Synthesis of NPCM paraffin and NPCM Glauber's salt*

Another objective of the research was to synthesise nano capsules with paraffins and Glauber's salt in the core and to bring the phase change temperature closer to the human skin comfort temperature. The NPCM paraffins were incorporated into polypropylene filament and compared to the previously developed MPCM yarn. The NPCM paraffin and Glauber's salt were also applied on cotton fabric via pad-dry-cure method. The following conclusions can be drawn:

- The nanocapsules containing paraffins and Glauber's salt in core were successfully synthesised using MF and PMMA shell respectively. The characterisations of capsules confirm the size in nanoscale range and the phase change temperature of the nanocapsules is closer to the human skin temperature. The prepared nanocapsules showed spherical shape with smooth surface and the diameter of the capsules was found in the range 320nm. Furthermore NPCM paraffins were successfully incorporated into polypropylene filament showing larger amount of latent heat than previously developed MPCM polypropylene filament.
- Cotton fabrics treated with the developed PCM nanocapsules showed better characteristics compared to that of treated with commercial microcapsules when subjected to multiple washing. This part of research also reveals the fact that nanocapsules bind well with fabrics in fibre level as an integral part of binder which enhances the resistance to washing.

7.2 **Limitations and future work**

- Core/sheath (bicomponent) filament provides the best solution for thermoregulating effect because of the large amount of phase change materials present in the core. These filaments were not manufactured because of the absence of the specific type of spinning machine. The fabric containing bicomponent filaments should be developed to increase the duration of thermoregulating effect.
- The NPCM paraffin can be used for the incorporation of multifilament polypropylene and spinneret can be designed for microfibre production. Furthermore these nanocapsules can be incorporated into other melt spun filaments such as polyester and nylon. Polyester and nylon usually degrade at high temperature with additives. The appropriate thermal and oxidative stabilizers can be found and used for the processing of polyester and nylon filaments.
- Encapsulated PCM can also be incorporated in nylon filaments through wet spinning process. This technique was not explored due to the absence of wet spinning facility. The polymer fibre forming solution can be made by dissolving nylon in formic acid up to certain extent to get the appropriate consistency and

then PCM capsules can be added into the solution. This solution can be wet spun to develop NPCM or MPCM incorporated nylon fibre.

- Further studies should be performed on different structures of woven and knitted fabrics and heat transfer analysis should be performed on fabrics using computation software. Thermoregulating effect can be predicted and compared for all types of fabrics to optimise fabric structure, design and manufacturing.
- To incorporate encapsulated PCM into filaments containing high melting temperature such as polyester and nylon needs thermal stable shell. For this purpose, further studies should be done regarding parametric study of shell formation or the selection of polymeric material to modify the shell to enhance the thermal stabilization. The shear and thermal stability may also be enhanced by increasing the thickness of the shell wall which can impair the phase change characteristics.
- A significant amount of solvents are used in the process of encapsulation of Glauber's salt. The further research is needed to optimise the process and minimise the use of solvent and reduce cost.

References

[1] P. S. Bhatkhande, "Development of Thermo-Regulating Fabric Using Phase Change Material (PCM)," Eastern Michigan University, Master's Theses and Doctoral Dissertations, 2011.

[2] G. Havenith, C. Smith, and T. Fukazawa, "The Skin Interface - Meeting Point of Physiology and Clothing Science," *Journal of Fiber Bioengineering and Informatics,* vol. 1, pp. 93-98, 2008.

[3] Q. H. Meng and J. L. Hu, "A poly(ethylene glycol)-based smart phase change material," *Solar Energy Materials and Solar Cells,* vol. 92, pp. 1260-1268, Oct 2008.

[4] H. Mattila, *Intelligent textiles and clothing* USA: Woodhead Publishing, July 2006.

[5] G. Havenith, "The Interaction of Clothing and Thermoregulationg," *Exogenous Dermatology,* vol. 1, pp. 221-230, 2002.

[6] A. Schwarz, L. Van Langenhove, P. Guermonprez, and D. Deguillemont, "A roadmap on smart textiles," *Textile Progress,* vol. 42, pp. 99-180, 2010.

[7] J. Mengjin, S. Xiaoqing, X. Jianjun, and Y. Guangdou, "Preparation of a new thermal regulating fiber based on PVA and paraffin," *Solar Energy Materials and Solar Cells,* vol. 92, pp. 1657-1660, 12// 2008.

[8] W. L. Cheng, N. Liu, and W. F. Wu, "Studies on thermal properties and thermal control effectiveness of a new shape-stabilized phase change material with high thermal conductivity," *Applied Thermal Engineering,* vol. 36, pp. 345-352, Apr 2012.

[9] R. Cox, "Synopsis of the new thermal regulating fiber Outlast," *Chemical fibers international,* vol. 48, 1998.

[10] G. Nelson, "Application of microencapsulation in textiles," *International Journal of Pharmaceutics,* vol. 242, pp. 55-62, 2002.

[11] S. Mondal, "Phase change materials for smart textiles–an overview," *Applied Thermal Engineering,* vol. 28, pp. 1536-1550, 2008.

[12] M. M. Farid, A. M. Khudhair, S. A. K. Razack, and S. Al-Hallaj, "A review on phase change energy storage: materials and applications," *Energy conversion and management,* vol. 45, pp. 1597-1615, 2004.

[13] D. Buddhi, R. Sawhney, P. Sehgal, and N. Bansal, "A simplification of the differential thermal analysis method to determine the latent heat of fusion of

phase change materials," *Journal of Physics D: Applied Physics*, vol. 20, p. 1601, 1987.

[14] M. Lacroix, "Study of the Heat-Transfer Behavior of a Latent-Heat Thermal-Energy Storage Unit with a Finned Tube," *International Journal of Heat and Mass Transfer*, vol. 36, pp. 2083-2092, May 1993.

[15] M. Pauken, N. Emis, and B. Watkins, "Thermal energy storage technology developments," *Space Technology and Applications International Forum - STAIF 2007*, vol. 880, pp. 412-420, 2007.

[16] A. Agbossou, Q. Zhang, G. Sebald, and D. Guyomar, "Solar micro-energy harvesting based on thermoelectric and latent heat effects. Part I: Theoretical analysis," *Sensors and Actuators a-Physical*, vol. 163, pp. 277-283, Sep 2010.

[17] C. Alkan, "Enthalpy of melting and solidification of sulfonated paraffins as phase change materials for thermal energy storage," *Thermochimica Acta*, vol. 451, pp. 126-130, Dec 1 2006.

[18] J. K. Choi, J. G. Lee, J. H. Kim, and H. S. Yang, "Preparation of microcapsules containing phase change materials as heat transfer media by in-situ polymerization," *Journal of Industrial and Engineering Chemistry*, vol. 7, pp. 358-362, Nov 2001.

[19] V. V. Tyagi and D. Buddhi, "PCM thermal storage in buildings: A state of art," *Renewable & Sustainable Energy Reviews*, vol. 11, pp. 1146-1166, Aug 2007.

[20] B. Zalba, J. M. Marin, L. F. Cabeza, and H. Mehling, "Review on thermal energy storage with phase change: materials, heat transfer analysis and applications," *Applied Thermal Engineering*, vol. 23, pp. 251-283, Feb 2003.

[21] D. Feldman, M. M. Shapiro, and D. Banu, "Organic-Phase Change Materials for Thermal-Energy Storage," *Solar Energy Materials*, vol. 13, pp. 1-10, Jan 1986.

[22] B. Pause, "Development of heat and cold insulating membrane structures with phase change material," *Journal of Industrial Textiles*, vol. 25, pp. 59-68, 1995.

[23] M. Hartmann, J. B. Worley, and M. North, "Cellulosic fibers having enhanced reversible thermal properties and methods of forming thereof," ed: Google Patents, 2012.

[24] W. Bendkowska and H. Wrzosek, "Experimental study of the thermoregulating properties of nonwovens treated with microencapsulated PCM," *Fibres & Textiles in Eastern Europe*, vol. 17, p. 76, 2009.

[25] A. Kürklü, "Thermal performance of a tapered store containing tubes of phase change material: cooling cycle," *Energy conversion and management,* vol. 38, pp. 333-340, 1997.

[26] B. Pause, "Driving more comfortably with phase change materials," *Technical Textiles International,* vol. 11, pp. 24-27, 2002.

[27] S. Canbazoğlu, A. Şahinaslan, A. Ekmekyapar, Ý. G. Aksoy, and F. Akarsu, "Enhancement of solar thermal energy storage performance using sodium thiosulfate pentahydrate of a conventional solar water-heating system," *Energy and Buildings,* vol. 37, pp. 235-242, 2005.

[28] A. Saito, S. Okawa, T. Shintani, and R. Iwamoto, "On the heat removal characteristics and the analytical model of a thermal energy storage capsule using gelled Glauber's salt as the PCM," *International journal of heat and mass transfer,* vol. 44, pp. 4693-4701, 2001.

[29] D. R. Biswas, "Thermal energy storage using sodium sulfate decahydrate and water," *Solar Energy,* vol. 19, pp. 99-100, 1977.

[30] S. Marks, "An investigation of the thermal energy storage capacity of Glauber's salt with respect to thermal cycling," *Solar Energy,* vol. 25, pp. 255-258, 1980.

[31] J. L. Zuckerman, R. J. Pushaw, B. T. Perry, and D. M. Wyner, "Fabric coating containing energy absorbing phase change material and method of manufacturing same," 2003.

[32] B. Pause, "Building conditioning technique using phase change materials," ed: Google Patents, 2001.

[33] K. Pielichowski and K. Flejtuch, "Differential scanning calorimetry studies on poly (ethylene glycol) with different molecular weights for thermal energy storage materials," *Polymers for Advanced Technologies,* vol. 13, pp. 690-696, 2002.

[34] D. Craig and J. Newton, "Characterisation of polyethylene glycols using differential scanning calorimetry," *International journal of pharmaceutics,* vol. 74, pp. 33-41, 1991.

[35] B. Hopp, T. Smausz, E. Tombácz, T. Wittmann, and F. Ignácz, "Solid state and liquid ablation of polyethylene-glycol 1000: temperature dependence," *Optics communications,* vol. 181, pp. 337-343, 2000.

[36] X. B. Yang, J. P. Zheng, Y. Bai, F. J. Tian, J. Yuan, J. Y. Sun, *et al.*, "Using lymphocyte and plasma Hsp70 as biomarkers for assessing coke oven exposure

among steel workers," *Environmental Health Perspectives,* vol. 115, pp. 1573-1577, Nov 2007.

[37] E. Onofrei, A. M. Rocha, and A. Catarino, "Textiles integrating PCMs – A review," *Buletinul Institutului Politehnic din Iaşi,* vol. 2, pp. 99-110, 2010.

[38] N. Sarier and E. Onder, "Organic phase change materials and their textile applications: An overview," *Thermochimica Acta,* vol. 540, pp. 7-60, Jul 20 2012.

[39] M. S. Uddin, H. J. Zhu, and M. N. A. Hawlader, "Effects of cyclic operation on the characteristics of a microencapsulated PCM storage material," *International Journal of Solar Energy,* vol. 22, pp. 105-114, 2002.

[40] Z. G. Jin, Y. D. Wang, J. G. Liu, and Z. Z. Yang, "Synthesis and properties of paraffin capsules as phase change materials," *Polymer,* vol. 49, pp. 2903-2910, Jun 10 2008.

[41] W. Chen, X. Liu, and D. W. Lee, "Fabrication and characterization of microcapsules with polyamide-polyurea as hybrid shell," *Journal of Materials Science,* vol. 47, pp. 2040-2044, Feb 2012.

[42] A. M. Borreguero, J. L. Valverde, J. F. Rodriguez, A. H. Barber, J. J. Cubillo, and M. Carmona, "Synthesis and characterization of microcapsules containing Rubitherm (R) RT27 obtained by spray drying," *Chemical Engineering Journal,* vol. 166, pp. 384-390, Jan 1 2011.

[43] C. Y. Zhao and G. H. Zhang, "Review on microencapsulated phase change materials (MEPCMs): Fabrication, characterization and applications," *Renewable & Sustainable Energy Reviews,* vol. 15, pp. 3813-3832, Oct 2011.

[44] Y. Shin, D. I. Yoo, and K. Son, "Development of thermoregulating textile materials with microencapsulated phase change materials (PCM). II. Preparation and application of PCM microcapsules," *Journal of Applied Polymer Science,* vol. 96, 2005.

[45] N. Sarier and E. Onder, "The manufacture of microencapsulated phase change materials suitable for the design of thermally enhanced fabrics," *Thermochimica Acta,* vol. 452, pp. 149-160, Jan 15 2007.

[46] G. Y. Fang, Z. Chen, and H. Li, "Synthesis and properties of microencapsulated paraffin composites with SiO2 shell as thermal energy storage materials," *Chemical Engineering Journal,* vol. 163, pp. 154-159, Sep 15 2010.

[47] M. G. Li, Y. Zhang, Y. H. Xu, and D. Zhang, "Effect of different amounts of surfactant on characteristics of nanoencapsulated phase-change materials," *Polymer Bulletin*, vol. 67, pp. 541-552, Jul 2011.

[48] F. Salaun, E. Devaux, S. Bourbigot, and P. Rumeau, "Development of Phase Change Materials in Clothing Part I: Formulation of Microencapsulated Phase Change," *Textile Research Journal*, vol. 80, pp. 195-205, Feb 2010.

[49] P. Sánchez, M. V. Sánchez-Fernandez, A. Romero, J. F. Rodríguez, and L. Sánchez-Silva, "Development of thermo-regulating textiles using paraffin wax microcapsule," *Thermochimica Acta*, vol. 498, pp. 16-21, 2010.

[50] A. Sari, C. Alkan, A. Karaipekli, and O. Uzun, "Microencapsulated n-octacosane as phase change material for thermal energy storage," *Solar Energy*, vol. 83, pp. 1757-1763, Oct 2009.

[51] H. J. Kwon, I. W. Cheong, and J. H. Kim, "Preparation of n-octadecane nanocapsules by using interfacial redox initiation in miniemulsion polymerization," *Macromolecular Research*, vol. 18, pp. 923-926, Sep 2010.

[52] J. K. Black, L. E. Tracy, C. P. Roche, P. J. Henry, J. B. Pesavento, and T. Adalsteinsson, "Phase Transitions of Hexadecane in Poly(alkyl methacrylate) Core-Shell Microcapsules," *Journal of Physical Chemistry B*, vol. 114, pp. 4130-4137, Apr 1 2010.

[53] S. Alay, F. Göde, and C. Alkan, "Preparation and characterization of poly(methylmethacrylate-coglycidyl methacrylate)/n-hexadecane nanocapsules as a fiber additive for thermal energy storage," *Fibers and Polymers*, vol. 11, pp. 1089-1093, 2010.

[54] M. Karthikeyan, T. Ramachandran, and O. L. Shanmugasundaram, "Synthesis, characterization, and development of thermally enhanced cotton fabric using nanoencapsulated phase change materials containing paraffin wax," *The Journal of The Textile Institute*, vol. 105, pp. 1279-1286, 2014.

[55] R. Arshaday, "Microspheres and Microcapsules, a Survey of Manufacturing Techniques Part II: Coacervation," *Polymer engineering and Science*, vol. 30, pp. 905-914, 1990.

[56] G. Nelson, "Microencapsulation in Textile Finishing," *Review of Progress in Coloration and Related Topics*, vol. 31, pp. 57-64, 2001.

[57] D. P. Colvin and Y. G. Bryant, "Thermally enhanced foam insulation," ed: Google Patents, 1997.

[58] R. J. Pushaw, "Coated skived foam and fabric article containing energy absorbing phase change material," ed: Google Patents, 1997.

[59] M. N. A. Hawlader, M. S. Uddin, and M. M. Khin, "Microencapsulated PCM thermal-energy storage system," *Applied Energy*, vol. 74, pp. 195-202, 2003.

[60] M. N. A. Hawlader, M. S. Uddin, and H. J. Zhu, "Preparation and Evaluation of a Novel Solar Storage Material: Microencapsulated Paraffin," *International Journal of Solar Energy*, vol. 20, pp. 227-238, 2000.

[61] M. I. Teixeira, L. R. Andrade, M. Farina, and M. H. M. Rocha-Leao, "Characterization of short chain fatty acid microcapsules produced by spray drying," *Materials Science & Engineering C-Biomimetic and Supramolecular Systems*, vol. 24, pp. 653-658, Nov 1 2004.

[62] A. Loxley and B. Vincent, "Preparation of poly(methylmethacrylate) microcapsules with liquid cores," *Journal of Colloid and Interface Science*, vol. 208, pp. 49-62, Dec 1 1998.

[63] F. Salaun, E. Devaux, S. Bourbigot, and P. Rumeau, "Preparation of multinuclear microparticles using a polymerization in emulsion process," *Journal of Applied Polymer Science*, vol. 107, pp. 2444-2452, Feb 15 2008.

[64] L. Sánchez, P. Sánchez, A. de Lucas, M. Carmona, and J. F. Rodríguez, "Microencapsulation of PCMs with a polystyrene shell," *Colloid and Polymer Science*, vol. 285, pp. 1377-1385, 2007.

[65] E. J. Sundberg and D. C. Sundberg, "Morphology development for three-component emulsion polymers: Theory and experiments," *Journal of Applied Polymer Science*, vol. 47, pp. 1277-1294, 1993.

[66] F. Salaun, "The Manufacture of Microencapsulated Thermal Energy Storage Compounds Suitable for Smart Textile," in *Developments in Heat Transfer*, M. A. D. S. Bernardes, Ed., ed, 2011.

[67] S. S. Deveci and G. Basal, "Preparation of PCM microcapsules by complex coacervation of silk fibroin and chitosan," *Colloid and Polymer Science*, vol. 287, pp. 1455-1467, Dec 2009.

[68] E. Onder, N. Sarier, and E. Cimen, "Encapsulation of phase change materials by complex coacervation to improve thermal performances of woven fabrics," *Thermochimica Acta*, vol. 467, pp. 63-72, 2008.

[69] B. Sumiga, E. Knez, M. Vrtacnik, V. Ferk-Savec, M. Staresinic, and B. Boh, "Production of Melamine-Formaldehyde PCM Microcapsules with Ammonia

Scavenger used for Residual Formaldehyde Reduction," *Acta Chim Slov,* vol. 58, pp. 14-25, Mar 2011.

[70] F. Salaun, E. Devaux, S. Bourbigot, and P. Rumeau, "Influence of process parameters on microcapsules loaded with n-hexadecane prepared by in situ polymerization," *Chemical Engineering Journal,* vol. 155, pp. 457-465, Dec 1 2009.

[71] Q. W. Song, Y. Li, J. W. Xing, J. Y. Hu, and C. W. M. Yuen, "Thermal stability of composite phase change material microcapsules incorporated with silver nano-particles," *Polymer,* vol. 48, pp. 3317-3323, May 21 2007.

[72] W. Li, X. X. Zhang, X. C. Wang, and J. J. Niu, "Preparation and characterization of microencapsulated phase change material with low remnant formaldehyde content," *Materials Chemistry and Physics,* vol. 106, pp. 437-442, Dec 15 2007.

[73] C. Berkland, M. King, A. Cox, K. K. Kim, and D. W. Pack, "Precise control of PLG microsphere size provides enhanced control of drug release rate," *Journal of Controlled Release,* vol. 82, pp. 137-147, 2002.

[74] J. Herrmann and R. Bodmeier, "Biodegradable, somatostatin acetate containing microspheres prepared by various aqueous and non-aqueous solvent evaporation methods," *European Journal of Pharmaceutics and Biopharmaceutics,* vol. 45, pp. 75-82, 1998.

[75] S. Freitas, H. P. Merkle, and B. Gander, "Microencapsulation by solvent extraction/evaporation: reviewing the state of the art of microsphere preparation process technology," *Journal of controlled release,* vol. 102, pp. 313-332, 2005.

[76] N. S. Berchane, F. F. Jebrail, K. H. Carson, A. C. Rice-Ficht, and M. J. Andrews, "About mean diameter and size distributions of poly (lactide-co-glycolide)(PLG) microspheres," *Journal of microencapsulation,* vol. 23, pp. 539-552, 2006.

[77] X. Li, X. Deng, M. Yuan, C. Xiong, Z. Huang, Y. Zhang, *et al.*, "Investigation on process parameters involved in preparation of poly-DL-lactide-poly (ethylene glycol) microspheres containing Leptospira Interrogans antigens," *International journal of pharmaceutics,* vol. 178, pp. 245-255, 1999.

[78] I. O. Salyer, "A clothing formed from a melt blends comprising a polyolefin selected from the group consisting of high density polyethylene, low density polyethylene, and a high melting polypropylene, an ethylene-vinyl acetate copolymer, silica," ed: Google Patents, 1999.

[79] T. L. Vigo, C. M. Zimmerman, J. S. Bruno, and G. F. Danna, "Temperature adaptable textile fibers and method of preparing same," ed: Google Patents, 1990.

[80] X. Zhang, X. Wang, X. Tao, and K. Yick, "Energy storage polymer/MicroPCMs blended chips and thermo-regulated fibers," *Journal of materials science,* vol. 40, pp. 3729-3734, 2005.

[81] B. Pause, "Nonwoven protective garments with thermo-regulating properties," *Journal of industrial textiles,* vol. 33, pp. 93-99, 2003.

[82] Y. Bryant and D. Colvin, "Fiber with reversible enhanced thermal storage properties and fabrics made there from, US Patent 4,756,958 (1988)," ed.

[83] Outlast. (27 November, 2015). *Outlast Technologies*. Available: http://www.outlast.com/en/applications/fiber

[84] X. Zhang, X. Wang, X. Tao, and K. Yick, "Structures and properties of wet spun thermo-regulated polyacrylonitrile-vinylidene chloride fibers," *Textile research journal,* vol. 76, pp. 351-359, 2006.

[85] M. H. Hartmann, "Stable phase change materials for use in temperature regulating synthetic fibers, fabrics and textiles," ed: Google Patents, 2004.

[86] G. Frank and R. Biastoch, "Low-formaldehyde dispersion of microcapsules of melamine-formaldehyde resins," 6224795, 2001.

[87] W. Li, J. Wang, X. Wang, S. Wu, and X. Zhang, "Effects of ammonium chloride and heat treatment on residual formaldehyde contents of melamine-formaldehyde microcapsules," *Colloid and Polymer Science*, vol. 285, pp. 1691-1697, 2007.

[88] Y. G. Bryant, "Melt spun fibers containing microencapsulated phase change material," *ASME-PUBLICATIONS-HTD*, vol. 363, pp. 225-234, 1999.

[89] M. H. Hartmann and M. C. Magill, "Melt spinable concentrate pellets having enhanced reversible thermal properties," 6793856 B2, 2004.

[90] M. C. Magill, M. H. Hartmann, and J. S. Haggard, "Multi-component fibers having enhanced reversible thermal properties and methods of manufacturing thereof," 6855422 B2, 2005.

[91] X. Gao, N. Han, X. Zhang, and W. Yu, "Melt-processable acrylonitrile–methyl acrylate copolymers and melt-spun fibers containing MicroPCMs," *Journal of materials science,* vol. 44, pp. 5877-5884, 2009.

[92] B. Hagström, "Temperature regulating textile fibers containing large amounts of phase change material," *Chemical Fibers International,* vol. 60, p. 221, 2010.

[93] Y. Shin, D. I. Yoo, and K. Son, "Development of thermoregulating textile materials with microencapsulated phase change materials (PCM). IV. Performance properties and hand of fabrics treated with PCM microcapsules," *Journal of Applied Polymer Science,* vol. 97, pp. 910-915, 2005.

[94] A. Khoddami, O. Avinc, and F. Ghahremanzadeh, "Improvement in poly (lactic acid) fabric performance via hydrophilic coating," *Progress in Organic Coatings,* vol. 72, pp. 299-304, 2011.

[95] E. P. G. Gohl and L. D. Vilensky, *Textile science*: Longman cheshire, 1983.

[96] W. Klein, *Man-made fibres and their processing*: Textile Institute, 1994.

[97] F. Fourne, "Synthetic Fibers: Machines and Equipments, Manufacture, Properties," *Hanser, Cincinnati,* 1999.

[98] P. Walsh, *The Yarn Book*: University of Pennsylvania Press, 2006.

[99] S. B. Warner, *Fiber science*: Prentice Hall Englewood Cliffs, NJ, 1995.

[100] B. Younes, "The statistical modelling of production processes of biodegradable aliphatic aromatic co-polyester fibres used in the textile industry," Heriot-Watt University, 2012.

[101] A. W. Rajput, "An investigation into the production of UHMWPE fibres and coatings for protective apparel," PhD, School of Textile & Design, Heriot Watt University, UK, 2013.

[102] John R. Carroll, Mark P. Givens, and R. Piefer, "DESIGN ELEMENTS OF THE MODERN SPINNING CONTROL SYSTEM," presented at the Textile, Fiber and Film Industry Technical Conference, 1994., IEEE 1994 Annual Greenville, SC 1994

[103] J. Maleyeff, "DEVELOPMENT OF AN INTERDISCIPLINARY SENIOR LABORATORY EXERCISE," presented at the International Conference on Engineering Education Chicago, Illinois, 1997.

[104] R. D. Yang, R. R. Mather, and A. F. Fotheringham, "The influence of fiber processing parameters on the structural properties of as-spun polypropylene fibers: a factorial design approach," *Journal of Applied Polymer Science,* vol. 93, pp. 568-576, Jul 15 2004.

[105] J. C. Moreland, J. L. Sharp, and P. J. Brown, "Lab-Scale Fiber Spinning Experimental Design Cost Comparison," *Journal of Engineered Fibers and Fabrics,* vol. 5, pp. 39-49, 2010.

[106] K. B. Clark and S. C. Wheelwright, *The product development challenge: competing through speed, quality, and creativity*: A Harvard business review book, 1995.

[107] T. Matsuo, "Recent specialty technologies of fibers and textiles in Japan," *Quality Textiles for Quality Life, Vols 1-4*, pp. 69-73, 2004.

[108] A. Ziabicki, L. Jarecki, and A. Wasiak, "Dynamic modelling of melt spinning," *Computational and Theoretical Polymer Science,* vol. 8, pp. 143-157, 1998.

[109] W. Ibrahim, "An investigation into textile applications of thermochromic pigments," Heriot-Watt University, 2012.

[110] Brydson J and D. Peacock, *Principles of Plastics Extrusion*, 1 ed.: Springer Netherlands, 1973.

[111] C. Rauwendaal, *Polymer Extrusion*, 5th Edition ed.: Carl Hanser Verlag GmbH & Co. KG 2014.

[112] C. X. Zhang, C. S. Wang, H. P. Wang, and Y. Zhang, "Multifilament model of PET melt spinning and prediction of As-spun fiber's quality," *Journal of Macromolecular Science Part B-Physics,* vol. 46, pp. 793-806, Jul-Aug 2007.

[113] L. Jarecki and Z. Lewandowski, "Mathematical Modelling of the Pneumatic Melt Spinning of Isotactic Polypropylene. Part III. Computations of the Process Dynamics," *FIBRES & TEXTILES in Eastern Europe,* vol. 17, pp. 75-80, 2009.

[114] M. L. Ottone and J. A. Deiber, "Modelling the melt spinning of polyethylene terephthalate," *Journal of elastomers and plastics*, vol. 32, pp. 119-139, 2000.

[115] H. H. George, "Model of Steady-State Melt Spinning at Intermediate Take-up Speeds," *Polymer Engineering and Science,* vol. 22, pp. 292-299, 1982.

[116] T. Gotz and S. S. N. Perera, "Optimal control of melt-spinning processes," *Journal of Engineering Mathematics,* vol. 67, pp. 153-163, Jul 2010.

[117] T. Gotz and S. S. N. Perera, "Stability analysis of the melt spinning process with respect to parameters," *Zamm-Zeitschrift Fur Angewandte Mathematik Und Mechanik,* vol. 89, pp. 874-880, Nov 2009.

[118] G. X. Wang and E. F. Matthys, "Modeling of Rapid Solidification by Melt Spinning - Effect of Heat-Transfer in the Cooling Substrate," *Materials Science and Engineering a-Structural Materials Properties Microstructure and Processing,* vol. 136, pp. 85-97, Apr 30 1991.

[119] K. Ravikumar and Y.-A. Son, "Process analysis and optimization for the ionic interactions of quaternary ammonium salts with nylon 66 fibers using statistical experimental design," *Dyes and Pigments,* vol. 75, pp. 199-206, 2007.

[120] J. G. Cook, *Hand book of Textile Fibres Part II : Man Made Fibres*, 5th ed. England: Merrow Publishing Co. Ltd, 1984.

[121] R. J. Crawford, *Plastic Engineering*, 3rd ed.: Elsevier, 1998.

[122] J. L. White, K. C. Dharod, and E. S. Clark, "Interaction of Melt Spinning and Drawing Variables on Crystalline Morphology and Mechanical-Properties of High-Density and Low-Density Polyethylene Fiber," *Journal of Applied Polymer Science*, vol. 18, pp. 2539-2568, 1974.

[123] R. Kolb, S. Seifert, N. Stribeck, and H. G. Zachmann, "Simultaneous measurements of small- and wide-angle X-ray scattering during low speed spinning of poly(propylene) using synchrotron radiation," *Polymer*, vol. 41, pp. 1497-1505, Feb 2000.

[124] S. Krimm and A. V. Tobolsky, "Quantitative x-ray studies of order in amorphous and crystalline polymers. Quantitative x-ray determination of crystallinity in polyethylene," *Journal of Applied Polymer Science*, vol. 7 pp. 57–76, 1951.

[125] W. C. Sheehan and T. B. Cole, "Production of super-tenacity polypropylene filaments," *Journal of Applied Polymer Science*, vol. 8, pp. 2359–2388, 1964.

[126] P. Smith and P. J. Lemstra, "Ultra-High-Strength Polyethylene Filaments by Solution Spinning-Drawing," *Journal of Materials Science*, vol. 15, pp. 505-514, 1980.

[127] R. Yang, "A systematic statistical approach to polypropylene fibre process technology," Heriot-Watt University, 2000.

[128] J. A. Brydson, *Plastics materials*: Butterworth-Heinemann, 1999.

[129] W. Sheehan and T. Cole, "Production of super-tenacity polypropylene filaments," *Journal of Applied Polymer Science*, vol. 8, pp. 2359-2388, 1964.

[130] R. C. Dutra, B. G. Soares, E. A. Campos, J. D. De Melo, and J. L. Silva, "Composite materials constituted by a modified polypropylene fiber and epoxy resin," *Journal of applied polymer science*, vol. 73, pp. 69-73, 1999.

[131] S. S. Chaudhari, R. S. Chitnis, and R. Ramkrishnan, "Waterproof Breathable active sports wear fabrics," *Man-made Textiles in India*, vol. 5, pp. 166-171, 2004.

[132] N. ÖZDİL and S. ANAND, "Recent Developments in Textile Materials and Products Used for Activewear and Sportswear," *Tekstil Teknolojileri Elektronik Dergisi*, vol. 8, pp. 68-83, 2014.

[133] D. Uttam, "Active sportswear fabrics," *International Journal of IT, Engineering and Applied Sciences Research (IJIEASR),* vol. 2, pp. 34-40, 2013.

[134] W. Zhang, J. Li, W. Chen, and S. Long, "Wetness comfort of fine-polypropylene-fibre fabrics," *Journal of the Textile Institute,* vol. 90, pp. 252-263, 1999.

[135] J. Karger-Kocsis, *Polypropylene: an AZ reference* vol. 2: Springer Science & Business Media, 2012.

[136] B. S. Babu, P. Senthilkumar, and M. Senthilkumar, "Effect of yarn linear density on moisture management characteristics of cotton/polypropylene double layer knitted fabrics," *INDUSTRIA TEXTILA,* vol. 66, pp. 123-130, 2015.

[137] M. Lokhande, L. Patil, and A. Awasare, "Suitability of Bi-Layer Knitted Fabric for Sportswear Application," in *International Journal of Engineering Research and Technology*, 2014.

[138] M. J. Abreu, A. P. Catarino, C. Cardoso, and E. Martin, "Effects of sportswear design on thermal comfort," 2011.

[139] X. Chen, "Modelling of Textile Structure for Advanced Applications," *Journal of Information and Computing Science,* vol. 5, pp. 71-80, 2010.

[140] M. O. R. Siddiqui, "Geometrical Modelling and Numerical Analysis of Thermal Behaviour of Textile Structures," PhD, School of Textile and Design, Heriot Watt University, United Kingdom, 2015.

[141] S. Vassiliadis, A. Kallivretaki, C. Provatidis, and D. Domvoglou, *Mechanical analysis of woven fabrics: The state of the art*: INTECH Open Access Publisher, 2011.

[142] H. Lin and A. Newton, "Computer representation of woven fabric by using B-splines," *Journal of the Textile Institute,* vol. 90, pp. 59-72, 1999.

[143] J. Hofstee and F. Van Keulen, "3-D geometric modeling of a draped woven fabric," *Composite structures,* vol. 54, pp. 179-195, 2001.

[144] R. Gong, B. Ozgen, and M. Soleimani, "Modeling of yarn cross-section in plain woven fabric," *Textile Research Journal,* vol. 79, pp. 1014-1020, 2009.

[145] D. Logan, *A first course in the finite element method*: Cengage Learning, 2011.

[146] M. A. G. Lazcano and W. Yu, "Thermal performance and flammability of phase change material for medium and elevated temperatures for textile application," *J Therm Anal Calorim,* vol. 117, pp. 9-17, 2014.

[147] G. E. R. Lamb and K. Duffy-Morris, "Heat Loss Through Fabrics Under Ventilation With and Without a Phase Transition Additive," *Textile Research Journal,* vol. 60, pp. 261-265, 1990.

[148] M. Nuckols, "Analytical modeling of a diver dry suit enhanced with micro-encapsulated phase change materials," *Ocean Engineering,* vol. 26, pp. 547-564, 1999.

[149] H. Shim, E. A. McCullough, and B. W. Jones, "Using Phase Change Materials in Clothing," *Textile Research Journal,* vol. 71, pp. 495-502, 2001.

[150] J. Kim and G. Cho, "Thermal Storage/Release, Durability, and Temperature Sensing Properties of Thermostatic Fabrics Treated with Octadecane-Containing Microcapsules," *Textile Research Journal,* vol. 72, pp. 1093-1098, 2002.

[151] K. Ghali, N. Ghaddar, J. Harathani, and B. Jones, "Experimental and numerical investigation of the effect of phase change materials on clothing during periodic ventilation," *Textile Research Journal,* vol. 74, pp. 205-214, 2004.

[152] L. I. Yi and Z. Qingyong, "A Model of Heat and Moisture Transfer in Porous Textiles with Phase Change Materials," *Textile Research Journal,* vol. 74, pp. 447-457, 2004.

[153] L. Fengzhi and L. Yi, "A computational analysis for effects of fibre hygroscopicity on heat and moisture transfer in textiles with PCM microcapsules," *Modelling and Simulation in Materials Science and Engineering,* vol. 15, p. 223, 2007.

[154] L. Fengzhi, "Numerical Simulation For Effect of Microcapsuled Phase Change Material (MPCM) Distribution on Heat and Moisture Transfer in Porous Textiles," *Modern Physics Letters B,* vol. 23, pp. 501-504, 2009.

[155] B. Ying, Y. Li, Y. Kwok, and Q. Song, "Mathematical Modeling Heat and Moisture Transfer in Multi-Layer Phase Change Materials Textile Assemblies," in *ICIECS (2009),* pp. 1-4.

[156] S. Alay, C. Alkan, and F. Göde, "Steady-state thermal comfort properties of fabrics incorporated with microencapsulated phase change materials," *Journal of the Textile Institute,* vol. 103, pp. 757-765, 2012.

[157] H. Yoo, J. Lim, and E. Kim, "Effects of the number and position of phase-change material-treated fabrics on the thermo-regulating properties of phase-change material garments," *Textile Research Journal* vol. 83, pp. 671-682, 2013.

[158] Y. Hu, D. Huang and Z. Qi, "Modeling thermal insulation of firefighting protective clothing embedded with phase change material," *Heat Mass Transfer*, vol. 49, pp. 567-573, 2013.

[159] M. O. R. Siddiqui and D. Sun, "Computational analysis of effective thermal conductivity of microencapsulated phase change material coated composite fabrics," *Journal of Composite Materials*, 2014.

[160] X. Zhao, X. Yi, Z. Xu, and Y. Xu, "Effects of spinneret structure on poly-ether-ether-ketone fibers by screw extrusion," *Journal of Central South University of Technology*, vol. 12, pp. 272-275, 2005.

[161] C. B. Weinberger, "Synthetic fiber manufacturing," *Departmant of Chemical Engineering, Drexel University*, 1996.

[162] H. F. Mark, *Encyclopedia of polymer science and technology, concise*: John Wiley & Sons, 2013.

[163] *ABAQUS User's Manual* version 6.12. (2012).

[164] W. Li, J. Wang, X. Wang, S. Wu, and X. Zhang, "Effect of Ammonium Chloride and heat treatment on residual formaldehyde contents of melamine formaldehyde microcapsules," *Colloid Polymer Science*, vol. 285, pp. 1691-1697, 2007.

[165] X. Zhang, Y. Fan, X. Tao, and K.Yick, "Fabrication and properties of microcapsules and nanocapsules containing n-octadecane," *Materials Chemistry and Physics*, vol. 88, pp. 300-307, 2004.